IMMUNOMODULATION BY SMALL MOLECULES FOR PREVENTION OR TREATMENT OF CANCER

By

Di Zhang

A DISSERTATION

Submitted to
Michigan State University
in partial fulfillment of the requirements
for the degree of

Pharmacology and Toxicology – Environmental Toxicology – Doctor of Philosophy

2020

ABSTRACT

IMMUNOMODULATION BY SMALL MOLECULES FOR PREVENTION OR TREATMENT OF CANCER

By

Di Zhang

Cancer is the second leading cause of deaths worldwide. Lung cancer and breast cancer, specifically, are two of the most common cancers in the U.S. except skin cancer. With the increasing medical and economic burden of these diseases, developing effective cancer prevention and treatment strategies is important and urgent. Cancer is characterized by uncontrolled cell proliferation. Targeting the tumor cells directly to inhibit their growth and increase cell death has been the major focus of cancer treatment since the last century. Cancer is also described as a wound that does not heal. Inflammation plays critical roles in cancer development and progression. The immune system is a powerful host defense mechanism against infections and diseases including cancer. However, tumor cells are able to edit and suppress the immune system to evade the immune attack. Targeting immune cells to unleash the power of immune surveillance has become a research priority. The recent breakthroughs in cancer immunotherapy have revolutionized the landscape of cancer treatment. As immunotherapy becomes the first line of therapy in cancer treatment, it is essential to understand how other drugs modulate the immune system, so that we can deliver more effective and less toxic combinations. In this thesis project, I focused on four therapeutic targets (bromodomain proteins, retinoid X receptors, Nrf2 transcription factors, poly (ADP-ribose) polymerase) and explored their effects on the immune cells. Small molecules targeting these proteins were tested in various preclinical mouse models in the context of either cancer

prevention or treatment. My studies not only demonstrated enhanced efficacy and reduced toxicity with all four classes of compounds but also provided some novel insights into the immunomodulatory effects of these clinically relevant signaling pathways. This work is highly translational and could have direct impact on human patients.

ACKNOWLEDGEMENTS

I always like to tell people how lucky I am having Dr. Karen Liby as my mentor. She and I joined MSU at the same time. I still remember how excited I was when I saw her research interests, because that is exactly what I wanted to work on. During the four years, she always leaves her door open for me. I feel more than comfortable talking to her at anytime. She is always patient, listens to me, and encourages me to think. She cares for every student in the lab. I still remember, at the beginning of my rotation, she went down with me to the animal room every week to give me hands-on training for handling mice and measuring tumors. I cannot thank her enough for trusting me and letting me lead multiple projects, so that I can be productive during my doctoral training. I also deeply appreciate all other supports she gave me on my career development. Without her support, I would not have been able to receive the F99/K00 transition award, work as a venture fellow at Spartan Innovations, practice as a summer intern at Charles River Laboratories. She sets a great example for me as a dedicated, enthusiastic, hard working and supportive mentor. I wish that one day I could become an outstanding scientist like her.

Thanks to my committee members Dr. Richard Neubig, Dr. Eran Andrechek, and Dr. Cheryl Rockwell. Thanks for all their invaluable inputs and guidance. I enjoyed every single committee meeting we had coming back with new ideas. All of them are always there whenever I need advice and support.

Thanks to everyone in Liby lab: Ana, Sarah, Lyndsey, Jess, Beth, Owen and Kayla. I feel so lucky working with all of them. They are always there offering help whenever I need. They made me enjoy coming into lab every day.

I also want to thank all my friends here: Vanessa, Robert, David, Kevin, Jon, Sean, Ted, Ryan, Jennifer, Salik, Ali, Hui, Pengfei, Mengzi, Shen. They are the reasons that I never feel lonely living in another country. They are the ones who made my life so much fun outside the lab.

Last but not least, I want to thank my parents for all their love and support. As the only child in the family, my parents always give me the best they can. Dad has forever been my role model. I know he is right there behind me whenever I need suggestions or courage for my career and life. He taught me how to be brave, strong, persistent, and independent. Mom is my best friend. I can share with her all my happiness and unhappiness. I know how much they miss me because I miss them so much as well. I would not have been able to come to another country by myself and accomplish all of these without their support and endless love. I am proud of being their child, and I hope I can become a person that they are proud of too.

TABLE OF CONTENTS

LIST OF TABLES

LIST OF FIGURES

KEY TO ABBREVIATIONS

ALK: anaplastic lymphoma kinase

ARE: antioxidant response element

ATM: ataxia-telangiesctasia mutated gene

ATR: ataxia telangiectasia and Rad3 related

BiTEs: bispecific T cells engagers

BMDMs: bone marrow-derived macrophages

Bmp6: bone morphogenetic protein 6

BRCA: breast cancer-associated gene

CAFs: cancer-associated fibroblasts

CAR: chimeric antigen receptor

Ccl9: chemokine (C-C motif) ligand 9

CDX: cell line derived xenograft

CHK1/2: checkpoint kinase 1/2

CML: chronic myelogenous leukemia

Csf1: colony stimulating factor 1

CTLA4: cytotoxic T lymphocyte-associated antigen 4

Cxcl1: chemokine (C-X-C motif) ligand 1

Cxcl12: chemokine (C-X-C motif) ligand 12

CXCR4: C-X-C chemokine receptor type 4

DCIS: ductal carcinoma in situ

DCs: dendritic cells

EBV: Epstein-Barr virus

Eef1a2: eukaryotic translation elongation factor 1 alpha 2

EGFR: epidermal growth factor receptor

ERK: extracellular signal–regulated kinases

ER: estrogen receptor

EPR: enhanced permeability and retention

FANCA: FA Complementation Group A

FANCD2: FA Complementation Group D2

Foxp3: forkhead box P3

FreeTLZ: free Talazoparib

GEMM: genetically engineered mouse model

Gpx3: Glutathione peroxidase 3

HATs: histone acetyltransferases

HBV: Hepatitis B virus

HCV: Hepatitis C virus

HDAC: histone deacetylase

HMTs: histone methyltransferases

HPV: human papillomavirus

HTLV: human T-lymphotropic virus

HR: homologous recombination

IBD: inflammatory bowel disease

ICIs: immune checkpoint inhibitors

IDC: invasive ductal carcinoma

Igfbp5: Insulin-like growth factor-binding protein 5

Igfbp6: Insulin-like growth factor-binding protein 6

IL13ra2: Interleukin-13 receptor subunit alpha-2

ILC: invasive lobular carcinoma

iNOS: inducible nitric oxide synthase

JNK: c-Jun N-terminal kinases

Keap1: Kelch-like ECH-associated protein 1

KO: Knockout

KSHV: Kaposi sarcoma herpesvirus

LCIS: lobular carcinoma in situ

LPS: lipopolysaccharide

MAPK: mitogen-activated protein kinase

MDSC: myeloid-derived suppressor cell

MHC-II: major histocompatibility complex-II

MMP12: matrix metalloproteinase 12

MMP25: matrix metalloproteinase 25

MMTV: mouse mammary tumor virus

Mybpc2: myosin binding protein C

Myh1: striated muscle myosin heavy chain 1

Myl1: myosin light chain 3

Mylpf: myosin light chain, phosphorylatable, fast skeletal muscle

NanoTLZ: Nano-Talazoparib

NK cells: natural killer cells

NNK: 4-(methylnitrosamino)-1-(3-pyridyl)-1-butanone

Nrf2 or NFE2L2: Nuclear factor (erythroid-derived 2)-like 2

NSAIDs: nonsteroidal anti-inflammatory drugs

NSCLC: non-small cell lung cancer

PARP: poly (ADP-ribose) polymerase

PEG: polyethylene glycol

RAE1: retinoic acid early transcript 1

RB: retinoblastoma protein

RES: reticuloendothelial system

PDX: patient-derived xenograft

PD-1: programmed cell death protein 1

PKC: protein kinase C

RIN: RNA integrity number

ROS: Reactive oxygen species

PTEN: phosphatase and tensin homolog

RXR: Retinoid X receptor

SCLC: small cell lung cancer

SERMs: selective estrogen receptor modulators

sMAF: small musculo-aponeurotic fibrosarcoma

Sod3: superoxide dismutase 3

SREBP: sterol regulatory element-binding protein

TAAs: tumor-associated antigens

TAMs: tumor-associated macrophages

TCR: T cell receptor

TGF-β: transforming growth factor beta

TIL: tumor-infiltrating lymphocyte

TNBC: triple negative breast cancer

TNFRSF19: tumor necrosis factor receptor superfamily, member 19

Top2a: topoisomerase II alpha

Tregs: regulatory T cells

VEGFs: vascular endothelial growth factor

WAP: whey acidic protein

WT: wildtype

CHAPTER 1

Overview - Targeting the immune system for cancer therapy

1.1 Cancer, “the emperor of all maladies”

Siddhartha Mukherjee has named cancer “the emperor of all maladies.” Cancer is a group of diseases that affect billions of people around the world. An estimated 18.1 million new cancer cases were diagnosed and 9.6 million deaths were reported worldwide from cancer in 2018 alone [1]. In the United States, it is estimated that approximately 1.8 million people will be diagnosed with cancer and over 600,000 cancer deaths recorded in 2019 [2]. The economic burden of cancer care has been steadily increasing. In 2010, $137.4 billion in medical expenditures were spent to care for cancer survivors in the United States [3]. As the population ages, cancer will continue to be a formidable adversary for human health.

1.1.1 Hallmarks of cancer

What is cancer? Although cancer encompasses over 200 diseases, they all share some common characteristics, which are classified as the hallmarks of cancer [4, 5]. Uncontrolled cell proliferation is a well-known hallmark of cancer. This is driven by acquired endogenous growth signals, lack of sensitivity to growth-inhibitory signals, evasion of programmed cell death, limitless replicative potential, and sustained angiogenesis. Tumor cells are characterized by genomic instability, abundant mutations, and the ability to evade immune surveillance. Normal cells only move from a quiescent state to a proliferative state after sensing mitogenic growth signals. In contrast, tumor cells are able to generate endogenous growth signals, by overexpressing growth factors and growth receptors, altering growth receptors structurally to become ligand independent, switching the types of extracellular matrix receptors that are expressed, and changing the components of downstream cytoplasmic circuitry [6]. In addition,

cancer cells can evade anti-proliferative signals by disrupting signaling pathways that govern the cell cycle [7].

Besides promoting the capabilities of proliferation, tumor cells also develop mechanisms to prevent cell death. For example, p53, a proapoptotic regulator, is mutated in more than 50% of human cancers [8]. The rapid growth of cancer cells certainly requires considerable supply of oxygen and nutrients. Angiogenesis and metabolism reprogramming, therefore, are crucial during tumor development [9]. Furthermore, even if the nutrients and space become limited at the primary site, tumor cells are able to survive by metastasizing to distant tissues [10].

1.1.2 Classification of cancer

Cancer can be classified into a wide variety of subtypes based on different criteria. In terms of organ origin, commonly diagnosed cancers include lung cancer, breast cancer, prostate cancer, colorectal cancer, skin cancer, bladder cancer, kidney cancer, lymphoma, leukemia, uterine cancer, pancreatic cancer, and thyroid cancer. This project will only focus on lung cancer and breast cancer, as they are the most commonly diagnosed lethal cancers. Not all tumors are cancerous. Originally, the term “tumor” referred to a swelling that could be either benign or malignant [11]. Benign tumors have well-defined borders and do not invade into nearby tissues and thus are often treated by surgical removal. Malignant tumors, in contrast, vary from well-differentiated to anaplastic, and frequently infiltrate local normal tissue or even metastasize to distant tissues. Depending on the tissue of origin, there are four main types of malignant cancers: carcinomas (epithelium), sarcomas (connective tissue), hematopoietic tumors (blood) and neuroectodermal tumors (nervous tissue) [12].

1.1.3 Risk factors

Cancer is caused by both external factors and internal factors. External risk factors include smoking [13], chemicals (e.g. asbestos, benzopyrene, vinyl chloride) [14], radiation [15], and infectious organisms (e.g. HPV, HBV, HCV) [16]. Internally, inherited mutations (e.g. *BRCA* mutations) [17], hormones [18], and immune system disorders [19] all contribute to tumor development. These factors may act together or in sequence as "hits" to initiate or promote carcinogenesis. Two hits are usually required to acquire phenotypic changes [20]. These risk factors often induce DNA damage either directly or indirectly. Failure of DNA repair leaves behind mutations. Beside environmental factors and inheritance, mutations in cancer cells can also result from DNA replication errors. In fact, DNA replication error-induced mutations are responsible for two-thirds of the mutations in human cancers [21]. If exogenous environmental factors are external enemies, reducing exposure will be the key to limiting the development of cancer, which is called primary prevention. Internal enemies, such as DNA replication errors, however, are not easily prevented. Therefore, early detection and secondary prevention (prevent the disease from getting worse) become alternative ways to defend against cancer.

1.1.4 Cancer treatment options

More treatment strategies for cancer have become available since the last century. Surgery, chemotherapy and radiotherapy are traditional treatment options for cancer patients. Surgery is most effective at early stages when the tumor is still localized. Surgery may also be used to provide comfort or enhance the effectiveness of other treatments. Neoadjuvant chemotherapy or radiotherapy can also be applied before surgery to shrink the tumor and lower the risk of recurrence. Chemotherapy was first

developed in the 1940s. Traditional chemotherapy includes alkylating agents, anti-metabolites, tumor antibiotics, topoisomerase inhibitors and microtubule inhibitors [22]. Because these cytotoxic agents target rapidly proliferating cells, they also induce significant side effects by acting on rapidly proliferating normal cells such as bone marrow stem cells, gastrointestinal mucosal cells, hair follicles and ovaries or testes.

Since 1990s, more targeted therapies have become available. These targeted therapies act by interfering in the processes of cell growth, division, or spread that tumor cells rely on for survival. Tyrosine kinase inhibitors were the first targeted therapy for cancer treatment. Hormone receptor modulators, epigenetic modifiers, proteasome inhibitors, angiogenesis inhibitors, apoptosis-inducing drugs, etc., are other targeted therapies [23].

Targeting the immune system to treat cancer is another important strategy in cancer treatment. Although this idea can be traced back to the 1950s, the blossoming of immunotherapy did not arrive until recently. As immune checkpoint inhibitors were approved for multiple cancers, immunotherapy has revolutionized the landscape of cancer therapy. Checkpoint inhibitors have become the first-line of treatment for advanced non-small cell lung cancer and have demonstrated prolonged survival benefits in multiple cancer types [24, 25]. In the era of immunotherapy, it is pivotal to understand not only the basic immunology of the cancer microenvironment, but also how other existing therapeutic options alter the effectiveness of immunotherapies. Although the achievements of immunotherapy observed in clinical trials are undeniable, only a small portion of the patients derives benefits. Rational drug combinations provide new opportunities to overcome some of these limitations.

1.2 Breast cancer

1.2.1 Statistics

Breast cancer is the most commonly diagnosed cancer and the second leading cause of cancer deaths in women. In 2019, an estimated 268,600 women will be diagnosed with breast cancer in the United States [26]. It is usually curable if the cancer is localized to the breast, with a 5-year survival rate of 99%. With advances in early detection and screening, over 60% breast cancer cases are diagnosed at this early stage. With regional spread into the lymph nodes, the average 5-year survival rate is 85%. However, if the cancer has spread to a distant tissue, the 5-year survival rate declines to only 27% [27].

1.2.2 Classification of breast cancer and treatment options

Breast cancer is a heterogeneous disease with distinct histological, molecular and clinical features. Breast cancer can be classified as luminal A, luminal B, $HER2^+$ and triple negative subtypes based on the molecular phenotypes [28]. Luminal A is the most common subtype of breast cancer and accounts for approximately 40% of breast cancer cases. Luminal A subtypes are usually low-grade tumors that express hormone receptors (estrogen receptor/progesterone receptor), and are therefore sensitive to endocrine therapies. The luminal B subtype, which represents about 20% of breast cancers, is estrogen-receptor and/or progesterone-receptor positive, HER2 positive or negative, with high levels of Ki67 expression. Luminal B tumors usually grow moderately faster than luminal A tumors and their prognosis is also slightly worse. HER2 positive breast cancers, as indicated in the name, express the human epidermal growth factor receptor 2 (HER2). Although HER2 positive cancers tend to be more aggressive than

other types, the prognosis is actually quite good because of the availability of targeted therapies such as Trastuzumab, an antibody which specifically targets the HER2 protein [29]. Triple negative breast cancers (15-20% of breast cancers) have the worst prognosis. Without the expression of either hormone receptor or the HER2 receptor, no targeted therapy is available, so chemotherapy remains the most effective option for triple negative breast cancer patients.

1.2.3 Animal models of breast cancer

Although *in vitro* assays using cancer cell lines are valuable methods to study cancer, it is critical to have *in vivo* models to study the complex biology of cancer and test new compounds for therapeutics. A wide variety of mouse models have been developed to study breast cancer. These mouse models mimic different subtypes of breast cancers in humans [30]. In general, there are three major ways to develop mammary gland tumors: implanting tumor cells directly into the mice (xenograft), genetically modifying the animals (GEMM) and carcinogen-induced tumor model (N-Methyl-N-nitrosurea, 7,12-Dimethylbenzanthracene, 2-Amino-1-methyl-6-phenylimidazo(4,5-b)pyridine, *etc.*).

To establish a xenograft model, either tumor cell lines (CDX) or human tumor fragments (PDX) are injected ectopically under the skin or orthotopically into a fat pad. To model colonization or metastasis, tumor cells can be injected directly into the circulation via the tail vein to study the process of extravasation and metastatic deposition in distant organs.

To generate GEMM models of breast cancer, regulatory elements only found in the mammary gland are used to drive the expression of gene of interest (e.g. tumor suppressor genes or oncogenes) selectively in the mammary gland. The most common

mammary-specific gene regulatory elements include the mouse mammary tumor virus long terminal repeat (MMTV-LTR) and milk protein gene promoters of the whey acidic protein (WAP) or the β-lactoglobulin (BLG) [31]. MMTV-PyMT, MMTV-Neu, BRCAfl/fl;MMTV-Cre are typical models representing triple negative, HER2 positive and BRCA-deficient breast cancers, respectively. Other GEMM models, such as MMTV-cyclin D1, MMTV-Myc, Stat1$^{-/-}$, have also been developed to study specific oncogenes or tumor suppressors [31].

Both xenograft models and GEMMs have their own advantages and disadvantages [30]. For xenograft models, inoculation of tumor cells is technically simple, tumors develop quickly, and human cancer cells are used. However, poorly differentiated cancer cells are required for tumor formation so that only advanced disease states are modeled. Additionally, the requirement to use immunocompromised hosts neglects the effects of an intact tumor microenvironment, which is critical in tumor initiation and progression. GEMMS maintain an intact immune system and thus a natural tumor microenvironment, and provide an opportunity to study both early and late stages of tumor development and progression. Nevertheless, GEMMs usually require extensive breeding and genotyping, and their genetics often do not fully represent the heterogeneity of human disease. Therefore, the selection of a mouse model needs to be carefully considered based on the scope of the research and confirmation of the results in more than one model will enhance rigor and confidence in the results.

1.3 Lung cancer

1.3.1 Statistics

Lung cancer is the second most commonly diagnosed cancer in both men and

women with an estimated 228,150 new cases in 2019 in the U.S. [2] Lung cancer is also the leading cause of cancer deaths, by far. More people die of lung cancer than of breast, prostate and colon cancers combined. The overall five-year survival rate for lung cancer is only 18% and had not improved in the last 30 years until the approval of immunotherapies. The survival rate (56%) is much higher when the disease is still localized, however, only 16% of lung cancers are diagnosed at an early stage. When the tumors spread to other organs, the five-year survival rate is only 5%. Smoking, as the main cause of lung cancer, is responsible for 80% of lung cancer cases; radon causes 10%; the other 10% is attributed to occupational exposures to carcinogens or exposures to outdoor air pollution [32]. The incidence of lung cancer in never-smokers is actually increasing especially in Asia. These cases of lung cancer in never smokers are usually associated with second hand smoke, indoor air pollution, occupational exposures, or genetic susceptibilities [33].

1.3.2 Classification of lung cancer

There are two major types of lung cancer: non-small cell lung cancer (NSCLC) and small cell lung cancer (SCLC). NSCLC is the most common subtype of lung cancer and accounts for 85% of lung cancer cases. NSCLC can be further divided into squamous cell carcinoma, adenocarcinoma and large cell carcinoma depending on the origin. SCLC accounts for the remaining 15% of lung cancers in the United States. SCLC often initiates in the bronchi and spreads to other organs much faster than NSCLC.

1.3.3 Treatment options for lung cancer

Besides conventional treatment strategies such as surgery, radiotherapy and chemotherapy, several targeted therapies are available for lung cancer depending on

their molecular profile. Mutations in *Kras* (25%) and *EGFR* (21%) are the most common driver mutations in adenocarcinomas followed by mutations in *Keap1, ALK, MET, HER2, BRAF, ROS1, RET, NTRK1, NRAS, PIK3CA*, etc [34]. EGFR inhibitors (e.g. erlotinib, afatinib, gefitinib, osimertinib, dacomitinib) can be used alone as first line treatment for advanced NSCLCs with mutations in the *EGFR* gene [35]. Drugs that target the abnormal ALK protein include crizotinib, certinib, alectinib, brigatinib, and lorlatinib. Some of these drugs have also shown some efficacy in *ROS1* altered cancers [36]. Other targeted therapies for lung cancer are a BRAF inhibitor (dabrafenib) or a MEK inhibitor (trametinib). They can be used in combination to treat metastatic NSCLC with a *BRAF* mutation ((BRAF^{V600E}) [37]. SCLC has a distinct molecular profile compared to adenocarcinomas. FGFR1 (20%), PK3CA (12%) and PTEN (10%) are the most commonly mutated genes in SCLC. Unlike NSCLC, chemotherapy remains the standard treatment strategy for SCLC.

Recently, a new chapter for lung cancer patients has emerged with the introduction of immunotherapy. Positive clinical trials led to the approval of four immune checkpoint inhibitors for lung cancer patients. Immunotherapy either alone or in combination with conventional treatments significantly improved patient outcomes in the clinic. Atezolizumab, durvalumab, nivoluman and pembrolizumab were approved by the FDA from 2015 to 2017 as checkpoint inhibitors targeting the PD-1/PD-L1 pathway, which is a critical mechanism in promoting self-tolerance and suppressing T cell activities [38, 39]. Among them, atezolizuman and pembrolizumab are now first-line therapy for treating advanced NSCLC patients. However, problems including low response rate, acquired resistance, toxicity, and lack of proper biomarkers for patient selection still limit the

benefits of immunotherapy.

1.3.4 Animal models of lung cancer

Animal models are essential tools to study disease onset, progression and response to treatment. To model lung cancer preclinically, generally three ways can be utilized to initiate the development of lung tumors. The first method is the same as other cancer types. Lung tumor cells can be injected ectopically under the skin. Orthotopic injection into the lung tissue is possible but technically more challenging. Limitations of these xenograft models have been discussed above.

The second strategy is to generate GEMMs, where genetic alterations are expressed in a specific cell type within the lung. Tumor induction can be achieved through Adeno-Cre virus infection, spontaneous recombination events [40], CCSP-rtTA transgene initiation with doxycyclin treatment, *etc* [41]. A number of mutations found in NSCLC have been introduced in mice, such as *Kras, p53, Braf, Egfr, Lkb1, Rac1,* and *NfkappaB*. These different models with various mutations possess shorter or longer latency periods, but all are aggressive with short life spans.

Third, lung cancer can be induced chemically via exposure to carcinogens including cigarette smoke, tar, polycyclic aromatic hydrocarbons, nitrosamines, urethane, vinyl carbamate, etc [42]. The susceptibility to carcinogens varies among different mouse strains. A/J and SWR mice are the most sensitive strains, while O20 and BALB/c have intermediate sensitivity, and C57BL/6 and DBA are almost complete resistant [42]. The relatively long latency in carcinogen-induced mouse models provides a window to intervene in tumor development for studying cancer prevention and treatment.

1.4 Immune system and cancer

1.4.1 Three phases of cancer immunoediting: surveillance, equilibrium, and escape

The first phase is immune surveillance. The immune system is a powerful host defense system against infections and diseases. It recognizes and eliminates “non-self” substances such as bacteria or viruses via a series of immune responses. Additionally, unhealthy cells like cancer are also under the surveillance of the immune system. The immune surveillance of cancer is supported by the finding of tumor-associated antigens in the host and the evidence that tumors can be suppressed by the immune system in tumor transplantation models [43]. Furthermore, immunodeficient mice are more susceptible to developing tumors induced by chemicals than immunocompetent mice [44]. Natural killer (NK) cells, NKT cells, and T cells, and the proteins including interferon-γ (IFN-γ) and perforin all play important roles in cancer immune surveillance [45, 46], which if lost would increase susceptibility to tumor formation.

Unfortunately, not all tumors are immunogenic. The second phase is an equilibrium state between the immune system and tumor cells. Genetically unstable tumor cells continue to evolve and edit the immune system to suppress immune recognition, which is called cancer immunoediting. Moreover, under pressure of immune selection, tumor cells with a non-immunogenic phenotype are more likely to survive. Tumors that went through T-cell mediated selection have better survival in hosts with functional T cells [47]. Continuous elimination of tumor cells and selection of resistant tumors reaches an equilibrium phase, which may last for years.

Eventually, tumor cells are able to escape from immune surveillance and grow into a detectable tumor. Signal transduction of cytotoxic immune cells is thus altered at this

stage. Loss of CD3 or T cell receptor (TCR) chains, apoptosis of T cells, recruitment and activation of immunosuppressive populations, and production of immunosuppressive cytokines are all known mechanisms that tumors use to evade an immune attack [48].

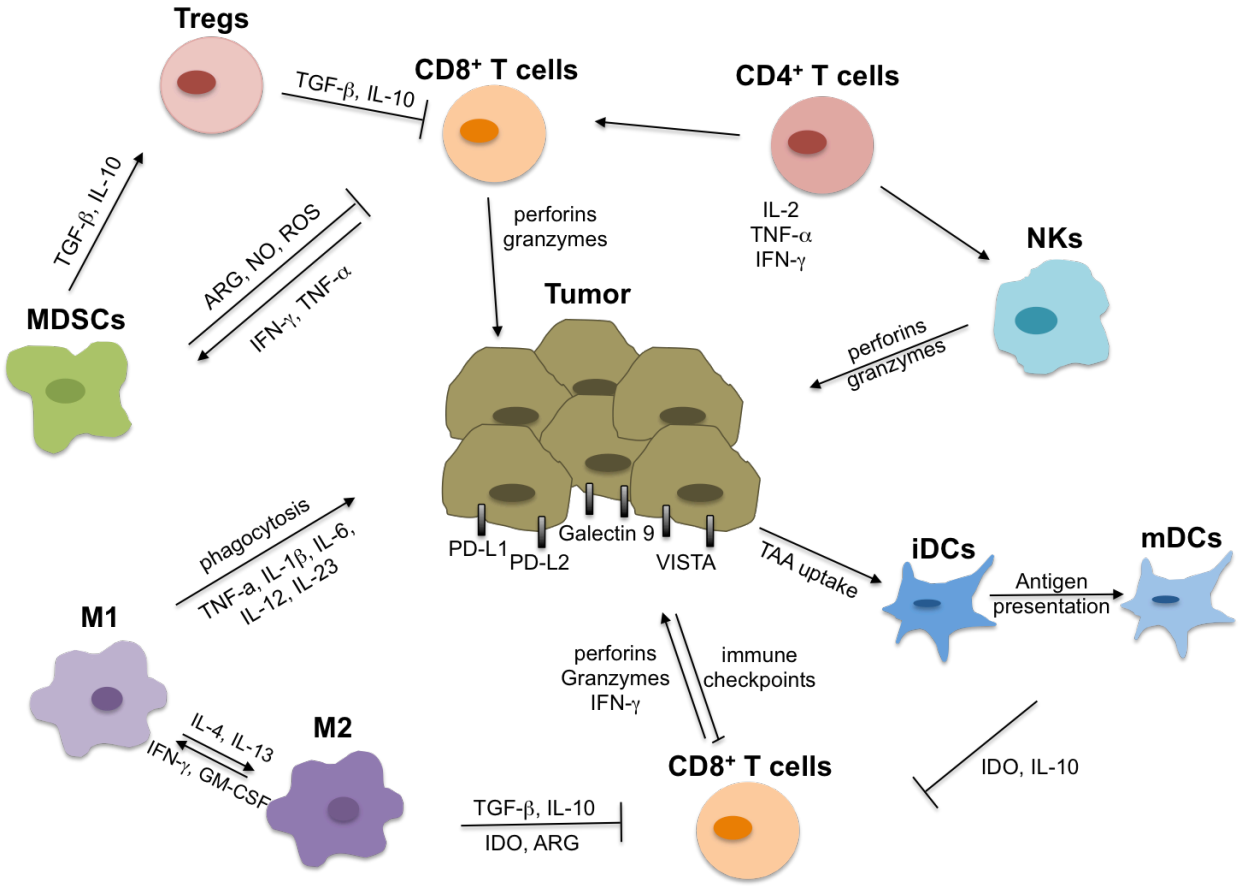

Figure 1.1 Cancer microenvironment. Immune cells actively interact with cancer cells. Different types of immune cells play various roles in promoting or inhibiting tumor development and progression. M, macrophages; iDCs, immature dendritic cells; mDCs, mature dendritic cells; Tregs, regulatory T cells; MDSCs, myeloid-derived suppressor cells; NKs, natural killer cells; TAA, tumor associated antigen; ARG, arginase.

1.4.2 The role of major immune cells in cancer

1.4.2.1 Macrophages

Different immune cells play various roles in cancer immunity from tumor initiation to metastatic progression (Figure 1.1) [49]. Macrophages are innate immune cells that

respond to infections or accumulating damaged cells. Macrophages are plastic cells with heterogeneous phenotypes that are determined by the surrounding microenvironment [50]. They generally present in two subtypes: M1 macrophages (classically activated) and M2 macrophages (alternatively activated). M1 macrophages, polarized by lipopolysaccharide (LPS) and/or Th1 cytokines (e.g. IFN-γ, GM-CSF), produce pro-inflammatory cytokines, such as TNF-α, IL-1β, IL-6, IL-12, and IL-23 [50]. M2 macrophages, polarized by Th2 cytokines (e.g. IL-4 and IL-13), produce anti-inflammatory cytokines, such as TGF-β and IL-10 [50]. Tumor-associated macrophages (TAMs) have been shown to express an M2-like phenotype. During carcinogenesis, M1 macrophages are involved in eliminating immunogenic tumor cells. As tumors progress, macrophages polarize to an M2 phenotype, which promotes tumor progression and resistance to chemotherapies.

As critical drivers of tumor-promoting inflammation, TAMs promote tumor growth, elicit tumor metastasis, and induce immunosuppression on other anti-tumor effector cells. A high infiltration of TAMs is usually correlated with poor prognosis and worse overall survival [51]. TAMs promote tumor progression through immune dependent and independent mechanisms [52, 53]. TAMs directly secrete epidermal growth factor (EGF) to fuel tumor growth [54], secrete proangiogenic factors such as vascular endothelial growth factor (VEGFs) to induce angiogenesis [55], and secrete metalloproteinases (MMPs) to remodel ECM for metastasis [56]. Besides these non-immune effects, TAMs also produce anti-inflammatory cytokines like IL-10 and TGF-β to impair the activity of cytotoxic T cells and maturation of dendritic cells (DC) [57, 58]. TAMs can induce direct suppression on T cell functions via expressing arginase 1 (ARG1) to exhaust L-arginine,

which is needed for the activation of T cells [59]. TAMs can also recruit other immunosuppressive populations such as regulatory T cells (Tregs) to suppress anticancer immune responses.

1.4.2.2 Myeloid-derived suppressor cells

Myeloid-derived suppressor cells (MDSCs) are another major player in immunosuppression within the tumor microenvironment [60]. MDSCs are a heterogeneous population of immune cells from the myeloid lineage. MDSCs are derived from bone marrow hematopoietic precursors and accumulate in pathological conditions such as chronic inflammation and cancer [61].

MDSCs have been well characterized in mice. They express high levels of CD11b, a classical myeloid lineage marker, and Gr1, a granulocytic marker [62]. Based on the expression level of Ly6G and Ly6C, MDSCs can be further divided into two major subtypes: polymorphonuclear MDSC (PMN-MDSC, $Ly6G^{+}/Ly6C^{lo}$) and monocytic MDSC (M-MDSC, $Ly6G^{-}/Ly6C^{hi}$) [62]. Although MDSCs are relatively less characterized in humans, their functions are similar to murine MDSCs. The same two subtypes are characterized as $Lin^{-}HLA\text{-}DR^{-/lo}CD11b^{+}CD14^{-}CD15^{+}CD33^{+}$ for PMN-MDSCs and $Lin^{-}HLA\text{-}DR^{-/lo}CD11b^{+}CD14^{+}CD15^{-}$ for M-MDSCs [63].

MDSCs induce immunosuppression via a wide variety of mechanisms: 1. Producing nitric oxide and reactive oxygen species, which impair antigen recognition via nitration of T cell receptors or induce apoptosis of T cells and NK cells [64]. 2. Depleting L-arginine and cysteine, critical nutrients needed for T cell function, to inhibit T cell proliferation [65]. 3. Secreting immunosuppressive cytokines, including IL-10 and TGF-β [66], or up-regulating the expression of the programmed death-ligand 1 (PD-L1) to suppress

anti-tumor T cell functions or activate other immunosuppressive populations (e.g. Tregs) [67]. 4. Reducing the expression of TCR ζ-chain, which is important in TCR-mediated antigen recognition. Besides suppressing anti-cancer immunity, MDSCs also promote angiogenesis through secretion of angiogenic factors directly [68] and enhance tumor growth by producing growth factors [69], thus greatly contributing to tumor progression.

1.4.2.3 Dendritic cells

Dendritic cells (DCs) are known as antigen-presenting cells. They are present in all tissues within the body, except the brain parenchyma [70]. The main function of DCs is to process and present antigens to T cells. Thus, DCs are critical in the connection between innate and adaptive immune system and priming naïve and memory T cells in anti-tumor immunity.

DCs can be classified into three major subtypes and each is independently regulated by distinct molecular cues. Classical type 1 DCs express CD8a (lymphoid) or CD103 (tissue) and they are BATF3- and IRF8-dependent. $CD11b^+$ and $CD127a^+$ DCs with IRF4-dependence are classical type 2 DCs. Another population of DCs is plasmacytoid DCs, which secrete IFN-α and depend on E2-2 signaling. Type 1 DCs are important to differentiate $CD4^+$ T helper type I and $CD8^+$ cytotoxic T cells from their precursors. DCs lacking $CD8a^+$ impair tumor rejection mediated by $CD4^+$ and $CD8^+$ T cells in a mouse model of fibrosarcoma [71]. $CD103^+$ DCs also play key roles in tumor antigen presentation in a melanoma, cervical and breast cancer mouse models [72, 73].

However, the activity of DCs is greatly hindered in cancer immunity. Chronic inflammation and tumor promoting pathways impair the ability of DCs to prime T cells, promote the exclusion of T cells from the tumor microenvironment or drive the expansion

of Tregs. PGE_2, a small molecule produced during inflammation, acts as a mediator that impairs the anti-tumor ability of myeloid cells. PGE_2 receptor knockout mice have inhibited tumor growth, enhanced DC differentiation and increased accumulation of T cells [74]. Fewer DCs infiltrate into tumors when PGE_2 production is elevated [75]. PGE_2 also activates β-catenin signaling in the TME; β-catenin signaling excludes T cells from the tumor. Forced expression of β-catenin decreased infiltration of $CD103^+$ and $CD8^+$ DCs and T cell priming [76].

1.4.2.4 Natural killer cells

Natural killer cells (NK cells) are the key cytotoxic lymphocytes in the innate immune system. NK cells reside mainly in peripheral blood, bone marrow, lymph nodes, and spleen, but they can also migrate to infection sites. NK cells respond rapidly to infections or tumor formation. Unlike other immune cells, NK cells have the ability to recognize cells in the absence of MHC. This is important in cancer immunity because cells without MHC I markers that cannot be destroyed by T lymphocytes can be detected by NK cells.

As a crucial defender in cancer surveillance, NK cells distinguish malignant cells from healthy ones via activation of the NK receptor NKG2D. NKG2D receptors recognize a wide variety of MHC I molecules on malignant cells. For example, abnormal cell proliferation induces the expression of ligand retinoic acid early transcript 1 (RAE1). Moreover, DNA damage [77] and RAS pathway activation [78] also up-regulate the expression of NKG2D ligands to alert the innate immune system. Besides NKG2D, there are many other receptors expressed on NK cells to activate them upon binding to tumor-derived ligands [79]. NK cells evoke the tumor killing mainly by the release of perforin and granzyme, which trigger apoptotic pathways and eventually eliminate the

tumor.

1.4.2.5 T cells

T cells, as major components of the adaptive immune system, are key players in killing cancer cells. When immunogenic antigens are presented during early tumor initiation, naïve T cells are primed in the draining lymph nodes and then activated and migrate to the tumor microenvironment. High level of T cell infiltration into the tumors is associated with better prognosis in many cancer types, including melanoma [80], lung [81], breast [82], ovarian [83], colorectal [84], prostate [85], gastric [86] and renal [87] cancer.

$CD8^+$ T cells, upon priming and activation, differentiate into cytotoxic T cells and produce perforin or granzymes to eliminate tumor cells. $CD4^+$ T helper 1 cells (Th1) also contribute to the anti-tumor attack by secreting proinflammatory cytokines, including IL-2, TNF-α and IFN-γ. These cytokines promote T cell priming and activation, antigen presentation, and even anti-tumor activity by macrophages and NK cells.

Unfortunately, tumors are good at evading immune recognition. Although most malignant cells express highly immunogenic antigens and get cleared by the immune response at early stages of tumor development, less immunogenic cells are able to escape and survive through the process of immune editing. They hijack the mechanisms of peripheral tolerance to suppress anti-tumor activities, such as upregulating immune checkpoints. CTLA-4 and PD-1 are two major players negatively regulating T cell functions. The engagement of CTLA-4 and PD-L1 has been reported in melanoma, lung, gastric, breast, and colorectal cancers [49]. Meanwhile, cancer cells recruit regulatory $CD4^+$ T cells (Tregs) to further facilitate immune escape. Tregs ($CD4^+CD25^+FOXP3^+$)

are essential for suppressing effector immune cells from priming, activating or killing cancer cells. Tregs can do so via either contact-dependent (expression of surface molecules including PD-L1, LAG-3, CTLA4, PD1 or CD39/73) or contact-independent mechanisms (production of immune-suppressive molecules including IL-2, TGF-β, adenosine, galectin-1 and prostaglandin E2) [88]. Infiltration of Tregs is associated with poor prognosis in breast cancer patients [89].

1.4.2.6 B cells

B cells, mediating humoral immunity, are another type of tumor-infiltrating lymphocyte. Accumulating studies suggest that B cells also play important roles in tumor immunology. However, unlike T cells, B cells remain understudied. The presence of B cells has been reported in melanoma, breast, ovarian and prostate cancer [90-92]. For example, tumor-infiltrating B cells represent up to 40% of tumor-infiltrating lymphocyte and about 25% of tumors in breast cancer [93].

B cells can modulate tumor immunity through three main mechanisms: antigen presentation, cytokine secretion and costimulation signaling. Similar to many other immune populations, B cells also have dual roles in cancer progression depending on the subtypes and can contribute to either pro- or anti-tumor immune responses. Recent evidence supports a tumor-promoting role for B cells as a robust cytotoxic T cell response was observed after B cell depletion vs. the restoration of tumor progression with adoptive transfer of B cells [94]. In addition, B cells produce IL-10 and TGF-β to recruit other immunosuppressive populations or directly repress T cell activation [95, 96]. On the other hand, $CD11c^+$ B cells serve as potent antigen-presenting cells in enhancing T cell activation [97]. Furthermore, infiltration of $CD20^+$ and $CD8^+$ lymphocytes is

associated with better survival in ovarian cancer compared to $CD8^+$ lymphocytes alone [98]. Further classification and study of B cells is required before we can understand their functions in cancer.

1.5 Targeting the immune system for cancer treatment

Rudolf Virchow first described the infiltration of immune cells into tumors in 1863. The first attempt at immunotherapy traces back to 1898: Coley's toxin. With the observations that infections after surgery correlate with tumor regression, William B. Coley began to treat inoperable cancers by injecting bacteria or bacterial products to stimulate the immune system [99]. He successfully treated over 1000 cancer patients. Despite these positive results, many doctors did not believe these results. Eventually, regulatory agencies stopped the toxins from being used. Since then, no further immunotherapies had been approved until a century later (Figure 1.2).

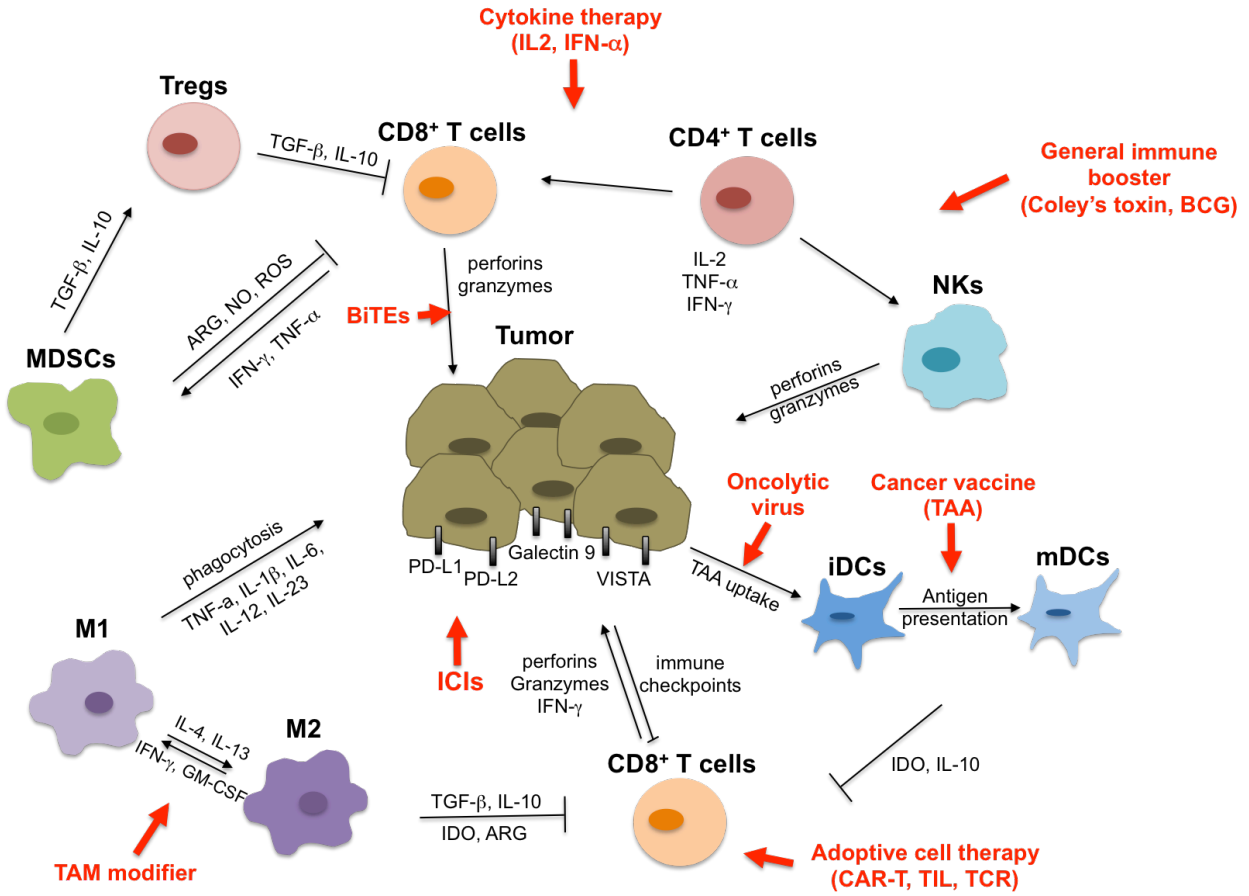

Figure 1.2 Targeting the immune system for cancer treatment. A series of strategies have been developed to target different immune cells to boost immune recognition and response to tumor cells. M, macrophages; iDCs, immature dendritic cells; mDCs, mature dendritic cells; Tregs, regulatory T cells; MDSCs, myeloid-derived suppressor cells; NKs, natural killer cells; TAA, tumor associated antigen; ARG, arginase; BCG, Bacillus Calmette-Guerin; TAM, tumor associated macrophages; ICIs, immune checkpoint inhibitors; BiTEs, bispecific T-cell engagers; CAR-T, chimeric antigen receptor T-cell therapy; TIL, tumor infiltrating lymphocyte; TCR, T cell receptor. Targets are indicated in red.

1.5.1 Current strategies of targeting immune system for cancer treatment

1.5.1.1 General immune boosters

Modern immunotherapy started with relatively non-targeted strategies. The goal was to activate the immune system to destroy cancer cells. Similar to the idea of Coley's toxins, Bacillus Calmette-Guerin (BCG) has been used to treat non-muscular invasive

bladder cancer since 1976. BCG is a bacterium which is similar to the ones responsible for the pathogenesis of tuberculosis. Bladder cancer cells internalize BCG and produce cytokines and chemokines to activate the immune system, including $CD4^+$ and $CD8^+$ T cells, NK cells, macrophages, and dendritic cells. BCG also initiates antigen presentation of cancer cells [100].

1.5.1.2 Cytokine therapies

Interleukin 2 (IL-2) was the first cytokine approved by the FDA for cancer treatment [101]. Recombinant IL-2 is approved to treat metastatic melanoma and advanced kidney cancer. IL-2 functions as a growth factor in the immune system by stimulating the expansion of T cells and NK cells [102]. Side effects of IL-2 include flu-like symptoms, diarrhea, nausea, low blood pressure, *etc*. Other interleukins, such as IL-7, IL-12 and IL-21, are currently under investigation.

Interferons are another class of cytokines that are used for cancer treatment. There are three types of interferons (IFN-α, IFN-β, and IFN-γ) but only IFN-α is being used clinically. IFN-α has been approved for the treatment of hairy cell leukemia, chronic myelogenous leukemia (CML), cutaneous T-cell lymphoma, follicular non-Hodgkin's lymphoma, kidney cancer and melanoma [103]. Side effects of IFN-α include flu-like symptoms, low white blood cell counts, skin rashes and thinning hair. IFN-α elicits anti-tumor activity via multiple mechanisms. It promotes the differentiation and activation of the host immune system, especially T cells and dendritic cells [104]. Although these cytokines are effective as single agents in certain cancers, accumulating studies suggest that combination therapy is needed to achieve a sustained response.

1.5.1.3 Oncolytic viruses

Oncolytic virus therapy is a strategy that uses tumor-targeting viruses to treat cancer. Some viruses can infect and kill tumor cells without harming normal cells. Talimogene laherparepvec (T-VEC), so far, is the only oncolytic virus therapy that has been approved to treat melanoma [105]. Although oncolytic viruses have long been thought to target tumor cells directly, we now know they also trigger an immune response against the cancer. When numerous copies of the virus bursts cancer cells, cellular materials, such as tumor antigens, are released and processed to allow the immune system to recognize tumors. This is an essential step to enhance the immune response and provides the rationale to include oncolytic viruses into the picture of immunotherapy. The combination of oncolytic virus therapy and immunotherapy has shown promising results in early-phase clinical trials [106].

1.5.1.4 Antibodies

Antibodies provide a more targeted approach for cancer treatment. They can bind to tumor antigens specifically and initiate an immune response against the target cancer cells. The simplest design is a so called “naked” monoclonal antibody. These antibodies bind to specific surface proteins expressed on tumor cells to directly disrupt tumor growth. At the same time, the back end of these antibodies also recruits immune cells to eliminate cancer cells via immune-mediated killing. Rituximab (anti-CD20 antibody) was the first FDA approved monoclonal antibody for cancer treatment (lymphoma) [107]. Since then, numerous monoclonal antibodies have received FDA approval, including trastuzumab (anti-HER2), cetuximab (anti-EGFR), dinutuximab (anti-GD2), and bevacizumab (anti-VEGF-α) [108]. These monoclonal antibodies are considered passive

immunotherapy because they target tumor cells directly rather than targeting the immune cells.

Bispecific antibodies are more active at stimulating an immune response by engaging the binding of tumor cells to immune cells. Bispecific T cell engagers (BiTEs) are effective in the clinic. Blinatumomab, a CD3/CD19 bispecific antibody, was approved for the treatment of acute lymphoblastic leukemia in 2014 [109]. Anti-CD20/CD3 bispecific antibodies have also been developed to treat B cell lymphoma [110]. Other bispecific antibodies are under investigation to target different tumor antigens. Notably, many tumor antigens are also expressed on normal cells. Avoiding the side effects brought on by on-target off-tumor activation is an important area of investigation.

1.5.1.5 Immune checkpoint inhibitors

The development of immune checkpoint inhibitors (ICIs) has been a major breakthrough for immunotherapy. Tumor cells can evade immunosurveillance through various mechanisms, one of which is to activate immune checkpoint pathways to suppress anti-tumor immunity. ICIs are designed to block these co-inhibitory signaling pathways to unleash the power of immune-mediated killing of cancer cells. Cytotoxic T lymphocyte-associated antigen 4 (CTLA4) was first discovered as a negative regulator of T cell activation in 1995 [111]. CTLA-4 is expressed on activated T cells and Tregs. CTLA-4 is homologous to CD28, the T cell co-stimulatory protein. In contrast to CD28, CTLA-4 transmits an inhibitory signal to T cells with a greater binding affinity to CD80/CD86 expressed on antigen-presenting cells. The anti-CTLA-4 antibody ipilimumab was the first immune checkpoint inhibitor approved for cancer treatment. Ipilimumab was initially approved for unresectable or metastatic melanoma in 2011, and

approval was then expanded to adjuvant therapy of stage 3 melanoma [112]. Because the inhibitory mechanism regulating immune system activation is blocked, the use of immune checkpoint inhibitors is often associated with autoimmune-like toxicities. Skin rash, colitis, hepatitis, and hypophysitis are common adverse events with anti-CTLA-4 therapy [113].

Programmed death-1 (PD-1) is another key player within the immune checkpoint pathways. PD-1 is expressed not only on activated T cells, but also on B cells and NK cells. PD-1 is phosphorylated upon binding with its ligands PD-L1 and PD-L2, which are mainly expressed on tumor cells. Binding leads to the recruitment of a SH2 domain containing a tyrosine phosphatase. Thus, activation and proliferation mediators, such as PI3K, are dephosphorylated, resulting in a suppression of T cell responses [114]. Tumor cells evade immune elimination by expressing PD-L1 on the surface. Over the past five years, anti-PD-1 or anti-PD-L1 antibodies have been approved for the treatment of over ten cancer types, including melanoma, NSCLC, renal cell carcinoma, urothelial bladder cancer, colorectal cancer, *etc.* Numerous clinical trials are still ongoing to extend the application of immune checkpoint inhibitors to more cancer types. Similar to anti-CTLA-4 treatment, immune-related adverse events also present with anti-PD1/PD-L1 therapy. However, the toxicity profile of anti-PD1/PD-L1 agents is slightly different than anti-CTLA-4 treatment. Hypothyroidism and pneumonitis are more commonly seen with anti-PD-1 therapy [113].

Additional immune checkpoints have been reported beyond CTLA-4 and PD-1. Lymphocyte-activation protein 3 (LAG-3) is expressed on activated T cells, NK cells, B cells and dendritic cells. LAG-3 outcompetes the binding of CD4 to major

histocompatibility complex-II (MHC-II) on APCs to directly disrupt TCR signaling [115]. T cell exhaustion in the tumor microenvironment is associated with upregulation of LAG-3 and PD-1/PD-L1. Ongoing clinical trials have shown promising survival benefits and durable response rates when combining the blockade of LAG-3 and PD-1 [116].

T cell immunoglobulin and mucin domain-3 (TIM3) is a type-I transmembrane glycoprotein. TIM3 is expressed on both tumor and immune cells, including type 1 T helper cells, CD8+ T cells, Tregs, *etc*. TIM3 is involved in immune tolerance and T cell exhaustion. Upon binding to its ligands, TIM3 triggers cell death and inhibits the immune response. TIM3 blockade enhances tumor antigen-specific T cell proliferation and the production of pro-inflammatory cytokines (e.g. TNF, IFN-γ) [117]. The B- and T-lymphocyte attenuator (BTLA), T-cell receptor with immunoglobulin and ITIM domain (TIGIT), V-domain Ig suppressor of T cell activation (VISTA), and Siglec-15 are other immune checkpoint inhibitory targets under investigation [118, 119].

Instead of blocking inhibitory signaling, activating stimulatory checkpoint pathways is another promising immunotherapy strategy. Agonists of stimulatory pathways (e.g. OX40, GITR, ICOS, 4-1BB, CD40) and molecules that target TME components (e.g. indoleamine 2,3-dioxygenase 1, Toll-like receptor) are under different stages of preclinical and clinical development [119].

1.5.1.6 Adoptive cell therapy

Adoptive cell therapy is a more active treatment approach that directly isolates immune cells from patients and then re-infuses cells after expansion and activation. This approach could potentially overcome the resistance of other immunotherapies due to the lack of functional immune killer cells. There are three forms of T-cell based adoptive cell

therapies: 1. Tumor-infiltrating lymphocyte (TIL) therapy; 2. Engineered T cell receptor (TCR) therapy; 3. Chimeric antigen receptor (CAR) T cell therapy. In contrast to the other two strategies, TIL utilizes existing T cells that are already capable of recognizing and eliminating cancer cells. TILs are isolated from tumor biopsy samples followed by a large-scale expansion *in vitro*. Expanded cells will then be infused back into the patient along with IL-2 as a growth factor. The first proof-of-principle study of TIL in treating preclinical tumors was performed by the Rosenberg group [120]. Later clinical trials exhibited a consistent objective response rate between 40-70% [121]. However, producing useable TIL products that pass the product-release criteria remains a challenge, and only 27%- 40% of patients who underwent tumor resection successfully received TIL therapy [122]. A TIL protocol developed by the Tran group significantly shortens the expansion phase and allows the production of TIL product within 4 weeks [122]. Further studies are still needed to optimize the protocol, improve the successful delivery rate, identify predictive markers for response, and select proper patients.

In contrast to TIL, TCR and CAR-T therapies take peripheral blood from patients to isolate T cells, and then engineer the T cells *in vitro* to enable them to recognize specific tumor antigens. TCR allows the recognition of antigens inside of tumor cells, but they have to be presented via MHC receptors. TCR therapies have been tested in certain types of synovial sarcoma and metastatic melanoma, but none have been approved by the FDA.

CAR-T cell therapy is so far the only approved cellular immunotherapy for cancer treatment. CAR-T cell therapy equips the patient's T cells with synthetic receptors that can bind to cancer cells independent of MHC presentation. CAR-T cells have evolved

through several generations [123]. The first generation of CAR-T contained an antibody-based recognition domain fused to a CD3zeta signaling domain. One (e.g. CD28 or 4-1BB) or two (e.g. CD28 and 4-1BB) co-stimulatory domains were then included to develop the second and third generation of CAR-T cells. Axicabtagene, ciloleucel and tisagenlecleucel are two FDA approved CD19-targeting CAR T cell immunotherapies for subsets of lymphoma or leukemia.

Despite success in blood cancers, CAR-T cell therapy in solid tumors is still facing major challenges [124]. Solid tumors present more complex and diverse surface proteins, making it difficult to find a common target for CARs. In addition, many targets are also expressed on normal tissues, causing severe toxicities due to on-target off-tumor effects [125]. Tumor-mediated immunosuppression is another hurdle limiting the efficacy of CAR-T cells to treat solid tumors. Attempts have been made to address each challenge, such as logic-gated tumor antigen recognition, safety switch, or immunostimulatory payload secreting CAR-T cells [126]. Further studies need to integrate these separate systems into a whole package to unleash the power of CAR-T cells in solid tumors.

1.5.1.7 Vaccines

Developing vaccines for cancer treatment has been challenging because of the lack of ideal common tumor antigens. The immunosuppressive tumor microenvironment further limits the efficacy of cancer vaccines. BCG treatment, as introduced earlier, is considered the first approved vaccine for cancer treatment. The other successful example is Sipuleucel-T (Provenge) [127]. It was approved in 2010 for treatment of men with metastatic prostate cancer. Provenge is an autologous cellular therapy based cancer vaccine. Autologous peripheral blood is obtained from each patient, and antigen

presenting cells (APCs) are isolated and cultured with a recombinant human protein (PAP-GM-CSF). PAP-GM-CSF is composed of an antigen expressed in prostate cancer tissue (prostatic acid phosphatase, PAP) and an immune cell activator (granulocyte-macrophage colony stimulating factor, GM-CSF). Activated APCs are infused back into the patient to facilitate the recognition and clearance of PAP^+ prostate cancer cells.

There are several other cancer vaccines being tested in clinical trials targeting a wide variety of cancers, including leukemia, myeloma, melanoma, bladder, breast, cervical, colorectal, kidney, lung, and pancreatic cancers. MAGE-3, for example, is a tumor antigen that is widely expressed on melanoma, non-small cell lung cancer and hematologic malignancies. High levels of MAGE-3 in lung adenocarcinoma are associated with poor survival [128]. However, anti-MAGE-3 vaccines have not provided clinical benefits.

1.5.2 Challenges and opportunities

Despite all of these breakthroughs, multiple challenges remain for cancer immunotherapy. Only a small portion of patients responds to immunotherapy. Tumors become resistant after treatment. Severe toxicities have been reported and are sometimes fatal. Predictive biomarkers are still needed to determine who should receive which treatment.

Combination therapy is an effective approach to address these challenges. It requires an orchestration among different cell types and signaling pathways to activate anti-tumor immunity successfully. Thus, a single agent targeting one step along the process often has limited effects. Anti-CTLA-4 antibodies act primarily in the priming phase, while

anti-PD-1/PD-L1 antibodies target the effector phase. Nivolumab (anti-PD-1) plus ipilimumab (anti-CTLA4) was the first combination immunotherapy approved in the U.S. for the treatment of advanced melanoma, advanced renal cell carcinoma and metastatic colon cancer. This combination therapy increased the response rate and prolonged survival better than each single agent.

In addition to the combination of immunotherapy agents, accumulating data have suggested better efficacy if immunotherapy is combined with chemotherapy, radiotherapy, or other targeted drugs. Pembrolizumab combined with a standard chemotherapy has been approved as the first line treatment for patients with metastatic non-squamous NSCLC. Radiation helps with releasing tumor antigens, upregulating chemokines and promoting T cell recruitment. The combination of radiotherapy and immunotherapy has shown promising results in both preclinical and clinical studies [129]. Many ongoing clinical trials are testing the combination of immune checkpoint inhibitors with targeted therapies, such as a BRAF inhibitor, EGFR inhibitor, ALK inhibitor, HER2 inhibitor, *etc.* Without doubt, immunotherapy is changing the landscape of cancer therapy. It is important to better understand the immunomodulation of existing therapeutic agents, so that we can combine therapies in rational way to deliver superior care to cancer patients.

1.6 Targeting the immune system for cancer prevention

1.6.1 Overview of cancer prevention

Cancer prevention aims to lower the risk of developing cancer. Considering millions of people are diagnosed with cancer every year, effective cancer prevention strategies are desperately needed to not only alleviate the physical problems and

emotional distress caused by cancer but also reduce the financial burden of treating cancer.

There are three levels of disease prevention: 1. Primary prevention aims to prevent the onset of the disease; 2. Secondary prevention includes early diagnosis and prompt treatment to prevent disease from progressing to a more severe stage; 3. Tertiary prevention aims to improve the treatment and recovery, so that it can limit the lasting effects of an ongoing disease.

Lifestyle modifications are important primary prevention strategies for cancer. Accumulating evidence has suggested that better dietary choices [130], eliminating tobacco and alcohol use [131], maintaining an active lifestyle and proper body weight [132] can reduce cancer risk.

Besides lifestyle changes, there are also drug interventions for cancer prevention. The most well-known example is selective estrogen receptor modulators (SERMs) for preventing breast cancer. Tamoxifen and raloxifene have been approved by the FDA to prevent breast cancer in high-risk women [133]. Many other chemopreventive agents have been tested in either preclinical animal models or clinical trials, such as 5-α-reductase inhibitors for prostate cancer, metformin for pancreatic and lung cancer, and curcumin for colorectal cancer [134].

Recruiting endogenous immune responses is another prominent strategy to prevent cancer (Figure 1.2). Effectively targeting the immune system is of great potential for cancer prevention [134].

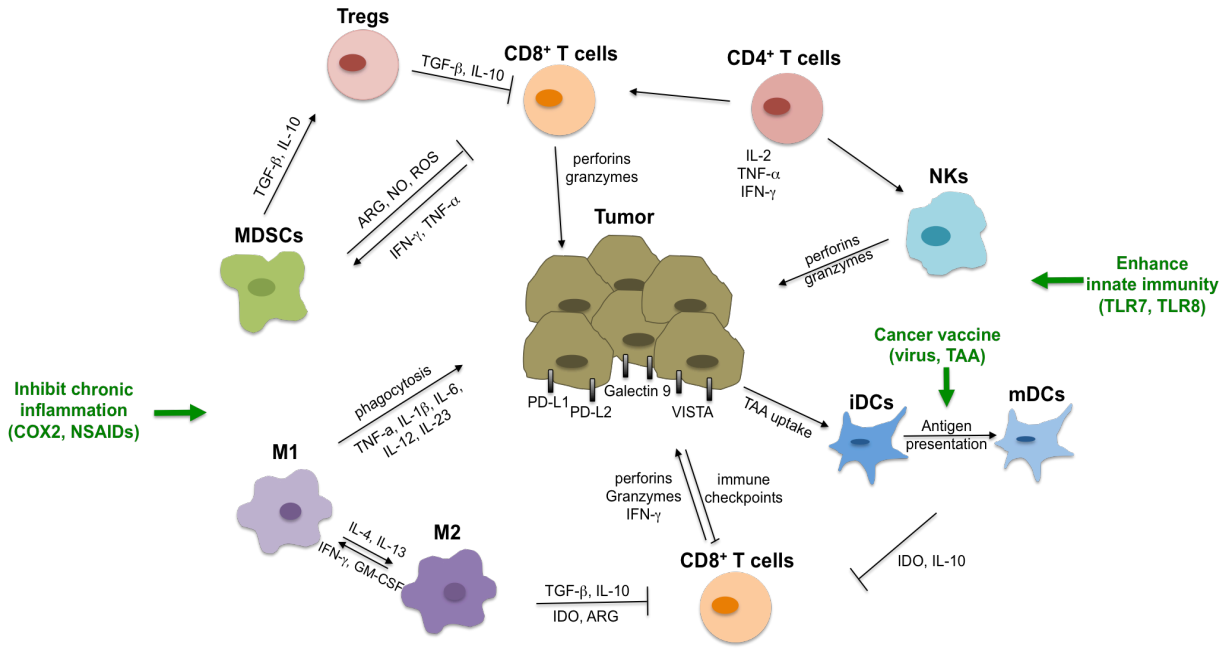

Figure 1.3 Targeting the immune system for cancer prevention. Chronic inflammation and infection from tumor-associated viruses are known risk factors for cancer development. Anti-inflammatory agents and cancer vaccines have been developed for cancer prevention. Targeting tumor-associated antigens or enhancing the innate immune response in general are other possibilities to prevent cancer development. M, macrophages; iDCs, immature dendritic cells; mDCs, mature dendritic cells; Tregs, regulatory T cells; MDSCs, myeloid-derived suppressor cells; NKs, natural killer cells; TAA, tumor associated antigen; ARG, arginase. Targets are indicated in green.

1.6.2 Current strategies of targeting immune system for cancer treatment

1.6.2.1 Anti-inflammatory agents

As championed by Harold F. Dvorak, “Cancer is a wound that does not heal” [135]. Inflammation is a critical component of wound healing and tumor development and progression. Chronic inflammation enhances the risk of developing many types of cancers. Up to 20% of human cancers are associated with chronic inflammation induced by infections or autoimmunity [136]. Inflammation induces the expression of proinflammatory transcription factors (e.g STAT3, NF-κB), which further stimulate the production of key cytokines, chemokines and inflammatory enzymes (e.g. COX-2).

These cytokines and chemokines recruit the infiltration of various immune cells, and in turn produce more inflammatory factors.

Anti-inflammatory agents have shown promising effects in both preclinical models and clinical trials for preventing cancer. Cyclooxygenase (COX)-2 enzymes drive tumorigenesis through the production of prostaglandins. Prostaglandins not only facilitate cancer cells to inhibit apoptosis and enhance cell migration but also act on stromal cells to promote angiogenesis. Nonsteroidal anti-inflammatory drugs (NSAIDs) are a family of compounds that inhibit the activity of COX enzymes and thus decrease the production of prostaglandins. The rationale for using NSAIDs in cancer prevention was based on observations that the use of NSAIDs induced regression of rectal polyp formation in patients with Gardener syndrome [137]. Since then, accumulating epidemiological data suggest a favorable effect of NSAIDs in cancer prevention. A large pooled analysis of observational and randomized trials was conducted to explore the effects of daily aspirin use on cancer development and dissemination in 2012 [138]. This analysis strongly supported the beneficial effects of aspirin in preventing the development of cancer. There are also multiple clinical trials that have tested the cancer-preventive effects of aspirin [139, 140]. These trials used colorectal adenomas as a surrogate primary end point for cancer. Post-hoc analyses and meta-analyses from multiple randomized clinical trials have also been done using non-cancer end points [141, 142]. All these studies suggested promising chemopreventive effects of aspirin in gastrointestinal cancers (esophageal and colorectal adenocarcinomas). In addition to aspirin, other NSAIDs have shown efficacy in cancer prevention trials, including Celecoxib (a selective inhibitor of COX2) [143] and

sulindac [144]. Unfortunately, the cardiovascular toxicities of COX2 inhibitors limited their widespread application in cancer prevention [145].

1.6.2.2 Vaccines

Vaccines are another approach that has been explored for decades in cancer prevention and treatment [146]. Because vaccines aims to activate the immune system to recognize and attack cancer cells, they have been more successful in cancer prevention than treatment. This success is likely attributed to a competent immune system that is still capable of producing robust anti-tumor immune responses before tumors have developed.

One strategy for developing cancer vaccines is to prevent the onset of infectious factors that are known to initiate tumorigenesis. Hepatitis B virus (HBV) is a major cause of hepatocellular carcinoma (HCC). The HBV vaccine reduced the incidence of HBV-specific HCC by an estimated 69% worldwide [147]. The Hepatitis C virus (HCV) also increases the risk of HCC, but HCV vaccines are still under development. Vaccines against human papillomavirus (HPV) have been developed in recent years. HPV infection is associated with increased risk of multiple cancers in both females and males, including cancers of the cervix, vulva, vagina, penis, anus, and oropharynx. Gardisil (targets HPV-6, 11, 16, 18) and Cervarix (targets HPV-16, 18) were approved by the FDA in 2006 and 2009, respectively for females between 9-26 years of age [134]. Additional efforts are ongoing to target other oncogenic strains of HPV. Besides HBV and HPV, several other viruses have been associated with cancer development. These include the Epstein-Barr virus (EBV, Burkitt's lymphoma, Hodgekin's lymphoma and NPC), human T-lymphotropic virus (HTLV, adult T cell leukemia or lymphoma), Kaposi

sarcoma herpes virus (KSHV, Kaposi's sarcoma), and merkel cell polyomavirus (Merkel cell skin cancer) [134]. Vaccines against these cancer-associated viruses are under various stages of development.

Another strategy for developing vaccines is to target tumor antigens directly. Tumor-specific antigens refer to those proteins that are only expressed in tumor cells and germ cells. Tumor-associated antigens (TAAs), in contrast, refer to those antigens that are also expressed in normal somatic cells but aberrantly expressed in tumor cells. Although the mechanisms of how aberrant proteins become immunogenic have not been fully understood, there are at least three possible ways: 1. Form stable mutations; 2. Overexpress TAAs; 3. Post-translational modifications of normal self-antigens. Vaccines targeting tumor antigens have mainly been tested in preclinical models. One exciting preclinical study is the vaccination against MUC1, which is expressed in both inflammatory bowel disease (IBD) and colon cancers. Anti-MUC1 vaccine not only delayed IBD, but also prevented the progression to colitis-associate colorectal cancer (CACC) in a mouse model [148]. Extensive preclinical studies have been focused on targeting ERBB2 for preventing breast cancer. Although complete protection has been achieved in mouse models, there were only limited responses in clinical setting [149, 150]. Other tumor antigens that have been explored are the carcinoembryonic antigen (CEA) [151], melanoma-associated protein 3 (MAGE3) [152], insulin-like growth factor binding protein 2 (IGFBP2) [153], cancer antigen 125 (CA125) [154], BCR-ABL [155], *etc.*

1.6.2.3 Nonspecific immune response enhancers

Besides targeting specific antigens, interventions that induce nonspecific

immunological responses have had several successes. Imiquimod and the related compound resiquimod, which activate toll-like receptors TLR7 and TLR8 in the innate immune system, have shown promising anti-tumor activities especially when combined with vaccines [156]. Carrageenans bind to TLR4, thus activating the innate immune system. They can also activate macrophages and stimulate the production of proinflammatory cytokines through the NF-κB and interleukin-8 pathway [157]. A clinical trial in high-risk and sexually active women showed that carraguard could effectively reduce HPV infection [158].

Moreover, increasing numbers of studies indicate that chemopreventive agents often elicit immunomodulatory effects and restore immunosurveillance. Curcumin, for example, inhibits immune suppressors like TGF-β and indoleamin-2,3-dioxygenase (IDO), decreases MDSCs, repolarizes macrophages to an M1 phenotype, and activates NK cells and T cells [159]. As more information regarding the efficacy and toxicity profiles of immune checkpoint inhibitors (anti-PD-1/PD-L1, anti-CTLA4) emerges from clinical trials, these agents will likely be further explored in prevention studies. The upregulation of PD-1 and CTLA4 in MSI CRCs provides a rationale for using immune checkpoint inhibitors in these high-risk patients [160]. In the future, it is critical to identify effective combinations of chemopreventive and immunopreventive agents with better efficacy and minimal toxicity to improve cancer prevention.

1.7 Scope of this project

In this project, I focused on four molecular targets and explored their roles in regulating the immune system in cancer prevention or treatment. These four targets are the epigenetic regulator bromodomain, nuclear receptor RXR (retinoid X receptor),

transcription factor Nrf2, and DNA repair enzyme PARP (Poly (ADP-ribose) polymerase). Small molecules targeting these pathways have either been FDA approved or are being tested in preclinical or clinical studies. Besides of their effects on tumor cells, it is important to understand how these molecules regulate the immune system. It will not only expand our knowledge on the role of these signaling pathways in immune cells, but also allow us better combine these compounds with immunotherapy drugs as immunotherapy is becoming the first line treatment in many cancers.

1.7.1 Bromodomain inhibitor

In addition to genetic mutations, epigenetic alterations also greatly contribute to the initiation and progression of cancer [161]. A number of epigenetic drugs have been developed for cancer treatment. Besides chromatin “writers” (e.g., histone acetyltransferases and histone methyltransferases) or “erasers” (e.g., HDACs and lysine demethylases), chromatin "readers" have emerged as promising epigenetic targets.

Bromodomains, containing a conserved binding motif, are the primary readers of acetylated lysine residues. Small molecules specifically targeting to the BET (bromodomain and extraterminal domain) family (BRD-2, 3, 4, T) of bromodomain proteins have been developed [162, 163]. The BET inhibitors have shown promising efficacy in various preclinical models and are being tested in clinical trials [162, 164]. However, very little is known regarding their chemopreventive potential in cancer. BET inhibitors are well known for their antiproliferative effects in cancer cells and for downregulating the key onco-protein c-Myc. Our lab has previously reported that I-BET 762 can inhibit cytokine secretion and decrease the number of tumor-associated macrophages and myeloid-derived suppressor cells in a preclinical model of pancreatic

cancer [165]. Because of these anti-inflammatory and immunomodulatory effects of the bromodomain inhibitors, we hypothesized that I-BET 762 regulates both epithelial cells and immune cells, and is efficacious for cancer prevention. In chapter 2, I-BET 762 was tested in clinically relevant mouse models of breast and lung cancer. The effects on both cancer and immune cells were investigated.

1.7.2 Retinoid X receptor agonist

Retinoid X receptors (RXR) belong to the nuclear receptor superfamily and regulate the expression of numerous genes through either heterodimerizing with other nuclear receptors or forming homodimers. Rexinoids are selective ligands for RXR and play important roles in regulating proliferation, differentiation, and apoptosis, which are highly relevant to cancer [166]. The rexinoid bexarotene has been approved by the FDA for the treatment of cutaneous T-cell lymphoma. However, existing rexinoids have not been widely used in the clinic mainly because of limited efficacy and undesired toxicities [167].

Our lab is dedicated to developing the next generation of rexinoids with better efficacy and limited toxicity to unleash the great potential of this class of drugs. To better identify new lead compounds, we need to further understand the mechanisms of action and develop *in vitro* assays that can predict *in vivo* efficacy or toxicities. Interestingly, the most potent rexinoid identified to date, LG100268, has very little activity for inhibiting cancer cell proliferation *in vitro* but has profound effects *in vivo* for both prevention and treatment of cancer [168]. In addition, rexinoids are known to regulate cytokine expression in myeloid cells [169]. These data led us to hypothesize that rexinoids play important roles in modulating the immune system in cancer prevention and treatment. In chapter 3, we for the first time investigated the effects of rexinoids on immune cells

during lung carcinogenesis and established a new screening paradigm to predict the efficacy and toxicities of novel rexinoids.

1.7.3 Nrf2-Keap1-ARE pathway

The Nrf2-Keap1-ARE pathway is a master defense mechanism protecting cells against oxidative and electrophilic stress. It regulates a number of cellular processes as diverse as metabolism, detoxification, redox-balancing, and proliferation [170]. The Nrf2 pathway possesses a dual role in cancer. In normal cells, transient activation of Nrf2 is chemopreventive. Nrf2 activators prevent carcinogenesis in various preclinical models [171-175]. However, in tumor cells, the constitutive activation of Nrf2 due to genetic alterations is cancer-promoting [170]. Nrf2 inhibitors, therefore, are desired as candidates for cancer treatment. This dual role of the Nrf2 pathway focuses on the opposite effects on normal epithelial cells vs. tumor cells. However, the effects of Nrf2 on immune cells within the tumor microenvironment have not been fully investigated. In chapter 4, I characterized the immune signature in Nrf2 WT vs. KO mice during carcinogenesis to explore the effects of Nrf2 in immune cells.

1.7.4 PARP inhibitor

The PARP inhibitors olaparib and talazoparib have recently been approved for treatment of *BRCA*-deficient breast cancer via the mechanism of inducing synthetic lethality [176, 177]. These drugs were the first targeted therapy for patients with *BRCA* mutations. Currently, PARP inhibitors are administered orally in the clinic. However, the limited bioavailability of talazoparib requires a higher dose to be administered to achieve the desired effect. Talazoparib is the most potent PARP inhibitor, but this potency also increases side effects. In chapter 5, I worked with collaborators to develop a novel

nanoparticle delivery system for talazoparib to overcome current limitations including poor bioavailability and subsequent toxicity. Nano-Talazoparib (NanoTLZ) was tested in a clinically relevant *BRCA*-deficient mouse model and compared directly with free Talazoparib (FreeTLZ) at the same dose. In addition, PARP inhibitors have recently been reported to upregulate PD-L1 expression [178], suggesting an immunomodulatory role in cancer treatment. Hence, we also evaluated the effects of NanoTLZ and FreeTLZ on immune populations within the tumor microenvironment in this BRCA-deficient mouse model.

REFERENCES

REFERENCES

1. Bray F, Ferlay J, Soerjomataram I, Siegel RL, Torre LA, Jemal A. Global cancer statistics 2018: GLOBOCAN estimates of incidence and mortality worldwide for 36 cancers in 185 countries. CA Cancer J Clin. 2018; 68: 394-424.

2. Siegel RL, Miller KD, Jemal A. Cancer statistics, 2019. CA Cancer J Clin. 2019; 69: 7-34.

3. Mariotto AB, Yabroff KR, Shao Y, Feuer EJ, Brown ML. Projections of the cost of cancer care in the United States: 2010-2020. J Natl Cancer Inst. 2011; 103: 117-28.

4. Hanahan D, Weinberg RA. The hallmarks of cancer. Cell. 2000; 100: 57-70.

5. Hanahan D, Weinberg RA. Hallmarks of cancer: the next generation. Cell. 2011; 144: 646-74.

6. Aaronson SA. Growth factors and cancer. Science. 1991; 254: 1146-53.

7. Fynan TM, Reiss M. Resistance to inhibition of cell growth by transforming growth factor-beta and its role in oncogenesis. Crit Rev Oncog. 1993; 4: 493-540.

8. Harris CC. p53 tumor suppressor gene: from the basic research laboratory to the clinic--an abridged historical perspective. Carcinogenesis. 1996; 17: 1187-98.

9. Hanahan D, Folkman J. Patterns and emerging mechanisms of the angiogenic switch during tumorigenesis. Cell. 1996; 86: 353-64.

10. Sporn MB. The war on cancer. Lancet. 1996; 347: 1377-81.

11. Wilson KJW, Ross JS. Ross and Wilson anatomy and physiology in health and illness. 6th ed. Edinburgh ; New York: Churchill Livingstone; 1987.

12. Weinberg RA. The biology of cancer. Second edition. ed. New York: Garland Science, Taylor & Francis Group; 2014.

13. Samet JM. Tobacco smoking: the leading cause of preventable disease worldwide. Thorac Surg Clin. 2013; 23: 103-12.

14. Wolf DC, Cohen SM, Boobis AR, Dellarco VL, Fenner-Crisp PA, Moretto A, et al. Chemical carcinogenicity revisited 1: A unified theory of carcinogenicity based on contemporary knowledge. Regul Toxicol Pharmacol. 2019; 103: 86-92.

15. Iglesias ML, Schmidt A, Ghuzlan AA, Lacroix L, Vathaire F, Chevillard S, et al.

Radiation exposure and thyroid cancer: a review. Arch Endocrinol Metab. 2017; 61: 180-7.

16. Xie Y. Hepatitis B Virus-Associated Hepatocellular Carcinoma. Adv Exp Med Biol. 2017; 1018: 11-21.

17. Rousset-Jablonski C, Gompel A. Screening for familial cancer risk: Focus on breast cancer. Maturitas. 2017; 105: 69-77.

18. Vanbrabant T, Fassnacht M, Assie G, Dekkers OM. Influence of hormonal functional status on survival in adrenocortical carcinoma: systematic review and meta-analysis. Eur J Endocrinol. 2018; 179: 429-36.

19. Felicetti F, Catalano MG, Fortunati N. Thyroid Autoimmunity and Cancer. Front Horm Res. 2017; 48: 97-109.

20. Wang LH, Wu CF, Rajasekaran N, Shin YK. Loss of Tumor Suppressor Gene Function in Human Cancer: An Overview. Cell Physiol Biochem. 2018; 51: 2647-93.

21. Tomasetti C, Li L, Vogelstein B. Stem cell divisions, somatic mutations, cancer etiology, and cancer prevention. Science. 2017; 355: 1330-4.

22. Chabner BA, Roberts TG, Jr. Timeline: Chemotherapy and the war on cancer. Nat Rev Cancer. 2005; 5: 65-72.

23. Padma VV. An overview of targeted cancer therapy. Biomedicine (Taipei). 2015; 5: 19.

24. Peron J, Lambert A, Munier S, Ozenne B, Giai J, Roy P, et al. Assessing Long-Term Survival Benefits of Immune Checkpoint Inhibitors Using the Net Survival Benefit. J Natl Cancer Inst. 2019; 111: 1186-91.

25. Nixon NA, Blais N, Ernst S, Kollmannsberger C, Bebb G, Butler M, et al. Current landscape of immunotherapy in the treatment of solid tumours, with future opportunities and challenges. Curr Oncol. 2018; 25: e373-e84.

26. DeSantis CE, Ma J, Gaudet MM, Newman LA, Miller KD, Goding Sauer A, et al. Breast cancer statistics, 2019. CA Cancer J Clin. 2019; 69: 438-51.

27. Ahmad A. Breast Cancer Statistics: Recent Trends. Adv Exp Med Biol. 2019; 1152: 1-7.

28. Provenzano E, Ulaner GA, Chin SF. Molecular Classification of Breast Cancer. PET Clin. 2018; 13: 325-38.

29. Maximiano S, Magalhaes P, Guerreiro MP, Morgado M. Trastuzumab in the Treatment of Breast Cancer. BioDrugs. 2016; 30: 75-86.

30. Holen I, Speirs V, Morrissey B, Blyth K. In vivo models in breast cancer research: progress, challenges and future directions. Dis Model Mech. 2017; 10: 359-71.

31. Sakamoto K, Schmidt JW, Wagner KU. Mouse models of breast cancer. Methods Mol Biol. 2015; 1267: 47-71.

32. Malhotra J, Malvezzi M, Negri E, La Vecchia C, Boffetta P. Risk factors for lung cancer worldwide. Eur Respir J. 2016; 48: 889-902.

33. Rivera GA, Wakelee H. Lung Cancer in Never Smokers. Adv Exp Med Biol. 2016; 893: 43-57.

34. Hirsch FR, Scagliotti GV, Mulshine JL, Kwon R, Curran WJ, Jr., Wu YL, et al. Lung cancer: current therapies and new targeted treatments. Lancet. 2017; 389: 299-311.

35. Singh M, Jadhav HR. Targeting non-small cell lung cancer with small-molecule EGFR tyrosine kinase inhibitors. Drug Discov Today. 2018; 23: 745-53.

36. Sgambato A, Casaluce F, Maione P, Gridelli C. Targeted therapies in non-small cell lung cancer: a focus on ALK/ROS1 tyrosine kinase inhibitors. Expert Rev Anticancer Ther. 2018; 18: 71-80.

37. Kelly RJ. Dabrafenib and trametinib for the treatment of non-small cell lung cancer. Expert Rev Anticancer Ther. 2018; 18: 1063-8.

38. Jain P, Jain C, Velcheti V. Role of immune-checkpoint inhibitors in lung cancer. Ther Adv Respir Dis. 2018; 12: 1753465817750075.

39. Salmaninejad A, Valilou SF, Shabgah AG, Aslani S, Alimardani M, Pasdar A, et al. PD-1/PD-L1 pathway: Basic biology and role in cancer immunotherapy. J Cell Physiol. 2019; 234: 16824-37.

40. Johnson L, Mercer K, Greenbaum D, Bronson RT, Crowley D, Tuveson DA, et al. Somatic activation of the K-ras oncogene causes early onset lung cancer in mice. Nature. 2001; 410: 1111-6.

41. Kwon MC, Berns A. Mouse models for lung cancer. Mol Oncol. 2013; 7: 165-77.

42. Meuwissen R, Berns A. Mouse models for human lung cancer. Genes Dev. 2005; 19: 643-64.

43. Dunn GP, Bruce AT, Ikeda H, Old LJ, Schreiber RD. Cancer immunoediting: from immunosurveillance to tumor escape. Nat Immunol. 2002; 3: 991-8.

44. Engel AM, Svane IM, Rygaard J, Werdelin O. MCA sarcomas induced in scid mice are more immunogenic than MCA sarcomas induced in congenic, immunocompetent mice. Scand J Immunol. 1997; 45: 463-70.

45. Kim R, Emi M, Tanabe K. Cancer immunoediting from immune surveillance to immune escape. Immunology. 2007; 121: 1-14.

46. Dunn GP, Bruce AT, Sheehan KC, Shankaran V, Uppaluri R, Bui JD, et al. A critical function for type I interferons in cancer immunoediting. Nat Immunol. 2005; 6: 722-9.

47. Shankaran V, Ikeda H, Bruce AT, White JM, Swanson PE, Old LJ, et al. IFNgamma and lymphocytes prevent primary tumour development and shape tumour immunogenicity. Nature. 2001; 410: 1107-11.

48. Mittal D, Gubin MM, Schreiber RD, Smyth MJ. New insights into cancer immunoediting and its three component phases--elimination, equilibrium and escape. Curr Opin Immunol. 2014; 27: 16-25.

49. Gonzalez H, Hagerling C, Werb Z. Roles of the immune system in cancer: from tumor initiation to metastatic progression. Genes Dev. 2018; 32: 1267-84.

50. Shapouri-Moghaddam A, Mohammadian S, Vazini H, Taghadosi M, Esmaeili SA, Mardani F, et al. Macrophage plasticity, polarization, and function in health and disease. J Cell Physiol. 2018; 233: 6425-40.

51. Zhang QW, Liu L, Gong CY, Shi HS, Zeng YH, Wang XZ, et al. Prognostic significance of tumor-associated macrophages in solid tumor: a meta-analysis of the literature. PLoS One. 2012; 7: e50946.

52. Kitamura T, Qian BZ, Pollard JW. Immune cell promotion of metastasis. Nat Rev Immunol. 2015; 15: 73-86.

53. Ostuni R, Kratochvill F, Murray PJ, Natoli G. Macrophages and cancer: from mechanisms to therapeutic implications. Trends Immunol. 2015; 36: 229-39.

54. O'Sullivan C, Lewis CE, Harris AL, McGee JO. Secretion of epidermal growth factor by macrophages associated with breast carcinoma. Lancet. 1993; 342: 148-9.

55. Shojaei F, Zhong C, Wu X, Yu L, Ferrara N. Role of myeloid cells in tumor angiogenesis and growth. Trends Cell Biol. 2008; 18: 372-8.

56. Kessenbrock K, Plaks V, Werb Z. Matrix metalloproteinases: regulators of the tumor microenvironment. Cell. 2010; 141: 52-67.

57. Dannenmann SR, Thielicke J, Stockli M, Matter C, von Boehmer L, Cecconi V, et al. Tumor-associated macrophages subvert T-cell function and correlate with reduced survival in clear cell renal cell carcinoma. Oncoimmunology. 2013; 2: e23562.

58. Rubtsov YP, Rasmussen JP, Chi EY, Fontenot J, Castelli L, Ye X, et al. Regulatory T cell-derived interleukin-10 limits inflammation at environmental interfaces. Immunity. 2008; 28: 546-58.

59. Hesse M, Modolell M, La Flamme AC, Schito M, Fuentes JM, Cheever AW, et al. Differential regulation of nitric oxide synthase-2 and arginase-1 by type 1/type 2 cytokines in vivo: granulomatous pathology is shaped by the pattern of L-arginine metabolism. J Immunol. 2001; 167: 6533-44.

60. Umansky V, Blattner C, Gebhardt C, Utikal J. The Role of Myeloid-Derived Suppressor Cells (MDSC) in Cancer Progression. Vaccines (Basel). 2016; 4.

61. Parker KH, Beury DW, Ostrand-Rosenberg S. Myeloid-Derived Suppressor Cells: Critical Cells Driving Immune Suppression in the Tumor Microenvironment. Adv Cancer Res. 2015; 128: 95-139.

62. Bronte V, Brandau S, Chen SH, Colombo MP, Frey AB, Greten TF, et al. Recommendations for myeloid-derived suppressor cell nomenclature and characterization standards. Nat Commun. 2016; 7: 12150.

63. Solito S, Marigo I, Pinton L, Damuzzo V, Mandruzzato S, Bronte V. Myeloid-derived suppressor cell heterogeneity in human cancers. Ann N Y Acad Sci. 2014; 1319: 47-65.

64. Nagaraj S, Gupta K, Pisarev V, Kinarsky L, Sherman S, Kang L, et al. Altered recognition of antigen is a mechanism of CD8+ T cell tolerance in cancer. Nat Med. 2007; 13: 828-35.

65. Raber P, Ochoa AC, Rodriguez PC. Metabolism of L-arginine by myeloid-derived suppressor cells in cancer: mechanisms of T cell suppression and therapeutic perspectives. Immunol Invest. 2012; 41: 614-34.

66. Ostrand-Rosenberg S, Sinha P. Myeloid-derived suppressor cells: linking inflammation and cancer. J Immunol. 2009; 182: 4499-506.

67. Noman MZ, Desantis G, Janji B, Hasmim M, Karray S, Dessen P, et al. PD-L1 is a novel direct target of HIF-1alpha, and its blockade under hypoxia enhanced MDSC-mediated T cell activation. J Exp Med. 2014; 211: 781-90.

68. Binsfeld M, Muller J, Lamour V, De Veirman K, De Raeve H, Bellahcene A, et al. Granulocytic myeloid-derived suppressor cells promote angiogenesis in the context of multiple myeloma. Oncotarget. 2016; 7: 37931-43.

69. Kumar V, Patel S, Tcyganov E, Gabrilovich DI. The Nature of Myeloid-Derived Suppressor Cells in the Tumor Microenvironment. Trends Immunol. 2016; 37: 208-20.

70. Mildner A, Jung S. Development and function of dendritic cell subsets. Immunity. 2014; 40: 642-56.

71. Hildner K, Edelson BT, Purtha WE, Diamond M, Matsushita H, Kohyama M, et al. Batf3 deficiency reveals a critical role for CD8alpha+ dendritic cells in cytotoxic T cell immunity. Science. 2008; 322: 1097-100.

72. Broz ML, Binnewies M, Boldajipour B, Nelson AE, Pollack JL, Erle DJ, et al. Dissecting the Tumor Myeloid Compartment Reveals Rare Activating Antigen-Presenting Cells Critical for T Cell Immunity. Cancer Cell. 2014; 26: 938.

73. Moynihan KD, Opel CF, Szeto GL, Tzeng A, Zhu EF, Engreitz JM, et al. Eradication of large established tumors in mice by combination immunotherapy that engages innate and adaptive immune responses. Nat Med. 2016; 22: 1402-10.

74. Yang L, Yamagata N, Yadav R, Brandon S, Courtney RL, Morrow JD, et al. Cancer-associated immunodeficiency and dendritic cell abnormalities mediated by the prostaglandin EP2 receptor. J Clin Invest. 2003; 111: 727-35.

75. Ahmadi M, Emery DC, Morgan DJ. Prevention of both direct and cross-priming of antitumor CD8+ T-cell responses following overproduction of prostaglandin E2 by tumor cells in vivo. Cancer Res. 2008; 68: 7520-9.

76. Fu C, Liang X, Cui W, Ober-Blobaum JL, Vazzana J, Shrikant PA, et al. beta-Catenin in dendritic cells exerts opposite functions in cross-priming and maintenance of CD8+ T cells through regulation of IL-10. Proc Natl Acad Sci U S A. 2015; 112: 2823-8.

77. Gasser S, Orsulic S, Brown EJ, Raulet DH. The DNA damage pathway regulates innate immune system ligands of the NKG2D receptor. Nature. 2005; 436: 1186-90.

78. Liu XV, Ho SS, Tan JJ, Kamran N, Gasser S. Ras activation induces expression of Raet1 family NK receptor ligands. J Immunol. 2012; 189: 1826-34.

79. Vivier E, Nunes JA, Vely F. Natural killer cell signaling pathways. Science. 2004; 306: 1517-9.

80. Clemente CG, Mihm MC, Jr., Bufalino R, Zurrida S, Collini P, Cascinelli N. Prognostic value of tumor infiltrating lymphocytes in the vertical growth phase of primary cutaneous melanoma. Cancer. 1996; 77: 1303-10.

81. Dieu-Nosjean MC, Antoine M, Danel C, Heudes D, Wislez M, Poulot V, et al. Long-term survival for patients with non-small-cell lung cancer with intratumoral lymphoid structures. J Clin Oncol. 2008; 26: 4410-7.

82. Oldford SA, Robb JD, Codner D, Gadag V, Watson PH, Drover S. Tumor cell expression of HLA-DM associates with a Th1 profile and predicts improved survival in breast carcinoma patients. Int Immunol. 2006; 18: 1591-602.

83. Kusuda T, Shigemasa K, Arihiro K, Fujii T, Nagai N, Ohama K. Relative expression levels of Th1 and Th2 cytokine mRNA are independent prognostic factors in patients with ovarian cancer. Oncol Rep. 2005; 13: 1153-8.

84. Tosolini M, Kirilovsky A, Mlecnik B, Fredriksen T, Mauger S, Bindea G, et al. Clinical impact of different classes of infiltrating T cytotoxic and helper cells (Th1, th2, treg, th17) in patients with colorectal cancer. Cancer Res. 2011; 71: 1263-71.

85. Vesalainen S, Lipponen P, Talja M, Syrjanen K. Histological grade, perineural infiltration, tumour-infiltrating lymphocytes and apoptosis as determinants of long-term prognosis in prostatic adenocarcinoma. Eur J Cancer. 1994; 30A: 1797-803.

86. Ubukata H, Motohashi G, Tabuchi T, Nagata H, Konishi S, Tabuchi T. Evaluations of interferon-gamma/interleukin-4 ratio and neutrophil/lymphocyte ratio as prognostic indicators in gastric cancer patients. J Surg Oncol. 2010; 102: 742-7.

87. Kondo T, Nakazawa H, Ito F, Hashimoto Y, Osaka Y, Futatsuyama K, et al. Favorable prognosis of renal cell carcinoma with increased expression of chemokines associated with a Th1-type immune response. Cancer Sci. 2006; 97: 780-6.

88. Beyer M, Schultze JL. Regulatory T cells in cancer. Blood. 2006; 108: 804-11.

89. Allaoui R, Hagerling C, Desmond E, Warfvinge CF, Jirstrom K, Leandersson K. Infiltration of gammadelta T cells, IL-17+ T cells and FoxP3+ T cells in human breast cancer. Cancer Biomark. 2017; 20: 395-409.

90. Chin Y, Janseens J, Vandepitte J, Vandenbrande J, Opdebeek L, Raus J. Phenotypic analysis of tumor-infiltrating lymphocytes from human breast cancer. Anticancer Res. 1992; 12: 1463-6.

91. Yang C, Lee H, Jove V, Deng J, Zhang W, Liu X, et al. Prognostic significance of B-cells and pSTAT3 in patients with ovarian cancer. PLoS One. 2013; 8: e54029.

92. Woo JR, Liss MA, Muldong MT, Palazzi K, Strasner A, Ammirante M, et al. Tumor infiltrating B-cells are increased in prostate cancer tissue. J Transl Med. 2014; 12: 30.

93. Marsigliante S, Biscozzo L, Marra A, Nicolardi G, Leo G, Lobreglio GB, et al. Computerised counting of tumour infiltrating lymphocytes in 90 breast cancer specimens. Cancer Lett. 1999; 139: 33-41.

94. Inoue S, Leitner WW, Golding B, Scott D. Inhibitory effects of B cells on antitumor immunity. Cancer Res. 2006; 66: 7741-7.

95. Schioppa T, Moore R, Thompson RG, Rosser EC, Kulbe H, Nedospasov S, et al. B regulatory cells and the tumor-promoting actions of TNF-alpha during squamous carcinogenesis. Proc Natl Acad Sci U S A. 2011; 108: 10662-7.

96. Olkhanud PB, Damdinsuren B, Bodogai M, Gress RE, Sen R, Wejksza K, et al. Tumor-evoked regulatory B cells promote breast cancer metastasis by converting resting CD4(+) T cells to T-regulatory cells. Cancer Res. 2011; 71: 3505-15.

97. Rubtsov AV, Rubtsova K, Kappler JW, Jacobelli J, Friedman RS, Marrack P. CD11c-Expressing B Cells Are Located at the T Cell/B Cell Border in Spleen and Are Potent APCs. J Immunol. 2015; 195: 71-9.

98. Nielsen JS, Sahota RA, Milne K, Kost SE, Nesslinger NJ, Watson PH, et al. CD20+

tumor-infiltrating lymphocytes have an atypical CD27- memory phenotype and together with CD8+ T cells promote favorable prognosis in ovarian cancer. Clin Cancer Res. 2012; 18: 3281-92.

99. McCarthy EF. The toxins of William B. Coley and the treatment of bone and soft-tissue sarcomas. Iowa Orthop J. 2006; 26: 154-8.

100. Redelman-Sidi G, Glickman MS, Bochner BH. The mechanism of action of BCG therapy for bladder cancer--a current perspective. Nat Rev Urol. 2014; 11: 153-62.

101. Yoshimoto T, Morishima N, Okumura M, Chiba Y, Xu M, Mizuguchi J. Interleukins and cancer immunotherapy. Immunotherapy. 2009; 1: 825-44.

102. Choudhry H, Helmi N, Abdulaal WH, Zeyadi M, Zamzami MA, Wu W, et al. Prospects of IL-2 in Cancer Immunotherapy. Biomed Res Int. 2018; 2018: 9056173.

103. Wadler S, Schwartz EL. New Advances in Interferon Therapy of Cancer. Oncologist. 1997; 2: 254-67.

104. Ferrantini M, Capone I, Belardelli F. Interferon-alpha and cancer: mechanisms of action and new perspectives of clinical use. Biochimie. 2007; 89: 884-93.

105. Fukuhara H, Ino Y, Todo T. Oncolytic virus therapy: A new era of cancer treatment at dawn. Cancer Sci. 2016; 107: 1373-9.

106. LaRocca CJ, Warner SG. Oncolytic viruses and checkpoint inhibitors: combination therapy in clinical trials. Clin Transl Med. 2018; 7: 35.

107. Boyiadzis M, Foon KA. Approved monoclonal antibodies for cancer therapy. Expert Opin Biol Ther. 2008; 8: 1151-8.

108. Chiavenna SM, Jaworski JP, Vendrell A. State of the art in anti-cancer mAbs. J Biomed Sci. 2017; 24: 15.

109. Koury J, Lucero M, Cato C, Chang L, Geiger J, Henry D, et al. Immunotherapies: Exploiting the Immune System for Cancer Treatment. J Immunol Res. 2018; 2018: 9585614.

110. Lu CY, Chen GJ, Tai PH, Yang YC, Hsu YS, Chang M, et al. Tetravalent anti-CD20/CD3 bispecific antibody for the treatment of B cell lymphoma. Biochem Biophys Res Commun. 2016; 473: 808-13.

111. Tivol EA, Borriello F, Schweitzer AN, Lynch WP, Bluestone JA, Sharpe AH. Loss of CTLA-4 leads to massive lymphoproliferation and fatal multiorgan tissue destruction, revealing a critical negative regulatory role of CTLA-4. Immunity. 1995; 3: 541-7.

112. Emens LA, Ascierto PA, Darcy PK, Demaria S, Eggermont AMM, Redmond WL, et al. Cancer immunotherapy: Opportunities and challenges in the rapidly evolving

clinical landscape. Eur J Cancer. 2017; 81: 116-29.

113. Marin-Acevedo JA, Chirila RM, Dronca RS. Immune Checkpoint Inhibitor Toxicities. Mayo Clin Proc. 2019; 94: 1321-9.

114. Seidel JA, Otsuka A, Kabashima K. Anti-PD-1 and Anti-CTLA-4 Therapies in Cancer: Mechanisms of Action, Efficacy, and Limitations. Front Oncol. 2018; 8: 86.

115. Goldberg MV, Drake CG. LAG-3 in Cancer Immunotherapy. Curr Top Microbiol Immunol. 2011; 344: 269-78.

116. Puhr HC, Ilhan-Mutlu A. New emerging targets in cancer immunotherapy: the role of LAG3. ESMO Open. 2019; 4: e000482.

117. Friedlaender A, Addeo A, Banna G. New emerging targets in cancer immunotherapy: the role of TIM3. ESMO Open. 2019; 4: e000497.

118. Wang J, Sun J, Liu LN, Flies DB, Nie X, Toki M, et al. Siglec-15 as an immune suppressor and potential target for normalization cancer immunotherapy. Nat Med. 2019; 25: 656-66.

119. Marin-Acevedo JA, Dholaria B, Soyano AE, Knutson KL, Chumsri S, Lou Y. Next generation of immune checkpoint therapy in cancer: new developments and challenges. J Hematol Oncol. 2018; 11: 39.

120. Spiess PJ, Yang JC, Rosenberg SA. In vivo antitumor activity of tumor-infiltrating lymphocytes expanded in recombinant interleukin-2. J Natl Cancer Inst. 1987; 79: 1067-75.

121. Rosenberg SA, Yang JC, Sherry RM, Kammula US, Hughes MS, Phan GQ, et al. Durable complete responses in heavily pretreated patients with metastatic melanoma using T-cell transfer immunotherapy. Clin Cancer Res. 2011; 17: 4550-7.

122. Schwartzentruber DJ, Hom SS, Dadmarz R, White DE, Yannelli JR, Steinberg SM, et al. In vitro predictors of therapeutic response in melanoma patients receiving tumor-infiltrating lymphocytes and interleukin-2. J Clin Oncol. 1994; 12: 1475-83.

123. Schmidts A, Maus MV. Making CAR T Cells a Solid Option for Solid Tumors. Front Immunol. 2018; 9: 2593.

124. D'Aloia MM, Zizzari IG, Sacchetti B, Pierelli L, Alimandi M. CAR-T cells: the long and winding road to solid tumors. Cell Death Dis. 2018; 9: 282.

125. Sun S, Hao H, Yang G, Zhang Y, Fu Y. Immunotherapy with CAR-Modified T Cells: Toxicities and Overcoming Strategies. J Immunol Res. 2018; 2018: 2386187.

126. Wu MR, Jusiak B, Lu TK. Engineering advanced cancer therapies with synthetic biology. Nat Rev Cancer. 2019; 19: 187-95.

127. Gardner TA, Elzey BD, Hahn NM. Sipuleucel-T (Provenge) autologous vaccine approved for treatment of men with asymptomatic or minimally symptomatic castrate-resistant metastatic prostate cancer. Hum Vaccin Immunother. 2012; 8: 534-9.

128. Gure AO, Chua R, Williamson B, Gonen M, Ferrera CA, Gnjatic S, et al. Cancer-testis genes are coordinately expressed and are markers of poor outcome in non-small cell lung cancer. Clin Cancer Res. 2005; 11: 8055-62.

129. Wang Y, Deng W, Li N, Neri S, Sharma A, Jiang W, et al. Combining Immunotherapy and Radiotherapy for Cancer Treatment: Current Challenges and Future Directions. Front Pharmacol. 2018; 9: 185.

130. Willett WC. Diet and cancer: one view at the start of the millennium. Cancer Epidemiol Biomarkers Prev. 2001; 10: 3-8.

131. Hecht SS. Tobacco carcinogens, their biomarkers and tobacco-induced cancer. Nat Rev Cancer. 2003; 3: 733-44.

132. Avgerinos KI, Spyrou N, Mantzoros CS, Dalamaga M. Obesity and cancer risk: Emerging biological mechanisms and perspectives. Metabolism. 2019; 92: 121-35.

133. Cuzick J, Powles T, Veronesi U, Forbes J, Edwards R, Ashley S, et al. Overview of the main outcomes in breast-cancer prevention trials. Lancet. 2003; 361: 296-300.

134. Umar A, Dunn BK, Greenwald P. Future directions in cancer prevention. Nat Rev Cancer. 2012; 12: 835-48.

135. Dvorak HF. Tumors: wounds that do not heal. Similarities between tumor stroma generation and wound healing. N Engl J Med. 1986; 315: 1650-9.

136. Crusz SM, Balkwill FR. Inflammation and cancer: advances and new agents. Nat Rev Clin Oncol. 2015; 12: 584-96.

137. Waddell WR, Loughry RW. Sulindac for polyposis of the colon. J Surg Oncol. 1983; 24: 83-7.

138. Algra AM, Rothwell PM. Effects of regular aspirin on long-term cancer incidence and metastasis: a systematic comparison of evidence from observational studies versus randomised trials. Lancet Oncol. 2012; 13: 518-27.

139. Baron JA, Cole BF, Sandler RS, Haile RW, Ahnen D, Bresalier R, et al. A randomized trial of aspirin to prevent colorectal adenomas. N Engl J Med. 2003; 348: 891-9.

140. Benamouzig R, Deyra J, Martin A, Girard B, Jullian E, Piednoir B, et al. Daily soluble aspirin and prevention of colorectal adenoma recurrence: one-year results of the APACC trial. Gastroenterology. 2003; 125: 328-36.

141. Rothwell PM, Fowkes FG, Belch JF, Ogawa H, Warlow CP, Meade TW. Effect of daily aspirin on long-term risk of death due to cancer: analysis of individual patient data from randomised trials. Lancet. 2011; 377: 31-41.

142. Rothwell PM, Price JF, Fowkes FG, Zanchetti A, Roncaglioni MC, Tognoni G, et al. Short-term effects of daily aspirin on cancer incidence, mortality, and non-vascular death: analysis of the time course of risks and benefits in 51 randomised controlled trials. Lancet. 2012; 379: 1602-12.

143. Arber N, Eagle CJ, Spicak J, Racz I, Dite P, Hajer J, et al. Celecoxib for the prevention of colorectal adenomatous polyps. N Engl J Med. 2006; 355: 885-95.

144. Meyskens FL, Jr., McLaren CE, Pelot D, Fujikawa-Brooks S, Carpenter PM, Hawk E, et al. Difluoromethylornithine plus sulindac for the prevention of sporadic colorectal adenomas: a randomized placebo-controlled, double-blind trial. Cancer Prev Res (Phila). 2008; 1: 32-8.

145. Bresalier RS, Sandler RS, Quan H, Bolognese JA, Oxenius B, Horgan K, et al. Cardiovascular events associated with rofecoxib in a colorectal adenoma chemoprevention trial. N Engl J Med. 2005; 352: 1092-102.

146. Lollini PL, Cavallo F, Nanni P, Forni G. Vaccines for tumour prevention. Nat Rev Cancer. 2006; 6: 204-16.

147. Schiller JT, Lowy DR. Vaccines to prevent infections by oncoviruses. Annu Rev Microbiol. 2010; 64: 23-41.

148. Beatty PL, Narayanan S, Gariepy J, Ranganathan S, Finn OJ. Vaccine against MUC1 antigen expressed in inflammatory bowel disease and cancer lessens colonic inflammation and prevents progression to colitis-associated colon cancer. Cancer Prev Res (Phila). 2010; 3: 438-46.

149. Dakappagari NK, Douglas DB, Triozzi PL, Stevens VC, Kaumaya PT. Prevention of mammary tumors with a chimeric HER-2 B-cell epitope peptide vaccine. Cancer Res. 2000; 60: 3782-9.

150. Cefai D, Morrison BW, Sckell A, Favre L, Balli M, Leunig M, et al. Targeting HER-2/neu for active-specific immunotherapy in a mouse model of spontaneous breast cancer. Int J Cancer. 1999; 83: 393-400.

151. Greiner JW, Zeytin H, Anver MR, Schlom J. Vaccine-based therapy directed against carcinoembryonic antigen demonstrates antitumor activity on spontaneous intestinal tumors in the absence of autoimmunity. Cancer Res. 2002; 62: 6944-51.

152. Disis ML, Bernhard H, Jaffee EM. Use of tumour-responsive T cells as cancer treatment. Lancet. 2009; 373: 673-83.

153. Park KH, Gad E, Goodell V, Dang Y, Wild T, Higgins D, et al. Insulin-like growth

factor-binding protein-2 is a target for the immunomodulation of breast cancer. Cancer Res. 2008; 68: 8400-9.

154. Yuan W, Xia G, Zhao C, Sui C, Ma J. Anti-idiotypic single chain mimicking CA125 linked with tuftsin provides protective immunity against ovarian cancer in mice. Mol Med Rep. 2012; 5: 388-94.

155. Bosch GJ, Joosten AM, Kessler JH, Melief CJ, Leeksma OC. Recognition of BCR-ABL positive leukemic blasts by human CD4+ T cells elicited by primary in vitro immunization with a BCR-ABL breakpoint peptide. Blood. 1996; 88: 3522-7.

156. Triozzi PL, Aldrich W, Ponnazhagan S. Inhibition and promotion of tumor growth with adeno-associated virus carcinoembryonic antigen vaccine and Toll-like receptor agonists. Cancer Gene Ther. 2011; 18: 850-8.

157. Bhattacharyya S, Gill R, Chen ML, Zhang F, Linhardt RJ, Dudeja PK, et al. Toll-like receptor 4 mediates induction of the Bcl10-NFkappaB-interleukin-8 inflammatory pathway by carrageenan in human intestinal epithelial cells. J Biol Chem. 2008; 283: 10550-8.

158. Buck CB, Thompson CD, Roberts JN, Muller M, Lowy DR, Schiller JT. Carrageenan is a potent inhibitor of papillomavirus infection. PLoS Pathog. 2006; 2: e69.

159. Johnson JJ, Mukhtar H. Curcumin for chemoprevention of colon cancer. Cancer Lett. 2007; 255: 170-81.

160. Llosa NJ, Cruise M, Tam A, Wicks EC, Hechenbleikner EM, Taube JM, et al. The vigorous immune microenvironment of microsatellite instable colon cancer is balanced by multiple counter-inhibitory checkpoints. Cancer Discov. 2015; 5: 43-51.

161. Coyle KM, Boudreau JE, Marcato P. Genetic Mutations and Epigenetic Modifications: Driving Cancer and Informing Precision Medicine. Biomed Res Int. 2017; 2017: 9620870.

162. Dawson MA, Prinjha RK, Dittmann A, Giotopoulos G, Bantscheff M, Chan WI, et al. Inhibition of BET recruitment to chromatin as an effective treatment for MLL-fusion leukaemia. Nature. 2011; 478: 529-33.

163. Filippakopoulos P, Qi J, Picaud S, Shen Y, Smith WB, Fedorov O, et al. Selective inhibition of BET bromodomains. Nature. 2010; 468: 1067-73.

164. Zuber J, Shi J, Wang E, Rappaport AR, Herrmann H, Sison EA, et al. RNAi screen identifies Brd4 as a therapeutic target in acute myeloid leukaemia. Nature. 2011; 478: 524-8.

165. Garcia PL, Miller AL, Kreitzburg KM, Council LN, Gamblin TL, Christein JD, et al. The BET bromodomain inhibitor JQ1 suppresses growth of pancreatic ductal adenocarcinoma in patient-derived xenograft models. Oncogene. 2016; 35: 833-45.

166. Evans RM, Mangelsdorf DJ. Nuclear Receptors, RXR, and the Big Bang. Cell. 2014; 157: 255-66.

167. Sherman SI, Gopal J, Haugen BR, Chiu AC, Whaley K, Nowlakha P, et al. Central hypothyroidism associated with retinoid X receptor-selective ligands. N Engl J Med. 1999; 340: 1075-9.

168. Liby KT, Sporn MB. Rexinoids for prevention and treatment of cancer: opportunities and challenges. Curr Top Med Chem. 2017; 17: 721-30.

169. Nunez V, Alameda D, Rico D, Mota R, Gonzalo P, Cedenilla M, et al. Retinoid X receptor alpha controls innate inflammatory responses through the up-regulation of chemokine expression. Proc Natl Acad Sci U S A. 2010; 107: 10626-31.

170. Menegon S, Columbano A, Giordano S. The Dual Roles of NRF2 in Cancer. Trends Mol Med. 2016; 22: 578-93.

171. Hayes JD, McMahon M, Chowdhry S, Dinkova-Kostova AT. Cancer chemoprevention mechanisms mediated through the Keap1-Nrf2 pathway. Antioxid Redox Signal. 2010; 13: 1713-48.

172. Hu R, Saw CL, Yu R, Kong AN. Regulation of NF-E2-related factor 2 signaling for cancer chemoprevention: antioxidant coupled with antiinflammatory. Antioxid Redox Signal. 2010; 13: 1679-98.

173. Iida K, Itoh K, Kumagai Y, Oyasu R, Hattori K, Kawai K, et al. Nrf2 is essential for the chemopreventive efficacy of oltipraz against urinary bladder carcinogenesis. Cancer Res. 2004; 64: 6424-31.

174. Khor TO, Huang MT, Prawan A, Liu Y, Hao X, Yu S, et al. Increased susceptibility of Nrf2 knockout mice to colitis-associated colorectal cancer. Cancer Prev Res (Phila). 2008; 1: 187-91.

175. Xu C, Huang MT, Shen G, Yuan X, Lin W, Khor TO, et al. Inhibition of 7,12-dimethylbenz(a)anthracene-induced skin tumorigenesis in C57BL/6 mice by sulforaphane is mediated by nuclear factor E2-related factor 2. Cancer Res. 2006; 66: 8293-6.

176. Farmer H, McCabe N, Lord CJ, Tutt AN, Johnson DA, Richardson TB, et al. Targeting the DNA repair defect in BRCA mutant cells as a therapeutic strategy. Nature. 2005; 434: 917-21.

177. Bryant HE, Schultz N, Thomas HD, Parker KM, Flower D, Lopez E, et al. Specific killing of BRCA2-deficient tumours with inhibitors of poly(ADP-ribose) polymerase. Nature. 2005; 434: 913-7.

178. Jiao S, Xia W, Yamaguchi H, Wei Y, Chen MK, Hsu JM, et al. PARP Inhibitor Upregulates PD-L1 Expression and Enhances Cancer-Associated Immunosuppression.

Clin Cancer Res. 2017; 23: 3711-20.

CHAPTER 2

Chemoprevention of preclinical breast and lung cancer with the bromodomain inhibitor I-BET 762

Reprinted with permission from *Cancer Prevention Research*. 2018. 11(3): 143-156

Di Zhang, Ana S. Leal, Sarah Carapellucci, Kayla Zydeck, Michael B. Sporn, and Karen T. Liby

Author contributions:
Participated in research design: Zhang, Leal, Liby
Conducted experiments: Zhang, Leal, Carapellucci, Zydeck
Performed data analysis: Zhang, Leal
Wrote or contributed to the writing of the manuscript: Zhang, Sporn, Liby

2.1 Abstract

Breast cancer and lung cancer remain the top two leading causes of cancer-related deaths in women. Because of limited success in reducing the high mortality of these diseases, new drugs and approaches are desperately needed. Cancer prevention is one such promising strategy that is effective in both preclinical and clinical studies. I-BET 762 is a new bromodomain inhibitor that reversibly targets BET (bromodomain and extraterminal) proteins and impairs their ability to bind to acetylated lysines on histones, thus interrupting downstream transcription. This inhibitor has anti-inflammatory effects and induces growth arrest in many cancers and is currently under clinical trials for treatment of cancer. However, few studies have investigated the chemopreventive effects of bromodomain inhibitors. Here, we found that I-BET 762 significantly delayed tumor development in preclinical breast and lung cancer mouse models. This drug not only induced growth arrest and downregulated c-Myc, pSTAT3 and pERK protein expression in tumor cells *in vitro* and *in vivo* but also altered immune populations in different organs. These results demonstrate the promising potential of using I-BET 762 for cancer prevention and suggest the striking effects of I-BET 762 are the result of targeting both tumor cells and the tumor microenvironment.

2.2 Introduction

Breast cancer and lung cancer are the top two leading causes of cancer deaths in women [1]. Even though the survival rates of estrogen receptor-positive (ER^+) breast cancer have gradually improved, primarily because of the benefits of endocrine therapy, the incidence and survival rates for ER-negative (ER^-) breast cancer have not noticeably shifted over the past 30 years [2]. Lung cancer is responsible for more cancer deaths

than breast, prostate, colon and pancreatic cancer combined, and the 5-year survival rates for lung cancer remain a disappointing 18% [1]. Therefore, new drugs as well as new approaches are greatly needed to reduce both the incidence and mortality of both of these diseases.

Prevention and early intervention in cancer are two underutilized strategies that have proven effective in both preclinical and clinical studies [3]. Fisher and colleagues reported a 49% reduction in the incidence of breast cancer in women taking tamoxifen compared with a placebo [4]. Raloxifene, a second-generation selective ER modulator (SERM), reduced the incidence of breast cancer by approximately 80% in early clinical trials [5]. Abundant clinical data confirm that antiestrogens or SERMs can prevent ER^+ breast cancer in women [6-9]. However, tamoxifen can induce rare but serious side effects, such as increasing the risk of uterine cancer [10], and there are no approved drugs available for the prevention of ER^- breast cancer. In contrast to breast cancer, drugs have been tested for the prevention of lung cancer in a variety of preclinical models, but these efforts have not been successfully translated into the clinic. Because smokers are at high risk of developing lung cancer, developing effective drugs with a good safety profile for the chemoprevention of lung cancer could greatly reduce the overall number of cancer deaths [11].

In addition to known genetic mutations that drive carcinogenesis, epigenetic events are also highly involved in the initiation and progression of cancer [12]. Unlike genetic mutations, epigenetic alterations are considered reversible, which makes them an appealing therapeutic target. A number of epigenetic drugs have been developed that can reverse the aberrations of DNA methylation or histone modifications in cancer.

Inhibitors of DNA methylation were the first epigenetic drugs designed for treatment of cancer; these nucleoside analogs inhibit DNA methylation by trapping DNA methyltransferases [13]. Drugs targeting histone modifications were then developed, and the histone deacetylase (HDAC) inhibitor suberoylanilide hydroxamic acid (SAHA) is approved by the FDA for the treatment of cutaneous T-cell lymphoma. Some of these epigenetic drugs have also been tested for chemoprevention [14]. The HDAC inhibitor valproic acid is currently being tested in a clinical trial (NCT02608736) for chemoprevention of head and neck squamous cell carcinoma.

Recently, chromatin “readers” have emerged as promising epigenetic targets. In contrast to “writers” (e.g. histone acetyltransferases and histone methyltransferases) or “erasers” (e.g. HDACs and lysine demethylases (KDMs)), readers bind to specific epigenetically modified sites. Bromodomains, which contain a conserved binding motif, are the primary readers of acetylated lysine residues, and over 40 human proteins express bromodomains [15]. Importantly, distinct small molecules that are specific to the BET (Bromodomain and extraterminal domain) family (BRD-2, 3, 4, T) of bromodomain proteins [16, 17] have been developed. The BET inhibitors have shown promising efficacy in preclinical models for treating cancers including NUT-midline carcinoma [18], hematological malignancies [16, 19], and pancreatic cancer [20], but little is known regarding the chemopreventive potential of bromodomain inhibitors in cancer.

JQ1 was one of the earliest BET inhibitors identified [17], and it blocks neoplastic transformation induced by 12-O-tetradecanoylphorbol-13-acetate [21] or visceral adipose tissue [22] in mouse skin epidermal JB6 P^+ cells and suppresses inflammation in many cell types [23, 24]. However, poor bioavailability and a short half-life make JQ1 an

impractical candidate for clinical development. In contrast, the bromodomain inhibitor I-BET 762 (also known as GSK525762) has good potency and pharmacokinetics following oral administration [25]. It is currently being evaluated in clinical trials (NCT01587703, NCT01943851, NCT02964507) for the treatment of NUT middle carcinoma and other cancers, including breast and lung cancer. In addition to its antiproliferative effects in cancer cells, I-BET 762 can inhibit cytokine secretion and decrease the number of tumor-associated macrophages and myeloid-derived suppressor cells in a preclinical model of pancreatic cancer [23]. Because of the known anti-inflammatory and immunomodulatory effects of the bromodomain inhibitors, we tested the efficacy of I-BET 762 for the prevention of breast and lung cancer in two clinically relevant mouse models (MMTV-PyMT ER^- breast cancer model and vinyl carbarmate-induced lung carcinogenesis model) and investigated its effects on both cancer and immune cells.

2.3 Materials and Methods

2.3.1 *In vivo* experiments

All animal studies were performed in accordance with protocols approved by the Institutional Animal Care and Use Committee at Michigan State University (East Lansing, MI). For the breast cancer studies, MMTV-PyMT mice were obtained from Dr. Jeffrey Pollard (Albert Einstein College of Medicine, Bronx, NY) and were genotyped as described [26]. Four-week-old female PyMT mice were randomized into either control group fed powdered 5002 rodent chow or I-BET 762 (60 mg/kg diet) mixed into powdered diet as described previously [27]; I-BET 762 (purity >95%) was synthesized [25] by J-Star Research (South Plainfield, NJ). Mice were palpated for tumors twice a

week. For the immune cell infiltration studies, 11-week-old female PyMT mice were gavaged (5% DMSO and 10% Tween 20 in saline) with 60 mg I-BET 762 /kg body weight daily for one week for a short-term protocol. In a longer-term protocol, four-week-old female PyMT mice were fed either powdered control diet or diet containing I-BET 762 (60 mg/kg diet) until 13 weeks of age. For both studies, tissues were harvested for analysis by flow cytometry and evaluation of biomarkers by Western blot or IHC.

For the lung cancer studies, 8-week old female A/J mice from The Jackson Laboratory were injected intraperitoneally with 0.32 mg vinyl carbamate (Toronto Research Chemicals) dissolved in saline. One week after injection, the mice were randomized into either control group fed AIN-93G semisynthetic diet (BioServ), I-BET 762 (40-120 mg/kg diet), LG100268 (40 mg/kg diet) or the combination of I-BET 762 and LG100268 (40 mg of each drug/kg diet). After 16 weeks on diet, lungs were harvested and inflated with PBS. Left lungs were fixed in neutral-buffered formalin (NBF) for histopathology. Right lungs were used immediately for flow cytometry (two lobes) or were flash frozen (the other two lobes). Samples were coded with random numbers to blind the investigators to the identity of the treatment group during analysis. Then tumor number, size and histopathology were assessed on two separate sections of the left lung by two independent investigators using published criteria [28].

2.3.2 Flow cytometry

The same two mammary glands or two lobes of the right lung were harvested from each PyMT mouse or A/J mouse, respectively, for flow cytometry. Fresh tissues were homogenized and incubated in digestion media containing 300 U/ml collagenase

(Sigma), 1 U/ml dispase (Worthington), and 2 U/ml DNAse (EMD Millipore) for 30 minutes at 37°C. Cells were passed through a 40 μm cell strainer (Falcon) to obtain a single-cell suspension and treated with a lysing solution (eBioscience) to eliminate red blood cells. Cells were then stained with 5 μg/ml anti-mouse Fc block (BioLegend) and two panels of validated antibodies [23] for 30 minutes on ice. Panel 1: CD45-VioGreen (3 μg/ml, Miltenyi Biotec), Gr-1-PE (3 μg/ml, Miltenyi Biotec), CD11b-FITC (3 μg/ml, Miltenyi Biotec). Panel 2: CD45-VioGreen (3 μg/ml, Miltenyi Biotec), CD3-PE (2 μg/ml, BioLegend), CD4-FITC (3 μg/ml, Miltenyi Biotec), CD8-PerCP/Cy5.5 (2 μg/ml, BioLegend), CD25-PE/Cy7 (2 μg/ml, BD Biosciences). Flow cytometry was performed using a LSR II flow cytometer with three laser sources (488 nm, 633 nm, 407 nm) and DIVA 6.2 software (BD Biosciences); data were analyzed by FlowJo x.10.0.7r2 software (Tree Star).

2.3.3 IHC

Upper right mammary glands and left lungs inflated with PBS were fixed in 10% NBF for 48 hours for histopathology and IHC. Citrate or EDTA buffer was used for antigen retrieval, and hydrogen peroxide was used to quench endogenous peroxidase activity. Sections were immunostained with pSTAT3 or pERK (1:50, Cell Signaling Technology) and biotinylated anti-rabbit secondary (Cell Signaling Technology), CD45 (1:100, BioScience) and anti-rat secondary (Vector), or PCNA (1:100 BioLegend) antibodies and biotinylated anti-mouse secondary (Cell Signaling Technology). Signal was detected using a DAB kit (Cell Signaling Technology). Sections were counterstained with hematoxylin (Vector).

2.3.4 Cell culture

MDA-MB-231 and A549 cells (ATCC) were cultured in DMEM or RPMI 1640, respectively, with 10% FBS and 1% penicillin/streptomycin. Primary PyMT tumor cells were isolated from female PyMT mice. Mammary tumors were dissected, homogenized and digested in DMEM with 10% FBS, 300 U/ml collagenase, 1.0 U/ml dispase and 2 U/ml DNase for 30 min at 37°C. The cell suspension was passed through a 40-μM cell strainer. After centrifugation at 220 x *g* for 10 minutes, cells were plated in DMEM with 10% FBS and 1% penicillin/streptomycin. All experiments were performed within 1 week of isolation. VC-1 cells were derived from lung tumors in A/J mice injected with vinyl carbamate, using the same protocol [28, 29]. Media and supplements were purchased from Corning Cellgro (Mediatech, Manassas, VA).

2.3.5 Western blotting

Cells treated with different concentration of I-BET 762 were lysed in RIPA buffer (1 mol/L Tris-Cl, 5 mol/L NaCl, pH 7.4, 0.5 mol/L EDTA, 25 mmol/L deoxycholic acid, 1% Triton-X, 0.1% SDS) with protease inhibitors. Mammary glands or lung tissues were homogenized and incubated in EBC buffer (5 mol/L NaCl, 1 mol/L Tris pH 8) with protease inhibitors and 10% NP-40 for 30 minutes. The BCA assay (Sigma-Aldrich) was performed to determine protein concentrations. Proteins were separated by SDS-PAGE and transferred to nitrocellulose membranes. p27KIP1, Cyclin D1, c-Myc, p-Erk 1/2, pSTAT3 and vinculin (all from Cell Signaling Technology) primary antibodies were used to analyze the corresponding proteins; secondary antibodies were purchased from Cell Signaling Technology. ImageJ was used to quantify the immunoblots. Images shown are representative of two to three independent experiments.

2.3.6 Statistical analysis

The *in vitro* experiments were repeated in at least three independent experiments. Results were analyzed using the t-test or one-way ANOVA (Prism 6). *In vivo* data were analyzed by one-way ANOVA followed by a Tukey test, or one-way ANOVA on ranks and the Dunn test if the data did not fit a normal distribution (SigmaStat 3.5). Results were expressed as the mean±SE unless otherwise noted. $p < 0.05$ was considered statistically significant.

2.4 Results

2.4.1 The bromodomain inhibitor I-BET 762 delays tumor development in the MMTV-PyMT model of breast cancer

To investigate whether I-BET 762 affects tumor development, we first tested this drug in MMTV-PyMT mice. In this ER^- breast cancer model, expression of the oncogenic PyMT protein is targeted to the mammary epithelium by the MMTV promoter [26]. This model mimics several key features of human breast cancer, including disease progression from hyperplasia to invasive carcinoma and the early infiltration of tumor-associated macrophages [30]. Female PyMT mice were fed control diet or diet containing I-BET 762 (60 mg/kg diet, which is approximately 15 mg/kg body weight) starting at 4 weeks of age. Treatment with I-BET 762 significantly ($p<0.05$) delayed the development of mammary tumors (Figure 2.1 A). The average time of the first palpable tumor increased from 13.1±0.8 weeks in the control group to 16.3±1.0 weeks with the I-BET 762 treatment (Figure 2.1 B; $p<0.05$). I-BET 762 was well tolerated at this dose, with no significant differences in weight between groups (average body weight of

24.1±1.6 g in control group vs. 24.5±1.8 g in I-BET 762 treated group at 17 weeks of age).

2.4.2 I-BET 762 induces growth arrest and downregulates c-Myc expression in breast cancer cells

Bromodomain inhibitors can inhibit c-Myc and induce growth arrest in many cell types [23, 31, 32]. In our studies, I-BET 762 inhibited proliferation of MDA-MB-231, a triple negative human breast cancer cell line, with an IC_{50} of 0.46±0.4 μmol/L in the MTT assay. At concentrations as low as 0.25 μmol/L, both I-BET 762 and JQ-1 upregulated p27 and downregulated c-Myc protein expression (Figure 2.1 C) in these cells. Next, primary cells were isolated from mammary tumors in PyMT mice and treated with I-BET 762 for 48 hours. In these cells, treatment with I-BET 762 increased protein levels of p27 and decreased Cyclin D1 (Figure 2.1 D); these changes are hallmarks of G_1-phase cell-cycle arrest [33]. I-BET 762 does arrest these cells in G1, as confirmed by flow cytometry (data now shown). C-Myc protein expression was also decreased by I-BET 762 (Figure 2.1 D).

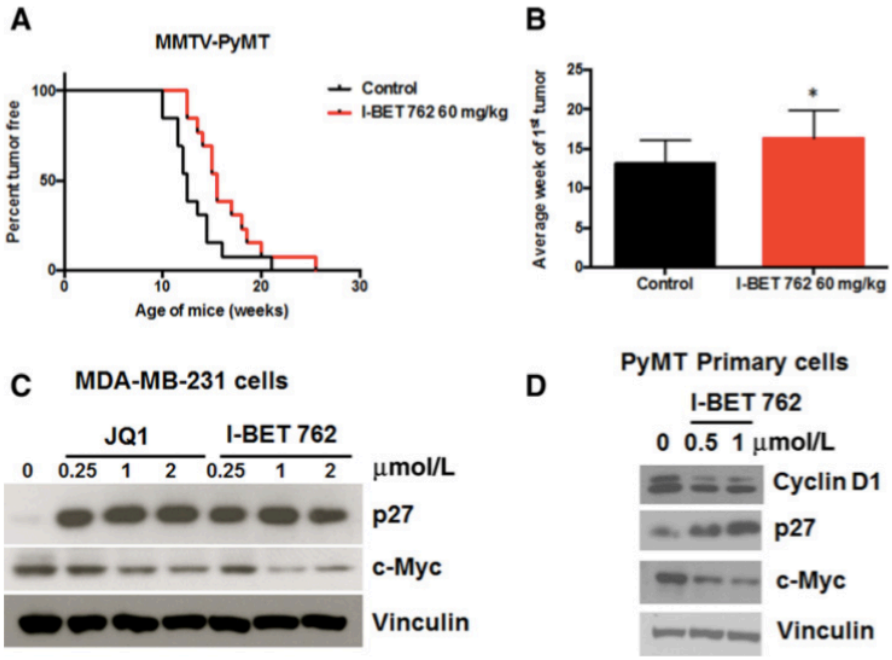

Figure 2.1. The bromodomain inhibitor I-BET 762 delays tumor development in the MMTV-PyMT model of ER$^-$ breast cancer. Female PyMT mice were started on either control diet or I-BET 762 (60 mg/kg in diet) at 4 weeks old. Mice were palpated twice a week for tumors. A. Treatment with I-BET 762 significantly ($p<0.05$) delayed development of the initial tumor compared with the control group. n=13 per group. B. Average time (in weeks) of the first tumor appearance. *, $p<0.05$ vs. control. Results, mean±SD. C. MDA-MB-231 cells were treated with different concentrations of JQ1 or I-BET 762 for 48 hours. p27 and c-Myc protein expression were detected by Western blotting. D. Primary tumor cells were isolated from tumors in PyMT mice. Cells were treated with I-BET 762 for 48 hours and lysates were immunoblotted with antibodies against Cyclin D1, p27, and c-Myc.

2.4.3 I-BET 762 modulates T-cell populations in the mammary gland and spleen and decreases pSTAT3 expression in the mammary gland

In addition to the antiproliferative role of I-BET 762 on tumor cells, this drug also modulates the tumor microenvironment. We and others have shown that bromodomain inhibitors suppress the production of proinflammatory molecules by macrophages [34] and have anti-inflammatory effects in pancreatic cancer [20, 23]. Because epigenetic modulators can have rapid effects on cells, a short-term *in vivo* study was performed. In

the PyMT model, 11-week-old female PyMT mice without palpable tumors were treated daily with either vehicle or I-BET 762 (60 mg/kg) by gavage for one week (short treatment protocol, Figure 2.2 A). This dose of I-BET 762 altered immune cell populations in a model of pancreatic cancer [23]. The time point was selected based on previous studies indicating that the highest infiltration of immune cells into the mammary gland occurred at 12 to 13 weeks of age in PyMT mice [35]. Both the mammary gland and spleen were harvested and analyzed by flow cytometry to obtain an overview of the immune cell populations in these tissues. The percentages of $CD45^+$ immune cells, total T cells ($CD45^+$, $CD3^+$), CD4 helper T cells ($CD45^+$, $CD3^+$, $CD4^+$) and CD8 cytotoxic T cells ($CD45^+$, $CD3^+$, $CD8^+$) and macrophages ($CD45^+$, $CD11b^+$, $F4/80^+$) were analyzed. After one week of treatment, the percentages of $CD45^+$ immune cells (Figure 2.2 B), total T cells (Figure 2.2 C), and CD4 helper T cells (Figure 2.2 D) were all significantly ($p<0.05$) higher in the spleen of the PyMT mice treated with I-BET 762. There were no significant changes in immune cell populations in the mammary glands after this limited treatment (data not shown). We then used a longer term treatment protocol (Figure 2.3 A) to evaluate the chronic effects of I-BET 762 on immune cell populations. Four-week old female PyMT mice were fed with either control diet or diet containing I-BET 762 (60 mg/kg diet) for 13 weeks. In these experiments, there was a small but significant ($p<0.05$) decrease of CD4 helper T cells in the mammary gland of mice treated with I-BET 762 (Figure 2.3 B). Activation of CD4 helper T cells was then evaluated by expression of the CD25 surface marker. A lower percentage of activated CD4 T cells was detected in I-BET 762 treated group ($p=0.08$, Figure 2.3 C). No other changes in immune cells in the mammary gland or the spleen were observed at this time point (data not shown).

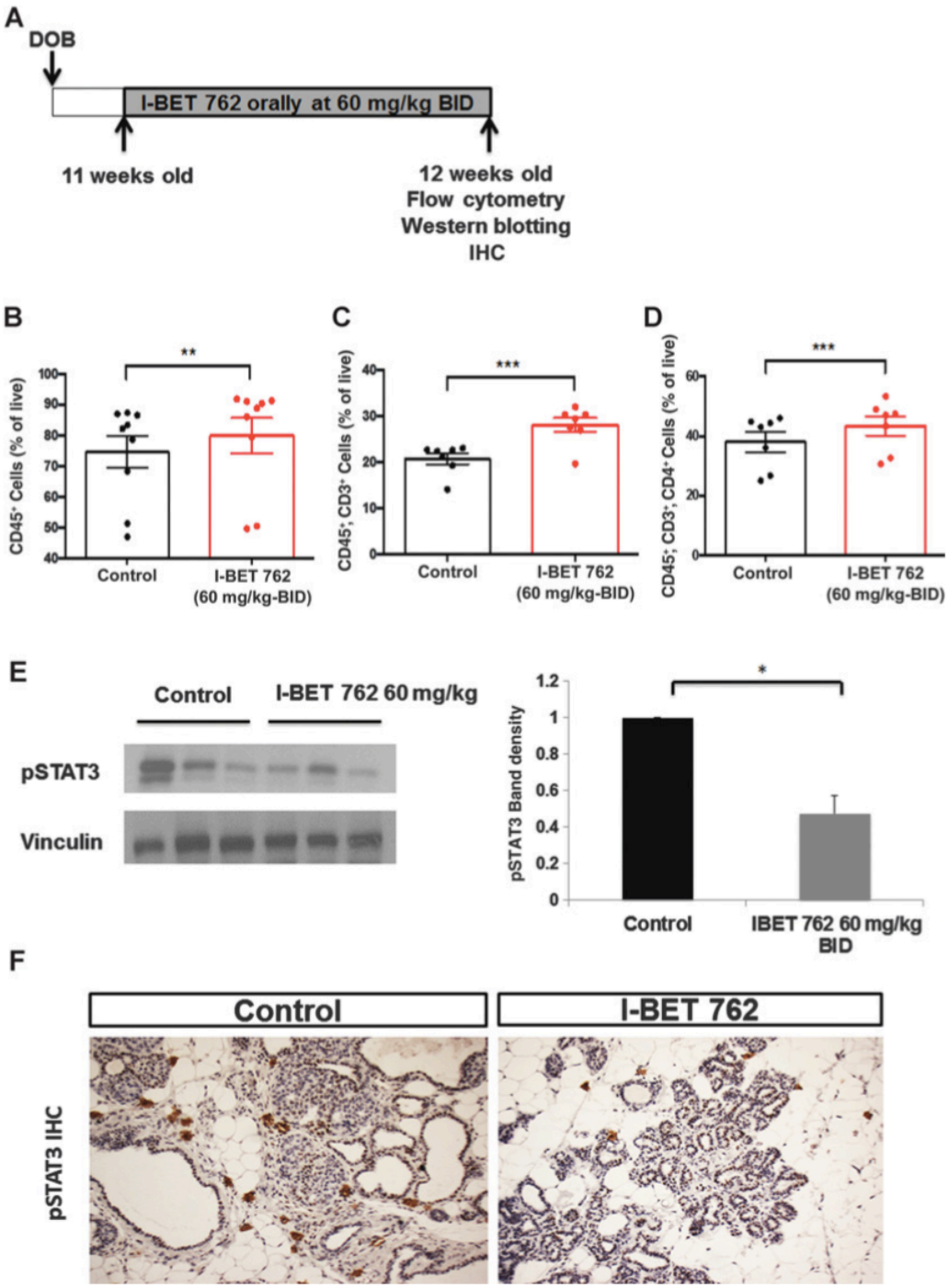

Figure 2.2. Short-term treatment with I-BET 762 increases CD45$^+$ immune cells and T-cell infiltration in the spleen and decreases pSTAT3 expression in the mammary gland. A. Diagram of short-term treatment protocol by gavage (n=9/group). The immune cell populations in mammary glands or spleen from PyMT mice were analyzed by flow cytometry. Percentages of total immune cells (CD45$^+$), total T cells (CD45$^+$, CD3$^+$), and Th cells (CD45$^+$, CD3$^+$, CD4$^+$) in the spleen are shown from B to D respectively. **, p<0.01; ***, p<0.001. E. Another mammary gland from the same mice

Figure 2.2 (cont'd)
was used to isolate total proteins. Lysates were immunoblotted with anti-pSTAT3 antibodies. Representative immunoblots are shown on the left and quantification of all samples by ImageJ is shown on the right. Results were normalized to vinculin and then expressed as fold control. *, $p<0.05$ vs control. F. Another mammary gland in the mice was fixed in formalin and sectioned for IHC. pSTAT3 staining is indicated in brown. Representative images are shown in F (x200 magnification). b.i.d., twice daily.

STAT3 plays a critical role in the crosstalk between cancer and immune cells [36]. As a point of convergence of many important oncogenic signaling pathways, STAT3 is constitutively activated in cell types. Activation of STAT3 inhibits the activation of dendritic cells, $CD8^+$ T cells and natural killer cells and enhances the production of immunosuppressive factors, which are associated with poor prognosis [37]. Hence, pSTAT3 expression was evaluated in the mammary gland by both Western blotting and IHC. Treatment with I-BET 762 significantly ($p<0.05$) decreased expression of pSTAT3 in both the short (Figure 2.2 E) and longer-term (Figure 2.3 D) protocols. With short-term treatment, decreased pSTAT3 expression (Figure 2.2 F) was mainly observed in immune cells surrounding early lesions, whereas pSTAT3 was also greatly decreased within tumor cells in the longer term protocol (Figure 2.3 E).

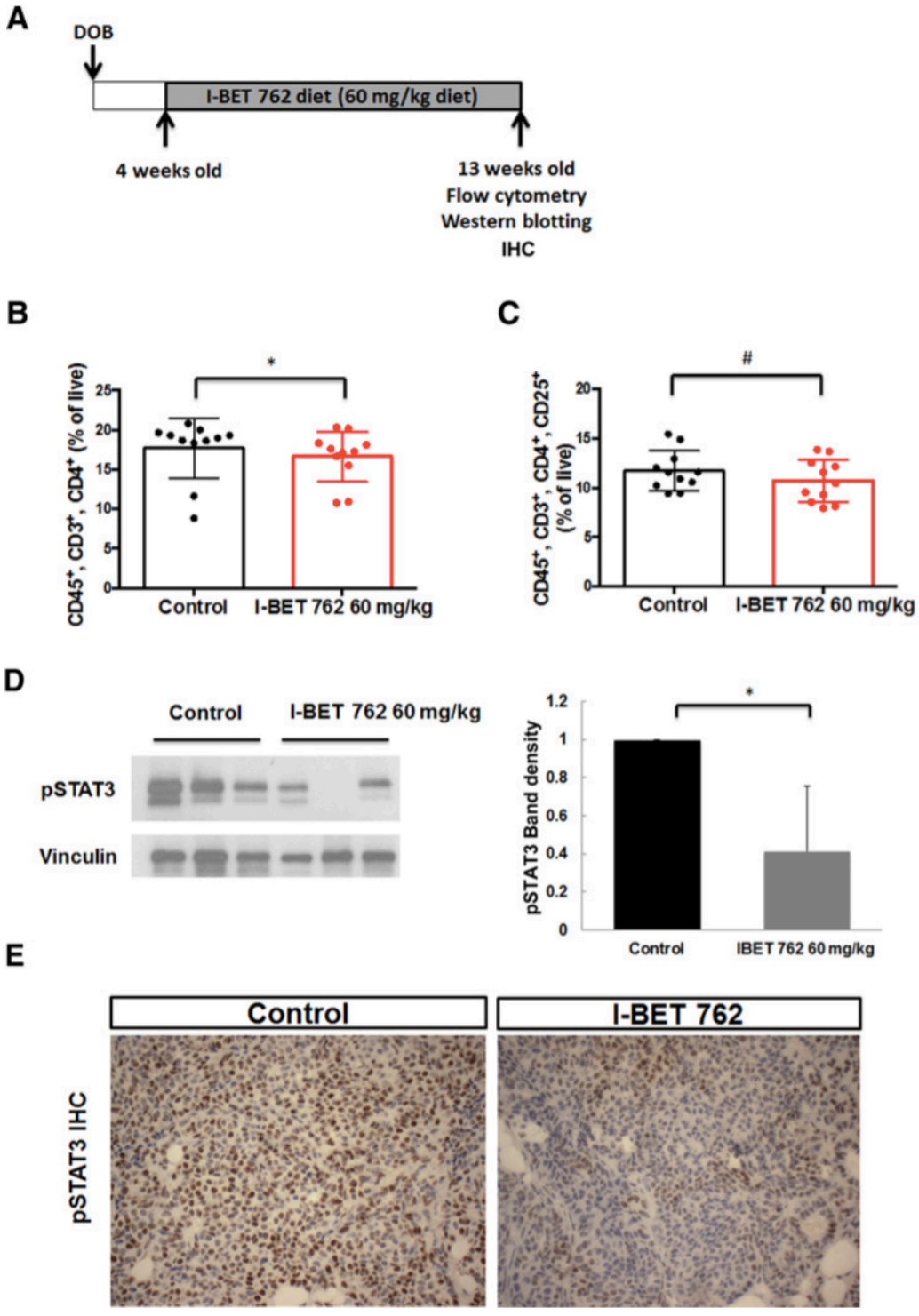

Figure 2.3. Long-term treatment with I-BET 762 reduces the infiltration of CD4$^+$ Th cells and decreases pSTAT3 expression in the mammary gland. A. Timeline of the longer term treatment protocol (n=11/group). The immune cell populations in the mammary glands from PyMT mice were analyzed by flow cytometry. B. The percentage of Th cells (CD45$^+$, CD3$^+$, CD4$^+$) in the mammary gland is significantly (*, $p<0.05$) lower

Figure 2.3 (cont'd)
in the group treated with I-BET 762 than controls. C. Percentage of activated T helper cells ($CD45^+$, $CD3^+$, $CD4^+$, $CD25^+$) in the mammary gland is also decreased (#, p=0.08 vs. controls). D. Protein extracts from the mammary gland were used to detect pSTAT3 expression by Western blotting. Representative immunoblots are shown on the left and quantification by ImageJ is shown on the right. Results were normalized to vinculin and expressed as fold control. *, $p<0.05$. E. pSTAT3 expression was confirmed by IHC on sections of mammary gland. Positive staining is indicated in brown. Representative pictures are shown at x400 magnification.

2.4.4 I-BET 762 prevents lung carcinogenesis in A/J mice challenged with vinyl carbamate

The anti-tumor effect of bromodomain inhibitors is not limited to a single cancer type. Besides breast cancer, these compounds have been shown to suppress growth of lung cancer cell lines and sensitize these cells to proapoptotic agents [38, 39]. However, the efficacy of bromodomain inhibitors for prevention of lung cancer has not been investigated. The A/J mouse model is widely used to evaluate chemopreventive agents for lung cancer [40, 41]. These mice can develop adenomas spontaneously in the lung, but injection of the carcinogen vinyl carbamate can induce invasive lung adenocarcinomas [28]. Vinyl carbamate induces *Kras* mutations [42], which are the most frequent mutations found in human lung cancers [43], especially in smokers and Caucasian patients [44]. Because urethane and carcinogens found in cigarette smoke such as NNK (a nitrosamine ketone derived from nicotine) only induce adenomas, the use of vinyl carbamate in A/J mice is more clinically relevant. In this study, female A/J mice were injected intraperitoneally with 0.32 mg vinyl carbamate to induce lung adenocarcinomas. One week after initiation, the mice were fed control diet or I-BET 762 in diet for 16 weeks. Then tumor number, size and histopathology were evaluated using published criteria [28]. In our first study, two doses of I-BET 762 (60 and 120 mg/kg diet

or approximately 15 and 30 mg/kg body weight) were tested (Table 2.1). Strikingly, treatment with I-BET 762 significantly ($p<0.05$) reduced the average number of grossly visible tumors on the inflated left lung from 12.4±0.6 tumors in the control group to only 3.7±0.6 in mice fed the highest concentration of I-BET 762, a reduction of 70%. Although the percentage of grossly visible small tumors (< 0.5 mm in diameter) was only 2.5% in the control group, 63% of the tumors in the I-BET 762 120 group were small ($p<0.05$ vs. control). Notably, not a single tumor in either group treated with I-BET was larger than 1 mm in diameter, while nearly 10% of the control tumors had grown to this size. To evaluate the histopathology, lungs were sectioned, randomized and the groups blinded. Impressively, the high dose of I-BET 762 significantly ($p<0.05$) reduced the average tumor number by 78% (from 3.84±0.25 to 0.86±0.19 per slide), average tumor size by 83% (from 0.33±0.03 mm^3 to 0.06±0.01 mm^3), and average tumor burden by 96% (from 1.26±0.14 mm^3 to 0.05±0.01 mm^3). Even with half of this dose (with 60 mg/kg diet), I-BET 762 still significantly ($p<0.05$) reduced the grossly visible tumors on the surface of left lung, and no large tumors (> 1mm in diameter) were found. At this lower dose, I-BET 762 also caused a 64% reduction in tumor size and a nearly 80% decrease in average tumor burden ($p<0.05$ vs. control for both characteristics).

Histopathology was evaluated based on two criteria (histological and nuclear), as published previously [28]. The percentage of high-grade tumor (HH), high for both histological and nuclear characteristics, such as fused trabecular architecture, distinct nucleoli and conspicuous mitoses, was 51% in the control group but only 5% to 13% in mice fed I-BET 762 ($p<0.05$). The percentage of low-grade tumors (LL) was also significantly higher in the treated groups (28%-32%) vs. the control group (2%). These

doses were well-tolerated with no observed adverse effects; average body weights at the end of the study were 21.7±2.4 g in the controls, 22.5±1.7 g in the I-BET 60 group, and 20.7±1.5 g in the I-BET 120 group.

Because impressive efficacy was observed in this first lung experiment, a lower dose of I-BET 762 (40 mg/kg diet or approximately 10 mg/kg body weight) was tested, alone and in combination with the rexinoid LG100268 (40 mg/kg diet). Rexinoids are selective ligands for RXRs (Retinoid X Receptors) with known anti-inflammatory and antitumor effects [29, 45]. LG100268 potently suppressed tumor development in this lung cancer model [27]. In addition, the combination of I-BET 762 and LG100268 was more effective than either drug alone for suppressing inducible nitric oxide synthase in macrophage-like cells (data not shown). This *in vitro* assay correlates well with efficacy in the A/J lung carcinogenesis model. The combination of I-BET 762 and LG100268 was therefore tested to investigate potential synergistic effects *in vivo*. Even though the concentration of I-BET 762 was reduced to only 40 mg/kg diet, a significant ($p<0.05$) reduction in tumor number (52%), size (60%), and burden (81%) were still observed in the mice (Table 2.2 and Figure 2.4 A). The efficacy in the combination group was not significantly different than I-BET 762 or LG100268 alone; lower doses of both drugs should be evaluated in future studies. The I-BET diets were well tolerated with no significant differences in body weight (23.6±3.4 g in control group vs. 24.1±2.5 g in the I-BET 762 group after 16 weeks on diet).

2.4.5 I-BET 762 induces growth arrest and downregulation of pSTAT3 and pERK in lung cancer *in vitro* and *in vivo*

To elucidate biomarkers of I-BET 762 efficacy in lung cancer, tumor cells were first

evaluated. Both A549 (a human non-small cell lung cancer cell line) and VC-1 (primary cells isolated from a lung tumor in an A/J mouse) cells were treated with I-BET 762 for 24-48 hours. With I-BET 762 treatment, protein levels of p27 increased, while Cyclin D1 and c-Myc expression decreased (Figure 2.4 B and C). Lungs from the mouse model were homogenized and immunoblotted. Cyclin D1, pSTAT3, pERK, and PCNA were all significantly decreased in the lungs of mice treated with I-BET 762 (Figure 2.4 D). C-Myc was expressed at very low levels in lung tissue, and no differences were detected between groups (data not shown). Kras mutations induced by vinyl carbamate activate downstream targets like ERK, and pERK expression was significantly decreased by I-BET 762 in the lung tumors (Figure 2.4 D), as confirmed by IHC (Figure 2.4 E). Proliferation in the tumor was also significantly inhibited by I-BET 762 treatment, as shown by PCNA staining (Figure 2.4 E).

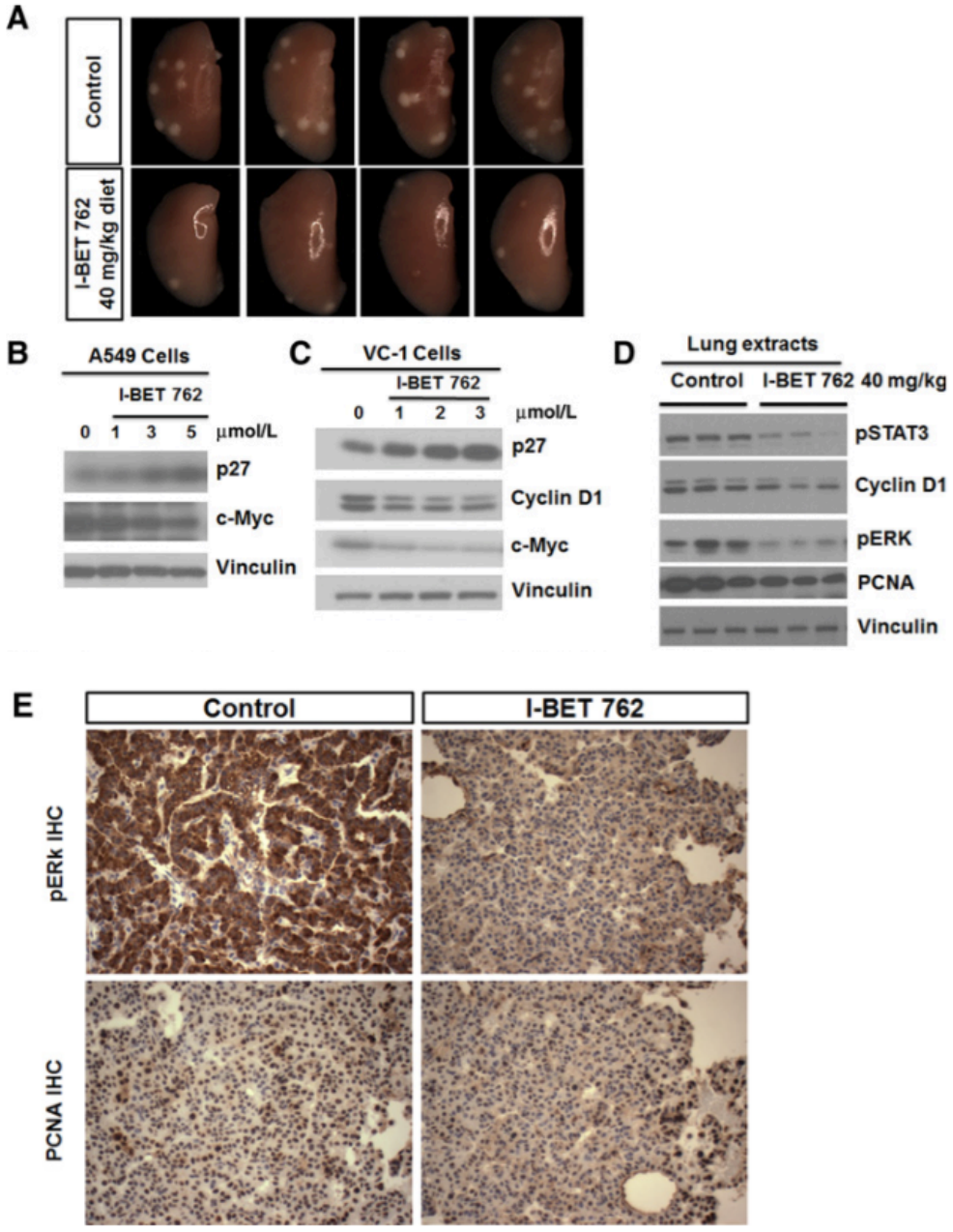

Figure 2.4. I-BET 762 prevents lung carcinogenesis in A/J mice. Female A/J mice were initiated with vinyl carbamate. The mice were then randomized and fed control diet or IBET 762 (40 mg/kg diet), starting one week after initiation with vinyl carbamate. After 16 weeks of treatment, lungs were harvested to examine tumor burden. A. Representative images of left lungs in each group (x10 magnification). A549 lung cancer cells (B) and primary VC-1 cells (C) isolated from lung tumors in A/J mice were treated with different concentrations of I-BET 762 for 48 or 24 hours, respectively. Protein expression in these cells or lung extracts (D) were analyzed by Western blotting. Changes in pERK and PCNA expression in the tumor were confirmed by IHC (E); positive staining is indicated in brown. Representative pictures are shown at x400 magnification, n=5 lungs per group.

2.4.6 I-BET 762 increases $CD45^+$ immune cells and decreases macrophages in the lung

JQ1 has been shown to attenuate the function of immunosuppressive T regulatory cells in an NSCLC model [46], indicating the potential immunomodulatory role of bromodomain inhibitors. Two lobes of the right lung were freshly homogenized and prepared for flow cytometry as described above. The $CD45^+$ immune cell population ($CD45^+$/live cells) was significantly ($p<0.05$) higher and the macrophage ($CD45^+$, $CD11b^+$, $Gr1^-$) population lower in the lungs of mice treated with I-BET 762 (Figure 2.5 A and B) vs. controls, but there were no significant differences in T-cell populations. The changes in $CD45^+$ (Figure 2.5 C) and macrophages (Figure 2.5 D) were confirmed by IHC on the lung sections. There was no difference in alveolar macrophages between groups as only macrophages near lung tumors were reduced in the group treated with I-BET 762.

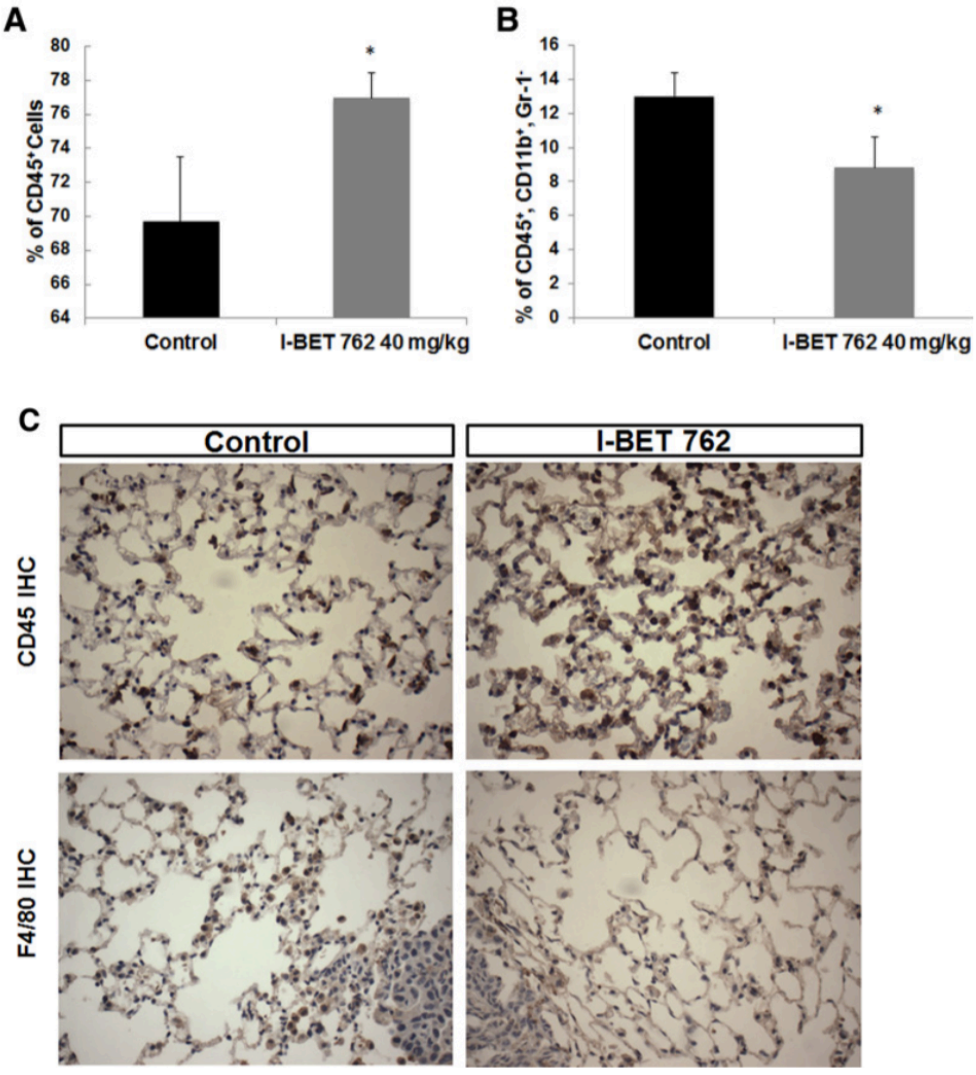

Figure 2.5. I-BET 762 increases the infiltration of CD45$^+$ immune cells and decreases the percentage of macrophages in the lungs of A/J mice challenged with vinyl carbamate. Two lobes of lung from A/J mice were isolated and processed immediately for flow cytometry to detect total immune cells (CD45$^+$, A) and macrophages (CD45$^+$, CD11b$^+$ Gr1$^-$ in B or F4/80$^+$ in C) in the lung. The changes were confirmed by IHC, as shown in C at x400 magnification. *, $p<0.05$ vs. control, n = 4-8 lungs per group.

2.5 Discussion

Bromodomains are an attractive target for cancer therapeutics and have been intensively studied as treatment in many cancer types [47]. Several studies reported the antiproliferative effects of bromodomain inhibitors in breast cancer cell lines and a

reduction of tumor mass in xenograft mouse models [48-50]. Arrested tumor growth by bromodomain inhibitors has also been shown in preclinical models of lung cancer. These drugs also triggered significant tumor regression and prolonged survival in mouse models of lung cancer initiated by KRAS mutations [51, 52]. In contrast to these previous treatment studies, our study provides direct evidence of effective chemoprevention by the potent bromodomain inhibitor I-BET 762 in relevant preclinical models of both breast and lung cancer. This bromodomain inhibitor not only significantly induced growth arrest and downregulation of oncoproteins and downstream effector proteins like c-Myc, pSTAT3 and pERK in tumor cells but also altered various immune populations within the tumor microenvironment.

Although I-BET 762 did not prevent the development of all tumors, but only delayed and reduced tumor burden in our models, no drug will be able to completely stop all tumor development. The available animal models used to study chemoprevention and carcinogenesis are genetically manipulated or challenged with high doses of carcinogens and thus develop multiple tumors with a very short latency. In humans, tumors are usually not detected until decades after the initiating event, even in smokers, and the incidence is not usually as high as in animal studies. However, any drug that significantly increases tumor latency or suppresses malignancy is likely to have a profoundly positive impact on the quality of life in people [53].

Interestingly, I-BET 762 was more effective and potent in the lung cancer model than in the breast cancer model. Notably, the lung tumors in A/J mouse model induced by vinyl carbamate are *Kras* dependent, whereas MMTV-PyMT tumors are driven by the polyomavirus middle T-antigen, which is not found in human breast cancer. Activating

mutations in *Ras* drive a variety of cancers, including melanomas, gliomas, pancreatic cancer and lung cancer [20, 51, 54], which are all sensitive to bromodomain inhibitors. In addition, a panel of lung cancer cell lines including NSCLC and small cell lung cancer harboring different oncogenic mutations have different susceptibilities to bromodomain inhibitors [39], indicating the involvement of the BET protein in different signaling pathways. Further studies are needed to better understand the mechanisms of bromodomain inhibitors in different cancer populations, and biomarkers need to be developed to predict the response in patients.

The immunomodulatory effects of bromodomain inhibitors for cancer prevention need to be emphasized in addition to the more widely studied suppression of oncogenic pathways. Inflammation is known to promote the progression of premalignant lesions and tumor growth [55]. As suggested by the “seed and soil” hypothesis, an appropriate host microenvironment (the soil) is necessary for the growth of tumor cells (the seed) [56]. In cancer prevention, when tumors are premalignant or too small to be detected, modulation of the stromal microenvironment is extremely important for preventing the development of immune tolerance and tumor progression [57, 58]. Notably, immunomodulatory activity has been reported for many chemopreventive agents [59], and emerging evidence supports the critical role of targeting the microenvironment for the efficacy of chemoprevention. Keenan and colleagues have reported that prevention of murine pancreatic ductal adenocarcinoma is feasible with Listeria vaccine and simultaneous depletion of proinflammatory immune cells [60]. In a recent clinical trial targeting MUC1 (Mucin 1, cell surface associated) in patients with premalignant colorectal adenomas, nonresponders had a significantly higher percentage of

immunosuppressive cells like myeloid-derived suppressor cells [61]. The finding of increased $CD45^+$ cells in the lungs of mice treated with I-BET 762 suggests a more active immune response that could halt or reverse tumor development, and we are designing new experiments to address this question. Although the magnitude of the changes in immune cell numbers are small, they are functionally significant as there is a decrease in activated Th cells ($CD25^+$), which are immunosuppressive and predict for poor survival in cancer patients [62]. In addition, we have previously shown that I-BET 762 decreases expression of markers of M2 tumor-promoting macrophages toward an antitumor M1 phenotype [23]. Bromodomain inhibitors also might be useful if used in combination with immunotherapy to enhance the anti-tumor response. JQ-1 has been shown to help maintain the function of $CD8^+$ cytotoxic T cells and enhance the persistence of T cells in adoptive immunotherapy models [63]. JQ-1 also downregulates the expression of PD-L1, and its combination with anti-PD-1 antibodies caused synergistic responses in Myc-driven lymphomas [64].

Despite the promising preclinical data with bromodomain inhibitors, some investigators are urging caution with the numerous clinical trials for these drugs and suggest that clinical efforts are “running ahead of the science” [65]. Bromodomain inhibitors have been shown to reactivate HIV in human cells [66] and inhibit erythroid maturation in both erythroid cells lines and primary mouse erythroblasts [67]. In addition, BET proteins are required for a variety of cellular activities, and each one regulates distinct transcriptional pathways. To understand the toxicity profile of bromodomain inhibitors, the role of each BET protein needs to be investigated; synthesis of drugs targeting specific BET protein appear to be feasible [68]. Optimized dosing and

treatment schedules also need to be further explored.

In drugs used for prevention, safety must be a top priority. In our studies, effective doses of I-BET 762 (40-60 mg/kg diet, approximately 10-15 mg/kg body weight) were strikingly 3-5 fold lower than used for treatment of cancer in preclinical models [69, 70]. The doses used for prevention were well-tolerated by the mice with no obvious toxicity, and it is possible that even lower concentrations could be used, especially if I-BET 762 is used in combination with other potent chemopreventive agents that work through different mechanisms. Drug combinations, intermittent dosing, and targeting high risk individuals are some of the strategies that can be used for effective cancer prevention in the clinic [3, 71]. Additional studies are needed to determine what dose, drug combinations, and molecular characteristics would be most appropriate for intervention or prevention with a safe and effective bromodomain inhibitor.

Table 2.1: I-BET 762 reduces lung carcinogenesis in A/J mice

	Control	I-BET 762 60 mg/kg diet	I-BET 762 120 mg/kg diet
Inflated lungs:			
# of mice/group	28	12	11
# of tumors/group	348	118	41
# of tumors/lung	12.4 ± 0.6	9.8 ± 0.9 *	3.7 ± 0.6 **
(% control)	(100%)	(79%)	(30%)
# of tumors < 0.5 mm (% of total tumors)	9 (2.5%)	20 (17%) **	26 (63%) **
# of tumors > 1 mm (% of total tumors)	33 (9.5%)	0**	0ǂ
Slides:			
# of slides/group	56	24	22
Average # of tumors/slide	3.84 ± 0.25	2.25 ± 0.36 *	0.86 ± 0.19 *
(% control)	(100%)	(58.6%)	(22.5%)
Average tumor size, mm^3	0.33 ± 0.03	0.12 ± 0.02 *	0.06 ± 0.01 *
(% control)	(100%)	(35.9%)	(17.2%)
Average tumor burden, mm^3	1.26 ± 0.14	0.27 ± 0.06 *	0.05 ± 0.01 *
(% control)	(100%)	(21%)	(3.9%)
Histopathology:			
Total # LL Grade (% of total tumors)	4 (2%)	15 (28%) **	6 (32%) **
Total # LH/HL Grade (% of total tumors)	102 (47%)	32 (59%)	12 (63%)
Total # HH Grade (% of total tumors)	109 (51%)	7 (13%) **	1 (5%) **

Note: Female A/J mice were injected i.p. with 0.32 mg vinyl carbamate and were randomized into either control group fed AIN-93G diet or treatment groups fed I-BET 762 in the diet, starting one week after initiation with vinyl carbamate. After 16 weeks of treatment, lungs were harvested. The tumor number, size and histopathology were assessed in a blinded fashion by two independent investigators. Results are presented as mean±SEM. *, $p < 0.05$ vs. control; **, $p < 0.001$ vs. control, ǂ, $p = 0.078$ vs. control.

Table 2.2: The combination of I-BET 762 and the rexinoid LG100268 for prevention of lung carcinogenesis

	Control	IBET 762 40 mg/kg diet	LG100268 40 mg/kg diet	I-BET762+LG268 40 mg each drug/kg diet
Inflated lungs:				
# of mice/group	24	12	12	12
# of tumors/group	188	60	62	57
# of tumors/lung (% control)	7.8±0.5 (100%)	5.0±0.5* (63.8%)	5.2±0.6* (66%)	4.8±0.7* (60.6%)
# of tumors < 0.5 mm (% of total tumors)	5 (2.7%)	7* (11.7%)	9** (14.5%)	13** (22.8%)
# of tumors > 1 mm (% of total tumors)	21 (11.2%)	1* (1.7%)	6 (9.7%)	1 (1.8%)
Slides:				
# of slides/group	48	24	24	24
# of tumors/group	92	22	39	19
Average # of tumors/slide (% control)	1.92±0.25 (100%)	0.92±0.15* (47.8%)	1.63±0.32 (84.8%)	0.79±2* (41.3%)
Average Tumor Size, mm^3 (% control)	0.24±0.09 (100%)	0.10±0.02* (39.8%)	0.11±0.02* (45.8%)	0.10±0.03* (42.5%)
Average Tumor Burden, mm^3 (% control)	0.47±0.19 (100%)	0.09±0.02* (19.1%)	0.18±0.04 (38.8%)	0.08±0.03* (17.5%)
Histopathology:				
Total # LL Grade	4 (4%)	1 (5%)	1 (3%)	3 (16%)

Table 2.2 (cont'd)

(% of total tumors)				
Total # LH/HL Grade (% of total tumors)	53 (58%)	16 (73%)	22 (56%)	12 (63%)
Total # HH Grade (% of total tumors)	35 (38%)	5 (23%)	16 (41%)	4 (21%)

Note: The same model was used as Table 1, but a lower concentration of I-BET 762 and a potent rexinoid (LG100268) were tested. The tumor number, size and histopathology were again assessed in a blinded fashion by two independent investigators. Results are shown as mean±SEM. *, $p < 0.05$ vs. control; **, $p < 0.001$ vs. control.

REFERENCES

REFERENCES

1. Siegel RL, Miller KD, Jemal A. Cancer Statistics, 2017. CA Cancer J Clin. 2017; 67: 7-30.

2. Gompel A. Breast cancer incidence rates in US women are no longer declining. Climacteric. 2011; 14: 690-1.

3. Meyskens FL, Jr., Mukhtar H, Rock CL, Cuzick J, Kensler TW, Yang CS, et al. Cancer Prevention: Obstacles, Challenges and the Road Ahead. J Natl Cancer Inst. 2016; 108: djv309.

4. Fisher B, Costantino JP, Wickerham DL, Redmond CK, Kavanah M, Cronin WM, et al. Tamoxifen for prevention of breast cancer: report of the National Surgical Adjuvant Breast and Bowel Project P-1 Study. J Natl Cancer Inst. 1998; 90: 1371-88.

5. Martino S, Cauley JA, Barrett-Connor E, Powles TJ, Mershon J, Disch D, et al. Continuing outcomes relevant to Evista: breast cancer incidence in postmenopausal osteoporotic women in a randomized trial of raloxifene. J Natl Cancer Inst. 2004; 96: 1751-61.

6. Goss PE, Ingle JN, Ales-Martinez JE, Cheung AM, Chlebowski RT, Wactawski-Wende J, et al. Exemestane for breast-cancer prevention in postmenopausal women. N Engl J Med. 2011; 364: 2381-91.

7. Vogel VG, Costantino JP, Wickerham DL, Cronin WM, Cecchini RS, Atkins JN, et al. Update of the National Surgical Adjuvant Breast and Bowel Project Study of Tamoxifen and Raloxifene (STAR) P-2 Trial: Preventing breast cancer. Cancer Prev Res (Phila). 2010; 3: 696-706.

8. Cuzick J, Sestak I, Bonanni B, Costantino JP, Cummings S, DeCensi A, et al. Selective oestrogen receptor modulators in prevention of breast cancer: an updated meta-analysis of individual participant data. Lancet. 2013; 381: 1827-34.

9. Mallick S, Benson R, Julka PK. Breast cancer prevention with anti-estrogens: review of the current evidence and future directions. Breast Cancer. 2016; 23: 170-7.

10. Fisher B, Costantino JP, Redmond CK, Fisher ER, Wickerham DL, Cronin WM. Endometrial cancer in tamoxifen-treated breast cancer patients: findings from the National Surgical Adjuvant Breast and Bowel Project (NSABP) B-14. J Natl Cancer Inst. 1994; 86: 527-37.

11. Lung cancer: despite advances, prevention is still best. Lancet. 2016; 388: 533.

12. Coyle KM, Boudreau JE, Marcato P. Genetic Mutations and Epigenetic Modifications: Driving Cancer and Informing Precision Medicine. Biomed Res Int. 2017; 2017: 9620870.

13. Sharma S, Kelly TK, Jones PA. Epigenetics in cancer. Carcinogenesis. 2010; 31: 27-36.

14. Huang J, Plass C, Gerhauser C. Cancer chemoprevention by targeting the epigenome. Curr Drug Targets. 2011; 12: 1925-56.

15. Chung CW, Witherington J. Progress in the discovery of small-molecule inhibitors of bromodomain--histone interactions. J Biomol Screen. 2011; 16: 1170-85.

16. Dawson MA, Prinjha RK, Dittmann A, Giotopoulos G, Bantscheff M, Chan WI, et al. Inhibition of BET recruitment to chromatin as an effective treatment for MLL-fusion leukaemia. Nature. 2011; 478: 529-33.

17. Filippakopoulos P, Qi J, Picaud S, Shen Y, Smith WB, Fedorov O, et al. Selective inhibition of BET bromodomains. Nature. 2010; 468: 1067-73.

18. French CA. NUT midline carcinoma. Cancer Genet Cytogenet. 2010; 203: 16-20.

19. Zuber J, Shi J, Wang E, Rappaport AR, Herrmann H, Sison EA, et al. RNAi screen identifies Brd4 as a therapeutic target in acute myeloid leukaemia. Nature. 2011; 478: 524-8.

20. Garcia PL, Miller AL, Kreitzburg KM, Council LN, Gamblin TL, Christein JD, et al. The BET bromodomain inhibitor JQ1 suppresses growth of pancreatic ductal adenocarcinoma in patient-derived xenograft models. Oncogene. 2016; 35: 833-45.

21. Zhang C, Su ZY, Wang L, Shu L, Yang Y, Guo Y, et al. Epigenetic blockade of neoplastic transformation by bromodomain and extra-terminal (BET) domain protein inhibitor JQ-1. Biochem Pharmacol. 2016; 117: 35-45.

22. Chakraborty D, Benham V, Bullard B, Kearney T, Hsia HC, Gibbon D, et al. Fibroblast growth factor receptor is a mechanistic link between visceral adiposity and cancer. Oncogene. 2017.

23. Leal AS, Williams CR, Royce DB, Pioli PA, Sporn MB, Liby KT. Bromodomain inhibitors, JQ1 and I-BET 762, as potential therapies for pancreatic cancer. Cancer Lett. 2017; 394: 76-87.

24. Hytti M, Tokarz P, Maatta E, Piippo N, Korhonen E, Suuronen T, et al. Inhibition of BET bromodomains alleviates inflammation in human RPE cells. Biochem Pharmacol. 2016; 110-111: 71-9.

25. Mirguet O, Gosmini R, Toum J, Clement CA, Barnathan M, Brusq JM, et al. Discovery of epigenetic regulator I-BET762: lead optimization to afford a clinical

candidate inhibitor of the BET bromodomains. J Med Chem. 2013; 56: 7501-15.

26. Guy CT, Cardiff RD, Muller WJ. Induction of mammary tumors by expression of polyomavirus middle T oncogene: a transgenic mouse model for metastatic disease. Mol Cell Biol. 1992; 12: 954-61.

27. Cao M, Royce DB, Risingsong R, Williams CR, Sporn MB, Liby KT. The Rexinoids LG100268 and LG101506 Inhibit Inflammation and Suppress Lung Carcinogenesis in A/J Mice. Cancer Prev Res (Phila). 2016; 9: 105-14.

28. Liby K, Royce DB, Williams CR, Risingsong R, Yore MM, Honda T, et al. The synthetic triterpenoids CDDO-methyl ester and CDDO-ethyl amide prevent lung cancer induced by vinyl carbamate in A/J mice. Cancer Res. 2007; 67: 2414-9.

29. Liby KT, Sporn MB. Rexinoids for prevention and treatment of cancer: opportunities and challenges. Curr Top Med Chem. 2017; 17: 721-30.

30. Lin EY, Nguyen AV, Russell RG, Pollard JW. Colony-stimulating factor 1 promotes progression of mammary tumors to malignancy. J Exp Med. 2001; 193: 727-40.

31. Delmore JE, Issa GC, Lemieux ME, Rahl PB, Shi J, Jacobs HM, et al. BET bromodomain inhibition as a therapeutic strategy to target c-Myc. Cell. 2011; 146: 904-17.

32. Mertz JA, Conery AR, Bryant BM, Sandy P, Balasubramanian S, Mele DA, et al. Targeting MYC dependence in cancer by inhibiting BET bromodomains. Proc Natl Acad Sci U S A. 2011; 108: 16669-74.

33. Toyoshima H, Hunter T. p27, a novel inhibitor of G1 cyclin-Cdk protein kinase activity, is related to p21. Cell. 1994; 78: 67-74.

34. Nicodeme E, Jeffrey KL, Schaefer U, Beinke S, Dewell S, Chung CW, et al. Suppression of inflammation by a synthetic histone mimic. Nature. 2010; 468: 1119-23.

35. Tran K, Risingsong R, Royce D, Williams CR, Sporn MB, Liby K. The synthetic triterpenoid CDDO-methyl ester delays estrogen receptor-negative mammary carcinogenesis in polyoma middle T mice. Cancer Prev Res (Phila). 2012; 5: 726-34.

36. Huynh J, Etemadi N, Hollande F, Ernst M, Buchert M. The JAK/STAT3 axis: A comprehensive drug target for solid malignancies. Semin Cancer Biol. 2017; 45: 13-22.

37. Yu H, Kortylewski M, Pardoll D. Crosstalk between cancer and immune cells: role of STAT3 in the tumour microenvironment. Nat Rev Immunol. 2007; 7: 41-51.

38. Klingbeil O, Lesche R, Gelato KA, Haendler B, Lejeune P. Inhibition of BET bromodomain-dependent XIAP and FLIP expression sensitizes KRAS-mutated NSCLC to pro-apoptotic agents. Cell Death Dis. 2016; 7: e2365.

39. Riveiro ME, Astorgues-Xerri L, Vazquez R, Frapolli R, Kwee I, Rinaldi A, et al. OTX015 (MK-8628), a novel BET inhibitor, exhibits antitumor activity in non-small cell and small cell lung cancer models harboring different oncogenic mutations. Oncotarget. 2016; 7: 84675-87.

40. Gorelik E, Herberman RB. Susceptibility of various strains of mice to urethan-induced lung tumors and depressed natural killer cell activity. J Natl Cancer Inst. 1981; 67: 1317-22.

41. Bauer AK, Malkinson AM, Kleeberger SR. Susceptibility to neoplastic and non-neoplastic pulmonary diseases in mice: genetic similarities. Am J Physiol Lung Cell Mol Physiol. 2004; 287: L685-703.

42. You M, Candrian U, Maronpot RR, Stoner GD, Anderson MW. Activation of the Ki-ras protooncogene in spontaneously occurring and chemically induced lung tumors of the strain A mouse. Proc Natl Acad Sci U S A. 1989; 86: 3070-4.

43. Jackman DM, Miller VA, Cioffredi LA, Yeap BY, Janne PA, Riely GJ, et al. Impact of epidermal growth factor receptor and KRAS mutations on clinical outcomes in previously untreated non-small cell lung cancer patients: results of an online tumor registry of clinical trials. Clin Cancer Res. 2009; 15: 5267-73.

44. Guibert N, Ilie M, Long E, Hofman V, Bouhlel L, Brest P, et al. KRAS Mutations in Lung Adenocarcinoma: Molecular and Epidemiological Characteristics, Methods for Detection, and Therapeutic Strategy Perspectives. Curr Mol Med. 2015; 15: 418-32.

45. Liby KT, Yore MM, Sporn MB. Triterpenoids and rexinoids as multifunctional agents for the prevention and treatment of cancer. Nat Rev Cancer. 2007; 7: 357-69.

46. Adeegbe D, Liu Y, Lizotte PH, Kamihara Y, Aref AR, Almonte C, et al. Synergistic Immunostimulatory Effects and Therapeutic Benefit of Combined Histone Deacetylase and Bromodomain Inhibition in Non-small Cell Lung Cancer. Cancer Discov. 2017; 7: 852-67.

47. Jung M, Gelato KA, Fernandez-Montalvan A, Siegel S, Haendler B. Targeting BET bromodomains for cancer treatment. Epigenomics. 2015; 7: 487-501.

48. Zhao Y, Bai L, Liu L, McEachern D, Stuckey JA, Meagher JL, et al. Structure-Based Discovery of 4-(6-Methoxy-2-methyl-4-(quinolin-4-yl)-9H-pyrimido[4,5-b]indol-7-yl)-3,5-dimethy lisoxazole (CD161) as a Potent and Orally Bioavailable BET Bromodomain Inhibitor. J Med Chem. 2017; 60: 3887-901.

49. Vazquez R, Riveiro ME, Astorgues-Xerri L, Odore E, Rezai K, Erba E, et al. The bromodomain inhibitor OTX015 (MK-8628) exerts anti-tumor activity in triple-negative breast cancer models as single agent and in combination with everolimus. Oncotarget. 2017; 8: 7598-613.

50. da Motta LL, Ledaki I, Purshouse K, Haider S, De Bastiani MA, Baban D, et al. The BET inhibitor JQ1 selectively impairs tumour response to hypoxia and downregulates CA9 and angiogenesis in triple negative breast cancer. Oncogene. 2017; 36: 122-32.

51. Shimamura T, Chen Z, Soucheray M, Carretero J, Kikuchi E, Tchaicha JH, et al. Efficacy of BET bromodomain inhibition in Kras-mutant non-small cell lung cancer. Clin Cancer Res. 2013; 19: 6183-92.

52. Adeegbe D, Liu Y, Lizotte PH, Kamihara Y, Aref AR, Almonte C, et al. Synergistic Immunostimulatory Effects and Therapeutic Benefit of Combined Histone Deacetylase and Bromodomain Inhibition in Non-small Cell Lung Cancer. Cancer Discov. 2017.

53. Sporn MB, Suh N. Chemoprevention: an essential approach to controlling cancer. Nat Rev Cancer. 2002; 2: 537-43.

54. De Raedt T, Beert E, Pasmant E, Luscan A, Brems H, Ortonne N, et al. PRC2 loss amplifies Ras-driven transcription and confers sensitivity to BRD4-based therapies. Nature. 2014; 514: 247-51.

55. Grivennikov SI, Greten FR, Karin M. Immunity, inflammation, and cancer. Cell. 2010; 140: 883-99.

56. Paget S. The distribution of secondary growths in cancer of the breast. 1889. Cancer Metastasis Rev. 1989; 8: 98-101.

57. Smit MA, Jaffee EM, Lutz ER. Cancer immunoprevention--the next frontier. Cancer Prev Res (Phila). 2014; 7: 1072-80.

58. Albini A, Sporn MB. The tumour microenvironment as a target for chemoprevention. Nat Rev Cancer. 2007; 7: 139-47.

59. Sharma SH, Thulasingam S, Nagarajan S. Chemopreventive agents targeting tumor microenvironment. Life Sci. 2016; 145: 74-84.

60. Keenan BP, Saenger Y, Kafrouni MI, Leubner A, Lauer P, Maitra A, et al. A Listeria vaccine and depletion of T-regulatory cells activate immunity against early stage pancreatic intraepithelial neoplasms and prolong survival of mice. Gastroenterology. 2014; 146: 1784-94 e6.

61. Kimura T, McKolanis JR, Dzubinski LA, Islam K, Potter DM, Salazar AM, et al. MUC1 vaccine for individuals with advanced adenoma of the colon: a cancer immunoprevention feasibility study. Cancer Prev Res (Phila). 2013; 6: 18-26.

62. Chen X, Du Y, Lin X, Qian Y, Zhou T, Huang Z. CD4+CD25+ regulatory T cells in tumor immunity. Int Immunopharmacol. 2016; 34: 244-9.

63. Kagoya Y, Nakatsugawa M, Yamashita Y, Ochi T, Guo T, Anczurowski M, et al. BET bromodomain inhibition enhances T cell persistence and function in adoptive

immunotherapy models. J Clin Invest. 2016; 126: 3479-94.

64. Hogg SJ, Vervoort SJ, Deswal S, Ott CJ, Li J, Cluse LA, et al. BET-Bromodomain Inhibitors Engage the Host Immune System and Regulate Expression of the Immune Checkpoint Ligand PD-L1. Cell Rep. 2017; 18: 2162-74.

65. Andrieu G, Belkina AC, Denis GV. Clinical trials for BET inhibitors run ahead of the science. Drug Discov Today Technol. 2016; 19: 45-50.

66. Banerjee C, Archin N, Michaels D, Belkina AC, Denis GV, Bradner J, et al. BET bromodomain inhibition as a novel strategy for reactivation of HIV-1. J Leukoc Biol. 2012; 92: 1147-54.

67. Stonestrom AJ, Hsu SC, Werner MT, Blobel GA. Erythropoiesis provides a BRD's eye view of BET protein function. Drug Discov Today Technol. 2016; 19: 23-8.

68. Liu Z, Wang P, Chen H, Wold EA, Tian B, Brasier AR, et al. Drug Discovery Targeting Bromodomain-Containing Protein 4. J Med Chem. 2017; 60: 4533-58.

69. Imayoshi N, Yoshioka M, Chauhan J, Nakata S, Toda Y, Fletcher S, et al. CG13250, a novel bromodomain inhibitor, suppresses proliferation of multiple myeloma cells in an orthotopic mouse model. Biochem Biophys Res Commun. 2017; 484: 262-8.

70. Berenguer-Daize C, Astorgues-Xerri L, Odore E, Cayol M, Cvitkovic E, Noel K, et al. OTX015 (MK-8628), a novel BET inhibitor, displays in vitro and in vivo antitumor effects alone and in combination with conventional therapies in glioblastoma models. Int J Cancer. 2016; 139: 2047-55.

71. Raj KP, Zell JA, Rock CL, McLaren CE, Zoumas-Morse C, Gerner EW, et al. Role of dietary polyamines in a phase III clinical trial of difluoromethylornithine (DFMO) and sulindac for prevention of sporadic colorectal adenomas. Br J Cancer. 2013; 108: 512-8.

CHAPTER 3

Testing Novel Pyrimidinyl Rexinoids: A New Paradigm for Evaluating Rexinoids for Cancer Prevention

Reprinted with permission from *Cancer Prevention Research*. 2019. 12(4): 211-224

Di Zhang, Ana S. Leal, Sarah Carapellucci, Pritika H. Shahani, Jaskaran S. Bhogal, Samir Ibrahim, San Raban, Peter W. Jurukta, Pamela A. Marshall, Michael B. Sporn, Carl E. Wagner, and Karen T. Liby

Author contributions:
Participated in research design: Zhang, Jurukta, Marshall, Wagner, Liby
Conducted experiments: Zhang, Leal, Carapellucci, Shahani, Bhogal, Ibrahim, Raban
Performed data analysis: Zhang, Liby
Wrote or contributed to the writing of the manuscript: Zhang, Jurukta, Marshall, Wagner, Sporn, Liby

3.1 Abstract

Rexinoids, selective ligands for retinoid X receptors (RXRs), have shown promise in preventing many types of cancer. However, the limited efficacy and undesirable lipidemic side-effects of the only clinically approved rexinoid, bexarotene, drive the search for new and better rexinoids. Here we report the evaluation of novel pyrimidinyl (Py) analogs of two known chemopreventive rexinoids, bexarotene (Bex) and LG100268 (LG268) in a new paradigm. We show that these novel derivatives were more effective agents than bexarotene for preventing lung carcinogenesis induced by carcinogen. In addition, these new analogs have an improved safety profile. PyBex caused less elevation of plasma triglyceride levels than bexarotene, while PyLG268 reduced plasma cholesterol levels and hepatomegaly compared to LG100268. Notably, this new paradigm mechanistically emphasizes the immunomodulatory and anti-inflammatory activities of rexinoids. We reveal new immunomodulatory actions of the above rexinoids, especially their ability to diminish the percentage of macrophages and myeloid-derived suppressor cells in the lung and to redirect activation of M2 macrophages. The rexinoids also potently inhibit critical inflammatory mediators including IL-6, IL-1β, CCL9 and nitric oxide synthase (iNOS) induced by lipopolysaccharide. Moreover, *in vitro* iNOS and SREBP (sterol regulatory element-binding protein) induction assays correlate with *in vivo* efficacy and toxicity, respectively. Our results not only report novel pyrimidine derivatives of existing rexinoids but also describe a series of biological screening assays that will guide the synthesis of additional rexinoids. Further progress in rexinoid synthesis, potency, and safety should eventually lead to a clinically acceptable and useful new drug for cancer patients.

3.2 Introduction

Rexinoids are selective ligands for retinoid X receptors (RXR), which regulate the expression of numerous genes [1]. Even though rexinoids were initially developed for metabolic disorders like diabetes [2], their important roles in proliferation, differentiation, and apoptosis are highly relevant to cancer [3, 4], making RXRs an attractive cancer target. The rexinoid bexarotene, is FDA approved for the treatment of cutaneous T-cell lymphoma. This drug has been tested in several clinical trials for lung cancer [5-9], and the combination of bexarotene and chemotherapeutic agents significantly improved median survival in a subset of patients with advanced non-small-cell lung cancer (NSCLC) [8, 10]. Rexinoids are also effective for prevention in a variety of preclinical cancer models, including breast cancer (MMTV-neu mouse model, nitrosomethylurea NMU rat model), lung cancer (vinyl carbamate induced A/J mouse model, and a genetically engineered mouse model of lung cancer), pancreatic cancer (KPC mouse model), and other cancers [3, 11-18]. Either as single agents or in combinations with other drugs, rexinoids significantly delayed tumor development and reduced tumor burden in prevention protocols.

In spite of their profound effects on many cellular pathways with direct relevance for the pathogenesis of human diseases [16], including cancer, diabetes, atherosclerosis and Alzheimer's disease, safe and effective rexinoids have not yet entered routine clinical practice, for either prevention or treatment of cancer or any other chronic diseases. Bexarotene has limited efficacy as a single agent. Moreover, triglyceride levels were elevated [5] and the thyroid axis suppressed in patients treated with this drug [19]. More potent and selective RXRs rexinoids have been developed, many with promising *in*

vitro activity [20-24]. LG100268 (LG268) is one of the most potent and selective of these newer rexinoids, with a 1,000 fold increase in selectivity for RXR binding compared to RAR binding [20], but elevated triglyceride levels and patent issues have prevented clinical development of this promising drug [3, 16]. Although the known side effects of rexinoids can be tolerated for treatment of cancer, they do not meet the elevated degree of safety required for long-term prevention protocols in humans.

Therefore, there is still a great need to develop new rexinoids with greater potency and less toxicity. Here, we present data from both *in vitro* and *in vivo* studies of new rexinoids, the pyrimidine (Py) derivatives of Bex and LG268. These new rexinoids were tested for their ability to prevent lung cancer and reduce side effects in a widely used A/J mouse model. When challenged with vinyl carbamate, these mice develop *Kras* mutations and adenocarcinomas, so the model is clinically relevant for evaluating new drugs for lung cancer [25]. As there is now abundant evidence that immunomodulatory and inflammatory effects play an essential role in carcinogenesis [26], we explored the immunomodulatory actions of rexinoids during lung carcinogenesis and their effects on macrophage polarization. We also screened 10 new rexinoids for their ability to suppress induction of the pro-inflammatory enzyme iNOS, an assay that correlates with suppression of carcinogenesis in this lung cancer model. In addition, their activation of RXR, as well as SREBP (sterol regulatory element-binding protein), a transcription factor involved in triglyceride synthesis, was used in initial screens to evaluate potency and toxicity, respectively. Upon validation, this set of *in vitro* assays will be used to guide the synthesis of additional compounds to generate drugs that are more effective and/or less toxic than existing rexinoids.

3.3 Materials and Methods

3.3.1 Drugs

Rexinoids were synthesized at Arizona State University as described [21, 22]. For *in vitro* assays, drugs were dissolved in DMSO to make 10 mmol/L stock concentrations and then diluted in the appropriate cell culture media (described below) to generate the final working concentrations listed in each figure or figure legend. Controls containing equivalent concentrations of DMSO were included in all experiments. For *in vivo* testing, drugs were incorporated in diet (40 mg/kg diet and 80 mg/kg diet) as previously described [14]. In brief, rexinoids were dissolved in 50 ml vehicle (1 part ethanol: 3 parts Neobee Oil, (Thermo Fisher Scientific), a highly purified coconut oil triglyceride used for formulation of drugs given to humans) per kg of diet and then mixed into powdered AIN-93M diet (BioServ, Flemington NJ) for 20 minutes using a commercial (KitchenAid) food mixer to assure homogeneity of drug in diet. Rexinoids are soluble in this vehicle, and providing drugs in diet yields better bioavailability and steady state drug levels than giving suspensions of drug as a bolus by gavage. The diets were stored in the cold room at 4°C for up to 4 weeks; we have confirmed the stability of multiple rexinoids in diet for this length of time by liquid chromatrography-mass spectometry.

3.3.2 Cell culture

RAW264.7 macrophage-like cells were purchased from the American Type Culture Collection (Manassas, VA) and cultured in DMEM media with 10% FBS and 1% penicillin/streptomycin. HepG2 cells were purchased from the American Type Culture Collection (Manassas, VA) and cultured in RPMI-1640 media with 10% FBS and 1% penicillin/streptomycin. Media and supplements were purchased from Corning Cellgro

(Mediatech, Manassas, VA). Bone marrow-derived macrophages (BMDMs) were isolated from the femurs of adult C57BL/6 mice as described previously [27]. Femurs were dissected out of the mice, and all remaining tissues removed before using scissors to cut the proximal and distal ends. The bone marrow was flushed out of the femur with 5 ml of RPMI using a 25G needle and syringe. All samples from a mouse were combined and resuspended in RPMI + 10% FBS and 1% penicillin/streptomycin.

3.3.3 iNOS (NO) assay

RAW264.7 cells were plated in 96-well plates (20,000 cells/well) and after overnight attachment, cells were treated with various concentrations of rexinoids (0-1000 nmol/L) and then stimulated with 1-2 ng/ml LPS (dissolved in saline) for 24 h. NO production was measured using the Griess reaction as described [14].

3.3.4 Cytokine RNA extraction and RT-qPCR analysis

RAW264.7 cells were treated with 300 nmol/L rexinoid and stimulated with 1 ng/ml LPS for 24 h. Bone marrow-derived macrophages (BMDMs) were cultured in RPMI 1640 media supplemented with 10% FBS and 20 ng/ml M-CSF (BioLegend) for 7 days to induce an M2 phenotype [27]. Then BMDMs were treated with 100 nM rexinoids and stimulated with 100 ng/ml LPS for 24 hours. Total RNA was isolated with TRIzol (Invitrogen, Carlsbad, CA). 2 μg of RNA was used to synthesize cDNA using the SuperScript III reverse transcriptase kit (Invitrogen, Carlsbad, CA). Validated IL-6 (PPM03015A), CCL9 (PPM02957F), IL-1β (PPM03109F), TNF-α (PPM03113G), IL-10 (PPM03017C) and β-actin (PPM02945B) primers were purchased from Qiagen (Valencia, CA). iQ SYBR Green Supermix (Bio-rad Laboratories, Hercules, CA) and the ABI 7500 FAST Real-Time PCR system were used to detect gene expression (95°C for

10 min followed by 40 cycles of 95°C for 15 s (melt) and 60°C (extend/anneal) for 1 min). The recommended protocol supplied by the manufacturer of each kit was followed for all experiments. Relative expression was calculated by the delta-delta Ct method [14].

3.3.5 Prevention of lung carcinogenesis *in vivo*

All animal studies were approved by the Institutional Animal Care and Use Committee (IACUC) at Michigan State University. Eight-week old female A/J mice (Jackson Laboratories, average weight = 20 g) were injected i.p. (16 mg/kg body weight) with vinyl carbamate (Toronto Research Chemicals). A 1.6 mg/ml stock solution of vinyl carbamate (dissolved in isotonic saline) was prepared, and approximately 200 µl injected into each mouse. One week after injection, the mice were randomized into the control group fed AIN-93G diet (BioServ, Flemington NJ) mixed with vehicle (1 part ethanol: 3 parts Neobee oil; 50 ml vehicle/kg diet) or fed rexinoids dissolved in the same vehicle and mixed into the diet [14]. After 16 weeks on diet, mice were euthanized and lungs were inflated with PBS. The entire left lobe of the lungs was fixed in neutral buffered formalin for histopathology. Right lungs were used immediately for flow cytometry (the superior and middle lobes) or were flash frozen (the other two lobes: inferior and post-caval). The tumor number, size, and histopathology were assessed on two separate sections of the left lung by two independent investigators. Sections were step sectioned (200 µM apart starting at the medial hilar section) and the slides stained with hematoxylin and eosin. The samples were coded with random numbers and then randomized before being read, thus blinding the investigators to the treatment group. The histopathology classifications were based on published criteria established by a lung pathologist [28].

3.3.6 Flow cytometry

The same two lobes (superior and middle) of the right lung were harvested from A/J mice for flow cytometry. Freshly harvested lung tissue was chopped and incubated in digestion media (DMEM media with 10% FBS and 1% penicillin/streptomycin) containing collagenase (300 U/ml, Sigma), dispase (1 U/ml, Worthington), and DNAse (2 U/ml, Calbiochem) for 30 minutes at 37°C. Cells were then passed through a 40-μm cell strainer (BD Falcon). Lysing solution (eBioscience) was used to eliminate red blood cells. Single-cell suspensions were stained with 5 μg/ml anti-mouse Fc block (eBioscience) and two optimized panels of validated antibodies for 30 min at 4°C. Panel 1: CD45-VioGreen (Miltenyi Biotec, clone 30F11，3 μg/mL), Gr-1-PE (Miltenyi Biotec, clone RB6-8C5, 3 μg/mL), CD11b-FITC (Miltenyi Biotec, clone M1/70, 3 μg/mL). Panel 2: CD45-VioGreen (Miltenyi Biotec, clone 30F11，3 μg/mL), CD4-FITC (Miltenyi Biotec, clone GK1.5, 3 μg/mL), CD3-PE (BioLegend, clone 145-2C11, 2 μg/mL), CD8-PerCP/Cy5.5 (BioLegend clone 53-6.7, 2 μg/mL). Flow cytometry was performed using a LSR II flow cytometer with DIVA 6.2 software (BD) and three laser sources (488, 633 and 407 nm). Data analysis was done using FlowJo x.10.0.7r2 software (Tree Star).

3.3.7 IHC

The entire lungs were inflated with PBS and then the entire left lobe of each lung was separated and fixed in 10% NBF for 48 hours. Lungs were then step-sectioned for histopathology and immunohistochemistry analysis. Citrate buffer (Vector, Cat. No: H3300) was used for antigen retrieval. Slides immersed in the buffer were microwaved to the boiling temperature and then kept around 90°C by microwaving another 3-5 seconds every 15-20 seconds for a total of 20 minutes. Endogenous peroxidase activity was

quenched in 3% hydrogen peroxide for 10 minutes. Sections were immunostained with CD45 (1:100, BioScience) and a biotinylated anti-rat secondary antibody (Vector Laboratories), or F4/80 (1:50, Invitrogen) antibodies and a biotinylated anti-rat secondary antibody (Vector). Signal was amplified by Vectastain ABC (Vector Laboratories) and detected using a DAB kit (Cell Signaling Technology). Sections were counterstained with hematoxylin (Vector Laboratories). Samples were coded, randomized and blinded as described above. Negative controls without primary antibody were also done to assure the quality and specificity of the primary antibodies.

3.3.8 Western blotting

HepG2 Cells treated with rexinoids were lysed in RIPA buffer (1 mol/L Tris-Cl, 5 mol/L NaCl, pH 7.4, 0.5 mol/L EDTA, 25 mmol/L deoxycholic acid, 1% Triton-X, 0.1% SDS) with protease inhibitors (1 mmol/L PMSF, 2 μg/ml aprotinin and 5 μg/ml leupeptin). The BCA assay (Sigma-Aldrich) was used to determine protein concentrations. Proteins (20 μg/well) were separated by 10% SDS-PAGE gels and transferred to nitrocellulose membranes. SREBP-1c (Active Motif, 1:1000) and vinculin (Cell Signaling Technology, 1:4000) primary antibodies were used to detect the corresponding proteins. Secondary antibodies (anti-rabbit or anti-mouse antibodies conjugated to horseradish peroxidase) were purchased from Cell Signaling Technology. Signal was detected using the ECL Western blotting substrate [14]. Images shown are representative of 3 independent experiments. Protein expression levels were quantified by ImageJ.

3.3.9 Lipid levels in plasma and liver

Sections of livers were homogenized in 5% NP-40/ddH_2O (50 mg tissue/ 1 ml solution), and total triglyceride levels in liver and plasma were evaluated using a

Triglyceride Quantification Assay Kit from Abcam. Cholesterol levels in plasma were measured using a Cholesterol Quantification Kit from Sigma-Aldrich. The recommended protocol supplied by the manufacturer of each kit was followed.

3.3.10 Screening assays for new rexinoids

New rexinoids were screened using the iNOS suppression assay described above in addition to RXR (EC_{50}) and SREBP activation. For screening, full dose-response curves were generated with ligand concentrations ranging from $1x10^{-9}$ to $0.3x10^{-5}$ mol/L in transfected HCT-116 cells (male *Homo sapiens* colorectal carcinoma epithelium) using an RXR mammalian two-hybrid system. Although not lung or liver cancer cells, these cells can be transfected with a variety of plasmids and are thus useful for screening. HCT-116 cells were plated overnight at 80,000 cells/well in 24 well plates and maintained in DMEM/high glucose (Hyclone) enhanced with 10% FBS (Invitrogen), 1 mmol/L sodium pyruvate (Invitrogen), 100 µg/mL streptomycin and 100 unit/mL penicillin. The cells were co-transfected using a human RXR binding domain (BD) vector, a human RXR activation domain (AD) vector, a luciferase reporter gene containing BD-binding sites and renilla control plasmid. Transfection was achieved via 2 µL/well of Express-IN transfection reagent (Thermo Fisher Scientific, Lafayette, CO), which was allowed to incubate for 24 h with the cells. The cells were subsequently treated with ethanol vehicle (0.1%) or analogs (1.0, 2.5, 5.0, 7.5, 10, 25, 50, 75, 100, 250, 500 nmol/L, 1, 2, 3 µmol/L) and incubated for 24 hours. The amount of rexinoid activity at each concentration was measured by luciferase output utilizing a dual-luciferase reporter assay system according to the manufacturer's protocol (Promega, Madison, WI) in a Sirus luminometer (Berthold Detection System, Pforzheim, Germany). Three independent assays were

conducted with triplicate samples for each treatment group. The EC_{50} values were derived from dose-response curves of ligand concentration versus normalized luciferase activity.

For SREBP-based screening, HCT-116 cells were maintained as above, followed by co-transfection of 250 ng of the pBP1c(6500)-Luc reporter gene which contains an LXRE in the context of about 6,500 base pairs of flanking DNA from the mouse SREBP-1c natural promoter [29] along with 50 ng of CMX-hLXRα, 50 ng of pSG5-hRXRα and 20 ng of the Renilla control plasmid. The transfection was initiated with 2 µL/well of Express-IN transfection reagent (Thermo Fisher Scientific, Lafayette, CO) used for liposome-mediated DNA delivery for 18 hours. The cells were then incubated for 24 hours post-transfection with ethanol vehicle, 10^{-7} mol/L T0901317 (LXR ligand), or 10^{-7} mol/L bexarotene or analogs. After a 24-hour incubation period, the amount of SREBP promoter activity was measured by luciferase output utilizing a dual-luciferase reporter assay system according to the manufacturer's protocol (Promega, Madison, WI) in a Sirius luminometer (Berthold Detection System, Pforzheim, Germany). Data were expressed as the percentage of T0901317-induced SREPB activation. Three independent assays were conducted with triplicate samples for each treatment group.

3.3.11 Statistical analysis

The *in vitro* experiments were performed in triplicate samples of each concentration of drug, and independent experiments were repeated at least three times. Results were expressed as the mean±SD or mean±SEM as indicated in each specific figure or table. For the *in vitro* and *in vivo* experiments, results were analyzed using the two-tailed t test when only two groups were compared (Figure 3.4 D); when more than two groups were

compared, data were analyzed using one-way ANOVA followed by a Tukey test for multiple comparisons (to control the type I error) if the data fit a normal distribution; the Kruskal-Wallis one-way ANOVA on ranks was used followed by the Dunn test for multiple comparisons if the data did not fit a normal distribution (SigmaStat 3.5). For the histopathology, McNemar's Z test was used to compare proportions. $p<0.05$ was considered statistically significant. A Benjamini-Hochberg procedure with false discovery rate of 25% was performed for the *in vivo* study (including tumor number, tumor size, tumor burden, liver weight and cholesterol level in the plasma), all the p values with this procedure were smaller than the original calculated p value.

3.4 Results

3.4.1 PyBex and PyLG268 are more effective than bexarotene for preventing lung carcinogenesis in A/J mice

In an effort to develop more potent and selective rexinoids, pyrimidine derivatives of LG268 (PyLG268) and bexarotene (PyBex) were synthesized (Figure 3.1 A). These two derivatives were tested *in vivo* because they were similar in potency to Bex but gave higher plasma concentrations at Cmax than Bex and produced differential gene expression in Sprague Dawley rats [30]. In the present experiments, A/J mice were injected i.p. with vinyl carbamate. As confirmed in our model, vinyl carbamate induced a mutation in codon 61 of the *Kras* gene as well as additional mutations across all of the chromosomes.

One week after initiation, the mice were fed control diet or rexinoids in diet (40-80 mg/kg diet) for 16 weeks. Tumor number, size, and burden were then evaluated, and Table 3.1 summarizes these results. Despite a trend toward lower tumor numbers in the

rexinoid-treated mice (Figure 3.1 B and Table 3.1), only high dose LG268 (80 mg/kg diet) significantly ($p<0.05$) reduced the average number of tumors, by 61%. All of the high dose (80 mg/kg diet) rexinoid groups significantly ($p<0.05$) reduced the average size of the lung tumors (Table 3.1) by 49-69% (range 0.07 ± 0.01 mm^3 to 0.12 ± 0.02 mm^3 vs. controls 0.24 ± 0.09 mm^3).

The average tumor burden on lung sections was markedly reduced by PyBex and PyLG268 by 59% and 53% (40 mg/kg diet doses) compared to the controls (from 0.47 ± 0.19 mm^3 in the control group to 0.19 ± 0.05 mm^3 in the group treated with PyBex and 0.22 ± 0.05 mm^3 in the PyLG268-treated group). In contrast, average tumor burden was 0.35 ± 0.08 mm^3 in the group treated with the low dose (40 mg/kg diet) of bexarotene, a reduction of only 26%. Again, LG268 was the best rexinoid and reduced average tumor burden by 88%, to 0.06 ± 0.02 mm^3 vs 0.47 ± 0.19 mm^3 in the control group.

Although the effects on tumor number and size were not changed with the low doses of rexinoids, the severity of the lesions was reduced. Notably, the percentage of high grade tumors (HH, both histological and nuclear characteristics such as tumefactive fused trabecular architecture, distinct nucleoli and conspicuous mitoses, as shown Figure 3.1 C) were significantly ($p<0.05$) higher (Figure 3.1 D) in the mice fed bexarotene (63%, 40 mg/kg diet) than in the control group (38%) or in the group treated with PyBex (34%, 40 mg/kg diet). While the increase in more advanced tumors (HH) was no longer found in the group fed the higher dose (80 mg/kg diet) of bexarotene (40%), the percentage of advanced tumors was still higher than any of the other groups (30% PyBex, 28% LG268, and 24% PyLG268) (Table 3.1).

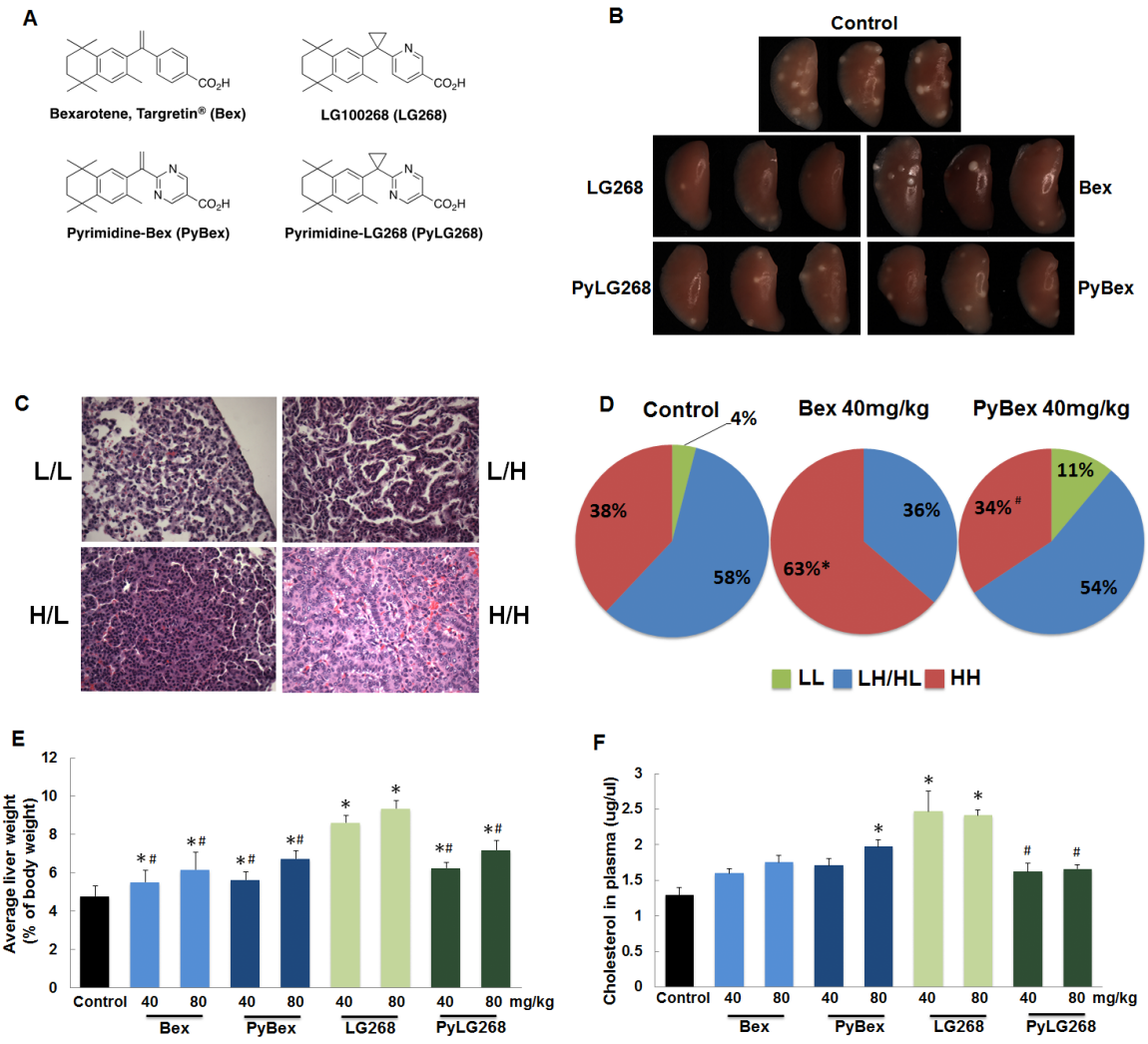

Figure 3.1: Evaluation of the efficacy and toxicity of rexinoids in preventing lung carcinogenesis in A/J mice. A. Structures of rexinoids used in these studies. PyBex and PyLG268 are new pyrimidine derivatives of bexarotene (Bex) and LG100268 (LG268), respectively. B. A/J mice were challenged with vinyl carbamate and then one week later, fed control diet or various rexinoids in diet for 16 weeks. Representative pictures of left lungs for each rexinoid at the end of the study. 10X magnification. C. Representative pictures of histopathology. Classification of tumor pathology was based on published histological (first letter) and nuclear (second letter) criteria. L = low; H = high. D. Quantitation of histopathology. *, $p<0.05$ vs. control; #, $p<0.05$ vs. Bex. Liver weights (N=12-24 mice/group; E) and plasma cholesterol levels (N=6 mice/group; F) were lower in A/J mice fed PyLG268 compared to LG268. Liver weights at the end of the lung prevention study (16 weeks on diet) were normalized to body weight. Results shown as mean±SEM. *, $p<0.05$ vs. control; #, $p<0.05$ vs. LG268 at the same concentration.

3.4.2 Superior lipid profile in A/J mice with PyLG268 and PyBex compared to LG268

Because of the known lipidemic properties of rexinoids, we measured lipid levels in the A/J mice. All the mice were weighed weekly, and the liver was weighed at the end of the study. The rexinoids were well-tolerated and did not cause weight loss, as there were no significant changes in weight across any of the groups throughout the study. As fatty livers and hepatomegaly are commonly seen in mice treated for prolonged periods with LG268, we normalized liver weights to body weight and compared groups (Figure 3.1 E). All four rexinoids significantly ($p<0.05$) increased the average liver weight (5.5-9.4%) compared to control mice (4.8%). However, the increase in liver weight observed with PyLG268 (6.2%) was significantly ($p<0.05$) reduced compared to LG268 (8.6%). There were no significant differences in liver weights between mice fed Bex and PyBex, but liver weights in these groups were significantly ($p<0.05$) lower than LG268**.**

In addition, triglyceride levels in the liver and plasma and cholesterol levels in the plasma were measured [14]. PyBex (40 mg/kg diet) reduced triglyceride levels (7.17 ± 0.92 µg/kg tissue) in the liver compared to bexarotene (40 mg/kg diet, 8.2 ± 0.93 µg/kg tissue) and plasma (3.6 ± 0.29 mg/ml vs. 4.8 ± 0.24 mg/ml, respectively, $p<0.05$). In the control group, the triglyceride level was 4.75 ± 0.95 µg/kg tissue in the liver and 4.90 ± 0.65 mg/ml in the plasma. PyLG268 significantly reduced cholesterol levels (Figure 3.1 F) in the plasma compared to LG268 (1.6± 0.28 µg/µl vs. 2.5± 0.68 µg/µl, respectively; $p<0.05$).

3.4.3 LG100268 and PyLG268 induce a favorable immune response *in vivo* and *in vitro*

Most rexinoids, at least as single agents, have limited activity for inhibiting proliferation or inducing apoptosis of epithelial cancer cells *in vitro*. Although we and

others have shown significant *in vitro* reduction of inflammatory cytokines and pathways by the rexinoids, the effects of rexinoids on immune cells *in vivo* in cancer studies have not been extensively investigated. Thus, we examined the modulation of immune cells by the two best rexinoids here. We harvested the superior and middle lobes of the right lung to characterize immune cell populations by flow cytometry. We evaluated levels of total immune cell populations ($CD45^+$), macrophages ($CD45^+$, $CD11b^+$, $Gr\text{-}1^-$), myeloid derived suppressor cells (MDSCs, $CD45^+$, $CD11b^+$, $Gr\text{-}1^+$), CD4 Th cells ($CD45^+$, $CD3^+$, $CD4^+$) and CD8 cytotoxic T cells ($CD45^+$, $CD3^+$, $CD8^+$), which are all very relevant to the pathogenesis and prognosis of lung cancer. MDSCs and tumor-associated macrophages are key players in immunosuppression and high infiltration of these cells is associated with poor prognosis [31, 32]. CD8 T cells are essential for killing tumor cells and for responding to immunotherapies like anti-PD-1/PD-L1 [33]. There was no increase of CD8 T cells with either LG268 or PyLG268 treatment. However, PyLG268, but not LG268, significantly increased total immune cell ($CD45^+$) infiltration into the lung (Figure 3.2 A). PyLG268 also significantly decreased the tumor associated macrophages and MDSCs in the lung (Figure 3.2 B and C, respectively). Changes in macrophage and MDSC populations were not significantly different in the LG268 groups, except for a decrease in macrophages in the high dose group (Figure 3.2 B). The changes in the $CD45^+$ populations in lung parenchyma and tumor associated macrophages near tumors were confirmed by IHC (Figure 3.2 D).

In addition to the immunomodulatory effects of LG268 and PyLG268 on the percentage of tumor associated macrophages (TAMs) in the lung, we further investigated the effects of these two rexinoids on macrophage polarization *in vitro*.

Macrophages with M1 and M2 phenotypes have opposite effects on lung cancer progression [34]. M1 (immuno-stimulatory) macrophages enhance antigen presentation and induce cell death of tumor cells, while M2 (immune-suppressive) macrophages promote tumor growth and invasion. Skewing the polarization of macrophages from an M2 to an M1 phenotype has been a promising strategy for cancer therapy. Here, we isolated primary bone marrow derived macrophages (BMDMs) from C57/BL6 wildtype mice and skewed them to an M2 phenotype by treating with M-CSF for 7 days. After differentiation, we treated the BMDMs with LG268 or PyLG268 and stimulated with LPS for 24 hours. Both LG268 and PyLG268 significantly ($p<0.05$ vs. control) increased the production of M1 cytokines (TNFα and IL-1β, Figure 3.2 E) and decreased the production of an M2 cytokine (IL-10, Figure 3.2 E). Furthermore, PyLG268 was significantly ($p<0.05$) more potent than LG268 in skewing the polarization of BMDMs. These experiments suggest that rexinoids, especially PyLG268, can reprogram the differentiation of macrophages from an M2 to an M1 phenotype.

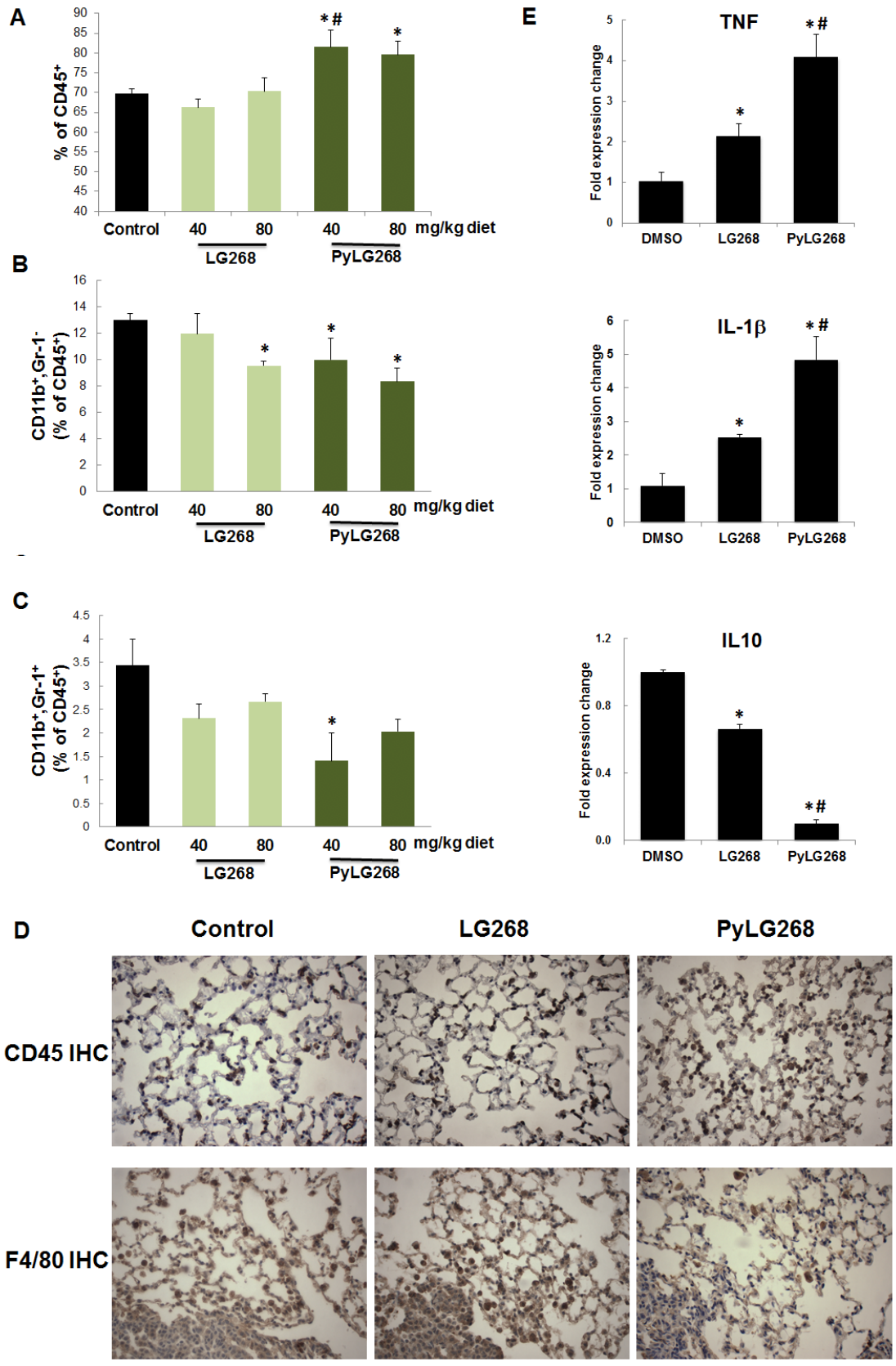

Figure 3.2: PyLG268 reduces the percentage of macrophages and myeloid derived

Figure 3.2 (cont'd)
suppressor cells in the lung and redirects the activation of macrophages to an M1 phenotype. A-C. Two lobes of the right lung from A/J mice injected with vinyl carbamate and fed rexinoids in diet for 16 weeks were removed at the end of the study to analyze immune populations by flow cytometry. Percentage of $CD45^+$ total immune cells, macrophages ($CD45^+$, $CD11b^+$, $Gr\text{-}1^-$), and myeloid derived suppressor cells ($CD45^+$, $CD11b^+$, $Gr\text{-}1^+$) in the lung are shown respectively from A to C. Results shown as mean±SEM. N=4-8 mice/group. *, $p<0.05$ vs. control; $^{\#}$, $p<0.05$ vs. LG268 40 mg/kg diet group. D. IHC staining of CD45 (immune cells) and F4/80 (macrophages) in the lung. E. BMDMs were isolated from mice and skewed to an M2 phenotype by treating with 20 ng/ml M-CSF for 7 days. The differentiated cells were then treated with DMSO or 100 nmol/L rexinoids and all cells stimulated with 100 ng/ml LPS for 24 hours. The expression of cytokines characteristic of M1 (TNFα and IL-1β) and M2 (IL-10) phenotypes were detected by real-time PCR. Results were normalized to DMSO controls. Results shown as mean±SD. *, $p<0.05$ vs. control; $^{\#}$, $p<0.05$ vs. LG268.

3.4.4 Anti-inflammatory properties of rexinoids *in vitro* correlate with the efficacy *in vivo*

Inflammation plays critical roles in tumor development [35]. We have previously shown that the rexinoids, LG100268, LG101506, and NRX194204 modulate the production of inflammatory cytokines and pathways induced by LPS in RAW264.7 macrophage-like cells [14, 36]. To characterize the anti-inflammatory effects of new pyrimidine rexinoids, we first performed the *in vitro* iNOS suppression assay [11]. RAW264.7 cells were treated with 10 nmol/L or 100 nmol/L rexinoids, challenged with 2 ng/ml LPS for 24 h, and NO was measured in the media. LG268 remained the most potent rexinoid for inhibiting the induction of NO and reducing lung carcinogenesis. PyLG268 is comparable in potency to LG268, and is significantly ($p<0.05$) more potent than bexarotene. PyBex is significantly ($p<0.05$) more potent for inhibiting iNOS than bexarotene, the parent compound (Figure 3.3 A). Notably, a correlation between *in vitro* efficacy in the iNOS assay and *in vivo* efficacy in the lung cancer model is observed with other published rexinoids. In previous work from our group, when the same concentration of five known rexinoids were directly compared in a separate iNOS assay,

the rank order was the same for iNOS suppression and reduction in tumor burden in the vinyl carbamate-induced lung cancer model [14, 28]. LG268 was the most effective rexinoid in both assays (100 ± 4% iNOS suppression at 10 nmol/L; 69% reduction in tumor burden), followed in order of potency by NRX194204 (98 ± 6% iNOS suppression; 64% reduction in tumor burden), PyLG268 (48 ± 10% iNOS suppression; 53% reduction in tumor burden), LG101506 (45 ± 8% iNOS suppression; 50% reduction in tumor burden) and bexarotene (31 ± 12% iNOS suppression; 26% reduction in tumor burden).

Next, the expression of a series of pro-inflammatory cytokines was compared by qPCR analysis. Total RNA was isolated from RAW264.7 cells treated with 300 nmol/L rexinoid and stimulated with 1 ng/ml LPS. CCL9 is a known downstream target of RXRs and plays an important role in leukocyte recruitment [37]; rexinoids suppressed CCL9 production (Figure 3.3 B) in a similar manner as in the NO assay. LG268, PyLG268 and PyBex were significantly ($p<0.05$) better for reducing CCL9 expression than Bex. IL-6 and IL-1β are not direct targets of RXR, but all four rexinoids almost completely abolished production of mRNA for these cytokines (Figure 3.3 C and D).

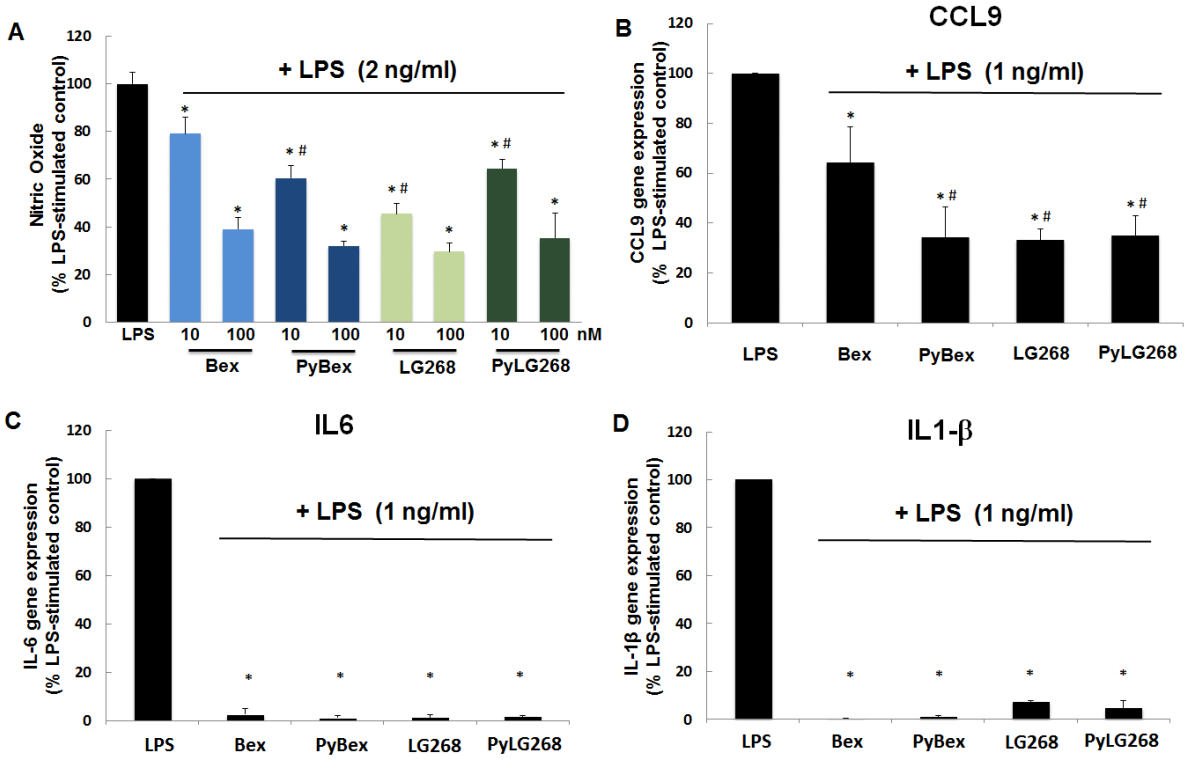

Figure 3.3: Rexinoids inhibit iNOS and cytokine production *in vitro*. A. RAW 264.7 cells were treated with 10-100 nmol/L rexinoids and then stimulated with 2 ng/ml LPS for 24 hours. Nitric oxide (NO) production was measured by the Griess assay, and results were normalized to LPS-stimulated controls. Results shown as mean±SD. *, $p<0.05$ vs. control; #, $p<0.05$ vs. Bex 10 nmol/L. B-D. RAW cells were treated with 300 nM rexinoids and 1 ng/ml LPS for 24 hours, and mRNA level of cytokines were measured by qPCR. Results were normalized to LPS-stimulated controls. All experiments were repeated independently more than three times. Results shown as mean±SD. *, $p<0.05$ vs. control; #, $p<0.05$ vs. Bex.

3.4.5 The expression and activity of SREBP vs. *in vivo* toxicity of rexinoids

The undesirable toxicities of rexinoids are a consequence of activation of heterodimers of RXR with other nuclear receptors, such as LXR, RAR and PPARγ. Activation of the LXR-RXR complex is usually associated with elevated plasma triglycerides due to the upregulation of SREBP-1c, a master regulator of cellular lipid metabolism and homeostasis [38]. Here, we evaluated the predictive value of SREBP elevation as a marker of *in vivo* toxicity in our lung cancer model. HepG2 cells were

treated with the four rexinoids, and expression of SREBP mRNA and protein levels were detected. LG268 induced the highest levels of SREBP mRNA (Figure 3.4 A) and protein (Figure 3.4 B). Consistent with the *in vivo* results, PyLG268 showed significantly ($p<0.05$) reduced expression of SREBP mRNA compared to LG268, even though the SREBP expression was still elevated compared to the control (Figure 3.4 A). Bexarotene and PyBex also increased SREBP mRNA expression compared to the control, but neither was as promising as PyLG268. In addition to mRNA and protein expression, the effects of rexinoids on transcriptional activity of SREBP were measured. A luciferase reporter gene containing the LXRE sequence from the mouse SREBP-1c promoter was transfected into HCT-116 cells. T0901317 (T0, a LXR ligand) was used as a positive control and results were normalized to induction with T0. All four rexinoids induced luciferase activity, but again PyLG268 was less lipogenic than LG268 (Figure 3.4 C).

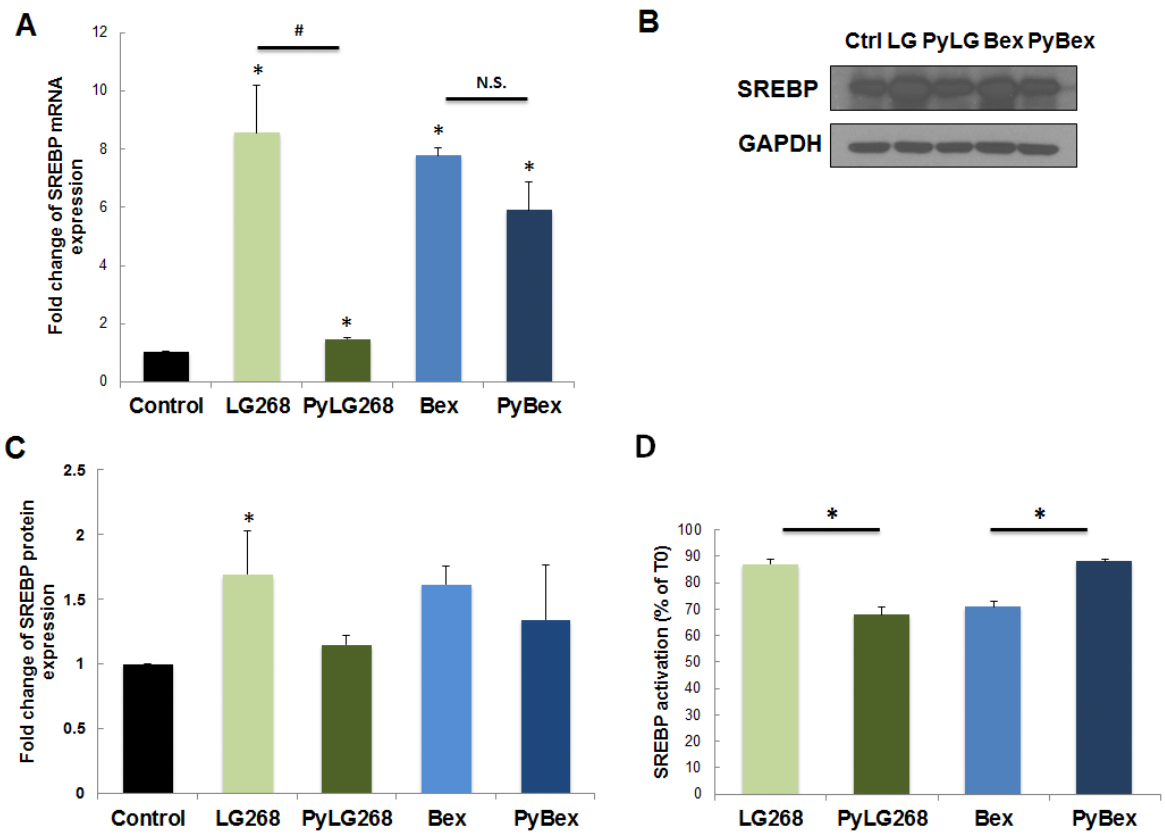

Figure 3.4: PyLG268 decreases the expression and activity of SREBP-1c compared to LG268. A. HepG2 cells were treated with 300 nmol/L rexinoids for 16 h. SREBP mRNA expression was detected by real time PCR, and values were normalized to GAPDH and the DMSO control. B and C. HepG2 cells were treated with 300 nmol/L rexinoids for 24 hours. Protein levels of SREBP-1c were detected by Western blotting (B) and quantified by ImageJ (C). Results were shown as mean±SD. *, $p<0.05$ vs. control. D. HCT-116 cells were transfected with a luciferase reporter gene containing an LXRE from the mouse SREBP-1c endogenous promoter. Transfected cells were treated with 10^{-7} mol/L T0901317 (LXR ligand and known SREBP activator) or 10^{-7} mol/L rexinoids. Luciferase activity was normalized relative to T0901317 treatment. Results were shown as mean±SD. *, $p<0.05$.

3.4.6 Screening assays for new rexinoids

With the *in vivo* and *in vitro* data supporting the value of the iNOS and SREBP assays, we then screened a series of 10 new rexinoids in three *in vitro* assays. Results are summarized in Table 3.2. Several of the new rexinoids inhibited NO secretion in the iNOS assay comparably to LG268, previously our most potent rexinoid, and some of

them (compounds 6, 8, 12, 13) were even more potent than LG268. RXR activation was better than Bex (EC_{50} = 55 nmol/L) for almost all of the new compounds. Induction of SREBP, a transcription factor that induces enzymes of triglyceride synthesis, was used as a biomarker of toxicity. SREBP was induced with T0901317, a LXR ligand and known SREPB activator, and data expressed as the percentage of T0901317-induced SREPB activation. SREBP activation was lower for compounds 12, 11, 7 and 10 compared to LG268 and Bex. On the basis of all of the *in vitro* screening assays listed in Table 3.2, compounds 7, 11 and 12 appear to be the most promising new rexinoids, with potentially lower toxicity and higher potency. To test our predictions, these compounds will be screened in our lung carcinogenesis assay. Once validated, these screening assays will be used to guide chemical synthesis and decision making for future *in vivo* testing.

3.5 Discussion

In the current study, two newly synthesized pyrimidine derivatives of bexarotene (PyBex) and LG268 (PyLG28) were evaluated in a preclinical lung cancer model. Both PyBex and PyLG268 were more efficacious than bexarotene for inhibiting lung carcinogenesis, particularly in reducing tumor burden. The reduction in the severity of the lesions also suggests that rexinoids can prevent tumor progression. In addition, in terms of toxicity, a better toxicity profile was observed with pyrimidine derivatives compared to their parent compound, with reduced hepatomegaly and lipids levels (triglycerides and cholesterol). This study supplied direct evidence showing the feasibility of using synthetic chemistry to produce superior rexinoids than bexarotene, the FDA approved rexinoid.

The lung cancer model we used in this study is highly clinically relevant. A/J mice are

widely used to evaluate chemopreventive agents. Although these mice can develop spontaneous adenomas in the lung, injection of a variety of carcinogens including urethane, vinyl carbamate, benzo(a)pyrene, and 4-(methylnitrosamino)-1-(3-pyridyl)-1-butanone (NNK) accelerates carcinogenesis [39-41]. Vinyl carbamate induces *Kras* mutations and lung adenocarcinomas in contrast to the adenomas induced by urethane and NNK [42]; there are currently no effective treatments for tumors driven by *Kras* mutations. Adenocarcinomas are the most common type of lung cancer and *Kras* mutations are found in 30% of lung adenocarcinomas [43], most frequently in smokers and Caucasian patients [44], making the A/J mouse model particularly relevant [25]. In addition, treatment with rexinoids was started post-initiation, in contrast to evaluation of many chemopreventive agents, which are administered before initiation with a carcinogen.

We have demonstrated immunomodulatory effects of rexinoids that are highly relevant in lung carcinogenesis, as increasing evidence supports the importance of the immune system in cancer progression [26]. The potent anti-inflammatory effects of rexinoids also support the important roles of these drugs on immune cells in the tumor microenvironment. PyLG268 decreased macrophage and myeloid derived suppressor cells, which is correlated with better clinical outcomes [32, 45]. Although the effects on macrophages were observed at both doses, the effect on myeloid-derived suppressor cells was only observed in the 40 mg/kg diet group, suggesting a concentration-dependent effect or a different mechanism in some immune populations. Future studies will address these questions. PyLG268 is also more potent than LG268 in skewing the polarization of macrophages from an M2 to an M1 phenotype. Future

studies will examine the functional consequences of these changes in immune cells in lung carcinogenesis as well as examine newly synthesized rexinoids. The incorporation of immunomodulatory and anti-inflammatory assays into the paradigm for evaluating new chemopreventive agents should help to further the practical development of new drugs for preventing cancer.

More importantly, we are not only reporting two new rexinoids, we also are developing a valuable *in vitro* screening system to guide our future rexinoid program for synthesizing superior rexinoids. On the basis of our years of experience on rexinoid development, a correlation between *in vitro* anti-inflammatory efficacy and *in vivo* chemopreventive efficacy was postulated and tested here. Combined with the activity of RXR activation *in vitro*, inhibition of iNOS may help us better predict the efficacy *in vivo*. Moreover, we also evaluated SREBP-1c expression and activity *in vitro* to determine if it could serve as a biomarker for predicting liver toxicity *in vivo*. As shown in Table 3.2, we have established these *in vitro* assays in a relatively high throughput way to rank the efficacy and toxicity of new rexinoids. Selection of the best compounds across our three *in vitro* screening assays will be tested *in vivo* in the lung cancer model for both efficacy (reduced tumor burden) and safety (reduced liver weight, triglycerides and cholesterol levels). If validated with additional compounds, this screening system provides us a more effective and efficient way to develop better rexinoids.

More and more studies support the potential clinical use of rexinoids for both cancer prevention and treatment, and RXR remains an attractive therapeutic target. We and other groups are making great efforts to push better rexinoids into the clinic. In addition to new efforts in synthetic chemistry, other strategies can be pursued. One way is

changing the delivery system. Zhang *et al.* reported that delivery of aerosolized bexarotene inhibits lung tumorigenesis without increasing plasma triglyceride and cholesterol levels [18], but this approach would be limited to lung cancer and other diseases of the lung. Another strategy is to utilize drug combinations to enhance efficacy and reduce side effects by using lower doses of complementary drugs. Previous work in many laboratories has shown notable effects with the combination of a rexinoid and other drugs [3, 16]. Lowering the dosing or using intermittent dosing [46, 47] can help balance between efficacy and toxicity. One more possibility is to design new rexinoids with appropriate interactions with co-activators and co-repressors, as has been successful for synthesis of new SERMs and other ligands targeting the nuclear receptor superfamily. With these strategies and better understanding of the mechanisms of rexinoids in cancer, there is great potential that the eventual goal of a clinically useful rexinoid will be achieved. Evaluation of the significant anti-inflammatory and immunomodulatory effects of rexinoids offers a new paradigm for such development.

Table 3.1. Rexinoids reduce lung carcinogenesis in A/J mice

	Control	Bexarotene		Pyrimidine-Bex		LG100268		Pyrimidine-LG268	
mg/kg **diet**		40	80	40	80	40	80	40	80
# of slides/ group	48	24	24	24	24	24	24	24	24
Average # tumors/slide (% control)	1.92±0.25 (100%)	1.75±0.25 (91.3%)	1.58±0.24 (82.6%)	1.46±0.26 (76.1%)	1.38±0.3 (71.7%)	1.63±0.32 (84.8%)	0.75±0.2* (39.1%)	1.46±0.23 (76.1%)	1.38±0.3 (71.7%)
Average tumor size, mm^3/tumor (% control)	0.24±0.09 (100%)	0.20±0.04 (80.7%)	0.11±0.02* (43.1%)	0.13±0.02 (54.4%)	0.10±0.02* (41.6%)	0.11±0.02* (45.8%)	0.07±0.01* (30.5%)	0.15±0.03 (62.1%)	0.12±0.02* (50.6)
Average tumor burden, mm^3/slide (% control)	0.47±0.19 (100%)	0.35±0.08 (73.7%)	0.17±0.04 (35.6%)	0.19±0.05 (41.4%)	0.14±0.03‡ (29.8%)	0.18±0.04 (38.8%)	0.06±0.02* (11.9%)	0.22±0.05 (47.3%)	0.17±0.06‡ (36.3%)
Total # LL Grade (% total)	4 (4%)	0	4 (10%)	4 (11%)	2 (6%)	1 (3%)	0	3 (9%)	0
Total # LH/HL Grade (% total)	53 (58%)	15 (36%)	19 (50%)	19 (54%)	21 (64%)	22 (56%)	13 (72%)	18 (51%)	25 (76%)
Total # HH Grade (% total)	35 (38%)	27 (64%)*	15 (40%)	12 (34%)#	10 (30%)	16 (41%)	5 (28%)	14 (40%)	8 (24%)

Note: Female A/J mice were injected i.p. with 0.32 mg vinyl carbamate. One week later, mice were randomized into either control group fed AIN-93G diet or experimental groups fed rexinoids in the same diet. After 16 weeks on diet, mice were euthanized. Tumor number, size and burden of lung tumors were measured. Values shown are mean±SEM. *, $p < 0.05$ vs. control; ‡, $p = 0.06$ or 0.07 vs control; #, $p<0.05$ vs. Bex 40; n = 12-24 mice per group.

Table 3.2. Activity of new rexinoids in iNOS, RXR and SREBP assays

Compound Structure	Name or Number	iNOS suppression (% LPS-stimulated control) (-/+ SD)	RXR activation (EC_{50}, nM) (-/+ SD)	SREBP activation (% of TO) (-/+ SD)	Original Reference
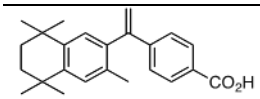	Bexarotene	24 (3)	55 (6)	71 (2)	[48]
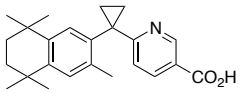	LG100268	15 (1)	15 (3)	87 (2)	[20]
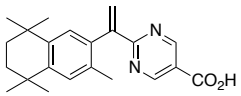	PyBex	20 (6)	44 (12)	88 (1)	[22]
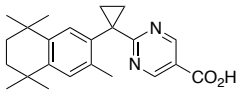	PyLG268	17 (6)	50 (10)	68 (3)	[22]
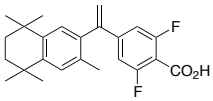	**5**	23 (6)	34 (6)	65 (5)	[49]
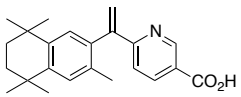	**6**	11 (2)	21 (2)	100 (7)	[20]
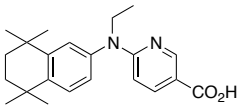	**7**	17 (5)	14 (0.8)	62 (5)	[50]
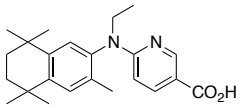	**8**	9 (5)	14 (1.5)	66 (5)	[51]
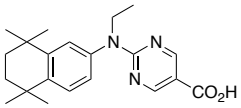	**9**	12 (4)	41 (0.6)	67 (12)	[51]
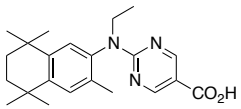	**10**	15 (1)	18 (0.4)	63 (6)	[51]
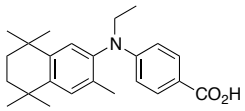	**11**	19 (7)	8 (0.4)	57 (6)	[52]
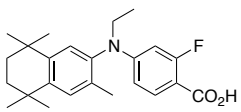	**12**	11 (0)	34 (0.1)	54 (5)	[51]
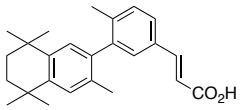	**13**	12 (3)	42 (3)	72 (13)	[22]
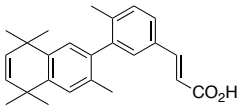	**14**	24 (9)	72 (11)	65 (15)	[22]

Table 3.2 (cont'd)
Note: To determine suppression of iNOS, RAW 264.7 cells were treated with 100 nM rexinoid and then challenged with 1 ng/ml LPS for 24 h. NO production was measured using the Griess assay, and results were normalized to the LPS-stimulated control. RXR and SREBP activation were evaluated as described in the Materials and Methods. T0 = T0901317, a LXR ligand and known SREPB activator.

REFERENCES

REFERENCES

1. Evans RM, Mangelsdorf DJ. Nuclear Receptors, RXR, and the Big Bang. Cell. 2014; 157: 255-66.

2. Mukherjee R, Davies PJ, Crombie DL, Bischoff ED, Cesario RM, Jow L, et al. Sensitization of diabetic and obese mice to insulin by retinoid X receptor agonists. Nature. 1997; 386: 407-10.

3. Liby KT, Sporn MB. Rexinoids for prevention and treatment of cancer: opportunities and challenges. Curr Top Med Chem. 2017; 17: 721-30.

4. Miller VA, Benedetti FM, Rigas JR, Verret AL, Pfister DG, Straus D, et al. Initial clinical trial of a selective retinoid X receptor ligand, LGD1069. J Clin Oncol. 1997; 15: 790-5.

5. Rizvi NA, Marshall JL, Dahut W, Ness E, Truglia JA, Loewen G, et al. A Phase I study of LGD1069 in adults with advanced cancer. Clin Cancer Res. 1999; 5: 1658-64.

6. Dragnev KH, Ma T, Cyrus J, Galimberti F, Memoli V, Busch AM, et al. Bexarotene plus erlotinib suppress lung carcinogenesis independent of KRAS mutations in two clinical trials and transgenic models. Cancer Prev Res (Phila). 2011; 4: 818-28.

7. Edelman MJ, Smith R, Hausner P, Doyle LA, Kalra K, Kendall J, et al. Phase II trial of the novel retinoid, bexarotene, and gemcitabine plus carboplatin in advanced non-small-cell lung cancer. J Clin Oncol. 2005; 23: 5774-8.

8. Blumenschein GR, Jr., Khuri FR, von Pawel J, Gatzemeier U, Miller WH, Jr., Jotte RM, et al. Phase III trial comparing carboplatin, paclitaxel, and bexarotene with carboplatin and paclitaxel in chemotherapy-naive patients with advanced or metastatic non-small-cell lung cancer: SPIRIT II. J Clin Oncol. 2008; 26: 1879-85.

9. Liu X RJ, Karakami M, Sanders M, Chandraratna R, Dmitrivsky E, Dragnev K. IRX4204 in combination with erlotinib to target distinct pathways in lung cancer cells. J Clin Oncol. 2017; 35: abstr e14095.

10. Ramlau R, Zatloukal P, Jassem J, Schwarzenberger P, Orlov SV, Gottfried M, et al. Randomized phase III trial comparing bexarotene (L1069-49)/cisplatin/vinorelbine with cisplatin/vinorelbine in chemotherapy-naive patients with advanced or metastatic non-small-cell lung cancer: SPIRIT I. J Clin Oncol. 2008; 26: 1886-92.

11. Liby KT, Yore MM, Sporn MB. Triterpenoids and rexinoids as multifunctional agents for the prevention and treatment of cancer. Nat Rev Cancer. 2007; 7: 357-69.

12. Brown PH, Subbaramaiah K, Salmon AP, Baker R, Newman RA, Yang P, et al. Combination chemoprevention of HER2/neu-induced breast cancer using a cyclooxygenase-2 inhibitor and a retinoid X receptor-selective retinoid. Cancer Prev Res (Phila). 2008; 1: 208-14.

13. Wu K, Zhang Y, Xu XC, Hill J, Celestino J, Kim HT, et al. The retinoid X receptor-selective retinoid, LGD1069, prevents the development of estrogen receptor-negative mammary tumors in transgenic mice. Cancer Res. 2002; 62: 6376-80.

14. Cao M, Royce DB, Risingsong R, Williams CR, Sporn MB, Liby KT. The Rexinoids LG100268 and LG101506 Inhibit Inflammation and Suppress Lung Carcinogenesis in A/J Mice. Cancer Prev Res (Phila). 2016; 9: 105-14.

15. Lubet RA, Clapper ML, McCormick DL, Pereira MA, Chang WC, Steele VE, et al. Chemopreventive efficacy of Targretin in rodent models of urinary bladder, colon/intestine, head and neck and mammary cancers. Oncol Rep. 2012; 27: 1400-6.

16. Uray IP, Dmitrovsky E, Brown PH. Retinoids and rexinoids in cancer prevention: from laboratory to clinic. Semin Oncol. 2016; 43: 49-64.

17. Wang Y, Zhang Z, Yao R, Jia D, Wang D, Lubet RA, et al. Prevention of lung cancer progression by bexarotene in mouse models. Oncogene. 2006; 25: 1320-9.

18. Zhang Q, Pan J, Zhang J, Liu P, Chen R, Chen DR, et al. Aerosolized bexarotene inhibits lung tumorigenesis without increasing plasma triglyceride and cholesterol levels in mice. Cancer Prev Res (Phila). 2011; 4: 270-6.

19. Sherman SI, Gopal J, Haugen BR, Chiu AC, Whaley K, Nowlakha P, et al. Central hypothyroidism associated with retinoid X receptor-selective ligands. N Engl J Med. 1999; 340: 1075-9.

20. Boehm MF, Zhang L, Zhi L, McClurg MR, Berger E, Wagoner M, et al. Design and synthesis of potent retinoid X receptor selective ligands that induce apoptosis in leukemia cells. J Med Chem. 1995; 38: 3146-55.

21. Wagner CE, Jurutka PW, Marshall PA, Groy TL, van der Vaart A, Ziller JW, et al. Modeling, synthesis and biological evaluation of potential retinoid X receptor (RXR) selective agonists: novel analogues of 4-[1-(3,5,5,8,8-pentamethyl-5,6,7,8-tetrahydro-2-naphthyl)ethynyl]benzoic acid (bexarotene). J Med Chem. 2009; 52: 5950-66.

22. Jurutka PW, Kaneko I, Yang J, Bhogal JS, Swierski JC, Tabacaru CR, et al. Modeling, synthesis, and biological evaluation of potential retinoid X receptor (RXR) selective agonists: novel analogues of 4-[1-(3,5,5,8,8-pentamethyl-5,6,7,8-tetrahydro-2-naphthyl)ethynyl]benzoic acid (bexarotene) and (E)-3-(3-(1,2,3,4-tetrahydro-1,1,4,4,6-pentamethylnaphthalen-7-yl)-4-hydroxypheny l)acrylic acid (CD3254). J Med Chem. 2013; 56: 8432-54.

23. Vuligonda V, Thacher SM, Chandraratna RA. Enantioselective syntheses of potent retinoid X receptor ligands: differential biological activities of individual antipodes. J Med Chem. 2001; 44: 2298-303.

24. Muccio DD, Atigadda VR, Brouillette WJ, Bland KI, Krontiras H, Grubbs CJ. Translation of a Tissue-Selective Rexinoid, UAB30, to the Clinic for Breast Cancer Prevention. Curr Top Med Chem. 2017; 17: 676-95.

25. Gorelik E, Herberman RB. Susceptibility of various strains of mice to urethan-induced lung tumors and depressed natural killer cell activity. J Natl Cancer Inst. 1981; 67: 1317-22.

26. Hollstein PE, Shaw RJ. Inflamed T cells and stroma drive gut tumors. Science. 2018; 361: 332-3.

27. Marim FM, Silveira TN, Lima DS, Jr., Zamboni DS. A method for generation of bone marrow-derived macrophages from cryopreserved mouse bone marrow cells. PLoS One. 2010; 5: e15263.

28. Liby K, Risingsong R, Royce DB, Williams CR, Ma T, Yore MM, et al. Triterpenoids CDDO-methyl ester or CDDO-ethyl amide and rexinoids LG100268 or NRX194204 for prevention and treatment of lung cancer in mice. Cancer Prev Res (Phila). 2009; 2: 1050-8.

29. Repa JJ, Liang G, Ou J, Bashmakov Y, Lobaccaro JM, Shimomura I, et al. Regulation of mouse sterol regulatory element-binding protein-1c gene (SREBP-1c) by oxysterol receptors, LXRalpha and LXRbeta. Genes Dev. 2000; 14: 2819-30.

30. Marshall PA, Jurutka PW, Wagner CE, van der Vaart A, Kaneko I, Chavez PI, et al. Analysis of differential secondary effects of novel rexinoids: select rexinoid X receptor ligands demonstrate differentiated side effect profiles. Pharmacol Res Perspect. 2015; 3: e00122.

31. Iriki T, Ohnishi K, Fujiwara Y, Horlad H, Saito Y, Pan C, et al. The cell-cell interaction between tumor-associated macrophages and small cell lung cancer cells is involved in tumor progression via STAT3 activation. Lung Cancer. 2017; 106: 22-32.

32. Fang Z, Wen C, Chen X, Yin R, Zhang C, Wang X, et al. Myeloid-derived suppressor cell and macrophage exert distinct angiogenic and immunosuppressive effects in breast cancer. Oncotarget. 2017.

33. Kamphorst AO, Pillai RN, Yang S, Nasti TH, Akondy RS, Wieland A, et al. Proliferation of PD-1+ CD8 T cells in peripheral blood after PD-1-targeted therapy in lung cancer patients. Proc Natl Acad Sci U S A. 2017.

34. Yuan A, Hsiao YJ, Chen HY, Chen HW, Ho CC, Chen YY, et al. Opposite Effects of M1 and M2 Macrophage Subtypes on Lung Cancer Progression. Sci Rep. 2015; 5: 14273.

35. Grivennikov SI, Greten FR, Karin M. Immunity, inflammation, and cancer. Cell. 2010; 140: 883-99.

36. Liby K, Royce DB, Risingsong R, Williams CR, Wood MD, Chandraratna RA, et al. A new rexinoid, NRX194204, prevents carcinogenesis in both the lung and mammary gland. Clin Cancer Res. 2007; 13: 6237-43.

37. Nunez V, Alameda D, Rico D, Mota R, Gonzalo P, Cedenilla M, et al. Retinoid X receptor alpha controls innate inflammatory responses through the up-regulation of chemokine expression. Proc Natl Acad Sci U S A. 2010; 107: 10626-31.

38. Bedi S, Hostetler HA, Rider SD, Jr. Mutations in Liver X Receptor Alpha That Impair Dimerization and Ligand Dependent Transactivation. Nucl Receptor Res. 2017; 4.

39. Kishi S, Yokohira M, Yamakawa K, Saoo K, Imaida K. Significance of the progesterone receptor and epidermal growth factor receptor, but not the estrogen receptor, in chemically induced lung carcinogenesis in female A/J mice. Oncol Lett. 2014; 8: 2379-86.

40. Yeo CD, Kim JW, Ha JH, Kim SJ, Lee SH, Kim IK, et al. Chemopreventive effect of phosphodieasterase-4 inhibition in benzo(a)pyrene-induced murine lung cancer model. Exp Lung Res. 2014; 40: 500-6.

41. Luettich K, Xiang Y, Iskandar A, Sewer A, Martin F, Talikka M, et al. Systems toxicology approaches enable mechanistic comparison of spontaneous and cigarette smoke-related lung tumor development in the A/J mouse model. Interdiscip Toxicol. 2014; 7: 73-84.

42. You M, Candrian U, Maronpot RR, Stoner GD, Anderson MW. Activation of the Ki-ras protooncogene in spontaneously occurring and chemically induced lung tumors of the strain A mouse. Proc Natl Acad Sci U S A. 1989; 86: 3070-4.

43. Jackman DM, Miller VA, Cioffredi LA, Yeap BY, Janne PA, Riely GJ, et al. Impact of epidermal growth factor receptor and KRAS mutations on clinical outcomes in previously untreated non-small cell lung cancer patients: results of an online tumor registry of clinical trials. Clin Cancer Res. 2009; 15: 5267-73.

44. Guibert N, Ilie M, Long E, Hofman V, Bouhlel L, Brest P, et al. KRAS Mutations in Lung Adenocarcinoma: Molecular and Epidemiological Characteristics, Methods for Detection, and Therapeutic Strategy Perspectives. Curr Mol Med. 2015; 15: 418-32.

45. Zaynagetdinov R, Sherrill TP, Polosukhin VV, Han W, Ausborn JA, McLoed AG, et al. A critical role for macrophages in promotion of urethane-induced lung carcinogenesis. J Immunol. 2011; 187: 5703-11.

46. Wu X, Lippman SM. An intermittent approach for cancer chemoprevention. Nat Rev Cancer. 2011; 11: 879-85.

47. Rendi MH, Suh N, Lamph WW, Krajewski S, Reed JC, Heyman RA, et al. The selective estrogen receptor modulator arzoxifene and the rexinoid LG100268 cooperate to promote transforming growth factor beta-dependent apoptosis in breast cancer. Cancer Res. 2004; 64: 3566-71.

48. Boehm MF, Zhang L, Badea BA, White SK, Mais DE, Berger E, et al. Synthesis and structure-activity relationships of novel retinoid X receptor-selective retinoids. J Med Chem. 1994; 37: 2930-41.

49. Furmick JK, Kaneko I, Walsh AN, Yang J, Bhogal JS, Gray GM, et al. Modeling, synthesis and biological evaluation of potential retinoid X receptor-selective agonists: novel halogenated analogues of 4-[1-(3,5,5,8,8-pentamethyl-5,6,7,8-tetrahydro-2-naphthyl)ethynyl]benzoic acid (bexarotene). ChemMedChem. 2012; 7: 1551-66.

50. Nakayama M, Yamada S, Ohsawa F, Ohta Y, Kawata K, Makishima M, et al. Discovery of a Potent Retinoid X Receptor Antagonist Structurally Closely Related to RXR Agonist NEt-3IB. ACS Med Chem Lett. 2011; 2: 896-900.

51. Heck MC, Wagner CE, Shahani PH, MacNeill M, Grozic A, Darwaiz T, et al. Modeling, Synthesis, and Biological Evaluation of Potential Retinoid X Receptor (RXR)-Selective Agonists: Analogues of 4-[1-(3,5,5,8,8-Pentamethyl-5,6,7,8-tetrahydro-2-naphthyl)ethynyl]benzoic Acid (Bexarotene) and 6-(Ethyl(5,5,8,8-tetrahydronaphthalen-2-yl)amino)nicotinic Acid (NEt-TMN). J Med Chem. 2016; 59: 8924-40.

52. Ohta K, Tsuji M, Kawachi E, Fukasawa H, Hashimoto Y, Shudo K, et al. Potent retinoid synergists with a diphenylamine skeleton. Biol Pharm Bull. 1998; 21: 544-6.

CHAPTER 4

Identification of an unfavorable immune signature in advanced lung tumors from Nrf2-deficient mice

Reprinted with permission from *Antioxidants & Redox Signaling*. 2018.29(16):1535-1552

Di Zhang, Jonathan Rennhack, Eran R. Andrechek, Cheryl E. Rockwell, and Karen T. Liby

Author contributions:
Participated in research design: Zhang, Liby
Conducted experiments: Zhang
Performed data analysis: Zhang, Rennhack
Wrote or contributed to the writing of the manuscript: Zhang, Andrechek, Liby

4.1 Abstract

Aims: Activation of the nuclear factor (erythroid-derived 2)- like 2 (Nrf2) pathway in normal cells inhibits carcinogenesis, whereas constitutive activation of Nrf2 in cancer cells promotes tumor growth and chemoresistance. However, the effects of Nrf2 activation in immune cells during lung carcinogenesis are poorly defined and could either promote or inhibit cancer growth. Our studies were designed to evaluate tumor burden and identify immune cell populations in the lungs of Nrf2 knockout (KO) *versus* wildtype (WT) mice challenged with vinyl carbamate.

Results: Nrf2 KO mice developed lung tumors earlier than the WT mice and exhibited more and larger tumors over time, even at late stages. T cell populations were lower in the lungs of Nrf2 KO mice, whereas tumor-promoting macrophages and myeloid-derived suppressor cells were elevated in the lungs and spleen, respectively, of Nrf2 KO mice relative to WT mice. Moreover, 34 immune response genes were significantly upregulated in tumors from Nrf2 KO mice, especially a series of cytokines (*Cxcl1, Csf1, Ccl9, Cxcl12, etc*.) and major histocompatibility complex antigens that promote tumor growth.

Innovation: Our studies discovered a novel immune signature, characterized by the infiltration of tumor-promoting immune cells, elevated cytokines, and increased expression of immune response genes in the lungs and tumors of Nrf2 KO mice. A complementary profile was also found in lung cancer patients, supporting the clinical significance of our findings.

Conclusion: Overall, our results confirmed a protective role for Nrf2 in late-stage carcinogenesis and, unexpectedly, suggest that activation of Nrf2 in immune cells may be advantageous for preventing or treating lung cancer.

4.2 Introduction

The Nrf2-Keap1-ARE pathway is a master defense mechanism protecting against oxidative and electrophilic stress. It helps regulate numerous cellular processes as diverse as metabolism, detoxification, redox-balancing, and autophagy [1]. Under basal conditions, Nrf2 (nuclear factor (erythroid-derived 2)-like 2) is bound to its internal negative regulator Keap1 (Kelch-like ECH-associated protein 1) and targeted to the proteasome for degradation [2]. Under stress conditions such as increased reactive oxygen species (ROS), Nrf2 is released from Keap1 and translocates to the nucleus to initiate transcription of a variety of downstream genes [1]. These target genes encode for proteins including (a) phase I/II/III metabolism enzymes that detoxify xenobiotics and enhance their elimination [3-5], (b) proteins to maintain cellular redox homeostasis [6], (c) enzymes involved in heme, lipid and glucose metabolism [7-9], (d) enzymes that regulate NADPH generation and pentose synthesis [10], and (e) proteins involved in apoptosis and autophagy [11, 12]. In addition to interaction with Keap1, additional mechanisms have been reported to regulate Nrf2 activity, including phosphorylation by kinases (PKC, MAPK/ERK/JNK, JUN/MYC), protein-protein interactions (e.g. RXRα), and epigenetic modifications (miRNAs, acetylation) [13]. The regulation of the Nrf2 pathway, therefore, is complex but profoundly important for numerous cellular processes [1].

As a “multi-organ protector” [14], activation of Nrf2 protects against many diseases driven by unresolved inflammation including cancer, cardiovascular diseases, and neurodegenerative diseases. Recently, the role of Nrf2 in cancer has been the topic of numerous interesting studies. Activation of Nrf2 was traditionally considered beneficial

for the prevention of cancer. As Nrf2 is the main cellular defense mechanism against both endogenous and exogenous insults, Nrf2 deficiency enhances the susceptibility to carcinogens [15]. This effect is not limited to certain types of cancer or restricted to certain types of insults. Carcinogenesis is consistently exacerbated in Nrf2 knockout (KO) vs. wildtype (WT) mice, whether induced by ultraviolet light or chemicals in skin, aflatoxin in the liver, polycyclic hydrocarbons in the forestomach, nitrosamines in the bladder, or inflammation in the colon [16-20]. Moreover, knockdown of Keap1, which elevates Nrf2 levels, increases resistance to cancer metastasis [21, 22]. In addition to affecting cancer susceptibility, Nrf2 also plays a crucial role in chemoprevention. Many Nrf2 activators, including a variety of natural products, can be used to prevent or delay tumor development, and these chemopreventive effects are greatly dampened in Nrf2 KO mice [18, 23].

However, increasing numbers of studies suggest a tumor-promoting role for Nrf2 [1]. The detoxifying and cytoprotective environment created by activation of the Nrf2 pathway helps tumor cells eliminate hypoxia and elevate ROS levels, thus promoting survival of tumor cells [24]. Gain-of function mutations in the *Nfe2l2* gene that encodes for Nrf2 and loss-of-function mutations in the *Keap1* gene are found in a subset of advanced cancers of the lung, liver, esophagus, bladder and other organs, but lung cancer has the highest frequency of *Nfe2l2* or *Keap1* alterations [1]. Epigenetic modifications of the *Keap1* or *Nfe2l2* promoters have also been found. All of these genetic and epigenetic alterations result in constitutively high levels of Nrf2 expression and activity, which is associated with chemoresistance and poor prognosis [1, 15, 25]. More recently, Ngo *et al.* reported that Nrf2 drives hepatocarcinogenesis [26], and Bauer

et al. reported that deletion of Nrf2 reduces lung tumor development induced by urethane [27]. Although these studies suggest the role of Nrf2 may be model and context dependent, they conclude that inhibiting Nrf2 activity should be beneficial in treating advanced cancers.

The complex tumor-promoting and tumor suppressing dual roles of Nrf2 in cancer have generated a great deal of interest, especially regarding the safety of long-term use of Nrf2 activators and the need to develop Nrf2 inhibitors for treating cancer. We recently reported that two drugs that can activate the Nrf2 pathway have opposite effects in a lung carcinogenesis model [28]. Dimethyl fumarate or Tecfidera®, approved by the FDA for the treatment of multiple sclerosis, increased the number and pathological grade of lung tumors. In contrast, synthetic oleanane triterpenoids [29] currently being tested in clinical trials for the treatment of chronic kidney disease, pulmonary hypertension and cancer, reduced the number, size and severity of lung tumors [28]. Additional experiments are needed to determine if these contradictory results are dependent on Nrf2, as both drugs are also potent anti-inflammatory agents that target the immune system and other specific protein targets.

Considering the conflicting reports regarding the role of Nrf2 in lung cancer and the importance of immunotherapy for treating lung cancer, understanding the regulation of immune cells by Nrf2 during carcinogenesis is necessary. The microenvironment regulates tumorigenesis, and a broad-spectrum integrative approach using natural products or pharmacological activators could be used to modulate this microenvironment for both cancer prevention and treatment [30]. As many Nrf2 modulators have anti-inflammatory effects, Nrf2 may be a potential target to modulate the

microenvironment. In our current studies, we used a relevant preclinical model to investigate the Nrf2 pathway in lung carcinogenesis. The potent carcinogen vinyl carbamate induces *Kras* mutations [31] and lung adenocarcinomas [32]. *Kras* mutations are the most common mutation found in lung cancer, especially in smokers, and adenocarcinomas are the most frequent type of lung cancer [33]. Notably, tumors driven by *Kras* mutations have been considered “undruggable” and are resistant to standard and targeted chemotherapies [33]. Although carcinogens found in cigarettes can also induce lung tumors, the traditional NNK model induces adenomas instead of adenocarcinomas [34]. *Kras* transgenic mice also develop lung cancer [35] but the rapid development of tumors and high tumor burden [35, 36] limit their utility for studying carcinogenesis and changes in the microenvironment over time. Here, we describe changes in tumor burden, immune cell populations, inflammatory cytokines, and immune signatures in the lungs of Nrf2 KO vs. WT mice challenged with vinyl carbamate.

4.3 Materials and Methods

4.3.1 *In vivo* lung carcinogenesis studies

All animal studies were performed in accordance with protocols approved by the Institutional Animal Care and Use Committee (IACUC) at Michigan State University. Nrf2-/- mice on a mixed C57Bl/6 and AKR background were generated as previously described and received as a generous gift from Dr. Jefferson Chan at the University of California San Francisco [37]. These mice were backcrossed onto a BALB/c background for eight generations and were found to be 99% congenic (analysis performed by Jackson Laboratory, Bar Harbor, ME). Age-matched female Nrf2 KO female mice and Nrf2 WT BALB/c mice (JAX) were injected i.p. once a week with 2-4 doses of vinyl

carbamate (0.32 mg/mouse/dose, approximately 16 mg/kg/dose), beginning when the mice were 6-8 weeks old. The mice were fed AIN-93G diet (BioServ, Flemington NJ) throughout the study and were weighed weekly. Age-matched cohorts of Nrf2 WT and KO mice (4 mice/group) were harvested from 4 to 8 weeks after initiation with carcinogen in the short-term study or 20 to 40 weeks after initiation with the carcinogen in the long-term study. Lungs were harvested *en bloc*, inflated with PBS, and tied off in two perpendicular directions. Left lungs were fixed in neutral buffered formalin (NBF) for histopathology. Right lungs were not fixed but instead immediately homogenized and processed for flow cytometry (two lobes) or were flash frozen and saved at -80°C (the other two lobes). Tumor parameters were assessed as previously described [38, 39] and include the number, size, and classification of the tumors.

4.3.2 RNA extraction and RT-qPCR analysis

Lung tumors were dissected and total RNA was isolated using the RNeasy Mini Kit (Qiagen, Valencia, CA). RNA concentrations are determined by NanoDrop, and cDNAs were synthesized by TaqMan Reverse Transcription reagents (Life Technologies, Carlsbad, CA). Total RNA from lung tissue was isolated with TRIzol (Invitrogen, Carlsbad, CA). Two μg RNA was used to synthesize cDNA using SuperScript III reverse transcriptase (Invitrogen, Carlsbad, CA). Validated Cxcl1, Ccl9, Csf1 and Cxcl12 primers were purchased from Qiagen (Valencia, CA). iQ SYBR Green Supermix (Bio-Rad, Berkeley, CA) and the ABI 7500 FAST Real-Time PCR system were used to detect gene expression. The delta-delta Ct method was used to calculate relative gene expression [40]. Values were normalized to the reference gene actin and expressed as fold induction compared with WT samples.

4.3.3 ELISA assay

Lung extracts were homogenized in EBC lysis buffer. Cytokine levels were detected in lung homogenates using ELISA kits and the manufacturer's instructions (R&D Systems).

4.3.4 Flow cytometry

The same two lobes of the unfixed right lung were harvested from each mouse for flow cytometry. Freshly harvested lung tissue and half of the spleen were homogenized and incubated in digestion media containing collagenase (300 U/ml, Sigma), dispase (1 U/ml, Worthington), and DNAse (2 U/ml, Calbiochem) for 30 minutes at 37°C. Cells were then passed through a 40 μm cell strainer (BD Falcon). Lysis solution (eBioscience) was used to eliminate red blood cells. Single cell suspensions were stained with 5 μg/ml anti-mouse Fc block antibody (eBioscience) and two optimized panels of antibodies [41] for 30 minutes at 4°C. Panel 1: CD45-VioGreen (Miltenyi, clone: 30F11, 3μg/mL), Gr-1-PE (Miltenyi, RB6-8C5, 3μg/mL), CD11b-FITC (Miltenyi, clone:M1/70, 3μg/mL), CD19-APC (BioLegend, clone:1D3/CD19, 2μg/mL), B220-PerCP/Cy5.5 (BioLegend, clone:RA3-6B2, 2μg/mL) Panel 2: CD4-FITC (Miltenyi, clone:GK1.5, 3μg/mL), CD3-PE (BioLegend, clone:145-2C11, 2μg/mL), CD8-PerCP/Cy5.5 (BioLegend, clone:53-6.7, 2μg/mL). Live cells were determined by propidium iodide staining (BioLegend, 5μg/mL), and only live cells were included in the analysis. Flow cytometry was performed using a LSR II flow cytometer with DIVA 6.2 software (BD) and three laser sources (488 nm, 633 nm, 407 nm); data were analyzed by FlowJo x.10.0.7r2 software (Tree Star).

4.3.5 RNAseq

Lung tumors were dissected out from the lung tissue and were pooled (3-4 tumors)

prior to isolating total RNA using the RNeasy Mini Kit (Qiagen, Valencia, CA). The RNA integrity number (RIN) was measured using the Aligent Bioanalyzer at the MSU Research Technology Support Facility Genomics Core facility. RNAseq and the bioinformatics analysis from two independent pools were performed by Novogene (Sacramento, CA). In brief, reads were processed and mapped. Raw data was stored in FASTQ format. After the removal of adaptors and low quality reads, reads were mapped to the mm10 mouse reference genome using TopHat2 [42]. Reads that mapped to genes were counted and normalized to gene length, then reported in FPKM (Fragments Per Kilo bases per Million reads) as previously described [43]. Routine identification of differentially expressed genes was performed using DESeq2 [44]. Raw and processed data were deposited on GEO and can be retrieved through record number GSE99338.

4.3.6 Over-representation analysis of differentially expressed genes

Up- and down regulated genes in tumors from NFR2 KO vs. WT mice were processed to identify over represented genes using PANTHER analysis as previously described [45]. To identify those over-represented genes up regulated with the alteration of Keap1 in human adenocarcinomas as identified by cBioPortal, significantly enriched genes were queried for over-represented gene ontologies using GATHER [46].

4.3.7 Human datasets

The impact of gene loss in human lung cancer patients was identified using the TCGA pan [47], adenocarcinoma [48] and squamous cell [49] lung cancer datasets. Figures were created using cbioportal.org [50, 51].

4.3.8 Statistical analysis

The *ex vivo* experiments were performed in triplicate and were repeated independently at least three times. Unless noted otherwise, data are presented as mean ± SEM. Results were analyzed using the t-test or one-way ANOVA (SigmaStat 3.5). *In vivo* data were analyzed by one-way ANOVA followed by Tukey test, or one-way ANOVA on ranks and the Dunn test if the data did not fit a normal distribution (SigmaStat 3.5). A p value < 0.05 was considered statistically significant. For RNAseq data, differential expression analysis of two conditions/groups was performed using the DESeq2 R package [44]. It provides accepted and routinely used statistical analysis for determining differential expression in digital gene expression data using a model based on the negative binomial distribution. If the readcount of the ith gene in the jth sample is Kij, there is: Kij NB(μij,σij2). The resulting p values were adjusted using the Benjamini and Hochberg's approach for controlling the false discovery rate.

4.4 Results

4.4.1 Lung carcinogenesis exacerbated in $Nrf2^{-/-}$ mice challenged with vinyl carbamate

To determine the effects of vinyl carbamate on Nrf2 knockout (KO) mice on a BALB/c background, female wildtype (WT) and KO mice were injected i.p. with two to four doses of vinyl carbamate, using protocols previously used with Nrf2 KO mice [22] or with vinyl carbamate [38]. Age-matched cohorts of Nrf2 WT and KO mice (4 mice/group/time point) were harvested beginning at 20 weeks after initiation and then every 4 weeks (24, 28, 32 weeks). More lung tumors were consistently visible over time (20-36 weeks) both (a) in Nrf2 KO mice vs. WT mice and (b) in mice injected with vinyl carbamate four times vs. two times in both WT and KO mice (average number = 2.7 ± 0.7 tumors with two doses

vinyl carbamate vs. 6.6 ± 0.6 tumors with four doses in WT mice, $p<0.05$; 7.95 ± 0.7 tumors with two doses vs. 10.9 ± 1.0 tumors with four doses in Nrf2 KO mice, $p<0.05$). Although the number and size of the tumors increased over time in both groups, these parameters were consistently higher in the Nrf2 KO mice (Figure 4.1 A). At 20 weeks, 4-12 tumors were visible on the surface of lungs in Nrf2 KO mice, while almost no visible tumors (0-1) were observed at this time in WT mice. By 32 weeks, an average of 6.5 ± 0.95 tumors per lung were found in the WT mice and 12.25 ± 2.6 tumors were found in the Nrf2 KO group. For all time points, the number of grossly visible surface tumors was significantly ($p<0.05$) higher in Nrf2 KO mice compared to WT mice (Figure 4.1 B), in the entire lung (unfixed) or in the intact left lung (after formalin fixation but before sectioning).

After gross evaluation, each left lung was then sectioned and stained with hematoxylin and eosin. The average tumor number (Figure 4.1 C) and total tumor volume (Figure 4.1 D) per slide were also significantly ($p<0.05$) higher in the lungs of Nrf2 KO mice vs. WT mice. There were no significant differences in tumor histopathology between groups as almost all of the tumors were high grade (tumefactive architecture, fused trabeculae, and distinct nucleoli and conspicuous mitoses within nuclei) by 20 weeks after initiation. Representative images demonstrating this histopathology are shown in Figure 4.1 E. As expected based on the larger tumor size, the tumors in the Nrf2 KO mice proliferate more rapidly than the WT tumors, as the percentage of proliferating cell nuclear antigen (PCNA) positive cells is significantly higher in the Nrf2 KO tumors.

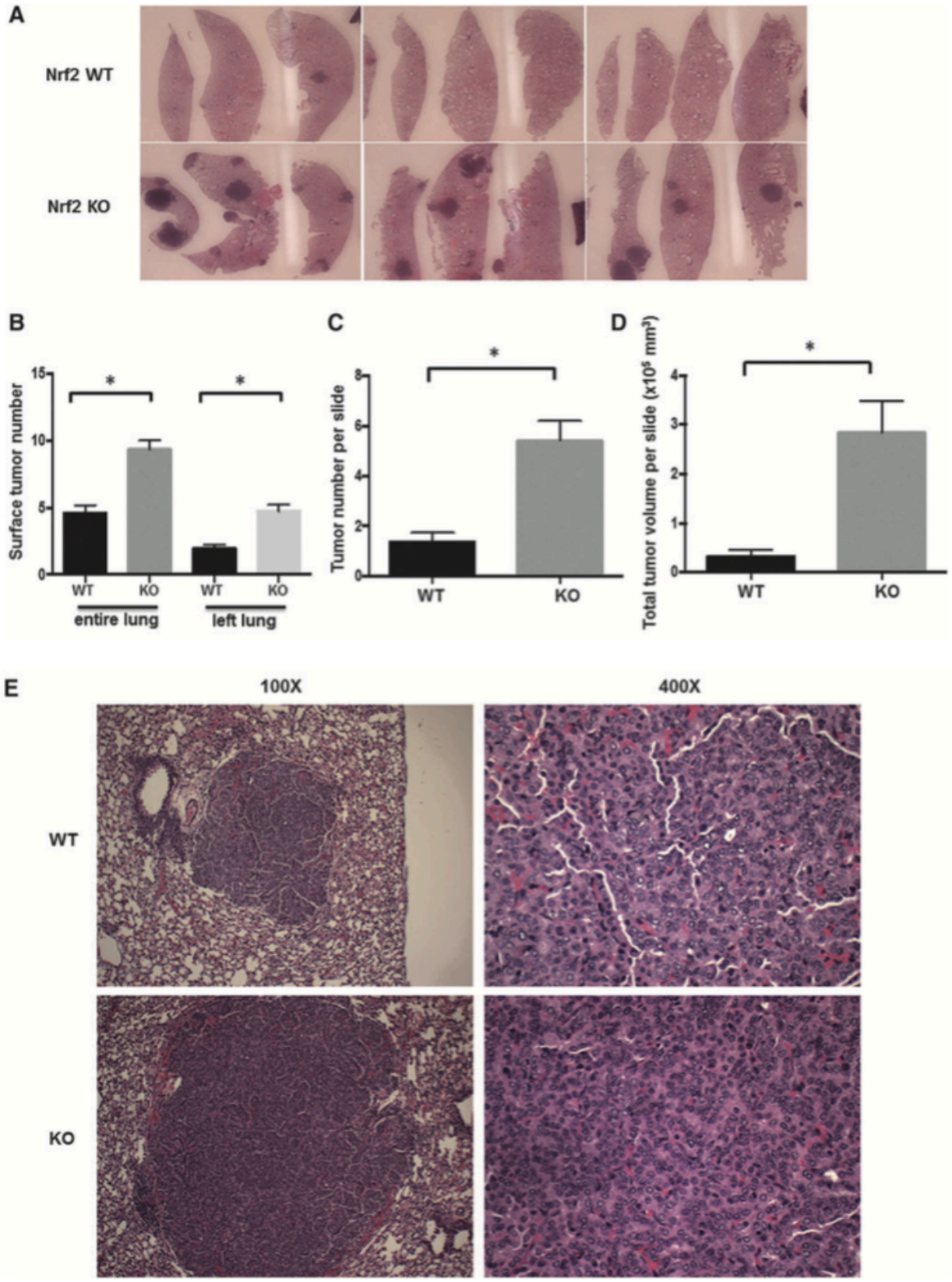

Figure 4.1: Nrf2 deficiency promotes lung carcinogenesis. Nrf2 knockout (KO) and

Figure 4.1 (cont'd)
wildtype (WT) mice were injected with vinyl carbamate between 6-8 weeks of age. Lungs from age-matched Nrf2 KO and WT mice were harvested over a period of 20-40 weeks after initiation with the carcinogen to examine tumor burden. A. Representative images of lung sections stained with hematoxylin and eosin; tumors are darkly stained purple areas (10X magnification). B. The average number of tumors on the surface of the entire lungs or on the left lung after fixation in formalin were counted, n = 31-42 mice per group C. Average tumor number (C) and total tumor volume (D) per slide was calculated in both Nrf2 WT and KO groups. N=20 mice per group. *, $p<0.05$. (E) Representative images of lung histopathology in WT and KO groups. KO, knockout; WT, wild-type.

4.4.2 Nrf2 deficiency decreases T cell populations during lung carcinogenesis

Next, we investigated immune cell populations in the lungs and spleens of Nrf2 WT and KO mice challenged with vinyl carbamate. The same two lobes of the right lung were always collected, and the fresh tissues were processed for flow cytometry using optimized antibody panels [41]. To obtain an overview of the immune cell populations in the lung, the percentages of $CD45^+$ immune cells as well as total T cells ($CD45^+$, $CD3^+$), CD4 helper T cells ($CD45^+$, $CD3^+$, $CD4^+$) and CD8 cytotoxic T cells ($CD45^+$, $CD3^+$, $CD8^+$), B cells ($CD45^+$, $CD19^+$, $B220^+$), macrophages ($CD45^+$, $CD11b^+$, $Gr\text{-}1^-$), and myeloid-derived suppressor cells (MDSCs) ($CD45^+$, $CD11b^+$, $Gr\text{-}1^+$) were analyzed. Although cohorts of paired, age-matched lungs (four mice/group) were collected 20-36 weeks after initiation with vinyl carbamate, unless otherwise noted, the changes in the Nrf2 KO vs. WT lungs was consistent over time, and Nrf2 KO and WT groups were pooled when appropriate.

As shown in Figure 4.2 A, the percentage of $CD45^+$ immune cells were significantly ($p<0.05$) lower in the lungs of Nrf2 KO mice than in WT mice, primarily because of changes in T cell populations. Nrf2 KO mice had a significantly ($p<0.05$) lower number of total T cells ($CD45^+$, $CD3^+$, 20-32 weeks; Figure 4.2 B), CD8 cytotoxic T cells (28-32

weeks; Figure 4.2 C) and CD4 helper T cells (24-32 weeks; Figure 4.2 D). CD4 T cells play a central role in immunity, but their contribution to antitumor immunity is complex as different types of CD4 T cells have diverse functions [52]. CD8 cytotoxic T cells recognize tumor cells and are essential for the response to immunotherapies such as PD-1/PD-L1 [53].

The percentage of macrophages was significantly ($p<0.05$) higher in the lungs of Nrf2 KO mice before 24 weeks (Figure 4.2 E), but this difference disappeared at later time points. Macrophages play a critical role in promotion of urethane-induced lung carcinogenesis [54]. Fewer and smaller lung tumors will develop if macrophages are depleted during tumor initiation and early promotion in this model. There was no significant difference in B cells between the two groups in the lung (data not shown). In the spleen, the only change was a small but significant ($p<0.05$; 20-40 weeks) increase in MDSCs in Nrf2 KO mice (Figure 4.2 F). MDSCs play important roles in immunosuppression. High infiltration of these cells is associated with poor prognosis in cancer patients [55-57], and the survival and function of MDSCs are regulated by Nrf2 [58]. All of the changes in immune populations were confirmed by immunohistochemistry and representative pictures are shown in Figure 4.2 G. As indicated in the pictures, the macrophages and CD8 cytotoxic T cells are located around the periphery of the tumors.

In addition, the decrease of $CD45^+$ population, $CD3^+$ T cells and $CD4^+$ T cells was similar at early time points (4 and 8 weeks after initiation, data not shown), while the percentage of $CD8^+$ T cells was significantly ($p<0.05$) higher in the lungs of Nrf2 KO mice compared to WT mice at early time points. There was no significant difference in immune

populations between saline injected mice and vinyl carbamate injected mice at these time points (data not shown).

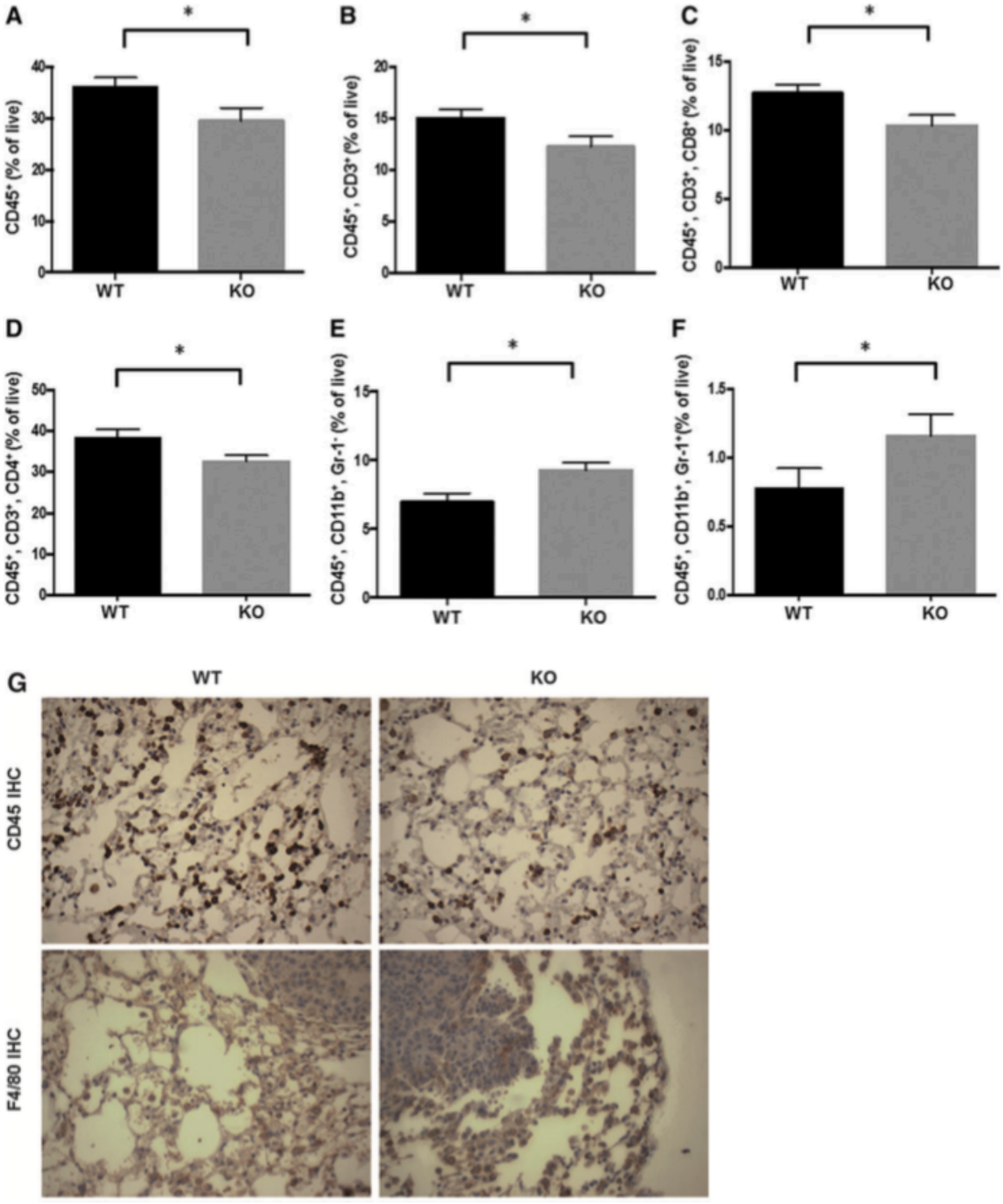

Figure 4.2: Nrf2-deficiency alters the immune cell populations in the lung and

Figure 4.2 (cont'd)
spleen of mice challenged with vinyl carbamate. The immune cell populations in the same two lobes of right lung (A-E) or spleen (F) from Nrf2 KO and Nrf2 WT were analyzed by flow cytometry. Percentages of total immune cells ($CD45^+$), total T cells ($CD45^+$, $CD3^+$), cytotoxic T cells ($CD45^+$, $CD3^+$, $CD8^+$), T helper cells ($CD45^+$, $CD3^+$, $CD4^+$), and macrophages ($CD45^+$, $CD11b^+$, $Gr\text{-}1^-$) in the lung (A-E) and myeloid derived suppressor cells ($CD45^+$, $CD11b^+$, $Gr\text{-}1^+$) in the spleen (F) are shown. *, $p<0.05$. The changes in immune cell populations were confirmed by IHC (G). F4/80 is a macrophage marker.

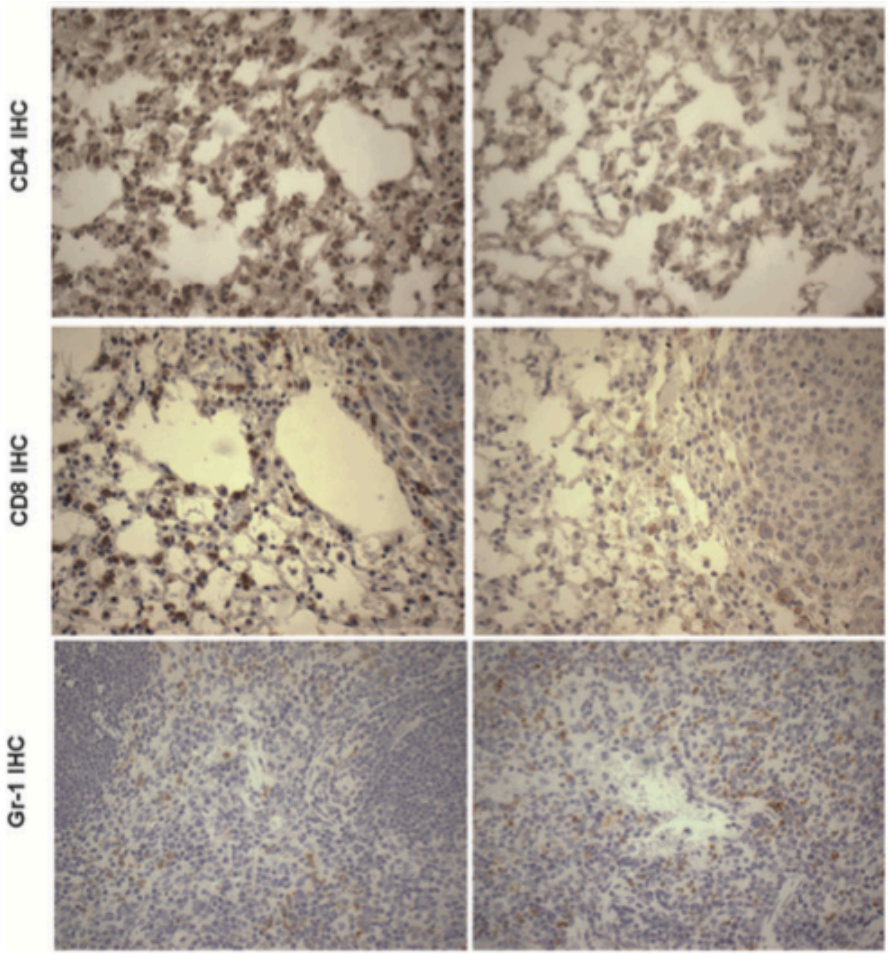

4.4.3 Altered gene signatures in lung tumors from Nrf2 KO vs. WT mice

To further investigate the differences between Nrf2 WT and KO mice at a molecular level, lung tumors were dissected out from the lung tissue and pooled (three to four

tumors). Total RNA from two independent samples per group was analyzed by RNA sequencing (RNAseq). Significantly ($p<0.05$) different expression patterns were detected for 376 genes in tumors from the lungs of Nrf2 WT vs. KO mice. Slightly more than half (197 out of 376) of the altered genes in the Nrf2 KO tumors were upregulated compared to WT tumors, and the rest were significantly downregulated (Figure 4.3 A).

Among the differentially regulated genes, the *NFE2L2* (Nrf2 gene) was the most significantly downregulated gene in Nrf2 KO tumors, which confirms the deletion of Nrf2. Additional confirmation that Nrf2 was deleted was obtained by genotyping the mice and analyzing lung extracts by western blotting (data not shown). Differentially regulated genes were then processed to identify over-represented genes using PANTHER analysis (Figure 4.3 B). As the Nrf2 cytoprotective mechanism was knocked out, the "response to stimuli gene set" (GO:0050896) including Sod3 (extracellular superoxide dismutase) and Gpx3 (Glutathione peroxidase 3) was downregulated in Nrf2 KO tumors. Notably, the "immune system process" (GO:0002376) was the gene set with the most significant change between groups. As listed in Table 4.1, a series of cytokines, chemokines and peptide antigens in this gene set were significantly upregulated in tumors from Nrf2 KO mice. Many of these factors, including Cxcl (1, 3, 12) and Ccl (9, 11, 17) are important for regulation and chemotaxis of immune cells, especially MDSCs, and the activation of M2 macrophages [59, 60] and will be discussed below. Cytokines can be released in response to inflammation to inhibit tumor development and progression, but alternatively, cancer cells can respond to cytokines that promote growth, inhibit apoptosis and facilitate metastasis [61]. In addition to the striking effects on the immune system, a metastatic signature also emerged. Genes involved in localization

(GO:0051179, Figure 4.3 B) and extracellular matrix (GO:0031012 and GO:0044421, Table 4.1), which regulates cell migration and metastasis, were differently expressed in these two groups. Overexpression of matrix metalloproteinase (MMP) 12, which is upregulated in KO tumors, plays a key role in modulating myelopoiesis, immune suppression, and lung tumorigenesis [62]. MMP25, which is elevated in many cancer types and promotes tumor invasion and metastasis through activation of MMP2, was also upregulated in Nrf2 KO tumors [63]. Notch signaling (Table 4.1) is known to crosstalk with the Nrf2 pathway, and aberrant crosstalk between Nrf2 and notch plays an important role in lung carcinogenesis [64]. The differential expression of Notch1 in the lung of Nrf2 WT vs. KO mice was confirmed by western blotting (data not shown). Consistent with the observation of more and larger tumors in Nrf2 KO vs. WT mice, cell growth related genes (Igfbp5, Igfbp6, Bmp6) were upregulated and cell death related genes (Srcap, Thsd4) downregulated in the Nrf2 KO lung tumors (Table 4.1). P27, an indicator of cell cycle arrest, was significantly down-regulated in Nrf2 KO mice vs. Nrf2 WT mice. Numerous genes involved in metabolic pathways were also significantly over represented, including heme transport (GO:0015886), negative regulation of cellular amide metabolic process (GO:0034249), and aldonic acid metabolic process (GO:0019520). The raw data and processed data are available on Gene Expression Omnibus (GEO, GSE99338).

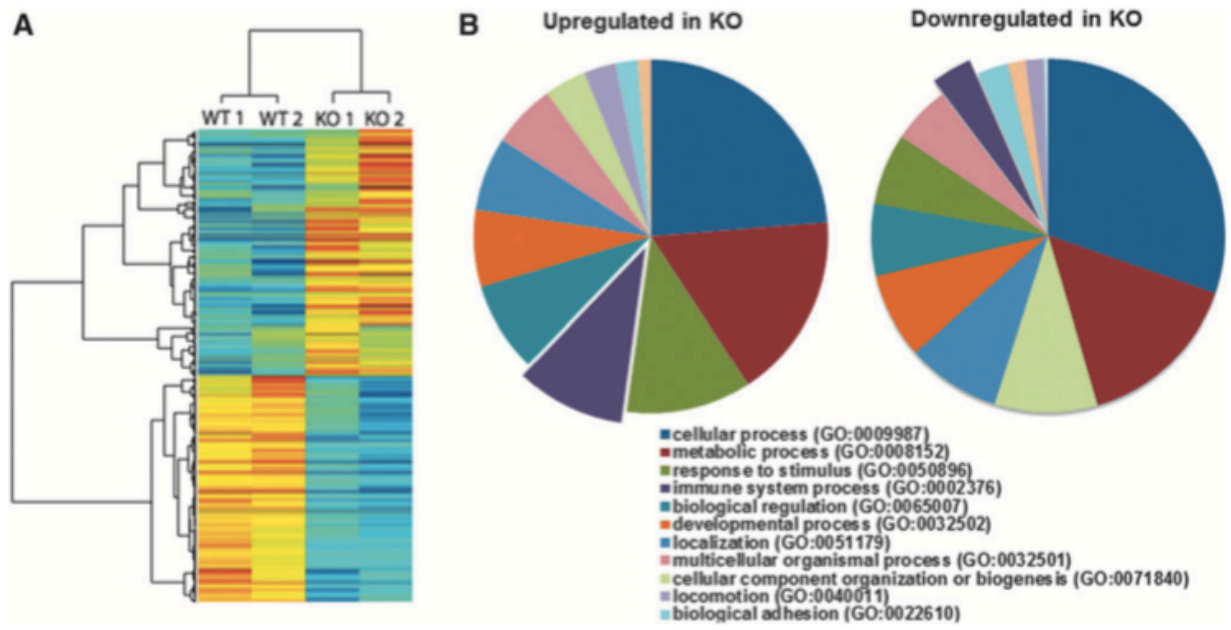

Figure 4.3: Nrf2-deficiency alters global transcription in tumors in the lungs of mice challenged with vinyl carbamate. A. An unsupervised-hierarchical clustering of Nrf2 WT and NRF2 KO tumors by differentially regulated genes shows unique transcriptional profile in the two tumor types. The NRF2 KO tumors have a distinct profile of upregulated (red) and downregulated (blue) genes which is reversed in the WT tumors. B. PANTHER analysis was performed on the upregulated genes (left) and downregulated genes (right) with NFR2 deletion. This analysis identified a number of significantly overrepresented gene ontologies between the WT and KO tumors, especially in the immune system related genes (GO:0002376) (purple).

4.4.4 Cytokines are up regulated in tumors and lungs from Nrf2 KO mice

Both the flow cytometry data and RNAseq data revealed the important role of Nrf2 on the immune system in this lung cancer model. To confirm these results, four cytokines listed in Table 4.1 were selected to validate *ex vivo*: Cxcl1, Cxcl12, Ccl9, and Csf1. These cytokines and chemokines are all highly relevant in cancer. Cxcl1 attracts MDSCs ($CD11b^+$, $Gr1^+$) into the tumor, which then produce chemokines that enhance tumor survival and inhibit CD8 cytotoxic T cells. It also recruits tumor-associated macrophages (TAMs) and cancer-associated fibroblasts (CAFs). High Cxcl1 levels are associated with higher metastatic potential and poor prognosis [60, 65, 66]. Chemokine Cxcl12, which is

the sole ligand of CXCR4, provides an attractive niche for tumor cell migration and colonization. It is highly expressed not only in primary lung cancer cells but also in the brain, liver, bone marrow, and adrenal glands, which are all common sites for lung cancer metastasis [67-70]. Ccl9 is highly induced in myeloid cells by TGF-β signaling and is also secreted by premetastatic tumor cells to recruit more myeloid cells, which enhances tumor cell survival and metastasis [71]. Csf1 is involved in cancer growth, survival, and metastasis. Blockade of CSF1/CSF1R reprograms TAMs to enhance antigen presentation, thus improving the therapeutic effects of immunotherapies [59, 72-74].

To validate the bioinformatics predictions (Figure 4.4A) of the upregulation of these cytokines and chemokines, aliquots of the same RNA samples analyzed by RNAseq were used for real-time PCR. All four cytokines were significantly upregulated in Nrf2 KO vs. WT tumors (Figure 4.4 B-E, $p<0.05$). To confirm these changes, total RNA was isolated from lung tissue, and real-time PCR was used to evaluate relative gene expression of the cytokines. Notably, significant increases in expression of these cytokines in Nrf2 KO lungs were still detected (Figure 4.4 F). *Cxcl1, Csf1, Cxcl12* (24 weeks) and *Ccl9* (32 weeks) were significantly upregulated in the lungs of Nrf2 KO mice (Figure 4.4 F). The expression of Cxcl1 and Cxcl12 protein was detected by ELISA. Cxcl1 (24-32 weeks, Figure 4.4 G) and Cxcl12 (32 weeks, Figure 4.4 H) are significantly upregulated in the Nrf2 KO lungs compared with those in the WT lungs.

To further validate the regulation of Nrf2 on cytokine expression and identify which cell type is expressing the cytokines, *in vitro* studies with both tumor cells and immune cells were performed. VC1 cells, a primary lung tumor cell line extracted from the vinyl

carbamate induced lung cancer model [38], were treated with CDDO-Im (a synthetic triterpenoid and potent Nrf2 activator), and the expression of the cytokines were detected by real-time PCR. Treatment with the Nrf2 activation significantly ($p<0.05$) decreased mRNA expression of these four cytokines in the lung cancer cells (Figure 4.5 A). Similarly, in RAW264.7 macrophage-like cells stimulated with LPS, activation of Nrf2 by CDDO-Im significantly ($p<0.05$) decreased Csf1 mRNA expression (Figure 4.5 B). *Cxcl1* and *Cxcl12* were expressed at very low levels in RAW264.7 cells, even after treatment with LPS or conditioned media from VC1 cells (data not shown), and there was no significant change in Ccl9 expression following treatment with CDDO-Im (Figure 4.5 B). These experiments suggest that Nrf2 regulates cytokines in both tumor cells and immune cells and that the expression of different cytokines is cell type dependent.

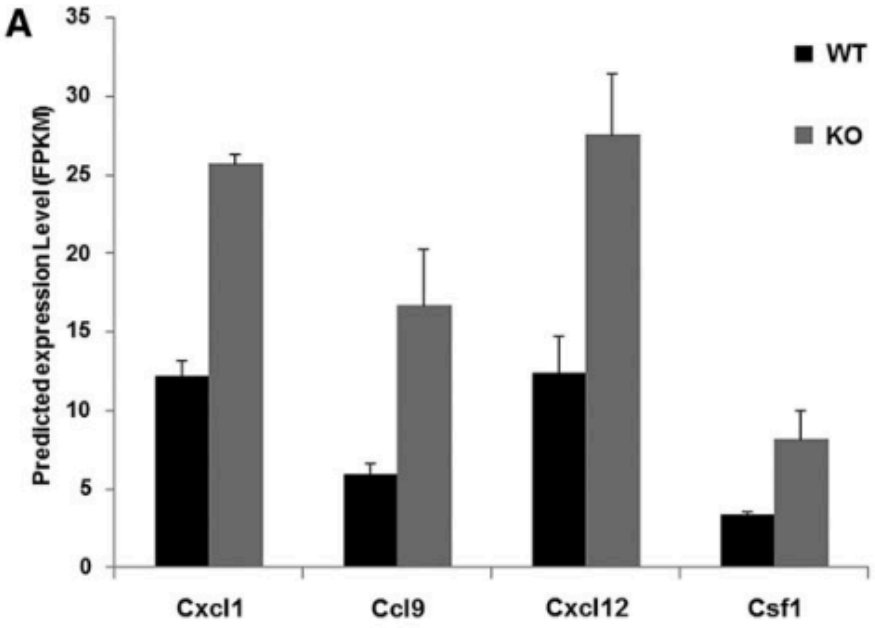

Figure 4.4: Differential gene expression of cytokines in the tumors and lungs of Nrf2 WT vs. KO mice. A. Predicted gene expression levels (FPKM) based on RNAseq data of lung tumors from Nrf2 WT and KO mice for *Cxcl1, Ccl9, Cxcl12* and *Csf1*. The same tumor RNA analyzed by RNAseq was used to confirm the cytokine gene expression using real-time PCR (B-E). *, $p<0.05$ WT vs KO. In F, lung tissues from mice challenged with vinyl carbamate were harvested at three time points, 24-32 weeks after

Figure 4.4 (cont'd)
initiation. Total RNA was extracted from the lung and relative gene expression of *Csf1*, *Cxcl1, Cxcl12* and *Ccl9* were analyzed by real time PCR. N=4 lungs per group at each time point. *, p<0.05 WT vs KO at 24 weeks (*Csf1, Cxcl1, Cxcl12*) or 32 weeks (*Ccl9*). The production of Cxcl1 (G) and Cxcl12 (H) in the lung was detected by ELISA assay. *, p<0.05 WT vs KO at 24-32 weeks with Cxcl1 and 32 weeks with Cxcl12. Data are presented as mean ± SEM.

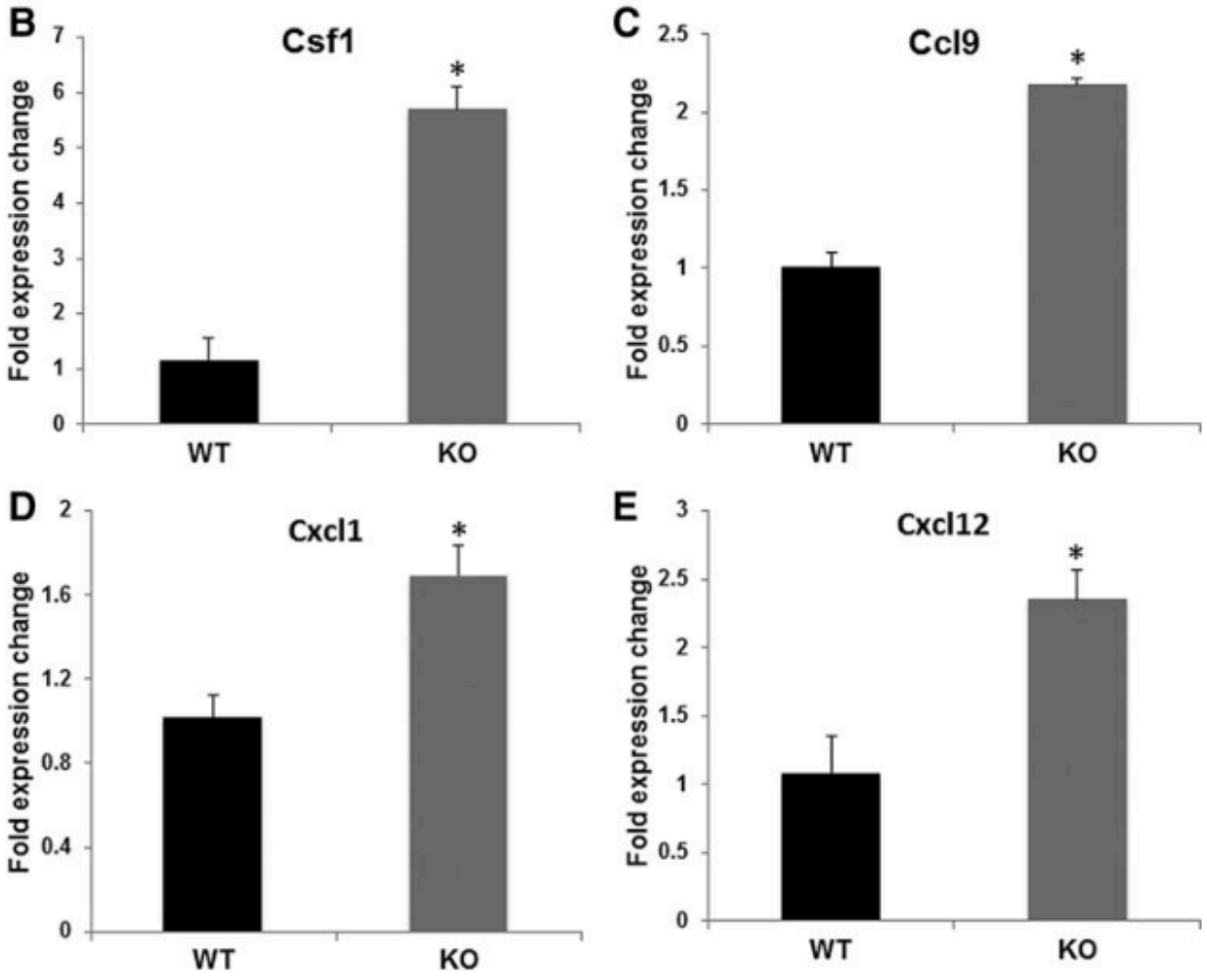

Figure 4.4 (cont'd)

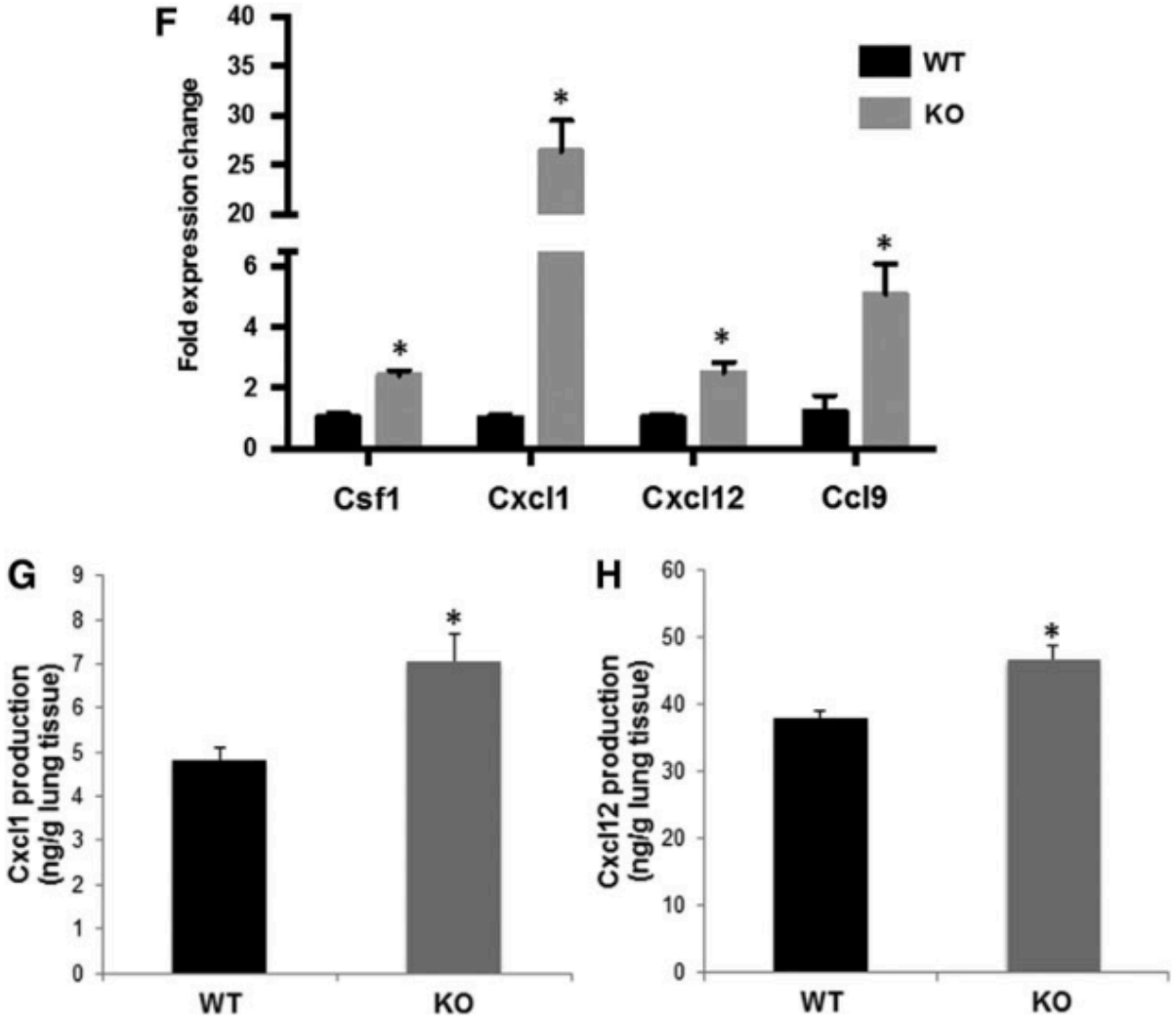

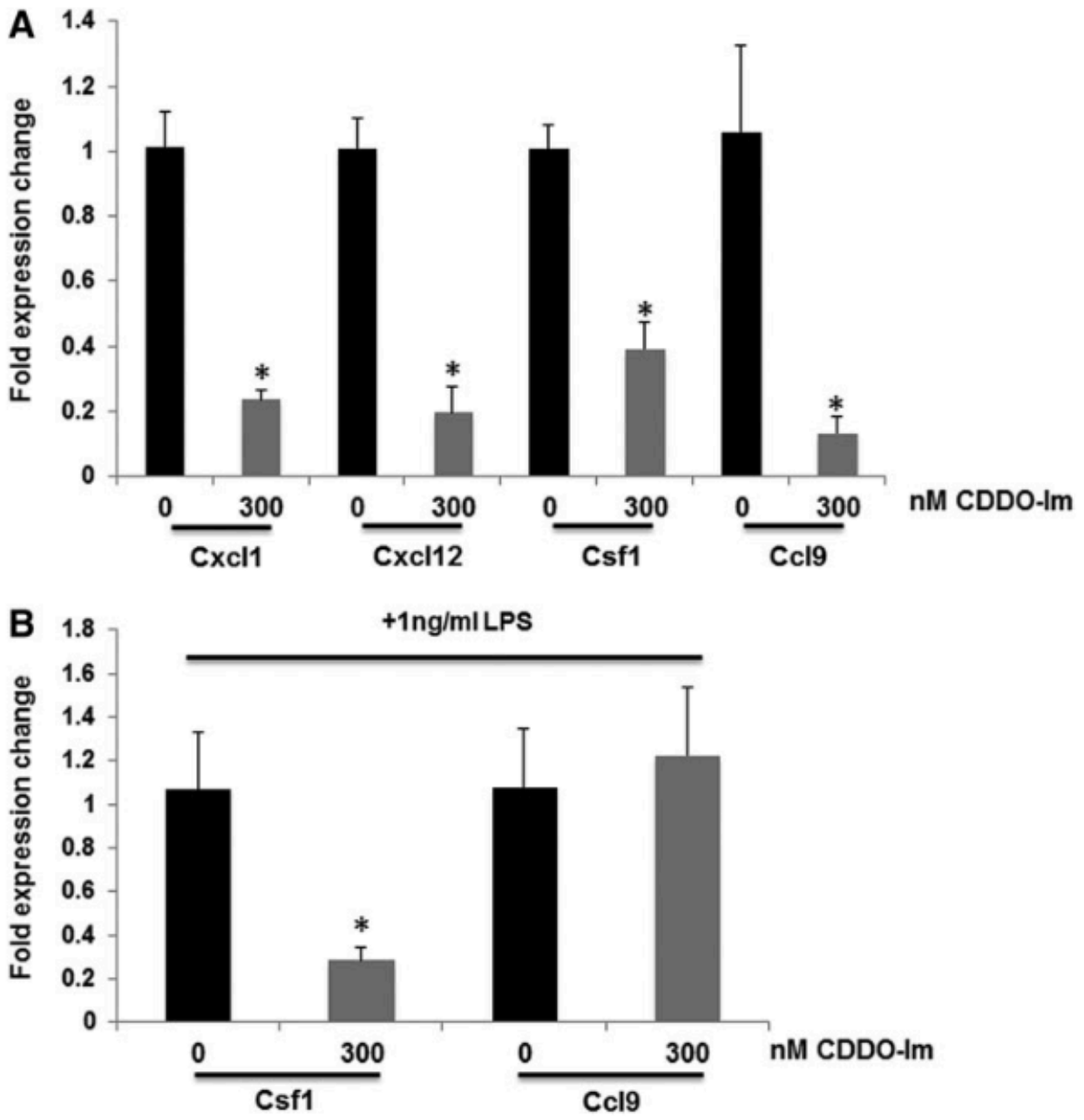

Figure 4.5: Nrf2 activation decreases cytokine production in both tumor cells and immune cells. VC1 (primary mouse lung cancer cells, A) and RAW264.7 (macrophage like cells, B) were treated with 300 nM CDDO-Im (a potent Nrf2 activator) for 24 hrs, and RAW264.7 cells were stimulated with 1 ng/ml LPS 20 mins after CDDO-Im treatment. Total RNA was extracted from the cells, and gene expression of *Cxcl1, Csf1, Ccl9* and *Cxcl12* were detected by real time PCR. *, $p<0.05$ CDDO-Im treated group vs. DMSO control for each cytokine.

4.4.5 The regulation of immune response in the mouse model is consistent with data from patients with lung adenocarcinomas

As a striking up-regulation of immune responses was found in lung tumors from Nrf2 KO mice, we wanted to verify if these results were consistent in human patients. We accessed genomic data from lung cancer patients through the TCGA human cancer database, and cBioPortal was used to analyze the genetic alterations in *Nfe2l2* and *Keap1* within lung cancer patients. As has been reported [15], *Keap1* alterations (mutations and deletions) are most frequent in lung adenocarcinoma patients, while *Nfe2l2* alterations (mutations and amplifications) are more frequent in lung squamous carcinoma. Both loss-of-function alterations of *Keap1* and gain-of-function alterations of *Nfe2l2* induce high constitutive Nrf2 activity. Oncoprints of *Keap1* genetic alterations in lung adenocarcinoma patients [48] (230 samples) and *Nfe2l2* genetic alterations in lung squamous carcinoma patients [49] (178 samples) are shown in Figure 4.6 A and C, respectively. Enrichment of gene ontologies was identified through Bayes factor. As shown in Table 4.2, the expression of immune response related gene ontologies (GO:0006955, GO:0019882, GO:0006959) was consistently preserved in human tumors. Then, gene expression of individual cytokines was analyzed, as cytokines were differentially regulated in our mouse model. *Cxcl1, 2, 10, 11, 12, 14, Ccl2, 3, 4L1, 13, 22*, *28* and *Csf1, 1R, 2RB, 3R* were all significantly downregulated in Keap1 altered adenocarcinoma patients. *Cxcl1, 2, 3, 6, 12, 17, Ccl15, 17, 22, 28,* and *Csf2, 3R* were significantly downregulated in Nrf2 altered squamous carcinoma patients. *Cxcl1, Cxcl12, Csf1*, the three cytokines upregulated in Nrf2 KO mice with adenocarcinomas, were consistently downregulated in Keap1 loss of function patients (Figure 4.6 B). These

results are consistent with the function of Keap1 as a negative regulator of Nrf2, as Nrf2 would be constitutively active in these samples instead of deleted as in the mouse model. *Cxcl1* was also downregulated in patients with gain of function Nrf2 amplifications and alterations (Figure 4.6 D). In summary, our findings suggest that Nrf2 regulation of cytokines in lung cancer can be found in both mice and humans.

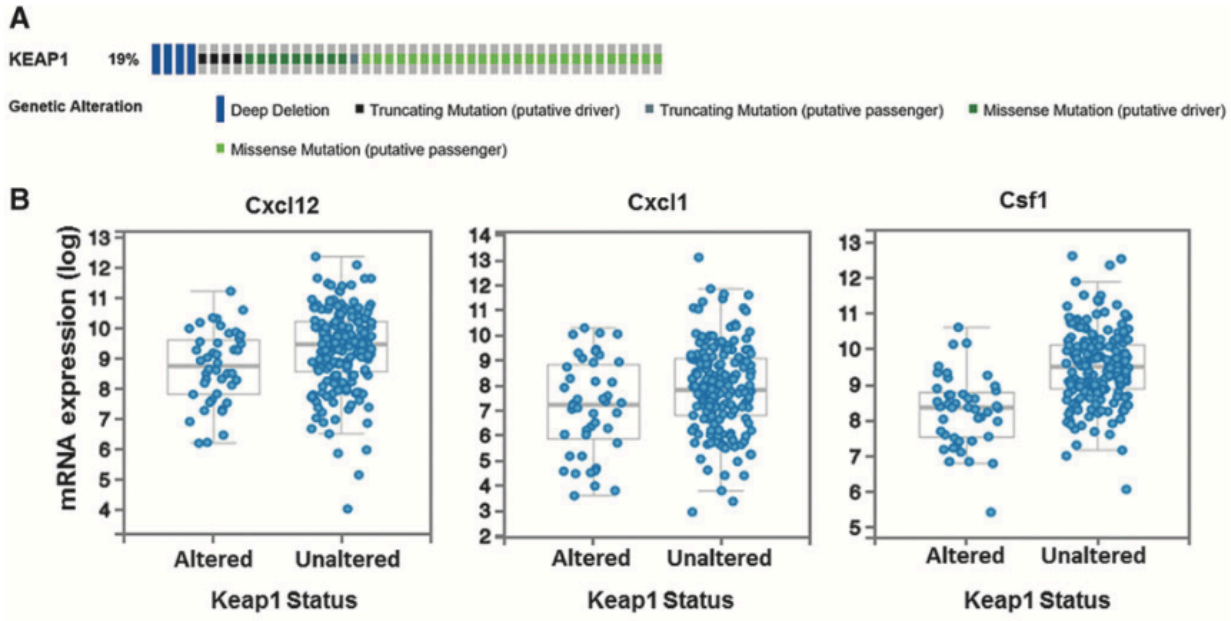

Figure 4.6: The regulation of immune response by Nrf2 in the mouse model is consistent with data in lung cancer patients. A. Oncoprint of *Keap1* genetic alterations in patients with lung adenocarcinoma [48] (230 samples). Unaltered patients are not shown. Alterations of *Keap1* are mainly deletions and mutations. B. Individual genes (*Cxcl12, Cxcl1, Csf1*) were downregulated in lung adenocarcinoma patients with *Keap1* alterations. $p<0.05$. Results are presented as box plot with maximum, third quartile, median, first quartile, and minimum (top to bottom). C. Oncoprint of *Nfe2l2* genetic alterations in lung squamous carcinoma patients [49] (178 samples). Unaltered patients are not shown. Alterations of *Nfe2l2* are mainly amplifications and mutations. D. *Cxcl1* was downregulated in lung squamous carcinoma patients with Nrf2 alterations. $p<0.05$. Results are presented as box plot with maximum, third quartile, median, first quartile, and minimum (top to bottom).

Figure 4.6 (cont'd)

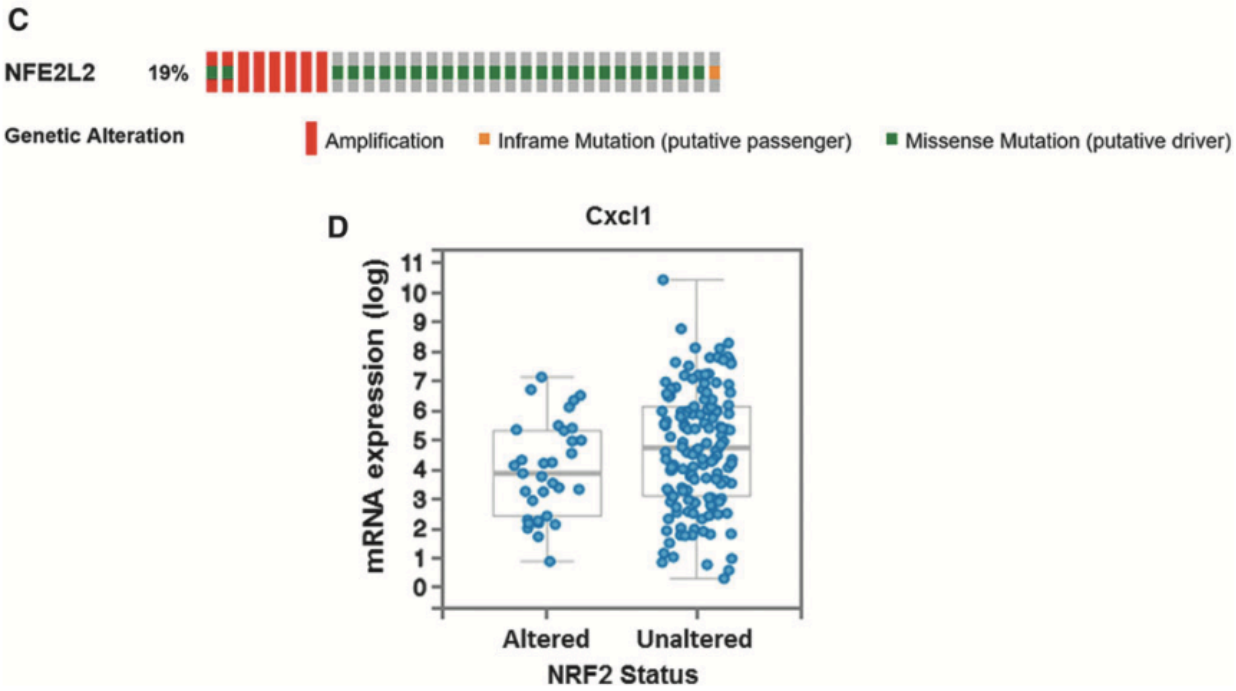

4.5 Discussion

This study confirmed the importance of Nrf2 as a cytoprotective mechanism for reducing tumor development in a relevant model of lung carcinogenesis. Nrf2 KO mice were more sensitive to vinyl carbamate-induced lung adenocarcinomas and developed more and larger tumors compared to Nrf2 WT mice. More importantly, this study provided evidence that Nrf2 regulated the immune cell infiltration that contributes to tumorigenesis. Deletion of Nrf2 significantly elevated the production of many cytokines and genes involved in antigen presentation and processing. Fewer T cells, including both CD8 cytotoxic T cells and CD4 helper T cells, were found in the lung, but higher populations of tumor-promoting macrophages and MDSCs were found in the lung and

spleen, respectively, in Nrf2 KO mice compared to WT mice with advanced tumors. These striking effects of Nrf2 on immune processes are consistent with changes found in lung cancer patients, making these findings clinically relevant.

There are many inconsistent results in the literature regarding the complex role of Nrf2 in tumor initiation and development, especially in lung cancer. Our study confirmed that Nrf2 deficiency makes mice more susceptible to the carcinogen vinyl carbamate, as *more and larger* tumors were found in the *Nrf2 KO* mice (Fig. 1). These results are consistent with the observation that Nrf2 deficient mice are more sensitive to carcinogens [23], as the enzymes that would normally detoxify the carcinogen are missing. Satoh *et al.* reported that Nrf2 prevented initiation of lung carcinogenesis, as Nrf2-deficient mice exhibited more tumor nodules than the wild type mice 4-8 weeks after urethane injection. However, at later time points (16 weeks after initiation), the number and size of the lung tumors in the Nrf2 KO mice were reduced, but the tumors were more aggressive in the Nrf2 KO mice than in WT mice [75]. Knockdown of Keap1 in mice, which results in *constitutive Nrf2 expression*, led to resistance to urethane-induced carcinogenesis and *fewer and smaller* surface tumors at an early stage (up to 16 weeks). In contrast to the results cited above, Bauer *et al.* reported that deletion of Nrf2 reduced the number of urethane-induced lung tumors, as Nrf2 had pro-survival effects in tumor cells and the lack of Nrf2 enhanced apoptosis in the lung [27].

There are a number of possible reasons for these discrepancies. The studies described above used mice on a variety of genetic backgrounds, with different carcinogens and protocols for initiating lung carcinogenesis, and with diverse time points chosen after initiation for final analysis. Although urethane is commonly used to induce

experimental lung cancer, initiation with urethane yields adenomas. In contrast, vinyl carbamate, the carcinogen used in our studies, bypasses the first step oxidation of urethane, induces invasive adenocarcinomas [38]. The most common mutations in NSCLC are in the *Kras* gene, and *Kras* mutations are prognostic for a poor outcome [76]. Both urethane and vinyl carbamate induce mutations in *Kras* [31, 77], but lung carcinogenesis is more aggressive when induced by vinyl carbamate, as the number, size and pathological grade of the tumors [39] increase in a reproducible, time-dependent manner. Moreover, vinyl carbamate is much more potent, as only 16 mg/kg are needed to induce lung carcinogenesis vs. 1 g/kg body for urethane [22].

In addition to the choice of carcinogen, a variety of mouse strains were used in these published studies, including BALB/cCR [27], ICR/CD-1 [75] and BALB/c strains. Mouse strains vary in their susceptibility to lung carcinogenesis, likely as a result of their response to inflammation [78]. Lungs were also harvested at different time points, and Nrf2 has different roles during early vs. late tumor progression [75]. In our studies, tumors were not harvested until 20 or more weeks after initiation, during late stage carcinogenesis, and thus the tumors were high-grade tumors.

Our most important finding is that Nrf2 regulates the immune cells and cytokines that can contribute to cancer development. Nrf2 has been shown to directly inhibit the transcription of pro-inflammatory cytokines [79]. To date, however, only a limited number of studies have investigated the effects of Nrf2 on the host immune system during carcinogenesis. Satoh *et al.* has shown that more inflammatory cells infiltrated into lungs of Keap1 knockdown mice than in WT Keap1 mice [21, 22], and these changes provided a more permissive environment for lung metastasis in the Lewis lung carcinoma model

[21]. Moreover, MDSCs, which suppress the activity of cytotoxic CD8 T cells, are regulated by Nrf2 [58], and the number and activity of splenic CD8 T cells were markedly diminished in tumor-bearing Nrf2 WT mice but not in Nrf2 KO mice [75]. However, in our study, we observed a reduced percentage of CD8 T cells in Nrf2 KO lungs compared to WT lungs, which is consistent with a higher tumor burden in the Nrf2 KO group. CD8 T cells are a major effector of antitumor immunity and are necessary for T cell-based immunotherapies against lung cancer. Dysfunctions in CD8+ T-cells in lung tumors are associated with a poor clinical response [80]. MDSCs also contribute to tumor growth by inhibiting CD8+ cytotoxic T cells (21).

Tumor associated macrophages are another important immune cell that can drive tumor progression [81], as long-term depletion of macrophages markedly reduced lung tumorigenesis induced by urethane [54]. The contribution of Nrf2 and other redox signaling for macrophage activation and polarization is an emerging area of investigation, in both health and disease [82]. Both the abundance and activation state of different cell types in the tumor microenvironment influence the balance between tumor promoting and tumor suppressing phenotypes. Although we have not yet explored the role of Nrf2 in macrophage polarization in our lung cancer model, additional studies will address this important question. However, the phenotype of increased percentages of macrophages and MDSCs and decreased CD8 T cell populations found in our model are associated with a poor prognosis in humans and are consistent with an important beneficial regulatory role for Nrf2 in cancer immunity. Moreover, the enhanced cytokine production in Nrf2 KO mice further confirmed the immune signature in the Nrf2 KO group. Elevated production of cytokines in Nrf2 KO tumors likely recruits macrophages and MDSCs, thus

promoting survival and growth of the tumor. These cytokines could be secreted by either tumor or other cells, including macrophages and fibroblasts [83].

The striking immune signatures found in our RNAseq analysis should draw more attention to the relatively unexplored function of Nrf2 on the immune system in lung carcinogenesis. A series of cytokines and MHC antigen genes are differentially expressed between Nrf2 WT and KO tumors, and higher expression levels in Nrf2 KO mice are associated with more and larger tumors. Admittedly, our approach did not differentiate the source of the immune signatures, but future studies will identify the relative contributions of cancer cells vs. immune cells. However, the regulation of immune responses by Nrf2 is also found in patients with lung cancer, indicating the potential value of Nrf2 status and immune signatures for predicting disease prognosis or treatment. With greater availability of sequencing or RNAseq analysis, tumor mutations and transcriptional profiles are being studied and are providing useful information. Gene signatures can potentially be used as diagnostic or prognostic markers and have been used successfully in breast cancer to guide clinical decisions [84]. In lung cancer, research into genetic signatures has been focused on early diagnosis of curable tumors, the need for new treatment regimens for patients with inoperable tumors, and the selection of effective therapies [85]. As diagnostic techniques advancing and understanding of biology accumulating, targeting Nrf2 under more circumstances in cancer will become more practical.

Because of the complexity of Nrf2 in cancer, targeting Nrf2 requires a deeper understanding of the role of Nrf2 at different stages of cancer (especially between tumor initiation and tumor progression) and on different components of the tumor

microenvironment (including tumor cells and immune cells). This information is especially relevant as there are already several compounds that activate the Nrf2 pathway that are being evaluated in the clinic. Dimethyl fumarate has been approved for relapsing multiple sclerosis. Synthetic triterpenoids are in clinical trials for pulmonary diseases, chronic kidney disease, melanoma, *etc*. Natural compounds including sulphoraphane and curcumin are being tested in clinical trials for cancer prevention. In contrast, there is still not a specific, potent Nrf2 inhibitor available, even though accumulating evidence suggests a tumor-promoting role for Nrf2 in advanced cancers. Treating patients appropriately with Nrf2 activators or inhibitors for prevention or treatment of cancer will require careful consideration of the genetic status of Nrf2/Keap1 and knowledge of the tumor stage.

It is also necessary to better understand the mechanisms of compounds that activate Nrf2 because of their potential off-target effects and the complex crosstalk between Nrf2 and other important pathways in cancer. It is well known that Nrf2 reciprocally interacts with HIF-1α, NF-κB, MAPK and phosphatases, and many of these important signaling pathways are enriched in redox-active cysteines that can be targeted by natural products and other redox sensitive drugs [86, 87]. Some of these proteins, such as HIF-1 and NF-κB, also regulate inflammation and immune responses [88, 89], and additional studies are needed to elucidate the crosstalk between Nrf2 and these pathways, especially regarding the regulation of the immune system in cancer.

In summary, our study demonstrates a protective role for Nrf2 in lung cancer and identifies an immune phenotype in tumors generated using a different model system than has been previously reported. Future studies will investigate the effects Nrf2 on

different types of immune cells and determine whether Nrf2 status is correlated with the response to immunotherapy or other therapies.

Table 4.1: Over-represented, differentially regulated genes in lung tumors from Nrf2 WT vs. KO mice

Description	Genes Up-Regulated in KO mice	Genes Down-Regulated in KO mice	GO accession	P value (Over-represented)
chemokine activity	Cxcl1,Cxcl12,Ccl17,Ccl9,Cxcl3,Ccl11		GO:0008009	1.07E-06
chemokine receptor binding	Cxcl3,Ccl11,Cxcl12,Ccl9,Ccl17,Cxcl1		GO:0042379	1.07E-06
cytokine activity	Csf1,Ccl11,Cxcl3,Cxcl1,Ccl9,Ccl17,Cxcl12		GO:0005125	3.35E-06
immune response	Ltb,Cxcl3,Ccl9,H2-Q6,H2-K1,H2-M5,Ccl11,Cxcl1, H2-M2,Ccl17,Cxcl12,Ms4a1	Dsp	GO:0006955	9.43E-06
immune system process	Ltb,Cxcl3,Ccl9,H2-K1,H2-Q6,H2-M5,Ccl11,Cxcl1, H2-M2,Ccl17,Cxcl12,Ms4a1	Dsp	GO:0002376	3.47E-05
cytokine receptor binding	Cxcl3,Ccl11,Ltb,Cxcl12,Ccl17,Ccl9,Cxcl1		GO:0005126	0.0008711
antigen processing and presentation	H2-Q6,H2-K1,H2-M2,H2-M5		GO:0019882	0.0087215
extracellular matrix	S100g,Des,S100a9,Mfap5,Mmp12,Mmp25,Fcer2a,Fgl2	Gpc3,Thsd4,Ppp3r2,Pls1, Gpc6	GO:0031012	0.00026772
extracellular region part	Tmcc2,S100a9,S100g,Des,Fcer2a,Fgl2,Gm26788 ,Mfap5	Myof,Gpc3,Afp,Pls1,Gpc6 ,Ppp3r2	GO:0044421	0.00036759
proteinaceous extracellular matrix	S100a9,S100g,Des,Fcer2a,Fgl2,Mfap5	Gpc3,Gpc6,Pls1,Ppp3r2	GO:0005578	0.00053867
Notch signaling pathway		Notch1,Notch2,Jag1	GO:0007219	0.01156
regulation of cell growth	Igfbp5,Igfbp6		GO:0001558	0.013648
insulin-like growth factor binding	Igfbp5,Igfbp6		GO:0005520	0.013648
cell growth	Igfbp5,Igfbp6		GO:0016049	0.013648
regulation of growth	Igfbp5,Igfbp6		GO:0040008	0.017012
Growth	Igfbp5,Bmp6,Igfbp6		GO:0040007	0.030478
growth factor binding	Igfbp6,Igfbp5		GO:0019838	0.028955
positive regulation of cell death		Srcap,Thsd4	GO:0010942	0.021795
positive regulation of apoptotic process		Srcap,Thsd4	GO:0043065	0.021795
positive regulation of programmed cell death		Srcap,Thsd4	GO:0043068	0.021795

Table 4.1 (cont'd)
Note: Total RNA from two independent samples per group were analyzed by RNA sequencing (RNAseq). Routine identification of differentially expressed genes was performed using DESeq2. 376 genes in tumors were detected with significantly ($p<0.05$) different expression patterns from the lungs of Nrf2 WT vs. KO mice. Cancer relevant gene sets are emphasized in this table.

Table 4.2. Differentially regulated gene ontologies in lung adenocarcinoma patients

Annotation	Total Genes With Annotation	ln(Bayes factor)
GO:0007186: G-protein coupled receptor protein signaling pathway	116	52.22
GO:0050877: neurophysiological process	90	45.06
GO:0007600: sensory perception	59	33.18
GO:0009581: detection of external stimulus	70	27.69
GO:0006955: immune response	271	22.42
GO:0050875: cellular physiological process	2391	22.28
GO:0006952: defense response	289	17.6
GO:0009607: response to biotic stimulus	323	17.37
GO:0044249: cellular biosynthesis	317	16.41
GO:0009058: biosynthesis	326	14.67
GO:0050794: regulation of cellular process	268	13.74
GO:0006412: protein biosynthesis	187	11.01
GO:0009059: macromolecule biosynthesis	204	10.46
GO:0007166: cell surface receptor linked signal transduction	272	9.62
GO:0051244: regulation of cellular physiological process	191	7.79
GO:0007155: cell adhesion	195	7.66
GO:0019882: antigen presentation	27	7.05
GO:0019226: transmission of nerve impulse	32	6.83
GO:0007268: synaptic transmission	31	6.58
GO:0007242: intracellular signaling cascade	306	6.56
GO:0006959: humoral immune response	67	5.78
GO:0006915: apoptosis	150	5.67
GO:0012501: programmed cell death	150	5.4
GO:0044260: cellular macromolecule metabolism	824	5.28

Note: Total RNA from two independent samples per group were analyzed by RNA sequencing (RNAseq). Routine identification of differentially expressed genes was performed using DESeq2. 376 genes in tumors were detected with significantly ($p<0.05$) different expression patterns from the lungs of Nrf2 WT vs. KO mice. Cancer relevant gene sets are emphasized in this table.

REFERENCES

REFERENCES

1. Menegon S, Columbano A, Giordano S. The Dual Roles of NRF2 in Cancer. Trends Mol Med. 2016; 22: 578-93.

2. Itoh K, Ishii T, Wakabayashi N, Yamamoto M. Regulatory mechanisms of cellular response to oxidative stress. Free Radic Res. 1999; 31: 319-24.

3. Itoh K, Chiba T, Takahashi S, Ishii T, Igarashi K, Katoh Y, et al. An Nrf2/small Maf heterodimer mediates the induction of phase II detoxifying enzyme genes through antioxidant response elements. Biochem Biophys Res Commun. 1997; 236: 313-22.

4. Rushmore TH, Kong AN. Pharmacogenomics, regulation and signaling pathways of phase I and II drug metabolizing enzymes. Curr Drug Metab. 2002; 3: 481-90.

5. Xu C, Li CY, Kong AN. Induction of phase I, II and III drug metabolism/transport by xenobiotics. Arch Pharm Res. 2005; 28: 249-68.

6. Cullinan SB, Diehl JA. PERK-dependent activation of Nrf2 contributes to redox homeostasis and cell survival following endoplasmic reticulum stress. J Biol Chem. 2004; 279: 20108-17.

7. Anwar AA, Li FY, Leake DS, Ishii T, Mann GE, Siow RC. Induction of heme oxygenase 1 by moderately oxidized low-density lipoproteins in human vascular smooth muscle cells: role of mitogen-activated protein kinases and Nrf2. Free Radic Biol Med. 2005; 39: 227-36.

8. Alam J, Stewart D, Touchard C, Boinapally S, Choi AM, Cook JL. Nrf2, a Cap'n'Collar transcription factor, regulates induction of the heme oxygenase-1 gene. J Biol Chem. 1999; 274: 26071-8.

9. Yuan X, Huang H, Huang Y, Wang J, Yan J, Ding L, et al. Nuclear factor E2-related factor 2 knockdown enhances glucose uptake and alters glucose metabolism in AML12 hepatocytes. Exp Biol Med (Maywood). 2017; 242: 930-8.

10. Kovac S, Angelova PR, Holmstrom KM, Zhang Y, Dinkova-Kostova AT, Abramov AY. Nrf2 regulates ROS production by mitochondria and NADPH oxidase. Biochim Biophys Acta. 2015; 1850: 794-801.

11. Ohtsubo T, Kamada S, Mikami T, Murakami H, Tsujimoto Y. Identification of NRF2, a member of the NF-E2 family of transcription factors, as a substrate for caspase-3(-like) proteases. Cell Death Differ. 1999; 6: 865-72.

12. Zhang L, Wang H, Fan Y, Gao Y, Li X, Hu Z, et al. Fucoxanthin provides

neuroprotection in models of traumatic brain injury via the Nrf2-ARE and Nrf2-autophagy pathways. Sci Rep. 2017; 7: 46763.

13. Guo Y, Yu S, Zhang C, Kong AN. Epigenetic regulation of Keap1-Nrf2 signaling. Free Radic Biol Med. 2015; 88: 337-49.

14. Lee JM, Li J, Johnson DA, Stein TD, Kraft AD, Calkins MJ, et al. Nrf2, a multi-organ protector? FASEB J. 2005; 19: 1061-6.

15. Sporn MB, Liby KT. NRF2 and cancer: the good, the bad and the importance of context. Nat Rev Cancer. 2012; 12: 564-71.

16. Hayes JD, McMahon M, Chowdhry S, Dinkova-Kostova AT. Cancer chemoprevention mechanisms mediated through the Keap1-Nrf2 pathway. Antioxid Redox Signal. 2010; 13: 1713-48.

17. Hu R, Saw CL, Yu R, Kong AN. Regulation of NF-E2-related factor 2 signaling for cancer chemoprevention: antioxidant coupled with antiinflammatory. Antioxid Redox Signal. 2010; 13: 1679-98.

18. Iida K, Itoh K, Kumagai Y, Oyasu R, Hattori K, Kawai K, et al. Nrf2 is essential for the chemopreventive efficacy of oltipraz against urinary bladder carcinogenesis. Cancer Res. 2004; 64: 6424-31.

19. Khor TO, Huang MT, Prawan A, Liu Y, Hao X, Yu S, et al. Increased susceptibility of Nrf2 knockout mice to colitis-associated colorectal cancer. Cancer Prev Res (Phila). 2008; 1: 187-91.

20. Xu C, Huang MT, Shen G, Yuan X, Lin W, Khor TO, et al. Inhibition of 7,12-dimethylbenz(a)anthracene-induced skin tumorigenesis in C57BL/6 mice by sulforaphane is mediated by nuclear factor E2-related factor 2. Cancer Res. 2006; 66: 8293-6.

21. Satoh H, Moriguchi T, Taguchi K, Takai J, Maher JM, Suzuki T, et al. Nrf2-deficiency creates a responsive microenvironment for metastasis to the lung. Carcinogenesis. 2010; 31: 1833-43.

22. Satoh H, Moriguchi T, Saigusa D, Baird L, Yu L, Rokutan H, et al. NRF2 Intensifies Host Defense Systems to Prevent Lung Carcinogenesis, but After Tumor Initiation Accelerates Malignant Cell Growth. Cancer Res. 2016; 76: 3088-96.

23. Ramos-Gomez M, Kwak MK, Dolan PM, Itoh K, Yamamoto M, Talalay P, et al. Sensitivity to carcinogenesis is increased and chemoprotective efficacy of enzyme inducers is lost in nrf2 transcription factor-deficient mice. Proc Natl Acad Sci U S A. 2001; 98: 3410-5.

24. Ganan-Gomez I, Wei Y, Yang H, Boyano-Adanez MC, Garcia-Manero G. Oncogenic functions of the transcription factor Nrf2. Free Radic Biol Med. 2013; 65: 750-64.

25. Wang XJ, Sun Z, Villeneuve NF, Zhang S, Zhao F, Li Y, et al. Nrf2 enhances resistance of cancer cells to chemotherapeutic drugs, the dark side of Nrf2. Carcinogenesis. 2008; 29: 1235-43.

26. Ngo HKC, Kim DH, Cha YN, Na HK, Surh YJ. Nrf2 Mutagenic Activation Drives Hepatocarcinogenesis. Cancer Res. 2017; 77: 4797-808.

27. Bauer AK, Cho HY, Miller-Degraff L, Walker C, Helms K, Fostel J, et al. Targeted deletion of Nrf2 reduces urethane-induced lung tumor development in mice. PLoS ONE. 2011; 6: e26590.

28. To C, Ringelberg CS, Royce DB, Williams CR, Risingsong R, Sporn MB, et al. Dimethyl fumarate and the oleanane triterpenoids, CDDO-imidazolide and CDDO-methyl ester, both activate the Nrf2 pathway but have opposite effects in the A/J model of lung carcinogenesis. Carcinogenesis. 2015; 36: 769-81.

29. Liby KT, Sporn MB. Synthetic oleanane triterpenoids: multifunctional drugs with a broad range of applications for prevention and treatment of chronic disease. Pharmacol Rev. 2012; 64: 972-1003.

30. Casey SC, Amedei A, Aquilano K, Azmi AS, Benencia F, Bhakta D, et al. Cancer prevention and therapy through the modulation of the tumor microenvironment. Semin Cancer Biol. 2015; 35 Suppl: S199-S223.

31. Hernandez LG, Forkert PG. Inhibition of vinyl carbamate-induced lung tumors and Kras2 mutations by the garlic derivative diallyl sulfone. Mutat Res. 2009; 662: 16-21.

32. Liby K, Royce DB, Risingsong R, Williams CR, Wood MD, Chandraratna RA, et al. A new rexinoid, NRX194204, prevents carcinogenesis in both the lung and mammary gland. Clin Cancer Res. 2007; 13: 6237-43.

33. Guibert N, Ilie M, Long E, Hofman V, Bouhlel L, Brest P, et al. KRAS Mutations in Lung Adenocarcinoma: Molecular and Epidemiological Characteristics, Methods for Detection, and Therapeutic Strategy Perspectives. Curr Mol Med. 2015; 15: 418-32.

34. Melkamu T, Qian X, Upadhyaya P, O'Sullivan MG, Kassie F. Lipopolysaccharide enhances mouse lung tumorigenesis: a model for inflammation-driven lung cancer. Vet Pathol. 2013; 50: 895-902.

35. Jackson EL, Willis N, Mercer K, Bronson RT, Crowley D, Montoya R, et al. Analysis of lung tumor initiation and progression using conditional expression of oncogenic K-ras. Genes Dev. 2001; 15: 3243-8.

36. Sheridan C, Downward J. Overview of KRAS-Driven Genetically Engineered Mouse Models of Non-Small Cell Lung Cancer. Curr Protoc Pharmacol. 2015; 70: 14 35 1-16.

37. Chan K, Lu R, Chang JC, Kan YW. NRF2, a member of the NFE2 family of transcription factors, is not essential for murine erythropoiesis, growth, and development.

Proc Natl Acad Sci U S A. 1996; 93: 13943-8.

38. Liby K, Royce DB, Williams CR, Risingsong R, Yore MM, Honda T, et al. The synthetic triterpenoids CDDO-methyl ester and CDDO-ethyl amide prevent lung cancer induced by vinyl carbamate in A/J mice. Cancer Res. 2007; 67: 2414-9.

39. Liby K, Black CC, Royce DB, Williams CR, Risingsong R, Yore MM, et al. The rexinoid LG100268 and the synthetic triterpenoid CDDO-methyl amide are more potent than erlotinib for prevention of mouse lung carcinogenesis. Mol Cancer Ther. 2008; 7: 1251-7.

40. Livak KJ, Schmittgen TD. Analysis of relative gene expression data using real-time quantitative PCR and the 2(-Delta Delta C(T)) Method. Methods. 2001; 25: 402-8.

41. Leal AS, Williams CR, Royce DB, Pioli PA, Sporn MB, Liby KT. Bromodomain inhibitors, JQ1 and I-BET 762, as potential therapies for pancreatic cancer. Cancer Lett. 2017; 394: 76-87.

42. Kim D, Pertea G, Trapnell C, Pimentel H, Kelley R, Salzberg SL. TopHat2: accurate alignment of transcriptomes in the presence of insertions, deletions and gene fusions. Genome Biol. 2013; 14: R36.

43. Mortazavi A, Williams BA, McCue K, Schaeffer L, Wold B. Mapping and quantifying mammalian transcriptomes by RNA-Seq. Nat Methods. 2008; 5: 621-8.

44. Anders S, Reyes A, Huber W. Detecting differential usage of exons from RNA-seq data. Genome Res. 2012; 22: 2008-17.

45. Mi H, Muruganujan A, Casagrande JT, Thomas PD. Large-scale gene function analysis with the PANTHER classification system. Nat Protoc. 2013; 8: 1551-66.

46. Chang JT, Nevins JR. GATHER: a systems approach to interpreting genomic signatures. Bioinformatics. 2006; 22: 2926-33.

47. Campbell JD, Alexandrov A, Kim J, Wala J, Berger AH, Pedamallu CS, et al. Distinct patterns of somatic genome alterations in lung adenocarcinomas and squamous cell carcinomas. Nat Genet. 2016; 48: 607-16.

48. Cancer Genome Atlas Research N. Comprehensive molecular profiling of lung adenocarcinoma. Nature. 2014; 511: 543-50.

49. Cancer Genome Atlas Research N. Comprehensive genomic characterization of squamous cell lung cancers. Nature. 2012; 489: 519-25.

50. Cerami E, Gao J, Dogrusoz U, Gross BE, Sumer SO, Aksoy BA, et al. The cBio cancer genomics portal: an open platform for exploring multidimensional cancer genomics data. Cancer Discov. 2012; 2: 401-4.

51. Gao J, Aksoy BA, Dogrusoz U, Dresdner G, Gross B, Sumer SO, et al. Integrative analysis of complex cancer genomics and clinical profiles using the cBioPortal. Sci Signal. 2013; 6: pl1.

52. Zanetti M. Tapping CD4 T cells for cancer immunotherapy: the choice of personalized genomics. J Immunol. 2015; 194: 2049-56.

53. Kamphorst AO, Pillai RN, Yang S, Nasti TH, Akondy RS, Wieland A, et al. Proliferation of PD-1+ CD8 T cells in peripheral blood after PD-1-targeted therapy in lung cancer patients. Proc Natl Acad Sci U S A. 2017.

54. Zaynagetdinov R, Sherrill TP, Polosukhin VV, Han W, Ausborn JA, McLoed AG, et al. A critical role for macrophages in promotion of urethane-induced lung carcinogenesis. J Immunol. 2011; 187: 5703-11.

55. Iriki T, Ohnishi K, Fujiwara Y, Horlad H, Saito Y, Pan C, et al. The cell-cell interaction between tumor-associated macrophages and small cell lung cancer cells is involved in tumor progression via STAT3 activation. Lung Cancer. 2017; 106: 22-32.

56. Wang R, Zhang J, Chen S, Lu M, Luo X, Yao S, et al. Tumor-associated macrophages provide a suitable microenvironment for non-small lung cancer invasion and progression. Lung Cancer. 2011; 74: 188-96.

57. Ortiz ML, Lu L, Ramachandran I, Gabrilovich DI. Myeloid-derived suppressor cells in the development of lung cancer. Cancer Immunol Res. 2014; 2: 50-8.

58. Beury DW, Carter KA, Nelson C, Sinha P, Hanson E, Nyandjo M, et al. Myeloid-Derived Suppressor Cell Survival and Function Are Regulated by the Transcription Factor Nrf2. J Immunol. 2016; 196: 3470-8.

59. Zhu Y, Knolhoff BL, Meyer MA, Nywening TM, West BL, Luo J, et al. CSF1/CSF1R blockade reprograms tumor-infiltrating macrophages and improves response to T-cell checkpoint immunotherapy in pancreatic cancer models. Cancer Res. 2014; 74: 5057-69.

60. Miyake M, Hori S, Morizawa Y, Tatsumi Y, Nakai Y, Anai S, et al. CXCL1-Mediated Interaction of Cancer Cells with Tumor-Associated Macrophages and Cancer-Associated Fibroblasts Promotes Tumor Progression in Human Bladder Cancer. Neoplasia. 2016; 18: 636-46.

61. Dranoff G. Cytokines in cancer pathogenesis and cancer therapy. Nat Rev Cancer. 2004; 4: 11-22.

62. Qu P, Yan C, Du H. Matrix metalloproteinase 12 overexpression in myeloid lineage cells plays a key role in modulating myelopoiesis, immune suppression, and lung tumorigenesis. Blood. 2011; 117: 4476-89.

63. Sohail A, Sun Q, Zhao H, Bernardo MM, Cho JA, Fridman R. MT4-(MMP17) and

MT6-MMP (MMP25), A unique set of membrane-anchored matrix metalloproteinases: properties and expression in cancer. Cancer Metastasis Rev. 2008; 27: 289-302.

64. Sparaneo A, Fabrizio FP, Muscarella LA. Nrf2 and Notch Signaling in Lung Cancer: Near the Crossroad. Oxid Med Cell Longev. 2016; 2016: 7316492.

65. Yuan M, Zhu H, Xu J, Zheng Y, Cao X, Liu Q. Tumor-Derived CXCL1 Promotes Lung Cancer Growth via Recruitment of Tumor-Associated Neutrophils. J Immunol Res. 2016; 2016: 6530410.

66. Wang D, Sun H, Wei J, Cen B, DuBois RN. CXCL1 Is Critical for Premetastatic Niche Formation and Metastasis in Colorectal Cancer. Cancer Res. 2017; 77: 3655-65.

67. Yang DL, Xin MM, Wang JS, Xu HY, Huo Q, Tang ZR, et al. Chemokine receptor CXCR4 and its ligand CXCL12 expressions and clinical significance in bladder cancer. Genet Mol Res. 2015; 14: 17699-707.

68. Guo Q, Gao BL, Zhang XJ, Liu GC, Xu F, Fan QY, et al. CXCL12-CXCR4 Axis Promotes Proliferation, Migration, Invasion, and Metastasis of Ovarian Cancer. Oncol Res. 2014; 22: 247-58.

69. Xie S, Zeng W, Fan G, Huang J, Kang G, Geng Q, et al. Effect of CXCL12/CXCR4 on increasing the metastatic potential of non-small cell lung cancer in vitro is inhibited through the downregulation of CXCR4 chemokine receptor expression. Oncol Lett. 2014; 7: 941-7.

70. Wang Z, Sun J, Feng Y, Tian X, Wang B, Zhou Y. Oncogenic roles and drug target of CXCR4/CXCL12 axis in lung cancer and cancer stem cell. Tumour Biol. 2016; 37: 8515-28.

71. Yan HH, Jiang J, Pang Y, Achyut BR, Lizardo M, Liang X, et al. CCL9 Induced by TGFbeta Signaling in Myeloid Cells Enhances Tumor Cell Survival in the Premetastatic Organ. Cancer Res. 2015; 75: 5283-98.

72. Ding J, Guo C, Hu P, Chen J, Liu Q, Wu X, et al. CSF1 is involved in breast cancer progression through inducing monocyte differentiation and homing. Int J Oncol. 2016; 49: 2064-74.

73. Aharinejad S, Salama M, Paulus P, Zins K, Berger A, Singer CF. Elevated CSF1 serum concentration predicts poor overall survival in women with early breast cancer. Endocr Relat Cancer. 2013; 20: 777-83.

74. Hung JY, Horn D, Woodruff K, Prihoda T, LeSaux C, Peters J, et al. Colony-stimulating factor 1 potentiates lung cancer bone metastasis. Lab Invest. 2014; 94: 371-81.

75. Satoh H, Moriguchi T, Takai J, Ebina M, Yamamoto M. Nrf2 prevents initiation but accelerates progression through the Kras signaling pathway during lung carcinogenesis.

Cancer Res. 2013; 73: 4158-68.

76. Roberts PJ, Stinchcombe TE. KRAS mutation: should we test for it, and does it matter? J Clin Oncol. 2013; 31: 1112-21.

77. You M, Candrian U, Maronpot RR, Stoner GD, Anderson MW. Activation of the Ki-ras protooncogene in spontaneously occurring and chemically induced lung tumors of the strain A mouse. Proc Natl Acad Sci U S A. 1989; 86: 3070-4.

78. Stathopoulos GT, Sherrill TP, Cheng DS, Scoggins RM, Han W, Polosukhin VV, et al. Epithelial NF-kappaB activation promotes urethane-induced lung carcinogenesis. Proc Natl Acad Sci U S A. 2007; 104: 18514-9.

79. Kobayashi EH, Suzuki T, Funayama R, Nagashima T, Hayashi M, Sekine H, et al. Nrf2 suppresses macrophage inflammatory response by blocking proinflammatory cytokine transcription. Nat Commun. 2016; 7: 11624.

80. Prado-Garcia H, Romero-Garcia S, Aguilar-Cazares D, Meneses-Flores M, Lopez-Gonzalez JS. Tumor-induced CD8+ T-cell dysfunction in lung cancer patients. Clin Dev Immunol. 2012; 2012: 741741.

81. Poczobutt JM, De S, Yadav VK, Nguyen TT, Li H, Sippel TR, et al. Expression Profiling of Macrophages Reveals Multiple Populations with Distinct Biological Roles in an Immunocompetent Orthotopic Model of Lung Cancer. J Immunol. 2016; 196: 2847-59.

82. Brune B, Dehne N, Grossmann N, Jung M, Namgaladze D, Schmid T, et al. Redox control of inflammation in macrophages. Antioxid Redox Signal. 2013; 19: 595-637.

83. Heneberg P. Paracrine tumor signaling induces transdifferentiation of surrounding fibroblasts. Crit Rev Oncol Hematol. 2016; 97: 303-11.

84. Arranz EE, Vara JA, Gamez-Pozo A, Zamora P. Gene signatures in breast cancer: current and future uses. Transl Oncol. 2012; 5: 398-403.

85. Kuner R. Lung Cancer Gene Signatures and Clinical Perspectives. Microarrays (Basel). 2013; 2: 318-39.

86. Bryan HK, Olayanju A, Goldring CE, Park BK. The Nrf2 cell defence pathway: Keap1-dependent and -independent mechanisms of regulation. Biochem Pharmacol. 2013; 85: 705-17.

87. Pantano C, Reynaert NL, van der Vliet A, Janssen-Heininger YM. Redox-sensitive kinases of the nuclear factor-kappaB signaling pathway. Antioxid Redox Signal. 2006; 8: 1791-806.

88. Palazon A, Goldrath AW, Nizet V, Johnson RS. HIF transcription factors, inflammation, and immunity. Immunity. 2014; 41: 518-28.

89. Del Prete A, Allavena P, Santoro G, Fumarulo R, Corsi MM, Mantovani A. Molecular pathways in cancer-related inflammation. Biochem Med (Zagreb). 2011; 21: 264-75.

CHAPTER 5

A nano-liposome formulation of the PARP inhibitor Talazoparib enhances treatment efficacy and modulates immune cell populations in mammary tumors of BRCA-deficient mice

Reprinted with permission from *Theranostics* 2019; 9(21):6224-6238

Di Zhang, Paige Baldwin, Ana S. Leal, Sarah Carapellucci, Srinivas Sridhar, Karen T. Liby

Author contributions:
Participated in research design: Zhang, Baldwin, Sridhar, Liby
Conducted experiments: Zhang, Baldwin, Leal, Carapellucci
Performed data analysis: Zhang, Baldwin
Wrote or contributed to the writing of the manuscript: Zhang, Baldwin, Sridhar, Liby

5. 1 Abstract

Two recently approved PARP inhibitors provide an important new therapeutic option for patients with BRCA-mutated metastatic breast cancer. PARP inhibitors significantly prolong progression-free survival in patients, but conventional oral delivery of PARP inhibitors is hindered by limited bioavailability and off-target toxicities, thus compromising the therapeutic benefits and quality of life for patients. Here, we developed a new delivery system, in which the PARP inhibitor Talazoparib is encapsulated in the bilayer of a nano-liposome, to overcome these limitations.

Methods: Nano-Talazoparib (NanoTLZ) was characterized both *in vitro* and *in vivo*. The therapeutic efficacy and toxicity of Nano-Talazoparib (NanoTLZ) were evaluated in BRCA-deficient mice. The regulation of NanoTLZ on gene transcription and immunomodulation were further investigated in spontaneous BRCA-deficient tumors.

Results: NanoTLZ significantly ($p<0.05$) prolonged the overall survival of BRCA-deficient mice compared to all of the other experimental groups, including saline control, empty nanoparticles, and free Talazoparib groups (oral and i.v.). Moreover, NanoTLZ was better tolerated than treatment with free Talazoparib, with no significant weight lost or alopecia as was observed with the free drug. After 5 doses, NanoTLZ altered the expression of over 140 genes and induced DNA damage, cell cycle arrest and inhibition of cell proliferation in the tumor. In addition, NanoTLZ favorably modulated immune cell populations *in vivo* and significantly ($p<0.05$) decreased the percentage of myeloid derived suppressor cells in both the tumor and spleen compared to control groups.

Conclusions: Our results demonstrate that delivering nanoformulated Talazoparib not only enhances treatment efficacy but also reduces off-target toxicities in BRCA-

deficient mice; the same potential is predicted for patients with BRCA-deficient breast cancer.

5.2 Introduction

Mutations in breast cancer-associated (*BRCA*) genes are the leading cause of hereditary breast cancer. Women with *BRCA* mutations have up to an 80% lifetime risk of developing breast cancer [1]. Furthermore, the majority of *BRCA1* mutated tumors are basal-like [2], a subtype associated with poor prognosis [3]. *BRCA1* functions as an important tumor suppressor that acts as a gatekeeper to protect against genomic instability [4]. Besides regulating numerous cellular functions [5, 6], including cell cycle, apoptosis and transcription, the BRCA1 protein is essential for repairing double-stranded DNA breaks through the homologous recombination (HR) pathway. Loss of function of the *BRCA1* gene forces cells to rely on more error-prone mechanisms such as non-homologous end joining to repair DNA damage [7]. PARP (poly (ADP-ribose) polymerase) is another protein that plays critical roles in DNA repair. PARP1 recognizes single-stranded DNA breaks and recruits proteins to assemble and activate DNA base excision repair machinery [8]. Single-stranded DNA breaks that cannot be repaired because of PARP deficiency will propagate into double-stranded DNA breaks and need to be repaired by the BRCA-initiated HR pathway. If the BRCA protein is dysfunctional, PARP is necessary for proper DNA repair. Because of the interdependence between PARP and BRCA, PARP inhibitors were developed to treat BRCA-deficient cancers by inducing synthetic lethality [9, 10]. Synthetic lethality occurs when a perturbation in either of two genes does not reduce cell survival, but the simultaneous perturbation of both genes results in a loss of cell viability. In the case of a *BRCA* mutation, PARP

inhibitors block the repair of single-strand DNA breaks, which are then converted into double-strand breaks during replication. Because the cell cannot proceed through homologous recombination, it must rely on error prone pathways which results in genomic instability and cell death.

Before PARP inhibitors were developed, no targeted therapy was available for patients with BRCA mutations who developed breast cancer. These tumors do not usually express estrogen, progesterone or HER2 receptors, so cytotoxic chemotherapy remained the standard of care for these mostly triple negative breast cancer (TNBC) patients. In January 2018, Olaparib became the first PARP inhibitor approved by the FDA for treating germline BRCA-mutated metastatic breast cancer. In October 2018, after the Phase 3 EMBRACA clinical trial showed that Talazoparib significantly extended progression-free survival in patients with metastatic breast cancer, Talazoparib was approved. This second PARP inhibitor to market was approved for treating germline BRCA-mutated, HER2-negative breast cancer, either locally advanced or metastatic [11]. Talazoparib is approximately 100 times more potent than Olaparib because of its higher capacity to induce “PARP trapping” [12]. Talazoparib not only inhibits the catalytic activity of PARP but also traps PARP at the site of DNA damage, thus inducing cell death. Notably, in addition to mutations in *BRCA1/2* genes, a wide range of other mechanisms produce a similar phenotypic trait of HR deficiency, which is called “BRCAness” [13]. The loss of HR can be the result of epigenetic silencing of *BRCA1/2* genes or genetic alterations in other key players such as *RAD51, ATR, CHK1/2, ATM, FANCD2* and *FANCA* along the HR pathway [14]. Recent studies reported that *MYC* amplification, *p53* mutations, and loss of *PTEN* all contribute to a

BRCA-like behavior [15, 16]. Therefore, PARP inhibitors could potentially impact more breast cancer patients beyond populations with *BRCA* mutations. A diverse collection of triple negative breast cancer patient-derived xenografts has confirmed the therapeutic activity of PARP inhibitors even in *BRCA1/2* wild-type tumors [17].

Currently, PARP inhibitors are formulated for daily oral administration based on their pharmacokinetic profiles. However, the bioavailability of Talazoparib is only 56% in rats, meaning a higher dose must be administered systemically to achieve the desired effect [18]. Talazoparib is the most potent PARP inhibitor, but this potency also increases side effects such as alopecia, fatigue, anemia, thrombocytopenia, neutropenia and decreased appetite [19]. Myelodysplastic syndrome, myelosuppression and embryo-fetal toxicity are included as warnings and precautions on the package insert. One method to overcome poor bioavailability and subsequent toxicity is the use of nanoparticle delivery systems.

Nanoparticles as drug delivery systems aim to increase bioavailability, minimize drug metabolism upon administration, prevent side effects, and increase the amount of drug delivered to the desired target [20]. Additionally, nanocarriers take advantage of the enhanced permeability and retention effect, in which tumors rapidly generate blood vessels that are considered “leaky” allowing for particles to extravasate and accumulate in the tumor microenvironment [21]. Liposomes are self-assembled phospholipid bilayers that form vesicles and are biologically inert and biocompatible. Due to the similar morphology to cell membranes and ability to incorporate both hydrophilic and lipophilic compounds, liposomes are thought to be ideal nanocarriers [22]. Although liposome efficacy can be limited by uptake into the reticuloendothelial system (RES),

polyethylene glycol (PEG) can be fused to the surface to extend the circulation time by conferring “stealth” properties to bypass some of the uptake by RES organs [23]. Here, we encapsulated Talazoparib in the bilayer of a nano-liposome and evaluated the efficacy and toxicity of Nano-Talazoparib (NanoTLZ) compared to free drug in BRCA-deficient mice.

5.3 Materials and Methods

5.3.1 Synthesis of NanoTLZ

Talazoparib for all experiments was purchased from Selleck Chemicals (Catalog # S7048, purity: 99.8%). NanoTLZ was synthesized using 1, 2-dipalmitoyl-*sn*-glycero-3-phosphocholine (DPPC), 1,2-dioleoyl-3-tri methyl-ammonium-propane (chloride salt) (DOTAP), cholesterol, 1,2-distearoyl-*sn*-glycero-3 phosphoethanolamine-N-[methoxy(polyethyleneglycol)-2000 (DSPE-PEG_{2000}, Avanti Polar Lipids), and Talazoparib. DOTAP was incorporated within the formulation because some literature suggests it can enhance the encapsulation of hydrophobic compounds [24, 25]. It also imparts a slightly positive surface charge, which allows better cell uptake, as cells more readily take up positively charged particles. DPPC, cholesterol, DOTAP and DSPE-PEG_{2000}, were individually dissolved in a methanol/ethanol mixture at a molar ratio of 65:29:2:4. 11.17 mM Talazoparib was added in dimethylformamide. Nanoparticles were formed via nanoprecipitation using the NanoAssemblr Benchtop. The total flow rate was 4 ml/min, and the aqueous to organic flow rate was 3:1. Organic solvents were removed by evaporation under argon followed by dialysis against phosphate buffered saline (PBS) for 30 minutes. The non-encapsulated drug which is insoluble in aqueous media was removed via syringe filter [26], and validation of the removal of free drug is shown in

Figure S5.1. Encapsulation efficiency was calculated using the formula ($C_{final}/C_{initial}$) x100, where C_{final} is the concentration of drug in 1 ml of particles after processing and $C_{initial}$ is the concentration of drug added to prepare 1 ml of particles. Drug loading was calculated using the following formula where C_{final} is the concentration of drug in 1 ml of particles after processing and W_{feed} is the weight of lipids in the feed to prepare 1 ml of formulation: drug loading (%) = C_{final}/W_{feed} x 100. Drug release was characterizd previously [27]. Vehicle nanoparticles (empty nanoparticles) were prepared following the same protocol without the addition of Talazoparib. Cyanine 5 (Cy5) labeled particles were synthesized by addition of Cy5 dye in the lipid mixture.

5.3.2 Characterization of NanoTLZ

The size and zeta potential of the nanoparticles was measured using a Brookhaven 90Plus analyzer equipped with ZetaPALS. Nanoparticles were diluted 1:100 in 0.2X PBS for all measurements. Stability was assessed by measuring size and zeta potential at predetermined times over the course of 2 months. The size was confirmed by transmission electron microscopy using a negative stain of 1.0% uranyl acetate. The concentration of encapsulated Talazoparib was measured via high performance liquid chromatography (HPLC) following nanoparticle lysis with methanol. HPLC was performed on an Agilent 1260 Infinity II instrument with a reverse phase C18 Supelco column. The mobile phase A consisted of acetonitrile with 0.1% phosphoric acid and the mobile phase B consisted of water with 0.1% phosphoric acid. The following gradient was applied 10-95% A (0-5.3 min), 95% A (5.3-8.5 min), 95-10% A (8.5-10.0 min), 10% A (10-11.5 min). The flow rate was 0.82 ml/minute, and Talazoparib was detected at a wavelength of 309 nm at ~4.2 minutes.

5.3.3 Cell Culture

W0069 and W780 cells derived from mammary tumors of BRCA-deficient mice were provided by Dr. Chu-Xia Deng (National Institutes of Health, Bethesda, MD) [28] and were cultured in DMEM+10% FBS+1% Pen/Strep (Corning Cellgro, Mediatech, Manassas, VA). In a dose response assay (Figure 5.1), cells were seeded into 96 well plates at 1000 cells per well. The following day cells were exposed to either Talazoparib or NanoTLZ at concentrations ranging from 0-100 nM. One week after seeding, cell viability was ascertained by the MTS assay to measure the metabolic activity of the cells. Data from the dose response experiment were plotted and fit using a variable slope four-parameter logistic equation constrained at 100 and 0. In the biomarker assay (Figure 5.1 E), cells were seeded in 6 well plates at 150,000 cells per well. The next day, cells were treated with Talazoparib or NanoTLZ at 5 and 10 mM. After 48 hrs of treatment, cells were harvested and proteins were extracted for western blotting.

5.3.4 Pharmacokinetics and Pharmacodynamics

All animal studies were performed in accordance with protocols approved by the Institutional Animal Care and Use Committees (IACUC) at Michigan State University and Northeastern University. An orthotopic xenograft model of human BRCA-mutated breast cancer was established via injection of $5x10^6$ HCC1937 cells (ATCC, Manassas, VA; cells were cultured in RPMI1640 with 10% FBS and 1% Pen/Strep) in the mammary fat pad of female NCr-nu/nu mice. Mice with tumors ~100 mm^3 in size were administered a single dose of 1 mg/kg i.v. NanoTLZ. Mice were euthanized at designated time points for sample collection. Blood was collected via cardiac puncture into K2 EDTA microtainers. Blood was centrifuged at 1600 *g* for 15 minutes at 4°C.

Plasma was separated and frozen at -80°C until processed. Acetonitrile was added to precipitate plasma proteins. Samples were centrifuged at 14,000 *g* for 5 minutes, and the supernatant was filtered with a 0.2 mm syringe filter. Each sample was dried overnight and reconstituted in 200 µl of 50:50 methanol:water solution for analysis via HPLC. HPLC conditions were as detailed above. A standard curve was prepared by processing plasma from untreated animals and spiking the samples with known amounts of Talazoparib when reconstituting the samples. A two compartment model was fit using PKSolver [29].

Tumors were collected and snap frozen in liquid nitrogen to stabilize PAR levels. Tumors were minced in lysis buffer (1% w/w deoxycholic acid, 1% w/w triton-x, 0.1% w/w sodium lauryl sulfate) with protease inhibitors (1 mM PMSF, 1 mM AEBSF•HCL, 800 nM aprotinin, 50 µM bestatin, 15 µM E-64, 5 mM EDTA, 20 µM leupeptin, and 10 µM pepstatin A). Total protein content was determined using the BCA assay (Pierce). Levels of PAR in the tumor lysates were determined by ELISA using PARP in vivo PD Assay II kit (Trevigen) following the manufacturer's instructions.

Brca1$^{Co/Co}$;MMTV-Cre;p53$^{+/-}$ mice bearing tumors (N=4) were injected i.v. with 100 ml nanoparticles encapsulated with the fluorescent dye Cy5. Mice were imaged using an IVIS imaging system (PerkinElmer) 24 hrs after the injection. Auto exposure setting was used to acquire the pictures. Major organs were dissected and imaged for biodistribution after whole body imaging.

To evaluate the cellular uptake of nanoparticles, W780 cells were plated in 12-well plates. Cells were treated with either 5% empty nanoparticles or 5% nanoparticles encapsulated with the fluorescent dye Cy5 for 1-2 hrs. Cells were then fixed with 10%

neutral buffered formalin (Sigma-Aldrich) for 15 minutes and mounted with Gold Antifade Mountant with DAPI (Invitrogen). Cy5 fluorescence (Green channel) and DAPI (UV channel) were detected using a fluorescence microscope (Nikon TE2000-U Inverted Microscope).

5.3.5 *In Vivo* Treatment Studies

The therapeutic efficacy of NanoTLZ was assessed in $Brca1^{Co/Co}$;MMTV-Cre;$p53^{+/-}$ mice [30, 31]. Treatment was started when a tumor was 4-5 mm in diameter and ended when it reached 10 mm in diameter. Mice with established tumors were randomized into five treatment groups: control (saline, i.v. N=5), empty nanoparticles (i.v., N=5), NanoTLZ (i.v., 0.33 mg/kg, N=8), free Talazoparib (i.v., 0.33 mg/kg, N=8), and free Talazoparib (gavage, 0.33 mg/kg, N=8). NanoTLZ was diluted in saline to the working concentration. Free Talazoparib was dissolved in DMSO and diluted in saline (DMSO in the final solution was 1%). Treatment was given three times a week (M, W, F). All the mice were weighed before each injection. Tumor size was measured using a caliper twice a week.

5.3.6 Western blotting

W780 and W0069 cells treated with Talazoparib or NanoTLZ were lysed in RIPA buffer (1 M Tris-Cl, 5 M NaCl, pH 7.4, 0.5 M EDTA, 25 mM deoxycholic acid, 1% triton-X, 0.1% SDS) with protease inhibitors (1 mM PMSF, 2 μg/ml aprotinin and 5 μg/ml leupeptin). Tumor samples dissected from BRCA-deficient mice were homogenized and lysed in EBC buffer (5 mol/L NaCl, 1 mol/L Tris pH 8) with protease inhibitors and 10% NP-40. Protein concentrations were determined using the BCA assay (Sigma-Aldrich). 20 μg of protein were separated by 10% SDS-PAGE gels and transferred to

nitrocellulose membranes. gH_2AX (Abcam, 1:1000), cleaved-caspase 3 (Cell Signaling, 1:1000), PARP/cleaved-PARP (Cell Signaling, 1:1000), Cyclin D1 (Cell Signaling, 1:1000), Cyclin E1 (Cell Signaling, 1:1000), PCNA (Santa Cruz, 1:1000), and vinculin (Cell Signaling, 1:4000) primary antibodies were used to detect the corresponding proteins. Secondary antibodies (anti-rabbit or anti-mouse linked to HRP) were purchased from Cell Signaling. ECL Western blotting substrate (GE Healthcare Life Sciences, UK) was used to detect the signal. Images shown are representative of 3 independent experiments. ImageJ was used to quantify protein expression.

5.3.7 Immunohistochemistry

Brca1$^{Co/Co}$;MMTV-Cre;p53$^{+/-}$ mice were treated with five doses (three times a week) of saline, i.v.TLZ or NanoTLZ (N=5/group). Tumor, mammary gland and spleen were then harvested and sectioned for histopathology and immunohistochemistry. EDTA (Cell Signaling, for CD3) or citrate buffer (Vector, Cat. # H3300, for all the other antibodies) was used for antigen retrieval. Endogenous peroxidase activity was quenched using hydrogen peroxide (3%) for 10 minutes. Sections were stained with CD45 (1:100, BioScience), CD3 (1:40, Biolegend), Gr-1 (1:50, R&D), F4/80 (1:50, Invitrogen), Foxp3 (1:25, BioScience), PCNA (1:200, Santa Cruz), or γH_2AX (1:100, Abcam) antibodies. Anti-rat secondary antibody was purchased from Vector. Anti-mouse and anti-rabbit secondary antibodies conjugated to HRP were purchased from Cell Signaling. Signal was detected using a DAB kit (Cell Signaling). Sections were counterstained with hematoxylin (Vector).

5.3.8 Flow cytometry

Brca1$^{Co/Co}$;MMTV-Cre;p53$^{+/-}$ mice (N=5/group) with established tumors (4-5 mm in diameter) were treated for five doses (three times a week) and then tumor, spleen and mammary gland were collected and digested for flow cytometry as published previously [32]. Panel 1: CD45-VioGreen (Miltenyi, 3 μg/mL), Gr-1-PE (Miltenyi, 3 μg/mL), CD11b-FITC (Miltenyi, 3 μg/mL), CD19-PerCP/Cy5.5 (BioLegend, 2 μg/mL). Panel 2: CD45-VioGreen (Miltenyi, 3 μg/mL), CD4-FITC (Miltenyi, 3 μg/mL), CD3-PE (BioLegend, 2 μg/mL), CD8-APC (BioLegend, 2 μg/mL), CD25-PE/Cy7 (BioLegend, 2 μg/mL).

5.3.9 RNAseq

Tumors from Brca1$^{Co/Co}$;MMTV-Cre;p53$^{+/-}$ mice treated with saline, free Talazoparib (i.v.), or NanoTLZ for five doses (three times a week) were harvested. Three samples were collected for each group. Total RNA was isolated using the RNeasy Mini Kit (Qiagen, Valencia, CA). The RNA integrity number (RIN) was detected using the Aligent Bioanalyzer at the MSU Research Technology Support Facility (RTSF) Genomics Core facility. RNAseq and the bioinformatics analysis were performed by Novogene (Sacramento, CA) as described in a previous publication [32]. Raw data and processed data were deposited on Gene Expression Omnibus (GEO) and are accessible through GSE125206.

5.3.10 RT-qPCR analysis

To validate the RNAseq data, aliquots of RNA samples from the tumor were used to run RT-qPCR analysis. RNA concentrations were determined by NanoDrop, and 2 μg RNA was used to synthesize cDNA using SuperScript III reverse transcriptase (Invitrogen, Carlsbad, CA). Primers were ordered from IDT, except Cxcl12. Validated

and optimized primers for Cxcl12 were purchased from Qiagen (Valencia, CA). iQ SYBR Green Supermix (Bio-Rad, Berkeley, CA) and the QuantStudio 7 Flex Real-Time PCR system were used to detect gene expression. The delta-delta Ct method was used to assess relative gene expression [33]. Values were normalized to the reference gene GAPDH and expressed as fold change compared to saline control samples.

5.3.11 Statistical Analysis

The *in vitro* experiments were performed in triplicate, and independent experiments were repeated at least three times. Results were expressed as mean ± SEM. For the *in vivo* experiments, results were analyzed using one-way ANOVA followed by a Tukey test if the data fit a normal distribution; the Kruskal-Wallis one-way ANOVA on ranks was used followed by the Dunn test for multiple comparisons if the data did not fit a normal distribution (Prism 6). A paired t-test was used to compare body weight before and after treatment. The log-rank (Mantel-Cox) test was used to compare survival curves. For the growth of tumors, a Chi-Square test was used to compare proportions. $p<0.05$ was considered statistically significant. For the RNAseq analysis, differential expression analysis was performed using the DESeq2 R package [34], and $padj<0.05$ was considered statistically significant.

5.4 Results

5.4.1 Validation of NanoTLZ *in vitro* and *in vivo*

To overcome the limitations of oral delivery, we developed a new formulation of Talazoparib. We encapsulated Talazoparib into liposomal nanoparticles with an average size of 74.5 ± 11.0 nm (Figure 5.1 A). The encapsulation efficiency was 83.0±5.9% and drug loading was 1.0 ± 0.1%. NanoTLZ is stable in size and zeta potential (15.3 ± 1.6

mV) at 4°C for 2 months (Figure 5.1 B-C). To validate the effects of NanoTLZ *in vitro*, BRCA-deficient cancer cell lines (W780 and W0069) were treated with NanoTLZ and free Talazoparib. Both W780 and W0069 cell lines were derived from independent tumors that developed in BRCA-deficient mice. W780 cells were derived from a tumor classified as an adenocarcinoma, while W0069 cells were derived from a fibro-adenoma tumor with strong stromal reaction [30]. NanoTLZ was similar in potency to free Talazoparib in both cell lines (Figure 5.1 D). Empty nanoparticles (vehicle) had no effects on cell viability (Figure S5.2). As reported previously for PARP inhibitors [35], NanoTLZ and Talazoparib induced DNA damage and apoptosis, as indicated by an increase of γH2AX, cleaved-caspase 3 and cleaved-PARP, respectively, in W780 and W0069 cells (Figure 5.1 E).

To evaluate the pharmacokinetics of NanoTLZ, an orthotopic xenograft model of human BRCA-mutated HCC1937 cells was established. Tumor bearing mice were dosed with 1 mg/kg NanoTLZ i.v., then blood and tumor samples were collected at different time points. The plasma data fits a two-compartment model with a terminal half-life of 37.5 hours (Figure 5.2 A). PAR levels, a marker of PARP activity, were detected in the tumor samples. The PAR level was significantly ($p<0.0001$) decreased 30 mins after injection and remained at lower levels than control tumors up to 72 hours post injection (Figure 5.2 B).

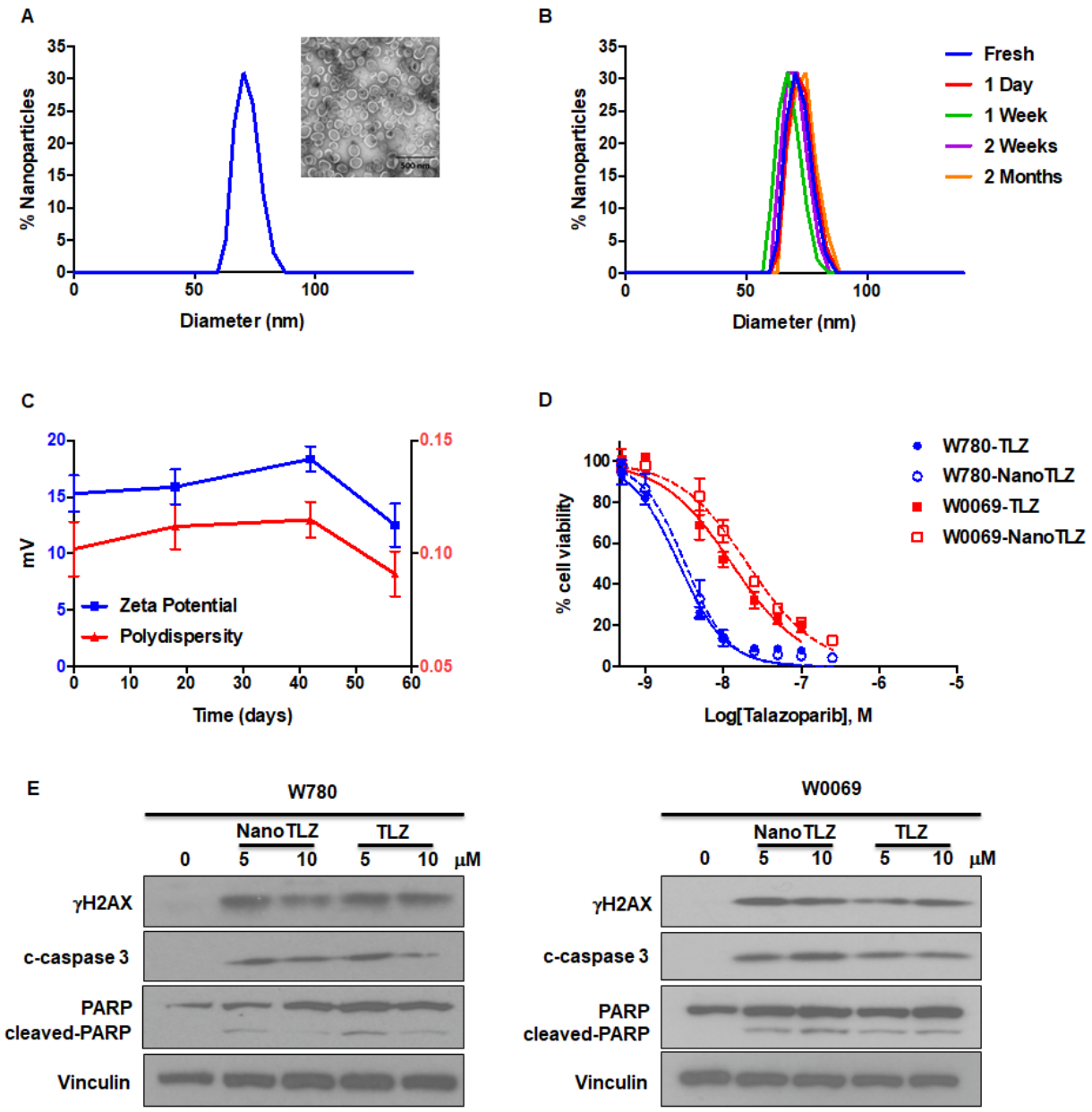

Figure 5.1. Characterization of Nano-Talazoparib (NanoTLZ). A. Physicochemical characterization of NanoTLZ via dynamic light scattering and (inset) transmission electron microscopy after staining with 1.0% uranyl acetate illustrates a monodisperse formulation with an average diameter of 75 nm. B and C. NanoTLZ is stable in size, zeta potential and polydispersity, for up to 2 months in storage at 4°C. D. W780 and W0069 cells were treated with NanoTLZ or free Talazoparib (TLZ) for 6 days. Cell viability was detected by the MTS assay. E. W780 and W0069 cells were treated with NanoTLZ or free Talazoparib (TLZ) for 48 hrs. NanoTLZ and TLZ increased the expression of γH2AX, cleaved-caspase 3 (c-caspase 3) and cleaved-PARP in these BRCA-deficient breast cancer cells.

To validate the enhanced permeability and retention effects of nanoparticles in our Brca1$^{Co/Co}$;MMTV-Cre;p53$^{+/-}$ model, we encapsulated the fluorescent dye Cy5 into nanoparticles using the same method as for Talazoparib and injected them i.v. into tumor-bearing BRCA-deficient mice. Mice and major organs were imaged using an IVIS system. At 24 hrs after injection, the fluorescent signal was mainly in the tumor, suggesting preferential accumulation in the tumor, although signal was also detected in the liver (Figure 5.2 C). In addition, the cellular uptake of nanoparticles was assessed in W780 cells *in vitro*. Cells were treated with 5% nanoparticles encapsulated with Cy5, and the fluorescent Cy5 signal was detected using a fluorescence microscope. Nanoparticles were visible inside of cells within 2 hours (Figure 5.2 D).

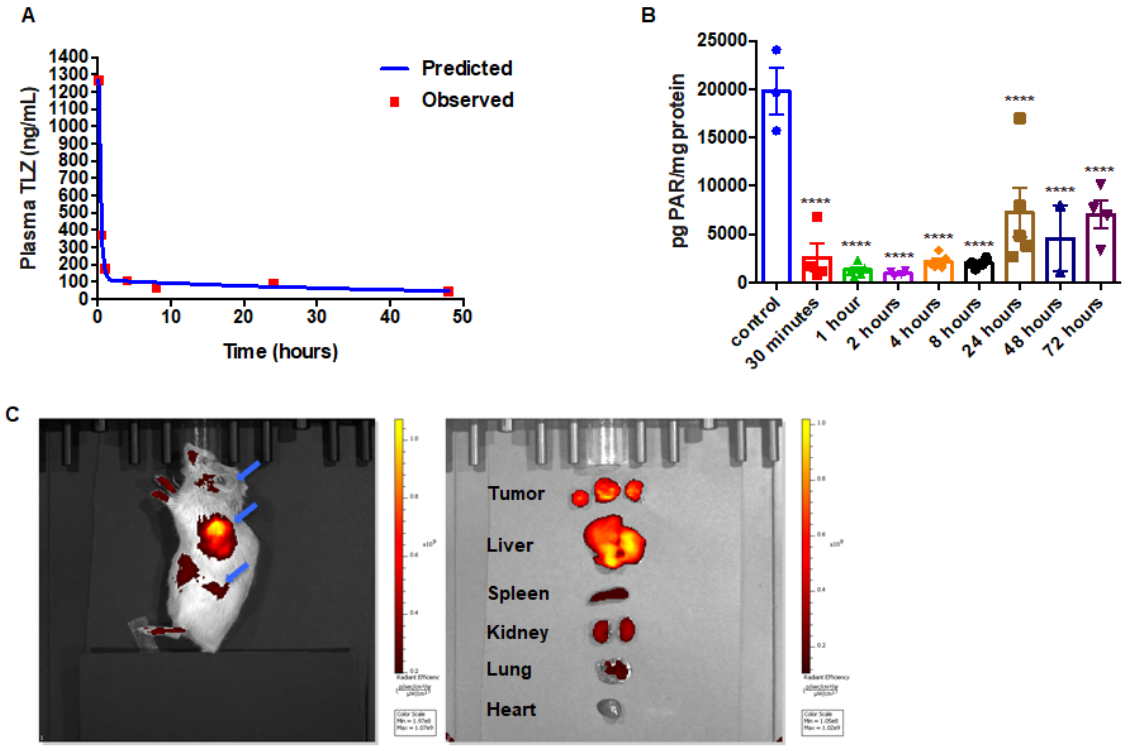

Figure 5.2. Pharmacokinetics and pharmacodynamics of NanoTLZ. A. Mice bearing orthotopic BRCA-mutated human HCC1937 xenografts were injected with 1 mg/kg

Figure 5.2 (cont'd)
NanoTalazoparib (i.v.). Plasma drug concentrations were detected via HPLC. A two-compartment model was fit to the plasma data using PKSolver. B. Tumor PAR levels were detected via ELISA. ****, $p<0.0001$ for all time points compared to control C. $Brca1^{Co/Co}$;MMTV-Cre;$p53^{+/-}$ mice (N=4) were injected with a single dose of Cy5-encapsulated nanoparticles, and the fluorescent signal was detected using a IVIS spectrum imaging system 24 hrs after injection. Major organs were dissected after *in vivo* imaging (left) and biodistribution of nanoparticles in these organs was detected (right). Blue arrows point to tumors. Representative images are shown. D. W780 cells were treated with 5% empty nanoparticles (vehicle) or Cy5-encapsulated nanoparticles for 1-2 hrs. Fluorescent Cy5 signal was detected with a fluorescence microscope. 200x magnification.

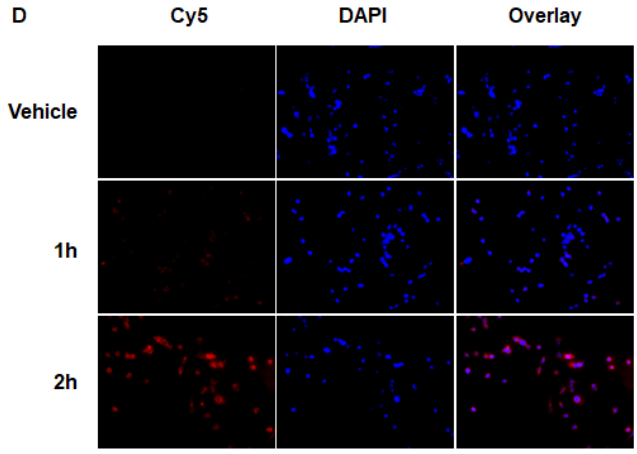

5.4.2 Nano-formulation enhances the efficacy of Talazoparib and reduces the toxicity in BRCA-deficient mice

Because of the tumor specificity of nanoparticles, we hypothesized that NanoTLZ would enhance the efficacy of Talazoparib and be more tolerable for treating BRCA-deficient breast cancer. When tumors in $Brca1^{Co/Co}$;MMTV-Cre;$p53^{+/-}$ mice reached 4 mm in diameter, they were randomized and enrolled into five experimental groups: saline (i.v.), vehicle (empty nanoparticle, i.v.), NanoTLZ (0.33 mg/kg, i.v.), free Talazoparib (0.33 mg/kg, i.v.) or free Talazoparib (0.33 mg/kg, oral). Mice were treated

three times a week (M, W, F) until a tumor reached 10 mm in diameter. All tumors in the saline control group grew exponentially (Figure 5.3 A) and lived an average of only 11.6±2.7 days once treatment started (Figure 5.3 B). Similarly to the saline treated group, empty nanoparticles did not have any therapeutic effect with overall survival in this group of 13.6±1.5 days. Drug treatment by all routes significantly ($p<0.05$) prolonged the overall survival (range 52.8-91.1 days) compared to the saline control, which validated the effectiveness of Talazoparib in treating BRCA-deficient tumors. There was no statistical significance observed between oral free Talazoparib and i.v. free Talazoparib in either overall survival (Figure 5.3 B) or progression-free survival (Figure 5.3 C). Progression was defined as a 50% increase in tumor volume. However, NanoTLZ treatment rapidly induced tumor regression (Figure 5.3 A) and significantly ($p<0.05$) prolonged both overall survival and progression-free survival compared to all of the other groups, including the free drug treatment groups (Figure 5.3 B-C). The average life span once treatment started was extended from 52.8±6.8 days in the oral free Talazoparib group and 61.1±8.3 days in the i.v. free Talazoparib group to 91.1±8.9 days in the NanoTLZ group. NanoTLZ was able to maintain its effectiveness longer than the free Talazoparib treatment.

Furthermore, NanoTLZ was also more effective than free Talazoparib in inducing tumor regression in BRCA-deficient mice. Tumors were classified into three categories: active growth (>50% increase in tumor volume), no change (<50% change in tumor volume), and regression (>50% decrease in tumor volume). Tumors in the control groups (saline and empty nanoparticles) were all actively growing. All of the tumors treated with NanoTLZ responded ($p<0.05$) to the treatment with no active growth (0%)

and 69% (9 out of 13) regressed after treatment (Figure 5.3 D). In comparison, 17% (2 out of 12) of tumors in the i.v. Talazoparib group and 11% (2 out of 19) in the oral Talazoparib group did not respond to the treatment and continued to grow (Figure 5.3 D). The majority of the tumors in these two groups achieved disease stabilization as only 33% (4 out of 12) tumors in the i.v. Talazoparib group and 21% (4 out of 19) in the oral Talazoparib group regressed (Figure 5.3 D). Notably, among the tumors that regressed, 56% (5 out of 9) tumors could no longer be palpated in the NanoTLZ group, while only 25% (1 out of 4) of the mice were tumor-free in the i.v. Talazoparib group and none (0 out of 4) were tumor-free in the oral Talazoparib group.

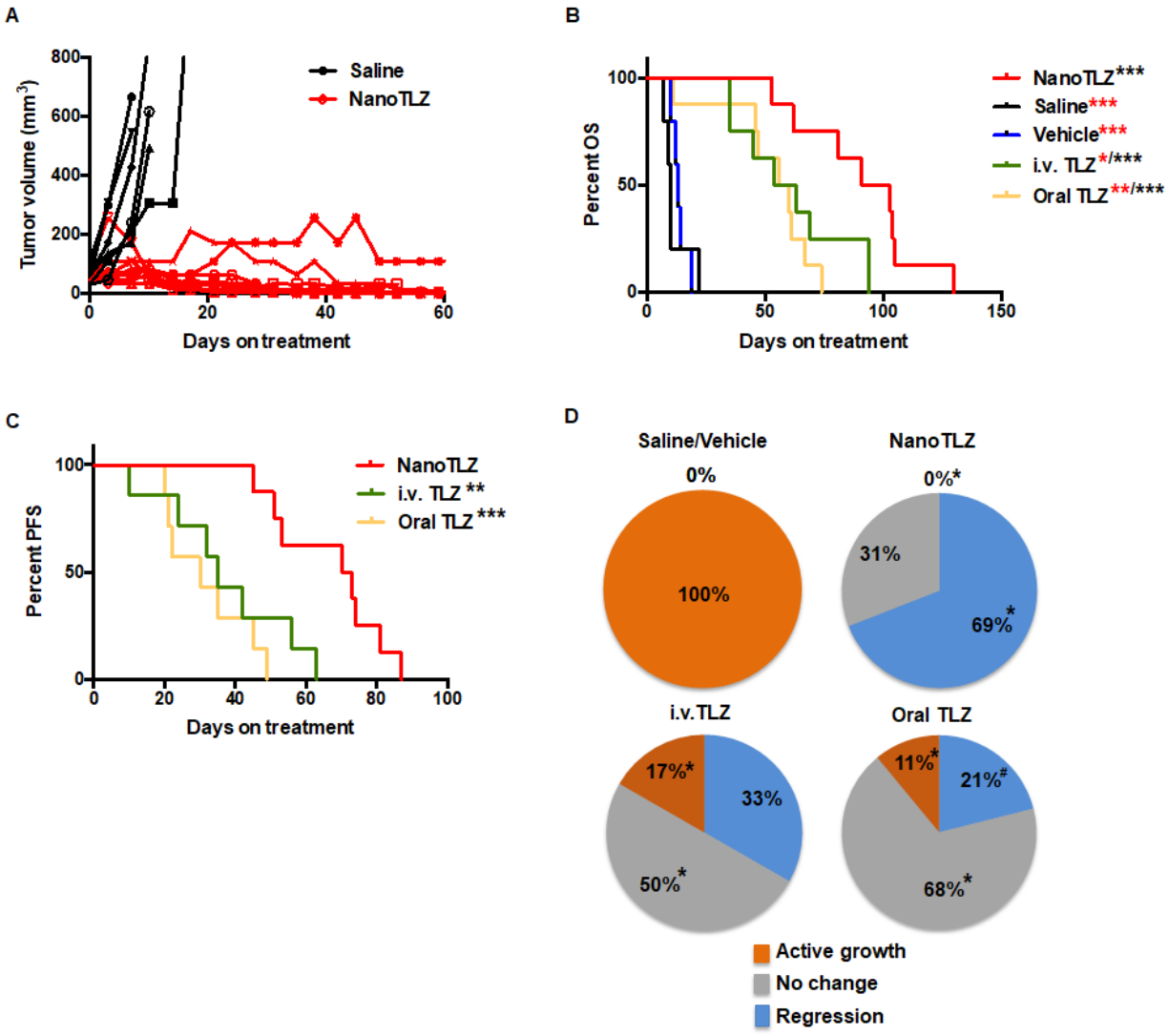

Figure 5.3. NanoTLZ prolongs overall survival and is more effective in inducing tumor regression compared to free Talazoparib in BRCA-deficient mice. Brca1$^{Co/Co}$;MMTV-Cre;p53$^{+/-}$ mice were started on treatment when tumors were 4 mm in diameter. The treatments were either control (saline, i.v.), empty nanoparticles (vehicle, i.v.), NanoTLZ (i.v., 0.33 mg/kg), free Talazoparib (i.v.TLZ, i.v., 0.33 mg/kg), or free Talazoparib (oral TLZ, gavage, 0.33 mg/kg). Treatment was given three times a week. Mice were sacrificed when the tumor reached 10 mm in diameter. A. Growth curves of individual tumors treated with saline or NanoTLZ. (N= 6 in saline and 9 in NanoTLZ groups) B. NanoTLZ significantly prolonged the overall survival of BRCA-deficient mice compared to controls, oral TLZ and i.v. TLZ. N=5 in saline and vehicle groups, N=8 in NanoTLZ and TLZ treatment groups. Symbols in red: *, p<0.05, **, p<0.0.1, ***, p<0.001 vs. NanoTLZ. Symbols in black: ***, p<0.001 vs. saline. C. NanoTLZ significantly improved the progression free survival of BRCA-deficient mice compared to i.v. TLZ and oral TLZ. N=8. **, p<0.0.1, ***, p<0.001 vs. NanoTLZ. D. All tumors were classified into three groups: regressing (tumor volume decreased more than 50%), no change (tumor volume did not increase or decrease by more than 50%), active growth (tumor

Figure 5.3 (cont'd)
continued to grow and tumor volume increased more than 50%). N=6-19/group. *, $p<0.05$. vs. saline; #, $p<0.05$ vs. NanoTLZ.

All mice were weighed immediately before each injection. Body weight was significantly ($p<0.05$) decreased in both the i.v. free Talazoparib (from 28.1±1.1 g to 26.1±0.7 g) and oral Talazoparib (from 31.1±0.9 g to 28.1±0.8 g) treatment groups after 10 doses (Figure 5.4 A). In contrast, NanoTLZ was better tolerated with no significant changes in body weight (from 30.0±1.4g to 28.6±1.1g, Figure 5.4 A). The dynamic changes in body weight over time are shown in Figure S5.3. Additionally, alopecia, a known side effect of Talazoparib in patients, was observed in both the i.v. Talazoparib (2 out of 8) and oral Talazoparib groups (2 out of 8), but no alopecia was observed in any of the mice in the NanoTLZ treatment group (0 out of 8). A representative image of alopecia is shown in Figure 5.4 B. No liver toxicity was observed after long-term treatment of NanoTLZ, based on the normal histology of all of the liver tissues.

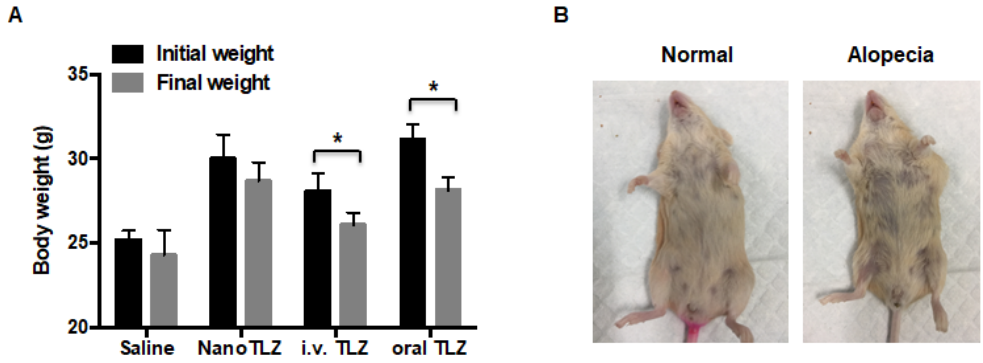

Figure 5.4. NanoTLZ is better tolerated than free Talazoparib in BRCA-deficient mice. A. $Brca1^{Co/Co}$;MMTV-Cre;$p53^{+/-}$ mice were treated three times a week and weighed prior to each treatment. Initial weight, the weight when the mice were started on treatment; final weight, weight after 10 injections of the corresponding treatment. Data presented as mean ± SEM. N=5 in saline group and N=8 in the NanoTLZ and Talazoparib treatment groups (i.v. TLZ and oral TLZ). *, $p<0.05$ vs. initial weight. B. Representative pictures of alopecia observed in free Talazoparib treatment groups.

5.4.3 RNAseq analysis of BRCA-deficient tumors treated with NanoTLZ and i.v. Talazoparib

Talazoparib, as a PARP inhibitor, induces DNA damage and cell death in BRCA-deficient breast cancer cell lines [35]. However, the global regulation of gene expression of Talazoparib vs. NanoTLZ treatment has not been characterized *in vivo*, especially in spontaneous BRCA-deficient mammary gland tumors. Here, we treated $Brca1^{Co/Co}$;MMTV-Cre;$p53^{+/-}$ mice with tumors 4 mm in diameter with 5 doses of i.v. Talazoparib or NanoTLZ (0.33 mg/kg/dose, 3 times a week). Total RNA was extracted from tumors and processed for RNAseq analysis. After five doses of treatment, i.v. Talazoparib significantly (padj<0.05) upregulated 39 genes and downregulated 41 genes. Cluster analysis indicated a similar expression pattern of NanoTLZ compared to Talazoparib (Figure 5.5 A). However, more genes were significantly (padj<0.05) regulated by NanoTLZ: 70 genes were upregulated and 78 genes were downregulated. The Venn diagram summarizes the number of differentially expressed genes compared to the saline group in each treatment group and the overlapping genes found between the comparisons (Figure 5.5 B). Raw data and processed data of the RNAseq were deposited on Gene Expression Omnibus (GEO, GSE125206).

Poly-ADP-ribosylation, a protein post-translational modification, regulates a variety of cellular processes including restarting stalled replication forks, DNA repair, transcription, mitosis and initiating a unique cell death pathway [36]. Not surprisingly, many genes involved in transcription, translation, cell cycle and cell death were differentially expressed in treatment groups compared to the saline control. *Ngfr* (Nerve growth factor receptor), a known tumor suppressor inhibiting cell growth in breast

cancer [37], was upregulated by both NanoTLZ and i.v. Talazoparib. *Bcl11a* (B cell CLL/lymphoma 11A) is overexpressed in triple-negative breast cancer and plays critical roles in stem and progenitor cells [38]; it was downregulated by i.v. Talazoparib and NanoTLZ. Oncogenes, like *Kit* and *Myb*, were also downregulated after treatment with i.v. Talazoparib or NanoTLZ, respectively. Downregulation of *Eef1a2* (eukaryotic translation elongation factor 1 alpha 2) and *Top2a* (topoisomerase II alpha) is consistent with growth arrest after treatment in both the i.v. Talazoparib and NanoTLZ groups. Interestingly, a group of myosin related genes were also regulated by Talazoparib treatment, including *Myl1, Myh1, Myh2, Myh4, Mybpc2* and *Mylpf*. Myosins play critical roles in various processes during tumor development, including cell adhesion, migration, and suppression of apoptosis. Accumulating studies suggest that many kinds of myosins are involved in the formation and development of cancer [39-41]. In addition, some genes that respond to the DNA damage were upregulated in the treatment groups, such as *Gadd45* and *Sod3*.

Notably, NanoTLZ regulated several immune-related genes including cytokines (e.g. *Cxcl12*, *IL13ra2*) and immunoglobulins (e.g. *Igha, Igkc, Ighg2b, Igj*), which were not affected by i.v. free Talazoparib. Cxcl12 enhances anti-cancer immunity and thus blocks both metastasis and primary tumor growth particularly in breast cancer [42]. IL13ra2 (Interleukin-13 receptor α2 chain) has also been shown to inhibit tumorigenicity of breast and pancreatic cancer in animal models [43].

A panel of genes was further validated by real-time PCR using RNA aliquots from the same samples as the RNAseq analysis and additional samples from other mice in each group (N=5 mice, Figure 5.5 C). The PCR results confirmed the RNAseq analysis

for *TNFRSF19, Eef1a2, Kit, Top2a, Sod3, and Cxcl12.* Although tumor samples treated with empty nanoparticles were not included in the original RNAseq comparison, they were analyzed using real-time PCR to evaluate the expression of a few genes that were significantly regulated by NanoTLZ. Interestingly, empty nanoparticles significantly ($p<0.05$) upregulated the expression of *Cxcl12,* suggesting an immune response was induced by the nanocarrier (Figure S5.5). However, as expected, genes like *Top2a* were not regulated by empty nanoparticles (Figure S5.5). Because regulation of proliferation, cell cycle arrest, and DNA damage were observed at the level of gene expression, protein expression of biomarkers in these cellular processes including PCNA, CyclinD1, CyclinE1, c-caspase 3, and gH2AX was analyzed by either western blotting or immunohistochemistry (Figure 5.5 D-E). PCNA, a biomarker of proliferation, was significantly ($p<0.05$) downregulated with NanoTLZ treatment (quantified in Figure S5.6). There was a striking decrease of Cyclin D1 and Cyclin E1 protein expression in the NanoTLZ treated tumor lysates, indicating cell cycle arrest. γH2AX was detected on tumor sections treated with NanoTLZ (Figure 5.5 E), demonstrating increased DNA damage after treatment. Similar effects on proliferation, cell cycle arrest and DNA damage were also observed in the i.v. TLZ group but at a lower magnitude than the nanoTLZ group (Figure S5.7 A-B).

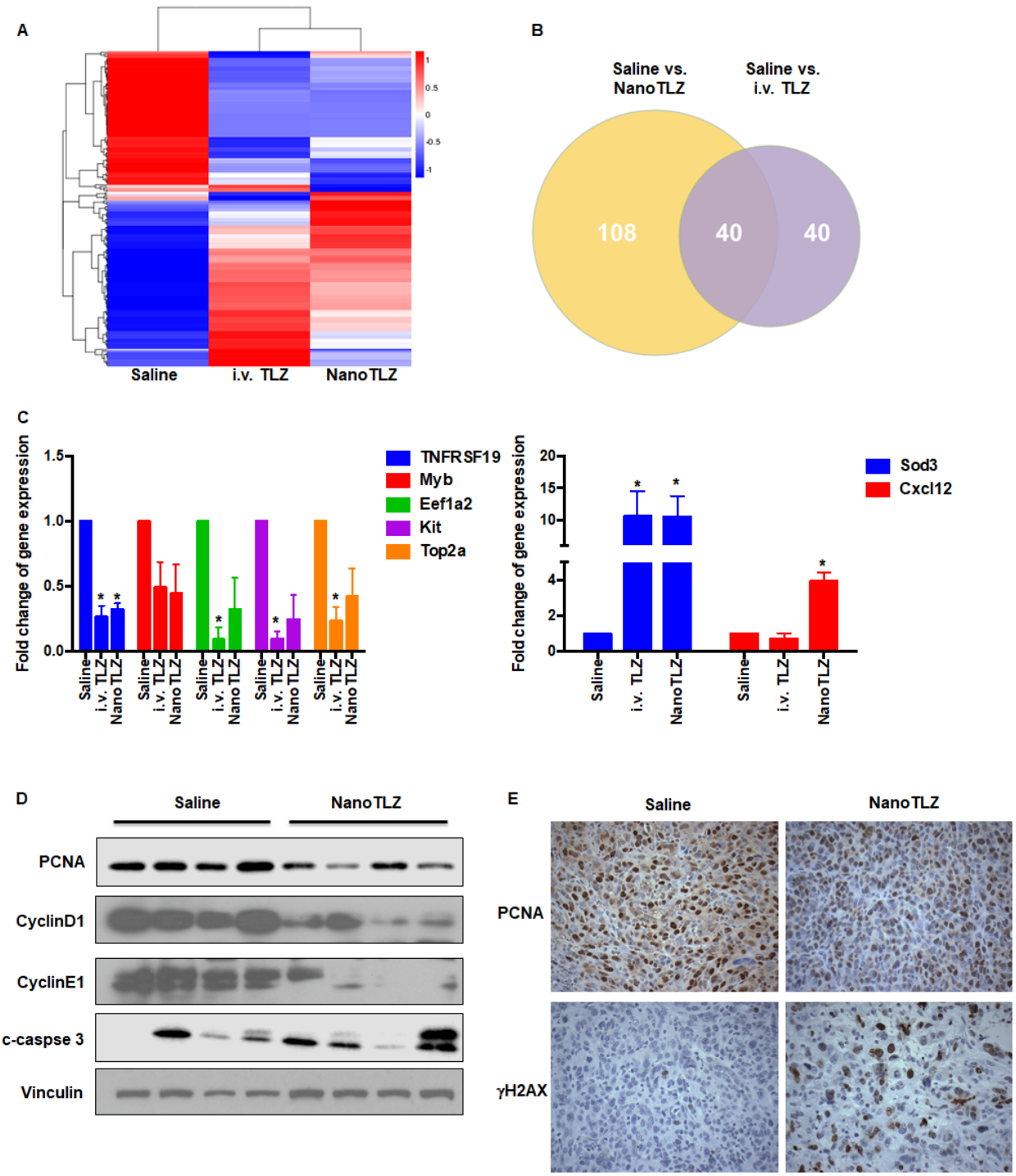

Figure 5.5. RNAseq analysis of tumors from BRCA-deficient mice treated with NanoTLZ or i.v. Talazoparib. When Brca1$^{Co/Co}$;MMTV-Cre;p53$^{+/-}$ mice developed tumors 4 mm in diameter, they were treated with either saline, NanoTLZ (0.33 mg/kg), or Talazoparib (i.v. TLZ, 0.33 mg/kg) by i.v. for 5 doses (3 times a week). Total RNA was isolated from the tumors and processed for RNAseq analysis. A. Cluster analysis of differentially expressed genes in each group. N=3 mice/group. B. Venn diagram of

Figure 5.5 (cont'd)
differentially expressed genes in NanoTLZ and i.v. Talazoparib group. C. Validation of gene expression by real-time PCR. Data presented as mean ± SEM. N=5 mice/group. *, $p<0.05$ vs. Saline. D. Protein expression of PCNA, CyclinD1, CyclinE1, cleaved-caspase (c-caspase) 3 in tumors treated with saline or NanoTLZ. Vinculin was used as the loading control. E. Immunohistochemistry of PCNA and γH2AX expression in tumor sections, 400x magnification.

5.4.4 NanoTLZ modulates immune cell populations in mammary gland, spleen and tumor

Because NanoTLZ regulated immune-associated genes in the tumor, we then examined the effects of NanoTLZ on immune populations within the tumor microenvironment. Here, we used our Brca1$^{Co/Co}$;MMTV-Cre;p53$^{+/-}$ mouse model and investigated the effects of saline, empty nanoparticle (vehicle), NanoTLZ and i.v. Talazoparib on immune populations. Mice bearing tumors (4 mm in diameter) were treated with either saline, empty nanoparticle, NanoTLZ or i.v. Talazoparib for 5 doses (0.33 mg/kg, 3 times a week). Fresh tumors, spleens and mammary glands without visible tumors were collected and processed for flow cytometry. No significant changes in immune populations were observed in empty nanoparticle treated mice compared to saline control (Figure 5.6 A-C). Both NanoTLZ and i.v. Talazoparib induced a decrease in the percentage of myeloid-derived suppressor cells (MDSCs - CD45$^+$, CD11b$^+$, Gr-1$^+$) in the spleen compared to saline group, but it is only statistically significant ($p<0.05$) in the NanoTLZ group (Figure 5.6 A). Interestingly, NanoTLZ significantly ($p<0.05$) increased the total immune cells (CD45$^+$) and total T cells (CD45$^+$, CD3$^+$) in the mammary gland (Figure 5.6 A). These changes were not observed with free i.v. Talazoparib treatment. Importantly, NanoTLZ also induced a striking and significant ($p<0.05$) decrease of MDSCs, a critical immune-suppressive population, in the tumors,

while the change was not significant in the free Talazoparib group (Figure 5.6 C). The results detected by flow cytometry were confirmed by immunohistochemistry (Figure 5.6 D). Although no significant difference was observed in the percentage of $CD4^+$ or $CD8^+$ T cells in either the NanoTLZ or i.v. Talazoparib group in tumors, the percentage of Foxp3 positive cells around the tumor was significantly ($p<0.01$) decreased in the NanoTLZ group compared to saline controls (Figure 5.6 D and quantified in Figure S5.8). The differences in $CD45^+$ cells and T cells in the mammary glands were observed at pre-lesion sites where no palpable lesions were detected.

Figure 5.6. NanoTLZ modulates immune cell populations in BRCA-deficient mice.

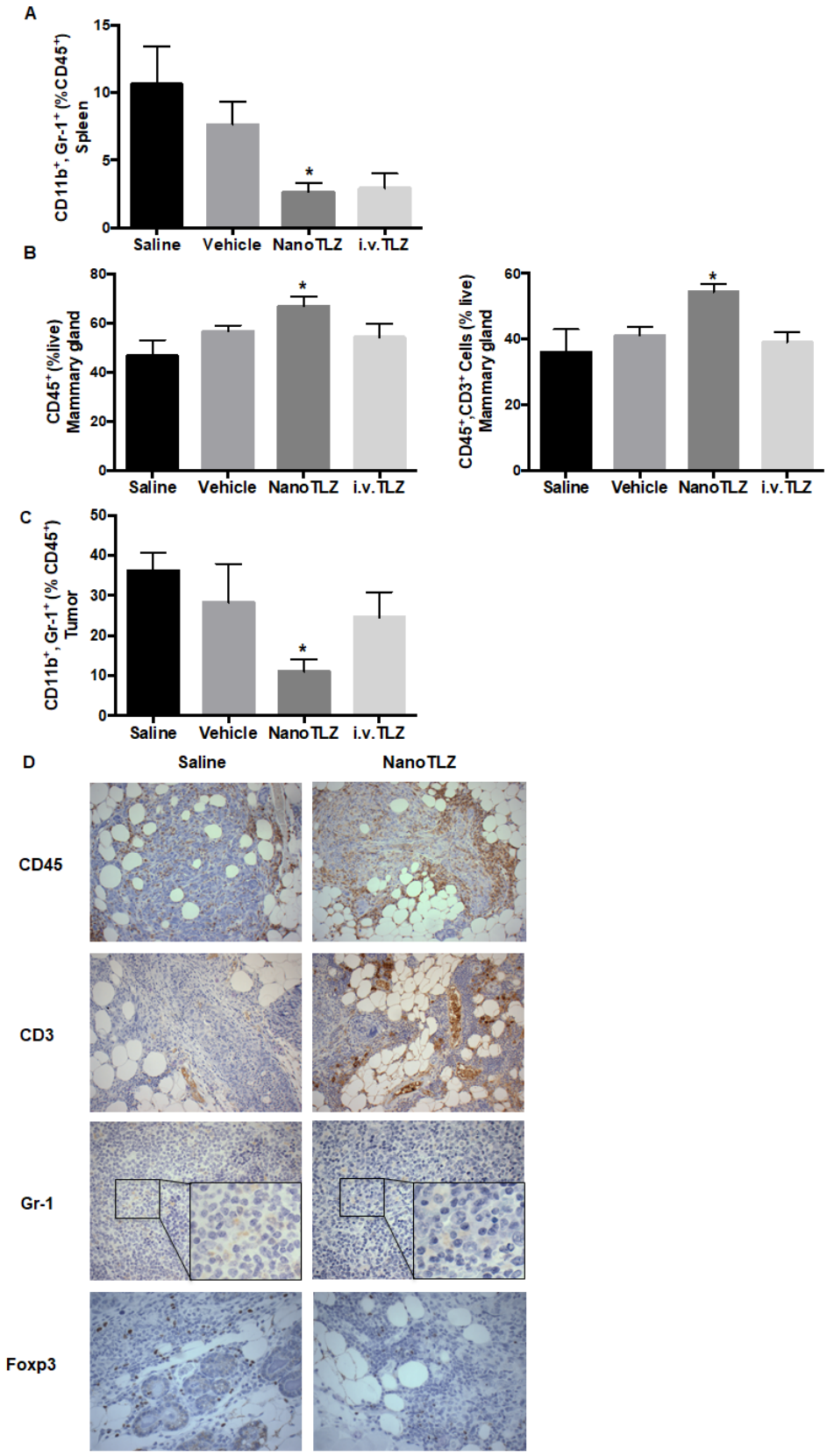

Figure 5.6 (cont'd)

Figure 5.6. NanoTLZ modulates immune cell populations in BRCA-deficient mice. Brca1$^{Co/Co}$;MMTV-Cre;p53$^{+/-}$ mice bearing tumors (4 mm in diameter) were treated with 5 doses of saline, empty nanoparticle (vehicle), free TLZ (i.v. TLZ) or NanoTLZ, and tumor, spleen and mammary gland without visible tumors were collected for flow cytometry. The percentage of immune populations with significant changes in spleen, mammary gland, or tumor are shown from A to C, respectively. N=5 mice/group. *, $p<0.05$ vs. saline. D. The changes of total immune cells (CD45) and T cells (CD3) in mammary gland were confirmed by immunohistochemistry. The changes in myeloid-derived suppressor cells (MDSCs, Gr-1) in the spleen were also validated using immunohistochemistry, 200x magnification. The change of Foxp3 expression around the tumor was shown by IHC at 400x magnification.

5.5 Discussion

To overcome the limitations of oral administration and increase the specific targeting of tumors, we encapsulated Talazoparib into nano liposomes. Our studies demonstrated that this nano-formulation enhanced the efficacy of Talazoparib with prolonged progression free survival and overall survival in BRCA-deficient mice. Compared to free Talazoparib, NanoTLZ was more effective with higher percentages of tumor regression and complete regression achieved, leading to greater overall survival and longer time to disease progression. Moreover, our nano-formulation also reduced the toxicity of Talazoparib.

Although Talazoparib is a more potent drug than Olaparib and thus administered at a lower dose, it is also more toxic clinically. 55% of patients receiving Talazoparib developed adverse grade 3-4 hematological events, mainly anemia, and 25% of patients treated with this PARP inhibitor presented with alopecia. Other common (≥20%)

adverse reactions with Talazoparib treatment in patients include fatigue, decreased appetite, vomiting, and nausea. Our BRCA-deficient mouse model mimics the toxicity observed in human patients after Talazoparib treatment. There was a significant ($p<0.05$) loss of body weight in the free Talazoparib treatment groups, and alopecia also was observed in both free Talazoparib groups. NanoTLZ, excitingly, had decreased toxicity, evident by the absence of weight loss and alopecia. In addition, worse toxicity has also been observed in clinical trials that combine PARP inhibitors with DNA damaging agents [44-50]. Severe side effects experienced during trials with PARP inhibitors and a number of chemotherapeutics required the dose and exposure of PARP inhibitors to be reduced, leading to subtherapeutic doses and ineffective combinations. A clinical trial of oral TLZ in combination with carboplatin required all patients to undergo treatment delay and dose reduction after cycle one due to adverse toxicity [50]. With our new nano-liposome formulation, NanoTLZ, which was better tolerated than free TLZ, significantly improved both PFS and OS compared to free TLZ. Future studies will investigate if similar efficacy and toxicity results are observed when NanoTLZ is combined with chemotherapy.

Because of the EPR effect, nano-carriers accumulated in the tumor of the BRCA-deficient mice and greatly improved the specificity of targeting to the tumor. Liposome-PEG nanocarriers also facilitate cellular uptake. In addition, NanoTLZ induced a striking decrease of MDSCs in the tumor, which was not found with free Talazoparib treatment. NanoTLZ also increased the infiltration of T cells into the pre-lesion sites in the mammary gland of BRCA-deficient mice. Although no significant differences in drug levels were detected in tumor lysates 24 hours after treatment with NanoTLZ and i.v.

TLZ , the multiple different effects that we describe when comparing NanoTLZ to free Talazoparib are important benefits of this novel delivery system. Although the EPR effect is model-dependent, the improvements to Talazoparib achieved by using a nanoparticle formulation could bring better therapeutic outcomes and improved quality of life during treatment for breast cancer patients if similar EPR effects are observed in humans.

With the advance of nanotechnology and its unique properties, nanomedicine has emerged as a promising approach in cancer therapeutics. Doxil (liposomal formulation of doxorubicin) and Abraxane (albumin-bound nanoparticle of paclitaxel) are two successful examples of drug delivery nanoparticles. Doxil, as the first FDA-approved nano-drug, has a prolonged circulation time with better effects than other forms of doxorubicin hydrochloride and fewer side effects [51]. Abraxane, nab-paclitaxel, was designed to overcome the barrier of effective drug delivery with the conventional formulation because of the lipophilic nature of taxane. To date, Abraxane has been approved for the treatment of metastatic breast cancer, non-small cell lung cancer, and pancreatic cancer. By choosing liposomes as the nano-carrier, our study is clinically relevant. Liposomes were the first approved drug-delivery vehicles because of their biocompatibility and biodegradability. Over ten liposomal formulations have been approved for different indications, and numerous other liposomes are being tested in clinical trials [22]. Liposomal-based drugs have a series of advantages including greater solubility, increased half-life, the ability to overcome drug resistance, and increased specificity to the target site. Although a drawback of liposomes is a rapid capture and

clearance by the RES, it can be overcome by PEGylation of the liposome, which induces steric hindrance.

Several other groups have made nanoformulated PARP inhibitors. A lipid-based injectable nanoformulation of Olaparib was developed to sensitize PTEN/TP53-deficient prostate cancer to radiation [52]. Tumor specific proteins can also be conjugated onto liposomes to enhance targeted drug delivery. For example, plectin-targeted liposomes enhance the therapeutic efficacy of a PARP inhibitor (AZ7379) in the treatment of ovarian cancer in animal models [53]. Recently, a solid lipid nanoparticle formulation of Talazoparib was reported and has been tested in *BRCA1* mutant triple negative breast cancer cell lines *in vitro*. The solid lipid formulated Talazoparib was more effective than Talazoparib in inhibiting cell growth in breast cancer cell lines and overcame HR-mediated resistance in TNBC cells [54] but was not tested *in vivo*. Here, we developed a novel liposome-based nanoformulation for Talazoparib and, to our knowledge, were the first to extensively evaluate its effects in a spontaneous and clinically relevant mouse model of breast cancer.

Notably, we also investigated the immunomodulatory effects of Talazoparib and compared it to NanoTLZ in this study. In a mouse model of ovarian cancer, Talazoparib increased peritoneal $CD8^+$ T cells and NK cells [55]. We, for the first time, have characterized immune populations within the tumor microenvironment in a BRCA-deficient breast cancer model. $Brca1^{Co/Co}$;MMTV-Cre;$p53^{+/-}$ mice develop tumors at an average age of 24-32 weeks and recapitulate BRCA-deficient breast cancer in humans. By using this spontaneous tumor model, an intact immune system is present, which allows us to study the endogenous tumor microenvironment. Notably, our data showed

that Talazoparib decreased the percentage of MDSCs, which is an immuno-suppressive population. NanoTLZ was more effective than free Talazoparib in reducing MDSCs in the tumor. MDSCs are known to inhibit the host immune response in breast cancer patients and limit the effectiveness of immunotherapies [56]. Meanwhile, Foxp3 expression, a marker of T regulatory cells, another immunosuppressive population, was decreased with NanoTLZ treatment. NanoTLZ also had additional effects beyond Talazoparib of modulating immune cells at the pre-lesion sites (Figure 5.6), suggesting a potential effect on newly developing tumors. RNAseq analysis (Figure 5.5) suggested that NanoTLZ, rather than Talazoparib, regulated immune-associated genes, which may explain the difference between NanoTLZ and Talazoparib on immune modulation. Interestingly, some effects on immune regulation may be induced by the nano-carriers, as empty nanoparticles upregulated *Cxcl12* expression. Additionally, our preliminary data suggests an increased activation of dendritic cells with NanoTLZ treatment compared to free TLZ, which will be fully explored in future studies.

In addition to the immunomodulation of NanoTLZ, PARP inhibitors have recently been shown to upregulate PD-L1 expression [57]. Therefore, there is a strong rationale for combining NanoTLZ with immunotherapies, such as PD1/PDL-1 immune checkpoint inhibitors. With its reduced toxicity, NanoTLZ is also a better compound for combining with other anti-cancer agents. In fact, the first positive results of a clinical trial in breast cancer patients using the combination of immunotherapy with nanomedicine was recently reported. Median progression-free survival was significantly ($p<0.05$) extended from 5.5 months in patients with metastatic TNBC treated with placebo plus nab-paclitaxel to 7.2 months in patients treated with atezolizumab (anti-PD-L1) plus nab-

paclitaxel [58]. In the future, we will explore the combination of NanoTLZ and immunotherapy (anti-PD1/PDL-1 antibodies) for treating BRCA-deficient breast cancer.

REFERENCES

REFERENCES

1. van der Kolk DM, de Bock GH, Leegte BK, Schaapveld M, Mourits MJ, de Vries J, et al. Penetrance of breast cancer, ovarian cancer and contralateral breast cancer in BRCA1 and BRCA2 families: high cancer incidence at older age. Breast Cancer Res Treat. 2010; 124: 643-51.

2. Larsen MJ, Kruse TA, Tan Q, Laenkholm AV, Bak M, Lykkesfeldt AE, et al. Classifications within molecular subtypes enables identification of BRCA1/BRCA2 mutation carriers by RNA tumor profiling. PLoS One. 2013; 8: e64268.

3. Petrucelli N, Daly MB, Feldman GL. Hereditary breast and ovarian cancer due to mutations in BRCA1 and BRCA2. Genet Med. 2010; 12: 245-59.

4. Scully R, Livingston DM. In search of the tumour-suppressor functions of BRCA1 and BRCA2. Nature. 2000; 408: 429-32.

5. Thangaraju M, Kaufmann SH, Couch FJ. BRCA1 facilitates stress-induced apoptosis in breast and ovarian cancer cell lines. J Biol Chem. 2000; 275: 33487-96.

6. Deng CX. BRCA1: cell cycle checkpoint, genetic instability, DNA damage response and cancer evolution. Nucleic Acids Res. 2006; 34: 1416-26.

7. Rodgers K, McVey M. Error-Prone Repair of DNA Double-Strand Breaks. J Cell Physiol. 2016; 231: 15-24.

8. Rouleau M, Patel A, Hendzel MJ, Kaufmann SH, Poirier GG. PARP inhibition: PARP1 and beyond. Nat Rev Cancer. 2010; 10: 293-301.

9. Farmer H, McCabe N, Lord CJ, Tutt AN, Johnson DA, Richardson TB, et al. Targeting the DNA repair defect in BRCA mutant cells as a therapeutic strategy. Nature. 2005; 434: 917-21.

10. Bryant HE, Schultz N, Thomas HD, Parker KM, Flower D, Lopez E, et al. Specific killing of BRCA2-deficient tumours with inhibitors of poly(ADP-ribose) polymerase. Nature. 2005; 434: 913-7.

11. Litton JK, Rugo HS, Ettl J, Hurvitz SA, Goncalves A, Lee KH, et al. Talazoparib in Patients with Advanced Breast Cancer and a Germline BRCA Mutation. N Engl J Med. 2018; 379: 753-63.

12. Murai J, Huang SY, Renaud A, Zhang Y, Ji J, Takeda S, et al. Stereospecific PARP trapping by BMN 673 and comparison with olaparib and rucaparib. Mol Cancer Ther. 2014; 13: 433-43.

13. Wang X, Shi Y, Huang D, Guan X. Emerging therapeutic modalities of PARP inhibitors in breast cancer. Cancer Treat Rev. 2018; 68: 62-8.

14. McCabe N, Turner NC, Lord CJ, Kluzek K, Bialkowska A, Swift S, et al. Deficiency in the repair of DNA damage by homologous recombination and sensitivity to poly(ADP-ribose) polymerase inhibition. Cancer Res. 2006; 66: 8109-15.

15. McLornan DP, List A, Mufti GJ. Applying synthetic lethality for the selective targeting of cancer. N Engl J Med. 2014; 371: 1725-35.

16. Saal LH, Gruvberger-Saal SK, Persson C, Lovgren K, Jumppanen M, Staaf J, et al. Recurrent gross mutations of the PTEN tumor suppressor gene in breast cancers with deficient DSB repair. Nat Genet. 2008; 40: 102-7.

17. Evans KW, Yuca E, Akcakanat A, Scott SM, Arango NP, Zheng X, et al. A Population of Heterogeneous Breast Cancer Patient-Derived Xenografts Demonstrate Broad Activity of PARP Inhibitor in BRCA1/2 Wild-Type Tumors. Clin Cancer Res. 2017; 23: 6468-77.

18. Wang B, Chu D, Feng Y, Shen Y, Aoyagi-Scharber M, Post LE. Discovery and Characterization of (8S,9R)-5-Fluoro-8-(4-fluorophenyl)-9-(1-methyl-1H-1,2,4-triazol-5-yl)-2,7,8,9-te trahydro-3H-pyrido[4,3,2-de]phthalazin-3-one (BMN 673, Talazoparib), a Novel, Highly Potent, and Orally Efficacious Poly(ADP-ribose) Polymerase-1/2 Inhibitor, as an Anticancer Agent. J Med Chem. 2016; 59: 335-57.

19. de Bono J, Ramanathan RK, Mina L, Chugh R, Glaspy J, Rafii S, et al. Phase I, Dose-Escalation, Two-Part Trial of the PARP Inhibitor Talazoparib in Patients with Advanced Germline BRCA1/2 Mutations and Selected Sporadic Cancers. Cancer Discov. 2017; 7: 620-9.

20. Torchilin VP. Targeted pharmaceutical nanocarriers for cancer therapy and imaging. AAPS J. 2007; 9: E128-47.

21. Maeda H. The enhanced permeability and retention (EPR) effect in tumor vasculature: the key role of tumor-selective macromolecular drug targeting. Adv Enzyme Regul. 2001; 41: 189-207.

22. Bozzuto G, Molinari A. Liposomes as nanomedical devices. Int J Nanomedicine. 2015; 10: 975-99.

23. Allen TM, Hansen C, Martin F, Redemann C, Yau-Young A. Liposomes containing synthetic lipid derivatives of poly(ethylene glycol) show prolonged circulation half-lives in vivo. Biochim Biophys Acta. 1991; 1066: 29-36.

24. Petrikovics I, Jayanna P, Childress J, Budai M, Martin S, Kuzmitcheva G, et al. Optimization of liposomal lipid composition for a new, reactive sulfur donor, and in vivo efficacy studies on mice to antagonize cyanide intoxication. J Drug Deliv. 2011; 2011: 928626.

25. Campbell RB, Balasubramanian SV, Straubinger RM. Influence of cationic lipids on the stability and membrane properties of paclitaxel-containing liposomes. J Pharm Sci. 2001; 90: 1091-105.

26. Zhang Y, Sriraman SK, Kenny HA, Luther E, Torchilin V, Lengyel E. Reversal of Chemoresistance in Ovarian Cancer by Co-Delivery of a P-Glycoprotein Inhibitor and Paclitaxel in a Liposomal Platform. Mol Cancer Ther. 2016; 15: 2282-93.

27. Baldwin P, Ohman AW, Medina JE, McCarthy ET, Dinulescu DM, Sridhar S. Nanoformulation of Talazoparib Delays Tumor Progression and Ascites Formation in a Late Stage Cancer Model. Front Oncol. 2019; 9: 353.

28. Kim EH, Deng C, Sporn MB, Royce DB, Risingsong R, Williams CR, et al. CDDO-methyl ester delays breast cancer development in BRCA1-mutated mice. Cancer Prev Res (Phila). 2012; 5: 89-97.

29. Zhang Y, Huo M, Zhou J, Xie S. PKSolver: An add-in program for pharmacokinetic and pharmacodynamic data analysis in Microsoft Excel. Comput Methods Programs Biomed. 2010; 99: 306-14.

30. Brodie SG, Xu X, Qiao W, Li WM, Cao L, Deng CX. Multiple genetic changes are associated with mammary tumorigenesis in Brca1 conditional knockout mice. Oncogene. 2001; 20: 7514-23.

31. Xu X, Wagner KU, Larson D, Weaver Z, Li C, Ried T, et al. Conditional mutation of Brca1 in mammary epithelial cells results in blunted ductal morphogenesis and tumour formation. Nat Genet. 1999; 22: 37-43.

32. Zhang D, Rennhack J, Andrechek ER, Rockwell CE, Liby KT. Identification of an Unfavorable Immune Signature in Advanced Lung Tumors from Nrf2-Deficient Mice. Antioxid Redox Signal. 2018; 29: 1535-52.

33. Livak KJ, Schmittgen TD. Analysis of relative gene expression data using real-time quantitative PCR and the 2(-Delta Delta C(T)) Method. Methods. 2001; 25: 402-8.

34. Anders S, Huber W. Differential expression analysis for sequence count data. Genome Biol. 2010; 11: R106.

35. Belz JE, Kumar R, Baldwin P, Ojo NC, Leal AS, Royce DB, et al. Sustained Release Talazoparib Implants for Localized Treatment of BRCA1-deficient Breast Cancer. Theranostics. 2017; 7: 4340-9.

36. Morales J, Li L, Fattah FJ, Dong Y, Bey EA, Patel M, et al. Review of poly (ADP-ribose) polymerase (PARP) mechanisms of action and rationale for targeting in cancer and other diseases. Crit Rev Eukaryot Gene Expr. 2014; 24: 15-28.

37. Reis-Filho JS, Steele D, Di Palma S, Jones RL, Savage K, James M, et al. Distribution and significance of nerve growth factor receptor (NGFR/p75NTR) in normal, benign and malignant breast tissue. Mod Pathol. 2006; 19: 307-19.

38. Khaled WT, Choon Lee S, Stingl J, Chen X, Raza Ali H, Rueda OM, et al. BCL11A is a triple-negative breast cancer gene with critical functions in stem and progenitor cells. Nat Commun. 2015; 6: 5987.

39. Li YR, Yang WX. Myosins as fundamental components during tumorigenesis: diverse and indispensable. Oncotarget. 2016; 7: 46785-812.

40. Ouderkirk-Pecone JL, Goreczny GJ, Chase SE, Tatum AH, Turner CE, Krendel M. Myosin 1e promotes breast cancer malignancy by enhancing tumor cell proliferation and stimulating tumor cell de-differentiation. Oncotarget. 2016; 7: 46419-32.

41. Cao R, Chen J, Zhang X, Zhai Y, Qing X, Xing W, et al. Elevated expression of myosin X in tumours contributes to breast cancer aggressiveness and metastasis. Br J Cancer. 2014; 111: 539-50.

42. Williams SA, Harata-Lee Y, Comerford I, Anderson RL, Smyth MJ, McColl SR. Multiple functions of CXCL12 in a syngeneic model of breast cancer. Mol Cancer. 2010; 9: 250.

43. Kawakami K, Kawakami M, Husain SR, Puri RK. Potent antitumor activity of IL-13 cytotoxin in human pancreatic tumors engineered to express IL-13 receptor alpha2 chain in vivo. Gene Ther. 2003; 10: 1116-28.

44. Khan OA, Gore M, Lorigan P, Stone J, Greystoke A, Burke W, et al. A phase I study of the safety and tolerability of olaparib (AZD2281, KU0059436) and dacarbazine in patients with advanced solid tumours. Br J Cancer. 2011; 104: 750-5.

45. Samol J, Ranson M, Scott E, Macpherson E, Carmichael J, Thomas A, et al. Safety and tolerability of the poly(ADP-ribose) polymerase (PARP) inhibitor, olaparib (AZD2281) in combination with topotecan for the treatment of patients with advanced solid tumors: a phase I study. Invest New Drug. 2012; 30: 1493-500.

46. Balmana J, Tung NM, Isakoff SJ, Grana B, Ryan PD, Saura C, et al. Phase I trial of olaparib in combination with cisplatin for the treatment of patients with advanced breast, ovarian and other solid tumors. Ann Oncol. 2014; 25: 1656-63.

47. Rajan A, Carter CA, Kelly RJ, Gutierrez M, Kummar S, Szabo E, et al. A Phase I Combination Study of Olaparib with Cisplatin and Gemcitabine in Adults with Solid Tumors. Clinical Cancer Research. 2012; 18: 2344-51.

48. Landrum LM, Brady WE, Armstrong DK, Moore KN, DiSilvestro PA, O'Malley DM, et al. A phase I trial of pegylated liposomal doxorubicin (PLD), carboplatin, bevacizumab, and veliparib (ABT-888) in recurrent, platinum-sensitive ovarian, primary peritoneal, and

fallopian tube cancer: A Gynecologic Oncology Group study. Gynecol Oncol. 2015; 137: 23-.

49. De Bono JS, Mina LA, Gonzalez M, Curtin NJ, Wang E, Henshaw JW, et al. First-in-human trial of novel oral PARP inhibitor BMN 673 in patients with solid tumors. Journal of Clinical Oncology. 2013; 31.

50. Dhawan MS, Aggarwal RR, Bartelink I, Leng J, Thomas S, Pawlowska N, et al. Efficacy and hematologic toxicity of carboplatin and talazoparib combination therapy in BRCA mutated patients. Journal of Clinical Oncology. 2016; 34.

51. Barenholz Y. Doxil(R)--the first FDA-approved nano-drug: lessons learned. J Control Release. 2012; 160: 117-34.

52. van de Ven AL, Tangutoori S, Baldwin P, Qiao J, Gharagouzloo C, Seitzer N, et al. Nanoformulation of Olaparib Amplifies PARP Inhibition and Sensitizes PTEN/TP53-Deficient Prostate Cancer to Radiation. Mol Cancer Ther. 2017; 16: 1279-89.

53. Dasa SSK, Diakova G, Suzuki R, Mills AM, Gutknecht MF, Klibanov AL, et al. Plectin-targeted liposomes enhance the therapeutic efficacy of a PARP inhibitor in the treatment of ovarian cancer. Theranostics. 2018; 8: 2782-98.

54. Guney Eskiler G, Cecener G, Egeli U, Tunca B. Synthetically Lethal BMN 673 (Talazoparib) Loaded Solid Lipid Nanoparticles for BRCA1 Mutant Triple Negative Breast Cancer. Pharm Res. 2018; 35: 218.

55. Huang J, Wang L, Cong Z, Amoozgar Z, Kiner E, Xing D, et al. The PARP1 inhibitor BMN 673 exhibits immunoregulatory effects in a Brca1(-/-) murine model of ovarian cancer. Biochem Biophys Res Commun. 2015; 463: 551-6.

56. Markowitz J, Wesolowski R, Papenfuss T, Brooks TR, Carson WE, 3rd. Myeloid-derived suppressor cells in breast cancer. Breast Cancer Res Treat. 2013; 140: 13-21.

57. Jiao S, Xia W, Yamaguchi H, Wei Y, Chen MK, Hsu JM, et al. PARP Inhibitor Upregulates PD-L1 Expression and Enhances Cancer-Associated Immunosuppression. Clin Cancer Res. 2017; 23: 3711-20.

58. Schmid P, Adams S, Rugo HS, Schneeweiss A, Barrios CH, Iwata H, et al. Atezolizumab and Nab-Paclitaxel in Advanced Triple-Negative Breast Cancer. N Engl J Med. 2018; 379: 2108-21.

CHAPTER 6

Conclusions and perspectives

6.1 Conclusions

This dissertation contributed to science in three aspects: 1. Tested new drugs for cancer prevention and treatment; 2. Demonstrated enhanced drug efficacy and reduced toxicity via various strategies; 3. Identified novel immunomodulatory effects of compounds or targets of interest.

As summarized earlier, cancer prevention is as important as cancer treatment. It is critical to develop effective and safe chemopreventive agents. In chapters 2 and 3, I evaluated the chemopreventive effects of the bromodomain inhibitor I-BET 762 and novel RXR agonists, respectively. The bromodomain inhibitor I-BET 762 significantly delayed tumor development in an ER^- breast cancer model. I-BET 762 was strikingly effective for reducing lung tumor burden induced by the carcinogen vinyl carbamate. I-BET 762 was well-tolerated in mice without any loss of body weight. More information about its toxicity profile will be learned from ongoing clinical trials. Rexinoids also showed significant efficacy in reducing tumor burden in the A/J lung carcinogenesis model. Notably, I-BET 762 can be combined with rexinoids, so that a lower dose of each can be used to further reduce any potential off-target side effects.

Rexinoids are effective for treating tumors as well. Bexarotene is FDA approved for treating cutaneous T-cell lymphoma. LG100268 significantly decreases tumor size and number when treating vinyl carbamate-induced lung tumors at a dose of 100 mg/kg diet [1]. LG100268 also induces rapid tumor regression when treating $HER2^+$ breast cancer in the MMTV-Neu mouse model [2]. Although new rexinoids reported here were only tested in a cancer prevention model, we predict that they possess the same efficacy for treating tumors if a higher dose is used.

Undesired side effects are often a primary obstacle limiting the use of a drug in the clinic especially for use in prevention. It is important to broaden the therapeutic window by enhancing drug efficacy and/or reducing toxicity. One possible strategy is to increase the delivery of drugs specifically to the tumor. We have collaborated with bioengineers to develop novel drug delivery platforms. Previously, we reported an intra-tumoral delivery system for the PARP inhibitor talazoparib [3]. Talazoparib was formulated into poly(lactic-co-glycolic acid) (PLGA) implants and were directly injected into the tumor in the mammary gland. This method bypassed the absorption and distribution steps required for oral delivery and targeted the drug specifically to tumors. This new formulation induced regression of *BRCA*-deficient tumors, whereas oral delivery at the same dose only slowed tumor growth. In chapter 5, we developed and tested another delivery system for talazoparib using a bilayer liposomal nanoparticle formulation. This novel delivery platform significantly improved therapeutic efficacy and reduced toxicity of talazoparib in *BRCA*-deficient mice.

Besides improving delivery systems, another strategy to increase the therapeutic window is to optimize the compound potency via synthetic chemistry. In chapter 3, we collaborated with medicinal chemists and synthesized novel rexinoids. Two new rexinoids are more effective than the FDA-approved bexarotene and less toxic than LG100268. This study demonstrated the possibility of synthesizing additional rexinoids that have sufficient efficacy and limited toxicity.

The bromodomain inhibitor, rexinoids, and PARP inhibitor all have immunomodulatory effects within the tumor microenvironment, although they were developed to target tumor cells rather than immune cells. I-BET 762 not only induced

growth arrest and downregulated the expression of oncoproteins in tumor cells but also altered various immune populations within the tumor microenvironment. Notably, I-BET 762 had distinct effects on immune cells in different cancer types, indicating the effects might be cancer type dependent. Anti-inflammatory effects of rexinoids play important roles in preventing tumor development in a lung carcinogenesis model. The ability of rexinoids to reduce NO production *in vitro* directly correlates with *in vivo* efficacy. PyLG268 also decreased the percentage of macrophages and MDSCs in the lung and skewed M2 macrophages to an M1 phenotype. It is worth noting that different rexinoids exhibit different effects on immune cells. Further studies will investigate whether these effects are RXR dependent. The PARP inhibitor talazoparib has been reported to upregulate the expression of PD-L1 [4]. NanoTLZ, interestingly, induced further immunomodulatory effects not observed with talazoparib, including decreasing the percentage of MDSCs in the tumors. Additional studies will determine whether these effects are induced by nanoparticles or a higher accumulation of drug in the tumors.

6.2 Perspectives – Developing new rexinoids

The retinoid X nuclear receptor is an attractive target for cancer therapy because it regulates many pathways that are relevant in cancer, including proliferation, apoptosis, differentiation, *etc*. As multifunctional agents, rexinoids can prevent and treat cancer in multiple preclinical models. Unlike conventional cytotoxic agents or monofunctional drugs, these compounds have unique molecular mechanisms. Unfortunately, despite great potential, rexinoids have not been widely used in clinic.

Bexarotene remains the only rexinoid that has been approved by the FDA. Both lack of efficacy and undesired toxicity limited the use of bexarotene in patients. Patent issues

prevented the further development of more advanced rexinoids, such as LG100268. Developing novel rexinoids with new patent protection and greater efficacy will provide new opportunities for this class of drug. The new paradigm I established here will accelerate the process of identifying promising rexinoids by using a series of predictive screening assays.

New compounds can be ranked based on the results of iNOS suppression and SREBP induction assays. Efficacy and toxicity must be balanced, as toxicity cannot be completely eliminated for any drug. Among compounds that have similar potency in inhibiting NO production, the ones with less induction of SREBP expression will be selected for additional study. The vinyl carbamate-induced lung cancer model in A/J mice is a very simple and reproducible model for testing new drugs. It provides a flexible study design to model both cancer prevention and treatment. We have established a method to monitor tumor growth in live animals using ultrasound imaging. With better understanding of the mechanisms of rexinoids in cancer, it is likely that rexinoids will eventually become clinically useful.

Interestingly, rexinoids seem to have greater efficacy in cancers that are driven by mutations in *Kras* or other growth factors [5]. Our lab has tested rexinoids in various models of breast cancer, lung cancer and pancreatic cancer [6, 7]. In addition to the vinyl carbamate induced lung cancer model (*Kras* mutation), rexinoids are also effective when treating tumors in the transgenic KPC model of pancreatic cancer (*Kras* and *p53* mutations) [7], ER^+ NMU model of breast cancer (*Hras* mutations) [8] and ER^- MMTV-neu model of breast cancer [6]. In contrast, rexinoids are not effective for preventing breast cancer in the ER^- PyMT and BRCA-deficient ($BRCA^{-/-}$;$p53^{-/+}$) breast

cancer models which are not driven by Ras or other growth factor signaling. *KRAS* is one of the most commonly mutated genes in cancer, and it has been considered an undruggable target for decades [9]. Although small molecules targeting a specific *KRAS* mutation (G12C) have been developed recently, they are still being evaluated in clinical trials [10]. Other *KRAS* mutations, such as the more common G12D mutation, remain undruggable. Developing successful rexinoids could potentially provide a valuable therapeutic option to treat *KRAS* mutant tumors.

The finding that rexinoids have limited effects on inducing cell death *in vitro* but have striking effects *in vivo* suggests an immune system dependent cell killing. My study suggests rexinoids can reduce immunosuppression within the microenvironment of lung cancer. Rexinoids not only decreased the percentage of TAMs and MDSCs but also repolarized M2 macrophages to tumor-killing M1 macrophages. In $HER2^+$ breast cancer, LG100268 decreased the infiltration of MDSCs and TAMs. LG100268 also increased cytotoxic activity of CD8 T cells [2]. These results indicate that rexinoids modulate the tumor microenvironment to become more immunoreactive. Further studies need to be performed to directly evaluate whether the efficacy of rexinoids is immune cell-dependent. If true, the mechanism of how rexinoids induce immune cell-mediated killing needs to be investigated.

6.3 Perspectives – Targeting the Nrf2 pathway in cancer

The Nrf2 pathway has become an important target in cancer research. Conventionally, Nrf2 was considered cancer-preventing. Activation of Nrf2 protects against many inflammatory diseases including cancer. Nrf2 serves as the main cellular defense mechanism against both endogenous and exogenous insults. Carcinogenesis is

exacerbated in Nrf2-knockout (KO) vs wildtype (WT) mice [11-15]. Knockdown of Keap1 increases resistance to cancer metastasis [16, 17]. Numerous Nrf2 activators, including natural products, can be used to prevent or delay tumor development, and these chemopreventive effects are greatly dampened in Nrf2 KO mice [13, 18].

However, accumulating studies suggest that there is also a tumor-promoting role for Nrf2. Mutations found in the *Nfe2l2* and *Keap1* genes promote tumor growth; the mutation rate in these genes is up to 30% in lung cancer [19]. Additionally, epigenetic modifications of the *Keap1* or *Nfe2l2* promoters have been found. All of these genetic and epigenetic alterations result in constitutively high levels of Nrf2 expression and activity, which is associated with chemoresistance and poor prognosis [19-21]. Nrf2 also promotes cell proliferation by reprogramming cellular metabolism [22, 23]. This tumor-promoting role of Nrf2 in tumor cells raised concerns regarding the long-term safety of Nrf2 activators for cancer prevention. Smokers, the patient population with the highest risk of developing lung cancer, are more likely to receive intervention by chemoprevention. However, it can be dangerous to activate Nrf2 chronically if cells are already transformed. On the other hand, the tumor-promoting role of Nrf2 has generated substantial interest in developing Nrf2 inhibitors for cancer treatment. Nrf2 inhibitors are expected to sensitize tumor cells to chemotherapies when used as an adjuvant therapy. A few Nrf2 inhibitors have been reported and provide *in vivo* proof-of concept [24].

In my dissertation research, I investigated the role of the Nrf2 pathway in immune cells during lung carcinogenesis. I identified an unfavorable immuno-suppressive signature in the tumors and lungs of Nf2 KO mice vs. Nrf2 WT mice [25]. These findings raise questions regarding the value of Nrf2 inhibitors for treating tumors in

immune-competent mice, which has never been tested. So far, reported Nrf2 inhibitors have only been tested in xenograft models established with either A549 cells or H460 human lung cancer cells; these models lack an intact immune system. It is critical to further test Nrf2 inhibitors in syngeneic models, such as the orthotopic Lewis lung carcinoma model, so that we can better determine whether we should inhibit this pathway for the treatment of lung cancer.

The effects of targeting Nrf2 pathways using Nrf2 inhibitors may also depend on the status of other genes. Targeting co-dependent vulnerabilities or synthetic lethal partners is often more effective and provides a promising therapeutic opportunity. Nrf2-mediated antioxidant activity can be upregulated by oncogenes, such as Kras, B-Raf, and myc, to detoxify the increased ROS [26]. Genetic deletion of Nrf2 impairs tumorigenesis driven by Kras [26]. Loss of NRF2 has also been shown to impair EGFR signaling, thus inhibiting cell proliferation in pancreatic cancer [27]. In KRAS-mutant lung adenocarcinoma patients, KEAP1 mutations often accompany the loss of LKB1. LKB1-deficient cells with Nrf2 activation have enhanced cell survival and better maintenance of energetic and redox homeostasis in a glutamine-dependent manner. They are more sensitive to glutamine inhibitors [28]. Further studies are needed to better understand the interactions of the Nrf2 pathway with other cell signaling pathways, so that we can determine which patient subpopulations would benefit the most from Nrf2 inhibitors.

Despite all these exciting studies, we still do not have a potent and specific Nrf2 inhibitor available. Unlike Nrf2 activators, a much smaller number of Nrf2 inhibitors have been reported. Brusatol, a natural product isolated from Bruceajavanica (L) Merr., has

emerged as a promising Nrf2 inhibitor with high potency. However, a mass spectrometry study suggested that brusatol regulates a series of fast turnover proteins by inducing a global inhibition of protein synthesis rather than being a specific inhibitor of Nrf2 [29]. Several other natural compounds were reported with inhibitory effects on Nrf2 activity, including ascorbic acid, flavonoids, trigonelline, and ochratoxin A [30-33]. Recently, high throughput drug screening has been used to identify novel Nrf2 inhibitors. AEM1 [34], IM3829 [35], ML385 [35], halofuginone [36], and clobetasol propionate [37] are all reported leads from different screens. Unfortunately, none of these compounds have adequate potency and specificity to be further developed for clinical trials. More studies need to be done to identify potent and selective Nrf2 inhibitors. To complement genetic deletion studies, powerful pharmacological tools will better illustrate the effects of inhibiting this important pathway in cancer.

6.4 Perspectives – Drug combinations

Cancer drugs are often more effective when given in combination. The idea is to combine drugs that function by different mechanisms. Considering the redundancy of compensatory signaling regulations, this approach could enhance the therapeutic benefits and potentially prevent drug resistance. Additionally, combinations could also potentially reduce side effects because each drug can be given at lower doses rather than at the maximum tolerated dose. Even when there is no synergistic or additive effect with the combination, combination cancer therapy still demonstrates superiority via patient-to-patient variability [38].

There are numerous successful strategies of using drug combination to sensitize or re-sensitize tumor cells. One example is to combine anti-cancer agents with multidrug

transporter blockers to keep drugs inside the cells. Up-regulation of ATP-binding cassette (ABC) transporters is a well-known mechanism of inducing chemoresistance [39]. Blocking these transporters will allow anticancer drugs to accumulate in tumor cells, thus boosting their effects. Another strategy is to target signal rewiring that induces drug resistance. Adaptive reprogramming of signaling pathways has been a major cause of acquired resistance. For example, EGFR family receptor targeted therapies can induce acquired resistance via upregulating other RTKs, including ERBB3, FGFR2, IFG1R, FAK, SRC family kinases, *etc* [40, 41]. Co-inhibition of EGFR and FGFR exhibits enhanced activity in lung cancer [42]. This rewiring can also be through epigenetic modifications. Patients develop high level of DNA methylation near the gene *hMLH1* after chemotherapy treatment, and decitabine (a DNA methylation inhibitor) can re-sensitize the tumors to cisplatin [43].

Besides acquired resistance, many patients are intrinsically resistant to treatment. It is estimated that only 12.5% patients with cancer respond to immune checkpoint inhibitors [44]. A lot of effort has focused on improving this low response rate by altering the tumor microenvironment. Eliciting a potent immune attack to the tumor cells requires cooperation along a series of steps, from antigen presentation and immune cell infiltration to T cell activation and T cell-mediated killing. Obviously, targeting only one step is often not sufficient. Thus, developing effective combinations with other therapeutic agents that enhance T cell infiltration and activation or decrease immunosuppression becomes a promising strategy to overcome resistance. Many studies have reported positive results when combining ICIs with other drugs including co-inhibitory receptors, anti-angiogenic molecules, microbiota modifiers, small molecules,

and oncolytic viruses [45]. Small molecules, including bromodomain inhibitors, rexinoids and PARP inhibitors, could not only arrest the tumor growth, but also prime a favorable microenvironment for immunotherapy. In the future, besides elucidating the respective combinations of each drug, it is also important to develop predictive *ex vivo* models to quickly evaluate the patient's likely response. If drug resistance and patient death could be substantially delayed, cancer will become manageable like many other chronic diseases.

REFERENCES

REFERENCES

1. Liby K, Risingsong R, Royce DB, Williams CR, Ma T, Yore MM, et al. Triterpenoids CDDO-methyl ester or CDDO-ethyl amide and rexinoids LG100268 or NRX194204 for prevention and treatment of lung cancer in mice. Cancer Prev Res (Phila). 2009; 2: 1050-8.

2. Leal AS, Zydeck K, Carapellucci S, Reich LA, Zhang D, Moerland JA, et al. Retinoid X receptor agonist LG100268 modulates the immune microenvironment in preclinical breast cancer models. NPJ Breast Cancer. 2019; 5: 39.

3. Belz JE, Kumar R, Baldwin P, Ojo NC, Leal AS, Royce DB, et al. Sustained Release Talazoparib Implants for Localized Treatment of BRCA1-deficient Breast Cancer. Theranostics. 2017; 7: 4340-9.

4. Jiao S, Xia W, Yamaguchi H, Wei Y, Chen MK, Hsu JM, et al. PARP Inhibitor Upregulates PD-L1 Expression and Enhances Cancer-Associated Immunosuppression. Clin Cancer Res. 2017; 23: 3711-20.

5. Liby KT, Sporn MB. Rexinoids for prevention and treatment of cancer: opportunities and challenges. Curr Top Med Chem. 2017; 17: 721-30.

6. Liby K, Royce DB, Risingsong R, Williams CR, Wood MD, Chandraratna RA, et al. A new rexinoid, NRX194204, prevents carcinogenesis in both the lung and mammary gland. Clin Cancer Res. 2007; 13: 6237-43.

7. Liby KT, Royce DB, Risingsong R, Williams CR, Maitra A, Hruban RH, et al. Synthetic triterpenoids prolong survival in a transgenic mouse model of pancreatic cancer. Cancer Prev Res (Phila). 2010; 3: 1427-34.

8. Suh N, Lamph WW, Glasebrook AL, Grese TA, Palkowitz AD, Williams CR, et al. Prevention and treatment of experimental breast cancer with the combination of a new selective estrogen receptor modulator, arzoxifene, and a new rexinoid, LG 100268. Clin Cancer Res. 2002; 8: 3270-5.

9. Cox AD, Fesik SW, Kimmelman AC, Luo J, Der CJ. Drugging the undruggable RAS: Mission possible? Nat Rev Drug Discov. 2014; 13: 828-51.

10. O'Bryan JP. Pharmacological targeting of RAS: Recent success with direct inhibitors. Pharmacol Res. 2019; 139: 503-11.

11. Hayes JD, McMahon M, Chowdhry S, Dinkova-Kostova AT. Cancer chemoprevention mechanisms mediated through the Keap1-Nrf2 pathway. Antioxid

Redox Signal. 2010; 13: 1713-48.

12. Hu R, Saw CL, Yu R, Kong AN. Regulation of NF-E2-related factor 2 signaling for cancer chemoprevention: antioxidant coupled with antiinflammatory. Antioxid Redox Signal. 2010; 13: 1679-98.

13. Iida K, Itoh K, Kumagai Y, Oyasu R, Hattori K, Kawai K, et al. Nrf2 is essential for the chemopreventive efficacy of oltipraz against urinary bladder carcinogenesis. Cancer Res. 2004; 64: 6424-31.

14. Khor TO, Huang MT, Prawan A, Liu Y, Hao X, Yu S, et al. Increased susceptibility of Nrf2 knockout mice to colitis-associated colorectal cancer. Cancer Prev Res (Phila). 2008; 1: 187-91.

15. Xu C, Huang MT, Shen G, Yuan X, Lin W, Khor TO, et al. Inhibition of 7,12-dimethylbenz(a)anthracene-induced skin tumorigenesis in C57BL/6 mice by sulforaphane is mediated by nuclear factor E2-related factor 2. Cancer Res. 2006; 66: 8293-6.

16. Satoh H, Moriguchi T, Taguchi K, Takai J, Maher JM, Suzuki T, et al. Nrf2-deficiency creates a responsive microenvironment for metastasis to the lung. Carcinogenesis. 2010; 31: 1833-43.

17. Satoh H, Moriguchi T, Saigusa D, Baird L, Yu L, Rokutan H, et al. NRF2 Intensifies Host Defense Systems to Prevent Lung Carcinogenesis, but After Tumor Initiation Accelerates Malignant Cell Growth. Cancer Res. 2016; 76: 3088-96.

18. Ramos-Gomez M, Kwak MK, Dolan PM, Itoh K, Yamamoto M, Talalay P, et al. Sensitivity to carcinogenesis is increased and chemoprotective efficacy of enzyme inducers is lost in nrf2 transcription factor-deficient mice. Proc Natl Acad Sci U S A. 2001; 98: 3410-5.

19. Menegon S, Columbano A, Giordano S. The Dual Roles of NRF2 in Cancer. Trends Mol Med. 2016; 22: 578-93.

20. Sporn MB, Liby KT. NRF2 and cancer: the good, the bad and the importance of context. Nat Rev Cancer. 2012; 12: 564-71.

21. Wang XJ, Sun Z, Villeneuve NF, Zhang S, Zhao F, Li Y, et al. Nrf2 enhances resistance of cancer cells to chemotherapeutic drugs, the dark side of Nrf2. Carcinogenesis. 2008; 29: 1235-43.

22. Mitsuishi Y, Taguchi K, Kawatani Y, Shibata T, Nukiwa T, Aburatani H, et al. Nrf2 redirects glucose and glutamine into anabolic pathways in metabolic reprogramming. Cancer Cell. 2012; 22: 66-79.

23. DeNicola GM, Chen PH, Mullarky E, Sudderth JA, Hu Z, Wu D, et al. NRF2 regulates serine biosynthesis in non-small cell lung cancer. Nat Genet. 2015; 47: 1475-81.

24. Cuadrado A, Rojo AI, Wells G, Hayes JD, Cousin SP, Rumsey WL, et al. Therapeutic targeting of the NRF2 and KEAP1 partnership in chronic diseases. Nat Rev Drug Discov. 2019.

25. Zhang D, Rennhack J, Andrechek ER, Rockwell CE, Liby KT. Identification of an Unfavorable Immune Signature in Advanced Lung Tumors from Nrf2-Deficient Mice. Antioxid Redox Signal. 2018; 29: 1535-52.

26. DeNicola GM, Karreth FA, Humpton TJ, Gopinathan A, Wei C, Frese K, et al. Oncogene-induced Nrf2 transcription promotes ROS detoxification and tumorigenesis. Nature. 2011; 475: 106-9.

27. Chio IIC, Jafarnejad SM, Ponz-Sarvise M, Park Y, Rivera K, Palm W, et al. NRF2 Promotes Tumor Maintenance by Modulating mRNA Translation in Pancreatic Cancer. Cell. 2016; 166: 963-76.

28. Galan-Cobo A, Sitthideatphaiboon P, Qu X, Poteete A, Pisegna MA, Tong P, et al. LKB1 and KEAP1/NRF2 Pathways Cooperatively Promote Metabolic Reprogramming with Enhanced Glutamine Dependence in KRAS-Mutant Lung Adenocarcinoma. Cancer Res. 2019; 79: 3251-67.

29. Vartanian S, Ma TP, Lee J, Haverty PM, Kirkpatrick DS, Yu K, et al. Application of Mass Spectrometry Profiling to Establish Brusatol as an Inhibitor of Global Protein Synthesis. Mol Cell Proteomics. 2016; 15: 1220-31.

30. Tarumoto T, Nagai T, Ohmine K, Miyoshi T, Nakamura M, Kondo T, et al. Ascorbic acid restores sensitivity to imatinib via suppression of Nrf2-dependent gene expression in the imatinib-resistant cell line. Exp Hematol. 2004; 32: 375-81.

31. Tang X, Wang H, Fan L, Wu X, Xin A, Ren H, et al. Luteolin inhibits Nrf2 leading to negative regulation of the Nrf2/ARE pathway and sensitization of human lung carcinoma A549 cells to therapeutic drugs. Free Radic Biol Med. 2011; 50: 1599-609.

32. Boesch-Saadatmandi C, Wagner AE, Graeser AC, Hundhausen C, Wolffram S, Rimbach G. Ochratoxin A impairs Nrf2-dependent gene expression in porcine kidney tubulus cells. J Anim Physiol Anim Nutr (Berl). 2009; 93: 547-54.

33. Boettler U, Sommerfeld K, Volz N, Pahlke G, Teller N, Somoza V, et al. Coffee constituents as modulators of Nrf2 nuclear translocation and ARE (EpRE)-dependent gene expression. J Nutr Biochem. 2011; 22: 426-40.

34. Bollong MJ, Yun H, Sherwood L, Woods AK, Lairson LL, Schultz PG. A Small Molecule Inhibits Deregulated NRF2 Transcriptional Activity in Cancer. ACS Chem Biol. 2015; 10: 2193-8.

35. Singh A, Venkannagari S, Oh KH, Zhang YQ, Rohde JM, Liu L, et al. Small Molecule Inhibitor of NRF2 Selectively Intervenes Therapeutic Resistance in KEAP1-Deficient NSCLC Tumors. ACS Chem Biol. 2016; 11: 3214-25.

36. Tsuchida K, Tsujita T, Hayashi M, Ojima A, Keleku-Lukwete N, Katsuoka F, et al. Halofuginone enhances the chemo-sensitivity of cancer cells by suppressing NRF2 accumulation. Free Radic Biol Med. 2017; 103: 236-47.

37. Choi EJ, Jung BJ, Lee SH, Yoo HS, Shin EA, Ko HJ, et al. A clinical drug library screen identifies clobetasol propionate as an NRF2 inhibitor with potential therapeutic efficacy in KEAP1 mutant lung cancer. Oncogene. 2017.

38. Palmer AC, Sorger PK. Combination Cancer Therapy Can Confer Benefit via Patient-to-Patient Variability without Drug Additivity or Synergy. Cell. 2017; 171: 1678-91 e13.

39. Choi YH, Yu AM. ABC transporters in multidrug resistance and pharmacokinetics, and strategies for drug development. Curr Pharm Des. 2014; 20: 793-807.

40. Garrett JT, Olivares MG, Rinehart C, Granja-Ingram ND, Sanchez V, Chakrabarty A, et al. Transcriptional and posttranslational up-regulation of HER3 (ErbB3) compensates for inhibition of the HER2 tyrosine kinase. Proc Natl Acad Sci U S A. 2011; 108: 5021-6.

41. Rexer BN, Arteaga CL. Intrinsic and acquired resistance to HER2-targeted therapies in HER2 gene-amplified breast cancer: mechanisms and clinical implications. Crit Rev Oncog. 2012; 17: 1-16.

42. Quintanal-Villalonga A, Molina-Pinelo S, Cirauqui C, Ojeda-Marquez L, Marrugal A, Suarez R, et al. FGFR1 Cooperates with EGFR in Lung Cancer Oncogenesis, and Their Combined Inhibition Shows Improved Efficacy. J Thorac Oncol. 2019; 14: 641-55.

43. Viet CT, Dang D, Achdjian S, Ye Y, Katz SG, Schmidt BL. Decitabine rescues cisplatin resistance in head and neck squamous cell carcinoma. PLoS One. 2014; 9: e112880.

44. Haslam A, Prasad V. Estimation of the Percentage of US Patients With Cancer Who Are Eligible for and Respond to Checkpoint Inhibitor Immunotherapy Drugs. JAMA Netw Open. 2019; 2: e192535.

45. Longo V, Brunetti O, Azzariti A, Galetta D, Nardulli P, Leonetti F, et al. Strategies to Improve Cancer Immune Checkpoint Inhibitors Efficacy, Other Than Abscopal Effect: A Systematic Review. Cancers (Basel). 2019; 11.